

Adam Mickiewicz University in Poznań
Faculty of Biology
Institute of Molecular Biology and Biotechnology
Human Molecular Genetics Research Unit



ADAM MICKIEWICZ
UNIVERSITY
POZNAŃ

The role of phosphorylation of ISGF3 components
in the regulation of ISG expression and viral protection

doctoral thesis

by

Hanna Nowicka

prepared under supervision of

Prof. dr hab. Hans A.R. Bluysen

Poznań 2022

Uniwersytet im. Adama Mickiewicza w Poznaniu,

Wydział Biologii

Instytut Biologii Molekularnej i Biotechnologii

Pracownia Genetyki Molekularnej Człowieka



ADAM MICKIEWICZ
UNIVERSITY
POZNAŃ

Rola fosforylacji komponentów kompleksu ISGF3 w regulacji ekspresji ISG i ochrony przeciwwirusowej

rozprawa w języku angielskim
ze streszczeniem w języku polskim

Autor:

Hanna Nowicka

przygotowana pod kierunkiem:

Prof. dr hab. Hans A.R. Bluysena

Poznań 2022

CONTENTS

1. INTRODUCTION.....	7
1.1. Interferons	8
1.2. IFN Type-I productions.....	11
1.3. Canonical IFN-Type I signalling pathway.	15
1.3.1. JAKs.....	15
1.3.2. STATs	16
1.3.2.1. STAT1	18
1.3.2.2. STAT2	21
1.3.3. IRFs.....	24
1.3.3.1. IRF9.....	25
1.3.3.2. IRF1	27
1.3.4. The role of the ISGF3 complex in the canonical IFN α -dependent signalling pathway	28
1.3.5. Negative regulation of the IFN Type-I signalling pathway.....	30
1.3.6. Prolonged ISGs expression	31
1.4. Non-canonical IFN-signalling pathways	32
1.4.1. Antiviral response in the absence of the STAT1 protein: the role of the STAT2/IRF9 complex	32
1.4.2. The role of the unphosphorylated STAT-based complexes in the IFN α -driven response ...	34
1.4.2.1. U-ISGF3	34
1.4.2.1. U-STAT2/IRF9.....	36
1.4.3. The role of the unphosphorylated STAT-based complexes in the basal ISGs expression regulation	38
1.5. Genome-wide studies of the IFN Type-I signalling pathway.....	39
1.5.1. IFN Type-I dependent	40
1.5.2. IFN Type-I independent	41
1.6. The regulation of <i>STAT1</i> , <i>STAT2</i> , <i>IRF9</i> and <i>IRF1</i> gene expression – the positive feedback loop model	42
1.7. Interferon stimulated genes	45
2. HYPOTHESIS AND OBJECTIVES.....	48
3. MATERIAL AND METHODS.....	49
3.1. Cell lines.....	49
3.1.1. Cell culture	49
3.1.2. Interferon treatment.....	50
3.2. Generation of the cell lines with stable overexpression of ISGF3 components	51

CONTENTS

3.3. RNA isolation and reverse transcription	52
3.4. qPCR method (Real-time PCR).....	53
3.5. RNA-Seq library preparation and sequencing.....	54
3.5.1. RNA-Seq data analysis	55
Differential gene expression analysis (DEG)	56
Gene ontology term enrichment analysis	56
Selection of commonly upregulated genes.....	56
3.6. Chromatin immunoprecipitation (ChIP).....	57
3.7. ChIP-Seq	59
3.7.1. ChIP-Seq data analysis	59
Top score peaks selection.....	61
Visualization in the Integrative Genomics Viewer	62
Binding profiles.....	62
Binding site motifs identification	62
3.8. Proteins isolation	63
3.9. Experiments with JAK Inhibitor I.....	66
3.10. Antiviral assay.....	66
4. RESULTS.....	68
<u>PART I</u>: The role of ISGF3 in time-dependent IFNα-activated transcriptional responses	68
4.1. Characterisation of 2fTGH and Huh7.5 cell lines	68
4.2. The genome-wide characterization of gene expression in 2fTGH and Huh7.5 cell lines	69
4.3. The genome-wide chromatin interactions in response to IFN α	74
4.4. The viral protection of 2fTGH upon long-term IFN α stimulation	79
<u>PART II</u>: The role of STAT2/IRF9 in time-dependent IFNα-activated transcriptional responses in the absence of STAT1	81
4.5. Characterisation of ST2-U3C and Huh7.7 STAT1 K.O. cell lines	81
4.6. The genome-wide characterization of gene expression in the ST2-U3C and Huh ST1 K.O. cell lines	83
4.7. The genome-wide chromatin interactions in response to IFN α	91
<u>PART III</u>: The role of phosphorylation of ISGF3 and STAT2/IRF9 in time-dependent IFNα- activated transcriptional responses	97
4.8. The role of phosphorylation of ISGF3 in the regulation of prolonged ISG expression under wild type conditions	97
4.9. The role of phosphorylation of STAT2/IRF9 in prolonged IFN α signalling in the absence of STAT1	101
4.10. The role of phosphorylation in viral protection of the 2fTGH cells.....	105

<u>PART IV A: The basal ISG expression regulation under conditions with the abundance of ISGF3 components</u>	107
4.11. The role of abundance of ISGF3 components in the regulation of the basal ISG expression .	107
4.12. The characterization of STAT1 K.O. U3C cell lines overexpressing the STAT1, STAT2 and IRF9 proteins.....	108
4.13. The genome-wide characterization of basal gene expression in cells overexpressing STAT1, STAT2 and IRF9	110
4.14. The role of unphosphorylated ISGF3 components in basal ISG expression	111
4.15. The basal chromatin binding of ISGF3 components in cells overexpressing these components	112
4.16. The role of unphosphorylated ISGF3 components in the viral protection in the absence of IFN α stimulation	114
<u>PART IV B: The role of abundance of ISGF3 components (U-ISGF3) in the regulation of IFN-activated ISG expression</u>	116
4.17. The role of phosphorylation in prolonged IFN α signalling under conditions with abundance of ISGF3 components	116
4.18. The role of phosphorylation in prolonged IFN α signalling in the cells overexpressing STAT1, STAT2 and IRF9	117
4.19. The role of phosphorylation in antiviral protection upon the abundance of STAT1, STAT2 and IRF9.....	118
5. DISCUSSION	122
5.1. The role of ISGF3 phosphorylation in time-dependent IFN α -activated regulation of ISGs	122
5.2. The role of STAT2/IRF9 in time-dependent IFN α -activated regulation of ISGs in the absence of STAT1	124
5.3. ISGF3 vs STAT2/IRF9.....	126
5.4. The role of U-ISGF3 and U-STAT2/IRF9 in basal and IFN-mediated expression of IFN α -induced genes.....	127
5.5. Increased complexity of basal and IFN α -dependent transcriptional responses.....	131
References	138
List of Figures	150
List of Tables	151
Abbreviations	152
List of publications	154
Acknowledgments	155
Funding	156
Summary	157
Streszczenie w języku polskim	159

1. INTRODUCTION

As in the late '90 effective treatment for controlling the human immunodeficiency virus (HIV) was established few viruses such as Ebola, Swine flu, avian influenza or MERS were causing epidemics, but none of them was considered to be as great a problem for modern societies as poverty, climate change or military conflicts. However, nowadays COVID-19 pandemic drew attention to the importance of viral diseases.

The new viral diseases are the consequence of the huge mutability and evolution of the already existing viruses. The reason for this is the transmission of animal viruses to humans due to the aggressive expansion of people to areas occupied by wild animals or insects that were so far isolated from humans (Kilbourne MD 1990)(Tapper 2006).

Viruses are unable to replicate without the host cell machinery and on account of this understanding the host-virus interactions is crucial for the development of new treatment and prevention methods.

In general, the immune response to viruses, same as the response to other pathogens, consists of two types: innate and adaptive. Innate immunity, also known as non-specific, is evolutionarily older than adaptive which is only found in jawed fish and higher vertebrates. Innate immunity is composed of cellular and humoral defence. The cellular defence based on the hematopoietic [such as dendritic cells, macrophages, neutrophils, eosinophils and natural killer (NK) cells] and non-hematopoietic cells (such as epithelial cells). The humoral component includes proteins and peptides that have antimicrobial functions such as complement proteins, defensins, LPS binding protein (LBP) and C-reactive protein (CRP). In general, innate immunity role is to:

- recruit immune cells to fighting with pathogens by producing cytokines (such as interferons),
- activate complement cascade that is responsible for recognition and removal of the bacteria and other pathogens
- remove foreign substances by the white blood cells (granulocytes and monocytes)
- remove infected or injured cells by NK cells
- activate the adaptive immune system via antigen presentation (Turvey and Broide 2010)

INTRODUCTION

Altogether, this provides time to develop an adaptive response mechanism which is more potent in combating infection (Randall and Goodbourn 2008). Adaptive immunity also consists of two systems: the cell-mediated and humoral response. The first one based on function of T lymphocytes, e.g. cytotoxic, that are able to kill infected cells. In turn, the humoral response is connected to specific antibody production by B lymphocytes. Both of these systems lead to creation of immunological memory that allow to combat the infection of already known pathogen much faster. However, in principle, one cannot speak of a real division as the boundary between innate and adaptive immunity is fluid, elements of those immunities are inseparable and they influence each other (Otto 2003)(Turvey and Broide 2010).

1.1. Interferons

Since discovered in 1957 by Isaacs and Lindenmann interferons (IFNs) and interferon-dependent signalling pathways were extensively studied as their role is not only the first line of host defence to the pathogens but also they are involved in many cellular mechanisms such as inflammation, cell growth, differentiation and apoptosis ending with adaptive immunity (Randall and Goodbourn 2008)(Lindenmann, Burke, and Isaacs A. 1957)(Sadler and Williams 2008)(Stark 2007). The interferon molecule was firstly observed to be produced by cells after influenza virus infection and its name comes from the ability of this cytokine to “interfere” with virus replication (Sadler and Williams 2008)(Fensterl and Sen 2009). IFN production is stimulated by pathogen products such as viral single or double-stranded RNA, dsDNA and other so-called PAMPs (pathogen-associated molecular patterns) e.g. bacterial lipopolysaccharide (LPS), flagellin, peptidoglycans or bacterial toxins (Randall and Goodbourn 2008)(Malterer, Glass, and Newman 2014). PAMPs are various microbial molecules sharing the ability to be recognized by the host immune system (Bianchi 2007) via pattern recognition receptors (PRRs). Among PRRs we distinguish: the toll-like receptor (TLR) family, localized on cell surface or in endosomes (Sue, Meir, and de la Morena 2018), RNA helicases retinoic acid-induced gene-I (RIG-I) and melanoma differentiation-associated gene-5 (MDA-5) receptors (Fensterl and Sen 2009). IFNs may also be produced as a consequence of damage-associated molecular patterns (DAMPs) recognition. DAMPs are equivalents of PAMPs, but with endogenous source – they are secreted by injured or dying cells (Bianchi 2007). DAMPs are, for example, ATP, heat shock proteins (HSPs), histones, fibrinogen or exposed mitochondria and other organelles that in normal conditions would not be found outside the cell. To DAMPs belongs also the nuclear

protein high mobility group box 1 (HMGB1) that is secreted by necrotic cells. Interestingly, IFN α , when produced by infected cells, also could be DAMP (Seong and Matzinger 2004)(Lotfi, Lee, and Lotze 2007)(Lotze, Deisseroth, and Rubartelli 2007)(Roh and Sohn 2018).

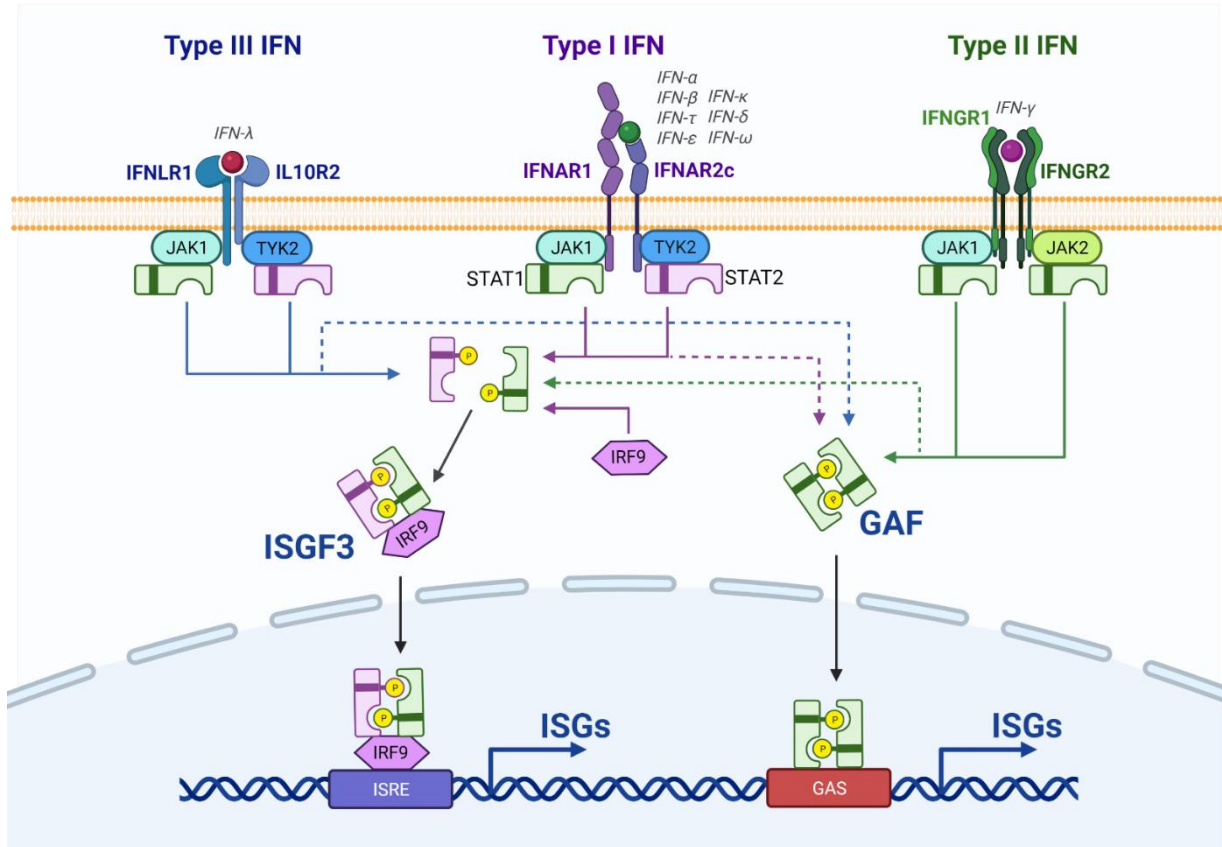


Figure 1.1 The Interferon signalling pathways

Various interferon types stimulate different cellular receptors. IFN Type-I binds to the IFNAR receptor built of the IFNAR1 and IFNAR2c subunits, IFN γ attaches to the IFNGR receptor consisting of four subunits (two IFNGR1 and two IFNGR2) and IFN λ s recognize the IFNLR receptor composed of IFNLR1 (known also as IL-28R1) and IL-10R2.

After IFN α stimulation the Janus kinases JAK1 and TYK2 phosphorylate STAT1 and STAT2 proteins which together with IRF9 form the ISGF3 complex, that translocates to the nucleus where it recognises the ISRE sequence in promoters of many genes with antiviral function, named as Interferon Stimulated Genes (ISGs).

IFN γ -receptor interactions evoke STAT1 phosphorylation and homodimerization into the GAF complex that is translocated to the nucleus where it recognizes the GAS sequence in promoters of ISGs.

Last but not least, IFN λ -receptor binding induces phosphorylation of the STAT1 and STAT2 proteins and triggers ISGF3 formation.

Under certain conditions IFN Type-I and -III can stimulate also GAF formation and IFN Type-II is involved in triggering of the ISRE containing genes expression.

INTRODUCTION

The basic function of interferon is triggering fast and robust antiviral response as its molecules are exceptionally potent regulators and are able to work effectively even though IFN production is limited to about 10 molecules per cell (Marcus 1999). Moreover, secretion of IFNs from infected cells brings neighbouring cells into a so-called antiviral state which provides readiness of the cells to fight with infection (Stark 2007).

IFNs are a family of cytokines secreted by the host cells in response to the pathogen appearance and in mammals according to their amino acid sequence homology and receptor specificity are divided into three groups: IFNs Type-I, -II and -III. In human IFN Type-I consists of 13 IFN α subtypes as well as IFN β , IFN κ , IFN ϵ and IFN- ω . Genes for all of them are clustered in chromosome 9 and, besides IFN κ , are devoid of introns (Lazear, Schoggins, and Diamond 2019). While IFN α and β can be secreted by most cell types, especially plasmacytoid dendritic cells (pDC), other Type-I IFNs production is more cell- or species-specific (Liu 2005). Human Type-II IFN contains a single IFN γ (gene located on 12 chromosome) which is produced mainly by activated T cells and NK cells (Fensterl and Sen 2009)(Samuel 2001). Last but not least, there is IFN Type-III which comprises INF λ 1, 2 and 3 known also as IL-29, IL-28A and IL-28B, respectively, as well as IFN λ 4 discovered in 2013. Genes for all of these cytokines, are clustered on chromosome 19 (Fensterl and Sen 2009)(Pestka 2007)(Prokunina-olsson et al. 2013). Structurally, the IFN λ group members are similar to the interleukin 10 (IL-10) family and are using the same receptor subunit, IL-10R2. Functionally, IFN λ s are similar to IFN Type-I, but IFN α / β are secreted ubiquitously, IFN lambdas are produced in mucosal tissues (such as in the gastrointestinal or respiratory tract, as well as the blood–brain barrier) especially by epithelial cells (Hemann, Gale, and Savan 2017)(Sadler and Williams 2008)(Sommerreyns et al. 2008). IFN Type-I binds to a ubiquitously expressed specific receptor built of IFNAR1 and IFNAR2 subunits, IFN Type-II recognizes a dimeric receptor complex consisting of two IFNARG1 and two IFNARG2 subunits (Michalska et al. 2018) while the Type-III receptor comprises of IL-10R2 and IFNLR1 (known also as IL-28R1)(Sadler and Williams 2008) (Figure 1.1). In general, specific receptor binding results in the activation of the JAK-STAT signalling pathway in case of all IFN subtypes (Sadler and Williams 2008) (Figure 1.1). IFN Type-I, as well as Type-III, promote phosphorylation of STAT1 (signal transducer and activator of transcription) and STAT2 by JAK1 and TYK2. As a consequence, phospho-STAT1-phosphoSTAT2 heterodimer, together with IRF9, form the Interferon-Stimulated Gene Factor 3 (ISGF3) complex. Next, ISGF3 is translocated to the nucleus where it recognizes a specific IFN-Stimulated Regulatory Element (ISRE) (Randall and Goodbourn 2008)(Lindenmann, Burke, and Isaacs A. 1957)(Sadler and

INTRODUCTION

Williams 2008)(Stark 2007)(Fensterl and Sen 2009) in promoters of more than 300 IGSs (interferon stimulated genes) with known antiviral function (Blaszczyk et al. 2016). Activation of the IFN γ -dependent signalling pathway is based on phosphorylated STAT1 dimerization and GAF (gamma activation factor) formation. Nuclear localization of GAF activates ISGs expression by binding to the gamma-activated sequence (GAS) in their promoters (Samuel 2001). An example of GAF targets are *IRF1*, *SOCS3*, as well as *STAT1*, *STAT2* and *IRF9* (Michalska et al. 2018). In general, IFN Type-I and -III activate ISRE-containing genes while IFN Type-II - GAS-containing genes. However, under certain conditions, the expression of the ISRE-containing genes can be activated by IFN Type-II and the GAS-containing genes - by IFN Type-I and -III (Michalska et al. 2018). This could explain the overlap between the gene subsets whose expression is triggered by these three different IFN types, even though they use distinct cell surface receptors.

IFNs function also as immunomodulators: Type-I promote dendritic cell and macrophage activation, thus MHC-I molecules upregulation, while Type-III has an impact on MHC class II expression by triggering IRF1 and CIITA (Class II Major Histocompatibility Complex Transactivator) production. Moreover, IFN γ is involved in the differentiation of T helper to Th1 cells, which then are secreting more IFN γ . T helper cells, on the other hand, are important in recognition of MHC class II molecule-antigen connections in the process called “antigen presentation” that further extend the immunological response to production of specific antibodies by B lymphocytes and provide readiness of the host cells to fight the re-infection with the same pathogen (Otto 2003).

1.2. IFN Type-I production

As briefly mentioned in the previous section, interferon production is a consequence of the pathogen exposure. The host cell defence mechanisms are sensitive to viral single or double-stranded RNA, exogenous DNA and PAMPs (pathogen-associated molecular patterns) (Figure 1.2). PAMPs are a group of diverse bacterial, parasite and viral molecules such as LPS, peptidoglycans, flagellin, extracorporeal nucleic acids or bacterial toxins. The common feature

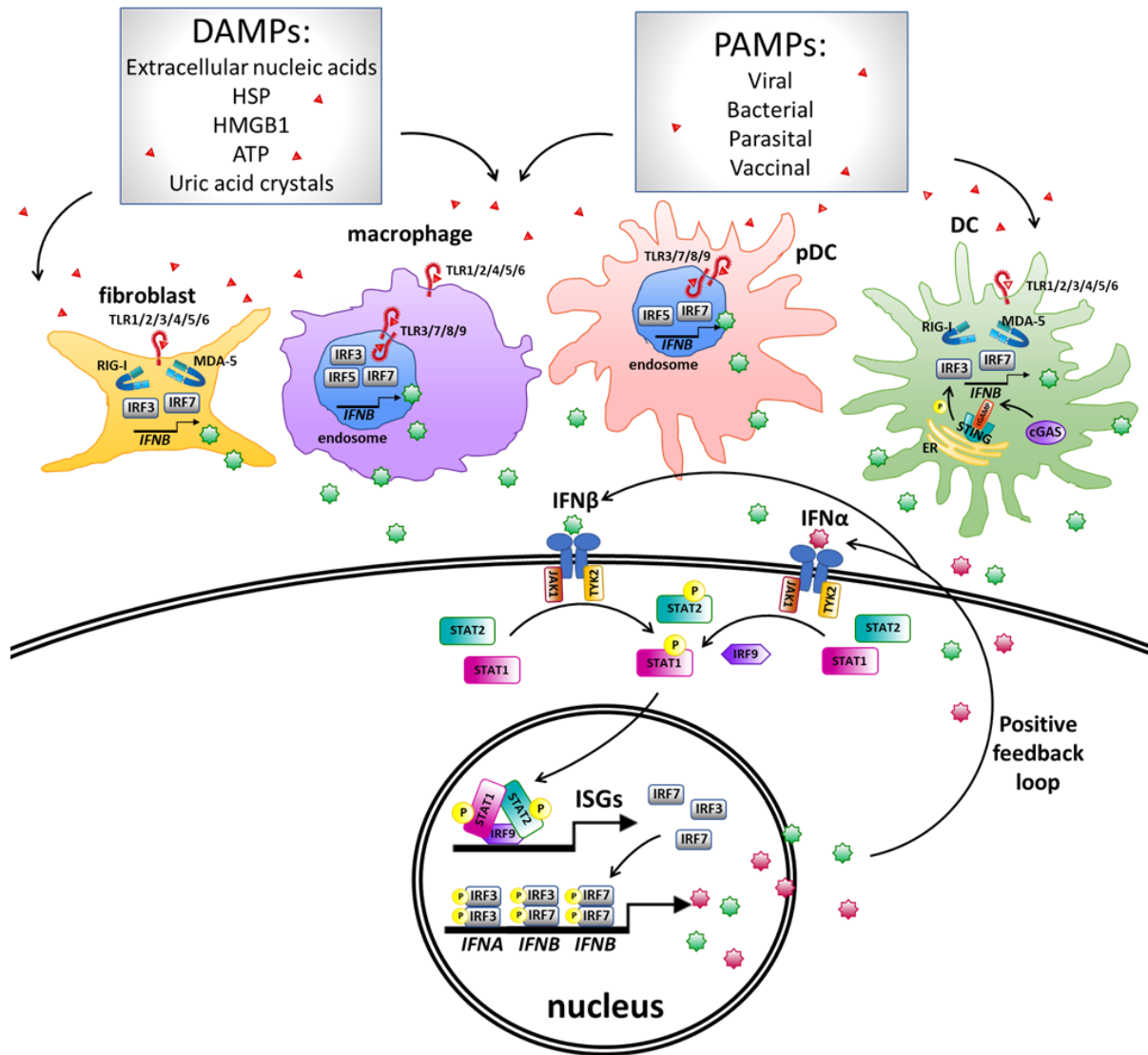


Figure 1.2 Simplified scheme of the IFN Type-I production

Immune cells are very responsive to pathogen-associated molecular patterns (PAMPs) or damage-associated molecular patterns (DAMPs). IFN β is produced by many types of immune cells, such as dendritic cells (DCs), plasmacytoid DCs (pDCs), macrophages (M ϕ) or fibroblasts. Recognition of PAMPs or DAMPs occurs through the: - Toll-like receptors (TLRs) localized in the cellular or endosomal membrane; - cytosolic RNA helicases retinoic acid-induced gene-I (RIG-I) and melanoma differentiation-associated gene-5 (MDA-5); - complex of cyclic guanosine monophosphate-adenosine monophosphate (cGAMP) synthase (cGAS)- stimulator of interferon genes (STING). Secreted IFN β promotes ISGF3 formation by triggering the JAK-STAT signalling pathway that leads to expression of ISGs, such as IRF7. Then, IRF7 and IRF3 are participating in the IFN α and IFN β gene expression initiation. The newly synthesized IFN α and β molecules are released from the cells and are binding to the IFNAR receptors of the same and neighbouring cells, thus providing the positive feedback loop for IFN Type-I production and the antiviral response (Pitha and Various 2007).

INTRODUCTION

of those PAMPs is recognizability by the host immune system via pattern recognition receptors (PRRs). Among PRRs toll-like receptor (TLR) family, RNA helicases retinoic acid-induced gene-I (RIG-I), melanoma differentiation-associated gene-5 (MDA-5) and cyclic guanosine monophosphate-adenosine monophosphate (cGAMP) synthase (cGAS)-STING receptors can be recognized. Likewise, interferons are produced also in response to DAMPs (Randall and Goodbourn 2008)(Malterer, Glass, and Newman 2014)(Bianchi 2007)(Sue, Meir, and de la Morena 2018)(Fensterl and Sen 2009).

In humans, TLR family consists of 10 members numbered from one to ten (Sue, Meir, and de la Morena 2018). While TLR 1, 2, 4, 5, and 10 are localized at the cell surface, TLR 2, 7, 8 and 9 are located on the membrane of endosomes (Sue, Meir, and de la Morena 2018). Many of TLRs are expressed in dendritic cells (DCs) and macrophages (M ϕ), especially TLR3 and 4. Upon TLR-dependent activation, DCs and M ϕ differentiate into antigen-presenting cells, thus initiating development of adaptive immunity (Pitha and Various 2007). It is worth noting that various PAMPs are recognized by different TLRs: lipoproteins are targets for TLR1, 2 and 6, LPS for TLR4, flagellin for TLR5, ssRNA for TLR7 as well as 8 and DNA for TLR9 (Kawai and Akira 2011). Nevertheless, to be recognized by TLRs all PAMPs need to possess an extracellular leucine-rich repeat (LRR) motif (or motifs). After ligand recognition, TLRs are recruiting to their cytoplasmic tail a variety of adaptor molecules possessing the TIR homology domain. Afterwards, myeloid differentiation primary response protein 88 (MyD88) or TIR domain-containing adapter-inducing IFN β (TRIF) are involved and activate transcription factors, including interferon regulatory factors (IRFs), NF- κ B and ATF-2/c-Jun (Pitha and Various 2007).

In contrast to TLRs, helicases RIG-I and MDA-5 are localized in the cytoplasm and are specialized in recognition of viral RNA which is accumulating in the cytoplasm during replication. At the RIG-I N-terminus, the caspase recruitment domain (CARD) is located. CARD is necessary for RIG-I functionality which is recognition of dsRNA. RIG-I activation depends on dsRNA binding, as well as ATP hydrolysis. Thus, C-terminus of RIG-I functions as a negative self-regulator via masking the CARD domain (Pitha and Various 2007). Helicase MDA-5 is structurally similar to RIG-I, however, differences in its CARD domain are responsible for the recognition of different virus types (Kato et al. 2006)(Kato et al. 2005)(Gitlin et al. 2006). Some studies on RIG-I and MyD88 revealed that various cell types differ in the

INTRODUCTION

signalling pathways usage. For example, in cDCs RIG-I, but not MyD88, is crucial, while inversely in pDCs MyD88, but not RIG-I, is necessary (Kato et al. 2005).

As cytosolic DNA is detected, cGAS synthase becomes activated and synthesizes 2'3'-cGAMP which interacts with the STING (stimulator of interferon genes) receptor located on the endoplasmic reticulum (ER). STING undergoes conformational changes, translocate to Golgi apparatus and recruits TBK1, which, as a consequence, phosphorylates itself and STING. Next, activated STING recruits IRF3 which becomes phosphorylated by TBK1 and is translocated to the nucleus what leads to IFN β production. Additionally, TBK1 activates NF- κ B (Cheng et al. 2020).

Pathogen recognition triggers diverse signalling pathways relying on TLRs, RIG-I or MDA-5, but all, eventually, result in IRF3 and IRF7 activation by phosphorylation and dimerization, thus in production of IFN β . IRF3 alone is enough to trigger production of IFN β , however IRF7 involvement is necessary for expression enhancement (Pitha and Various 2007)(Erickson and Gale 2008). It has been proven that IRF7 is also pivotal for IFN α production, as in IRF7 $^{-/-}$ mice IFN α signalling pathway is severely impaired (Honda et al. 2005). It is worth noting, that while IRF3 is expressed ubiquitously and constitutively, IRF7 expression is restricted to some lymphoid cells and plasmacytoid dendritic cells (pDC) and is dependent on ISGF3 (Pitha and Various 2007). The recognition of PAMPs by TLRs leads to IRF3 activation and IFN β production. Secreted IFN β binds to the receptors on the surface of the same and neighbouring cells, thus activating IRF7 production. As a consequence, accumulation of IRF7 stimulates further IFN α production. (Fensterl and Sen 2009)(Randall and Goodbourn 2008)(Sadler and Williams 2008)(Pitha and Various 2007)(Jefferies 2019). This process creates a positive feedback loop that boosts the antiviral response in uninfected and already infected cells (Randall and Goodbourn 2008)(Marie 1998).

An uncontrolled feedback loop can lead to a pathological condition which results in various diseases and needs to be regulated. The mechanism of this regulation is described in detail in subsection 1.6.

Apart from IRF3 and IRF7, also other IRFs participate in triggering IFN Type-I production. Among them, IRF1 and IRF5 need to be mentioned. It was observed that, while IRF7 induces IFN α 1 subtype, IRF5 takes part in production of IFN α 8. Interestingly, IRF1/IRF7 double knock-out myeloid dendritic cells (mDC) after viral infection produce relatively normal levels of IFN β . IRF5 (previously identified in connection to induction of proinflammatory cytokines,

such as TNF- α , IL-6 and IL-12, downstream to TLR7 and MYD88) has been proven to be responsible for this process (Lazear et al. 2013). Also IRF1 was observed to induce IFN β production, however its presence is not necessary (Pitha and Various 2007).

In fact, IFNs Type-I are produced in all cells over the body, however, the biggest producers are pDCs which possess TLR7 and 8, as well as TLR9 receptors, thus their main role is connected to recognizing bacterial DNA and viral RNA, respectively (Pitha and Various 2007). Nevertheless, also macrophages, cDCs and monocytes as well as fibroblasts and epithelial cells act synergistically providing a broad spectrum of IFN α sources, ensuring full protection against viral infections (Ali et al. 2019).

1.3. Canonical IFN-Type I signalling pathway

In this thesis, we focus on the IFN α signalling pathway and all of following subsections will refer to this type of interferon.

The classical IFN Type-I-dependent response, similar to other IFN types, is based on triggering JAK/STAT signalling pathway which engages proteins from two families: JAKs and STATs (Fensterl and Sen 2009). Specific receptor for IFN Type-I is composed of two subunits IFNAR1 and IFNAR2c to which JAK family members TYK2 and JAK1, respectively, are connected (X. Li et al. 1997). IFN binding promotes transphosphorylation of these JAK proteins which, in turn, phosphorylate tyrosine residues in the cytoplasmic tail of IFNAR thus creating docking site for STAT family members. As mentioned in detail in subsection 1.1 and shown on Figure 1.1, the consequence of IFNAR stimulation is ISGF3 formation and ISG production. It is worth highlighting, that different IFN Type-I molecules use the same receptors but cause distinct biological consequences. This phenomenon could be explained by several separate binding sites for different IFNs within receptor subunits and domains (van Boxel-Dezaire, Rani, and Stark 2006).

1.3.1. JAKs

As IFN Type-I receptor does not have kinase activity itself indispensable phosphorylation event is provided by attached proteins JAK1 and TYK2 which together with JAK1 and JAK3 are members of JAK family (Samuel 2001)(Zanin et al. 2021). Besides JAK3,

INTRODUCTION

all of the JAKs are necessary for interferon signalling activation and play a crucial role in antiviral response (Stark 2007). JAKs are protein tyrosine kinases (PTK) - enzymes able to transfer phosphate groups from ATP to the substrate proteins (Ghoreschi, Laurence, and O'Shea 2009) and this activity ensures STAT phosphorylation events that are essential for JAK-STAT signalling. JAK1 is involved in all of the IFN type responses, JAK2 is part of the IFN gamma receptor complex and TYK2 participates in Type-I and -III signalling pathways (Sadler and Williams 2008) (Figure 1.1).

All JAKs are large proteins that have an homologous structure. Seven Jak homology regions, named JH1-7, have been described (Ghoreschi, Laurence, and O'Shea 2009)(Kisseleva et al. 2002). The JH1 domain ensures kinase catalytic activity. JH2 is a pseudo-kinase domain and has a self-inhibitory role. The SH2-like and FERM (Four-point-one, Ezrin, Radoxin, Moesin) domains (built from JH3-JH4 and JH4-JH7, respectively) are responsible for protein-receptor interactions (Kisseleva et al. 2002)(Ferrao and Lupardus 2017)(Huang, Constantinescu, and Lodish 2001). The pseudo-kinase domain is inactive due to the lack of conserved residues that are critical for phosphoryl group transfer. Interestingly, studies of Ungureanu and colleagues (Ungureanu et al. 2011) proved that the JH2 domain of JAK2 provides dual-specificity protein kinase activity. Autophosphorylation of Ser523 is the first step in activation of JH2 domain, enhancing phosphorylation of Tyr570 the next. And both ensure JAK2 low-activity without cytokine stimulation. Interestingly, Ser523 residue is the only one, that is constitutively phosphorylated in the absence of stimuli. Activated JAK2 becomes phosphorylated on approximately 20 tyrosine residues, among them, some enhance JAK2 activity (e.g. Tyr813), whereas some are negative regulators (e.g. Tyr119). Upon ligand binding to the receptor and its spatial reorganization activation-loop tyrosine residues at positions 1007–1008 of JAK2 JH1 domain become phosphorylated. This event leads to activation of JAK2, which, in turn, phosphorylate receptor tyrosine residues. This promote creation of docking sites for SH2 domain of the STAT proteins.

1.3.2. STATs

The STAT family consists of 7 members: STAT1, STAT2, STAT3, STAT4, STAT5 α , STAT5 β and STAT6 (Samuel 2001)(Shuai 1999) with size in the range of 750-900 amino acids. Genes for STAT1 and STAT4 are located on chromosome 2, for STAT2 and STAT6 – on

INTRODUCTION

chromosome 12 and for STAT3, 5a and 5b – on chromosome 17. For fulfilling their role as transcription factors, STATs need to be translocated to the nucleus.

STATs share similar structure of 6 conserved domains (described in more detail below)(Szlag et al. 2016): the N-terminal domain (ND), the coiled-coil domain (C-C), the DNA binding domain (DBD), the linker domain (LD), the Src homology 2 domain (SH2), the transcription activation domain (TAD) and the tyrosine phosphorylation site which is important for activity of STATs and located between the SH2 and TAD domains (Shuai 1999) (Figure 1.3 and 1.4).

The N-terminal domain participates primarily in forming various STAT dimer complexes (observed in untreated cells, also in unphosphorylated forms (Stark 2007)(Neculai et al. 2005) as well as in STATs methylation (Mowen et al. 2001)(Zouein et al. 2015).

The Coiled-coil domain mediates interplay of the STATs with other transcription factors e.g. ensures interaction of STAT1 and STAT2 with IRF9 during ISGF3 formation, as well as provides interaction of STAT5 with heat shock protein 90 (HSP90) (Weijing Xu et al. 2004)(Wesoly, Szweykowska-Kulinska, and Bluysen 2007).

The DNA-binding domain, besides its DNA-binding function, mediates STAT protein nuclear trafficking by providing a nuclear localization signal (NLS).

The linker domain is the region rich in Gly, Pro and hydrophilic residues involved in maintenance of appropriate spatial conformation of adjacent domains as well as nuclear export, DNA binding and transcriptional activity. The amino acid structure of the linker enables flexibility for interaction of the phosphotyrosine tail of one STAT protein to the SH2 domain of the other, but, at the same time, is too short to interact with its own SH2 (Lim and Cao 2006).

The SH2 domain is necessary for the interaction of STATs with IFN receptors (Randall and Goodbourn 2008). It also facilitates STATs dimerization – a prerequisite for nuclear translocation, DNA-binding and the antiviral response cascade activation (Samuel 2001).

The TAD domain of STATs has a role in transcriptional activation e.g. it is involved in interaction with CBP/p300 coactivators (Wojciak et al. 2009). In the absence of stimulus STATs TAD is structurally disordered because it is rich in proline residues and highly acidic (Lim and Cao 2006). Spatial organization and folding of these proteins takes place upon stimulation and dimerization.

At the border of the STAT's SH2 and TAD domains, tyrosine residues are located, that are essential for the canonical IFN-dependent response (Szelag et al. 2015). Tyrosine phosphorylation (pTyr) allows the STAT proteins to create homo- and heterodimers by interactions of pTyr of one STAT with the SH2 domain of another STAT (Kiu and Nicholson 2012). The phosphorylation event was thought to be a key factor for antiviral gene expression regulation, however, some studies suggested unphosphorylated STATs to be functional as well (see subsection 1.4.2).

The characteristic feature of the IFN-dependent signalling pathway is its rapid activation and subsequent decay determined by phosphorylation-dephosphorylation events, dimerization and the balance of STATs being shuttled from the cytoplasm to the nucleus and back. The balance shifted toward nuclear accumulation is an effect of STATs activation/dimerization which depends on nuclear localization signal (NLS). On the other hand, STATs translocation back to cytoplasm depends on three mechanism: NES (nuclear export signal) activity, dephosphorylation and interactions with negative regulators such as SOCS or PIAS (Schindler, Levy, and Decker 2007) described in more detail in subsection 1.3.5.

In following subsections we focus on the components of the ISGF3 complex: STAT1, STAT2 and IRF9.

1.3.2.1. STAT1

STAT1 gene is clustered on chromosome 2 together with *STAT4*. The STAT1 protein has a weight of 91 kDa and is activated by Tyr701 phosphorylation as a consequence of stimulation by all IFN types (Reich 2013). The phosphorylated STAT1 homodimer, known as GAF (the γ -activated factor), is the main component of the IFN γ -dependent signalling pathway. GAF triggers expression of genes containing GAS sequence (in consensus form of TTCCNGGAA, as described by Decker) (Decker, Kovarik, and Meinke 1997). Among these genes *IRF1*, *IRF8*, *GBP* and *SOCS1* are examples. In the IFN Type-I-dependent response STAT1 takes part in the ISGF3 formation, where main role of STAT1 is to stabilize ISGF3-DNA interaction (Bluyssen and Levy 1997).

The N-terminal domain of STAT1 takes part in formation of U-STAT1 dimers, as well as in promoting dephosphorylation (Mertens et al. 2006). The C-C domain is engaged in interactions with non-STAT factors, such as IRF9. DBD, except for its participation in

STAT1

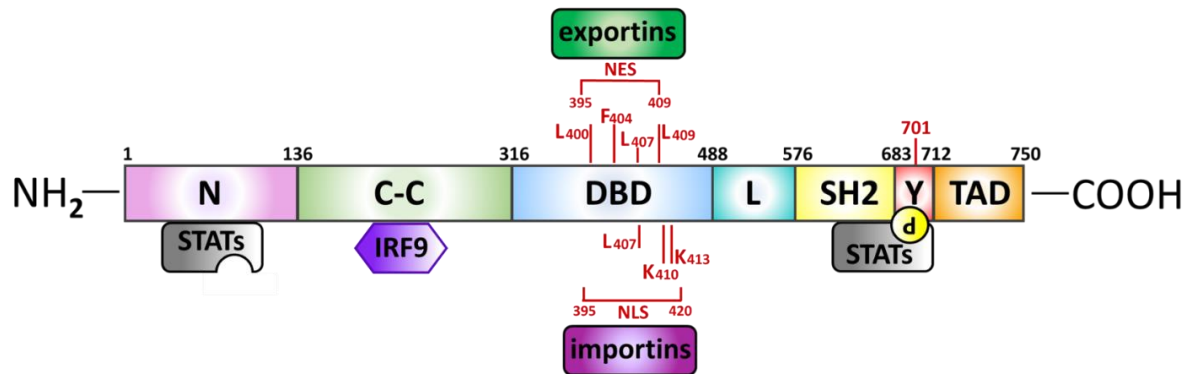


Figure 1.3 The STAT1 protein structure

Similar to the other STAT family members, STAT1 consists of 6 domains: N-terminal (N), Coiled-coil (C-C), DNA binding (DBD), Linker (L), Src homology 2 (SH2) and Transcription activation (TAD) at the carboxyl terminus. At the border of SH2 and TAD, at position 701, there is tyrosine residue (Y) undergoing phosphorylation. The N-terminus takes part in dimerization of STAT1 with other STATs in their unphosphorylated form. C-C domain is responsible for interactions with non-STAT proteins, such as interferon regulatory factor 9 (IRF9), during complex formation. The DBD, besides participation in DNA binding, is involved in the STAT1 nuclear import and export, as nuclear localization signal (NLS) and nuclear export signal (NES) are located in this domain. These signals are recognized by importins and exportins, respectively. In red colour crucial amino acids and their positions are shown (Szelag et al. 2016)(D. Xu et al. 2012).

recognition and connection with gene promoters (from which its name comes from), has pivotal role in nuclear import and export as NLS and NES sequences (recognized by importins and exportins, respectively) are located in that domain (Reich 2013). Next to DBD linker domain is located. This rich in Gly, Pro and hydrophilic residues region is crucial for STAT1 transcriptional activity. Point mutation of amino acids at position 544 and 545 of this domain resulted in abolished transcriptional responsiveness to IFN γ (Edward Yang et al. 1999). This domain contains NLS, that is important in nuclear trafficking and depends on STAT1 phosphorylation and dimerization (Kevin M. McBride et al. 2002). The STAT1-SH2 interacts with IFNGR1 receptor subunit where this transcription factor is phosphorylated (Randall and Goodbourn 2008). SH2 domain is responsible for dimerization of active, tyrosine-phosphorylated proteins. This crucial tyrosine residue is located at position 701 of amino acid chain. Crystallography experiments showed that STAT1/STAT1 cross-interaction is mediated by the SH2 domains. Interestingly, unphosphorylated proteins stick to each other in

INTRODUCTION

“head-to-head” position known as anti-parallel, while phosphorylation event changes that spatial arrangement to parallel and stabilizing it (Reich 2013). Moreover, STAT1/STAT2 dimerization is also facilitated by the STAT1-SH2 (Samuel 2001). Interestingly, hemiphosphorylated STAT1/STAT2 complexes are unable to translocate to the nucleus, as in IFN Type-I-related response U-STAT1 blocks P-STAT2 trafficking, and *vice versa* (Majoros et al. 2017). Last, but not least, the C-terminal domain ensures transcriptional activity of the STAT1 protein as it is utterly essential for recruitment of RNA polymerase II. C-terminus truncated STAT1 β isoforms could not effectively mediate the binding of transcription machinery to the subset of the genes, among them *IRF8* and *IRF1* (Parrini et al. 2018).

Phosphorylation of STAT1 Ser727, located in TAD, maximizes the STAT1 transcriptional activity of a gene subset and is not dependent on tyrosine phosphorylation. However, activated JAK2 is necessary for both of Ser727 and Tyr701 phosphorylation events (Zhu et al. 1997). Moreover, the STAT1 β isoform lacking TAD (together with Ser727 residue) has attenuated functionality (Chodisetti et al. 2020).

The signalling pathway stimulation and repression depends on the nuclear trafficking of STATs proteins (Meyer and Vinkemeier 2004). Nuclear import of phosphorylated STAT1 is facilitated by interactions of DBD-located NLS with importin- α 5/importin- β 1 heterodimer. In case of unphosphorylated STAT1 the spatial arrangement precludes recognition of NLS by importin- α 5/importin- β 1 heterodimer. Thus, U-STAT1 is not able to be translocated into the nucleus (Reich 2013). Surprisingly, U-STAT1 was still detectable in the nucleus (Meyer and Vinkemeier 2004)(Marg et al. 2004). The mechanism that explains this phenomenon may be connected to the transportation of STAT1 by the nuclear pore complex (NPC) directly, as STAT1 connection to nucleoporins Nup153 and Nup214 was evidenced (Marg et al. 2004). Inversely, STAT1 export from the nucleus relies on the NES signal (which overlap NLS in the DBD) and is strongly dependent on dephosphorylation (D. Xu et al. 2012). The STAT1-NES remains hidden, when this protein is attached to DNA. Loss of the phosphoryl group forces detachment from DNA and reveals NES making it accessible for Crm1 exportin – primary mediator of STAT1 nuclear export (K. M. McBride 2000). Thus, nuclear export of STAT1 depends on dephosphorylation and the N-terminal domain has been reported to play a role in this process (Mertens et al. 2006).

STAT1 was observed to form many dimers. The basic is STAT1/STAT1, known as GAF, but also others were described. STAT1/STAT2 exists in the resting cells and together

with STAT2/IRF9 was proposed to form ISGF3, STAT1-STAT3 can be formed in response to IL-6 and IL-27 and STAT1-STAT4 is induced by IL-35 (Delgoffe and Vignali 2013).

The STAT1 role in pathogenesis was also described. The studies on mice lacking STAT1 have shown increased susceptibility of these animals to the tumorigenesis induced by the chemical carcinogens. Deficiency of both, STAT1 and p53, made mice develop tumours more rapidly and frequently when compared with these lacking p53 alone. Moreover, double K.O. mice develop a broader spectrum of cancer types (Kaplan et al. 1998). Due to the STAT1 role in promoting apoptosis (Kumar et al. 1997)(Janjua, Stephanou, and Latchman 2002)(Sironi and Ouchi 2004), this protein was regarded as a tumour suppressor. However, more recent studies have shown that *STAT1* functions as an oncogene in the malignant pleural mesothelioma (MPM) (Arzt et al. 2014). Similarly, *STAT1* as an oncogene connected to tumorigenesis induced by ETV6-NTRK3 (EN) fusion gene, was described in paper of Park and colleagues (Park et al. 2018). This chromosomal rearrangement is associated with many tumours, among them, gastrointestinal stromal tumour, acute myeloblastic leukaemia and congenital fibrosarcoma.

1.3.2.2. STAT2

The molecular weight of STAT2 is 113 kDa what makes it the largest protein among the STAT family and - as the only one - it does not have isoforms. Its gene is clustered together with *STAT6* on chromosome 12 (Lim and Cao 2006). Structurally, STAT2 does not differ from other family members. The N-terminal domain was described to play a role in interactions of STAT2 with IFNAR receptor (X. Li et al. 1997). The N-terminus has also pivotal role in the STAT2-dependent activation of STAT1 (X. Li et al. 1997) and is involved in the interaction between STAT1 and CREB-binding domain of CBP/p300 (Stark 2007). The C-C domain role is connected to the interactions with non-STAT factors, especially IRF9 during ISGF3 formation (Martinez-Moczygemba et al. 1997).

The STAT2 DNA binding domain has no ability to binding DNA directly (Bluyssen and Levy 1997), but it is possessing NLS/NES signals. Arginine at position 409 and lysine at position 415 have been proven to play a crucial role in STAT2 nuclear trafficking (Fagerlund et al. 2002). Interestingly, STAT2 was found to be the only STAT which nuclear transport is dependent on having an dimerization partner with active NLS (e.g. STAT1 or IRF9) (Blaszczyk et al. 2016). Leucine Additional, constantly active NES is located also in the TAD domain, at position 740-751 (Banninger and Reich 2004).

STAT2

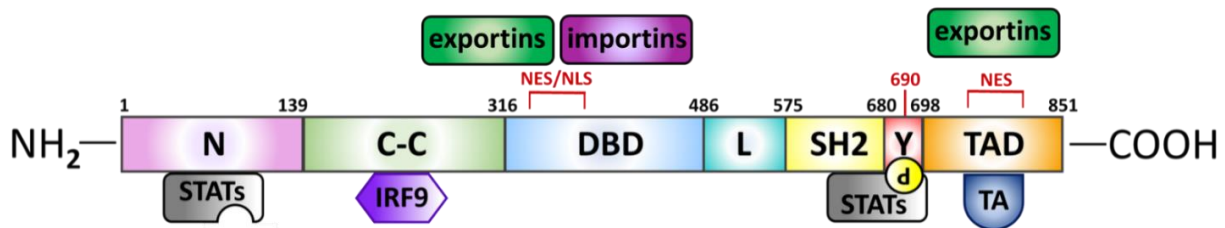


Figure 1.4 The STAT2 protein structure

STAT2, similar to the other STAT family members, is built of 6 domains: N-terminal (N), Coiled-coil (C-C), DNA binding (DBD), Linker (L), Src homology 2 (SH2) and Transcription activation (TAD) at the carboxyl terminus. At the border of SH2 and TAD, at position 690, tyrosine residue (Y) is located, which undergoes phosphorylation process. The N-terminus is responsible for dimerization with other STATs in their unphosphorylated form. C-C domain takes part in interactions with non-STAT proteins [such as interferon regulatory factor 9 (IRF9)], during complex formation. The DBD, besides its role in DNA binding, is involved in the nuclear import and export of STAT2, as nuclear localization signal (NLS) and nuclear export signal (NES) are located in that domain and amino acids at position 419 and 415 play crucial role. The second, constantly active NES, is in the TAD (amino acids 740-751). NLS and NES are recognized by importins and exportins, respectively (Szelag et al. 2016)(Blaszczyk et al. 2016)(D. Xu et al. 2012)(Banninger and Reich 2004).

It was established, that the SH2 domain of STAT2 has a critical role in IFN α / β -dependent signalling via interaction with the cytoplasmatic tail of the tyrosine-phosphorylated IFNAR1 subunit (Stark 2007)(Nguyen et al. 2002). Moreover, STAT2-SH2 interacts with IFNAR2, however, researchers are not in agreement if this connection is, or is not required for IFN α / β -related signal transduction (X. Li et al. 1997)(Nguyen et al. 2002). Some studies showed that STAT2 serves as an adaptor for STAT1 to IFNAR2 where STAT1 is being activated by phosphorylation, thus making STAT2-IFNAR2 connection pivotal for signalling cascade triggering (X. Li et al. 1997). In contrast, other studies did not provide evidence for STAT2-IFNAR2 binding requirement in IFN α -mediated signalling (Nguyen et al. 2002). Besides this, STAT2 helps STAT1 to interact with IRF9 for the ISGF3 complex formation (Tang et al. 2007). Nonetheless, STAT2 protein holds great importance in IFN Type-I signalling pathway, despite its inability to the direct DNA binding.

INTRODUCTION

Between the DBD and the SH2 the linker domain is located. As in case of other STATs, linker is responsible for the maintenance of the appropriate spatial conformation of the adjacent domains.

At the carboxyl end of STAT2, the TAD domain is located. The STAT2-TAD, apart from its transcriptional activation role, has the constantly active NES inside. This second NES, together with NLS of IRF9, ensures the STAT2/IRF9 heterodimer shuttling between the cytoplasm and the nucleus (Banninger and Reich 2004). The TAD domain has also been reported to bind the transcription coactivator p300/GBP (Bhattacharya et al. 1996), GCN5 (Paulson et al. 2002), as well as the MED14 enzyme (known also as DRIP150) which is one of the factors directing initiation of transcription by the RNA II Polymerase apparatus (Harper and Taatjes 2018)(Lau et al. 2003).

At the border of the SH2 and the TAD domains, the tyrosine 690 residue is situated, that is crucial for STAT2 activation. This amino acid undergoes phosphorylation as a consequence of binding of IFN Type-I to IFNAR and subsequent JAK1/TYK2 activation. Phosphorylation of the Y690 residue participates in homo- or heterodimerization of STAT2 with other STATs (e.g. STAT1 and STAT6) where cross-interaction of SH2 and Y-Tyr is essential (Kiu and Nicholson 2012)(Delgoffe and Vignali 2013).

The studies of Wang and colleagues (Y. Wang et al. 2021), showed that phosphorylation on threonine 404 residue located in STAT2 DBD domain is not only promoting changing anti- to parallel conformation of the STAT1/STAT2 heterodimer, but also increases the affinity of IGSF3 to the ISRE element of ISGs and expedites tyrosine phosphorylation of both STAT1 and STAT2 proteins. In T403A/T403A (equivalent of T404 in humans) mutant mice brain accumulation of the viral RNA was also observed, pointing to impaired virus clearance due to inability of inactive STAT1/STAT2 heterodimers to change conformation and trigger fast and robust antiviral response. However, this phosphorylation event seems to be important in case of a gene subset to which classical ISGs do not belong.

In 2013, Steen and colleagues (Steen et al. 2013) published the results of their studies on the role of STAT2 Ser287 phosphorylation. Contrasted to the serine residues of other STAT proteins, STAT2 Ser287 is the negative regulator of IFN Type-I antiviral effect. The point mutation of serine to alanine increased tested ISGs expression significantly and changed its profile to prolonged. Interestingly, S287A mutant cells exhibits prolonged profile of the STAT1 and STAT2 tyrosine phosphorylation in response to IFN α . Moreover, S287A-STAT2 mutant

cells are more protected from VSV infection than WTs. Conversely, the point mutation to aspartate, which is mimicking serine phosphorylation, diminished the IFN α -dependent ISGs expression and protection from viruses (Steen et al. 2013).

The role of STAT2 in carcinogenesis was described recently by Lee and colleagues (Lee et al. 2020). Researchers have found, that STAT2 interacts with the tumour suppressor FBXW7 which promotes the STAT2 destabilization and ubiquitination-mediated degradation in proteasomes. STAT2 protein levels were increased in melanoma and STAT2 knock-down impaired tumour cells proliferation. Thus, STAT2 functioned as the promoter of oncogenesis.

Additionally, the STAT2, as well as STAT1, role in multiple sclerosis (MS) was established by Manoochehrabadi and colleagues (Manoochehrabadi et al. 2019). Researchers have found that in MS patients *STAT2* expression was downregulated, while *STAT1* – upregulated, however, it is not clear if the expression changes are the cause or the result of the disease.

1.3.3. IRFs

The IRF family consists of nine members: IRF1, IRF2, IRF3, IRF4, IRF5, IRF6, IRF7, IRF8 and IRF9 (Samuel 2001). In humans, genes for these proteins are located on different chromosomes (Barnes, Lubyova, and Pitha 2002). Structurally, these proteins are homologous in the N-terminal region of 115 amino acid, where the DNA binding domain is located. The helix-turn-helix DBD has five conserved tryptophan-rich repeats (Paul, Tang, and Ng 2018). The more divergent carboxyl end is responsible for interactions within the IRF family as well as with other transcription factors. The C-terminus of IRFs can have, either an IRF-associated domain 1 (IAD1), or IAD2. IAD2 is specific for IRF1 and IRF2, while IAD1 is conserved in all of the remaining IRF family members (Zhao, Jiang, and Li 2015). In contrast to the DBD, the IAD is not as much conserved. This variability correlates with specificity of IRFs. Moreover, IAD imposes the transcriptional role of the complex formed by IRF and its partner and defines the nucleotide sequence adjacent to the core IRF-binding motif, that is recognized by the particular transcriptional complex (Yanai, Negishi, and Taniguchi 2012)(Paul, Tang, and Ng 2018).

IRFs, similar to STATs, are transcription factors that regulate the IFN-dependent immunological response (Samuel 2001). IRFs are also required during the differentiation

INTRODUCTION

immune cells such as myeloid, dendritic, natural killer (NK) as well as B and T-lymphocytes. Apart from this, they play a role in a multitude of metabolic processes, as well as apoptosis, and abnormalities in their expression were described as a cause of diseases such as hepatic steatosis, insulin resistance (Zhao, Jiang, and Li 2015), carcinogenesis (Lei et al. 2021)(de Oliveira et al. 2021)(Yuemaier et al. 2020) or multiple autoimmune syndromes such as rheumatoid arthritis (RA), systemic lupus erythematosus (SLE), inflammatory bowel disease (IBD), Sjogren's syndrome (SS) and systemic sclerosis (SSc) (Kaur et al. 2018)(Gallucci, Meka, and Gamero 2021). Also cardiovascular disorders (like atherosclerosis and hypertension) and neurological diseases (like multiple sclerosis (MS) or stroke) are connected to the function of IRFs (Zhao, Jiang, and Li 2015). A common feature of IRF DNA binding sites is possessing the consensus GAAA tandem sequence separated by 1-3 nitrogenous bases. However, IRF1 recognizes only one GAAA segment (Fujii et al. 1999). All IRFs recognize the same element, named as the IRF-E, that is represented by the sequence $G(A)AAA^{G/T}/C/GAAA^{G/T}/C$. Interestingly, the above described sequence is almost identical to the ISRE element $A/GNGAAANNGAAACT$ (Taniguchi et al. 2001). For this reason, IRFs regulate both, IFN production and ISG expression.

1.3.3.1. IRF9

IRF9 is crucial in IFN signalling, because of its unique interaction with STAT1 and STAT2, leading to ISGF3 formation. Similar to other IRFs, IRF9 protein is built of a DNA binding domain at the N-terminus and an IRF-associated domain at the carboxyl end, which are separated by a linker (Paul, Tang, and Ng 2018). The gene coding IRF9 is located on chromosome 14 and contains both, GAS and ISRE elements and its expression is regulated by ISGF3, as well as GAF complexes (Michalska et al. 2018). In case of the IFN Type-I signalling pathway, IRF9 plays an important role as part of the ISGF3 complex, where, in principle, it is responsible for the ISRE recognition and binding. It can also bind DNA in complex with the STAT2 homodimer (Bluyssen and Levy 1997)(Błaszczuk et al. 2015) and the STAT1 homodimer (Bluyssen, Durbin, and Levy 1996), similar to ISGF3 complex. Moreover, IRF9, as a component of ISGF3, that has an active nuclear localization signal (NLS) (built of two segments at positions 66-70 and 81-85, separated by 10 amino acids that provides flexibility), was thought to be crucial for ISGF3 nuclear translocation. It was observed to be present in both, nucleus and cytoplasm, independent of IFN-treatment (Samuel 2001). Even though, IRF9 is

IRF9

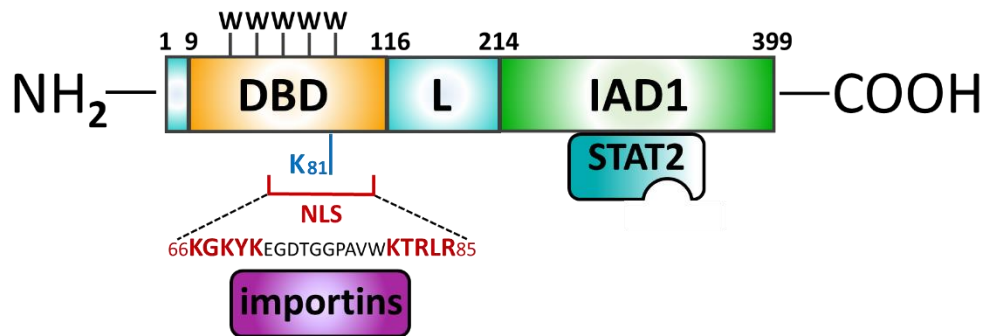


Figure 1.5 The IRF9 protein structure

Similar to other IRF family members, IRF9 consists of 2 domains and a linker between them. Closer to the N-terminus, the evolutionarily conserved DNA binding domain is located. In the DBD five tryptophan-rich repeats (W) can be found, that are necessary for interaction with DNA. In this domain is also located a bipartite nuclear localization signal (NLS) (at positions 66–70 and 81–85), which, via recognition by importins, provides IFN-stimulation-independent nuclear import of IRF9. The basic amino acids of IRF9's NLS are marked in red. Acetylation of lysine at position 81 (K81, marked in blue) is pivotal for both, DNA binding and ISGF3 formation. The second domain of IRF9 is the IRF-associated domain 1 (IAD1) which mediates the interaction with the coiled-coil (C-C) domain of STAT2 and STAT1 (Antonczyk et al. 2019)(Blaszczyk et al. 2016)(Paul, Tang, and Ng 2018)(Bluyssen, Durbin, and Levy 1996).

necessary for DNA binding, it requires STAT partner's TAD to drive transcription and antiviral response. It has been proven, that in the carboxyl terminus of IRF9 binding sites for STAT1 and STAT2 are located, the IRF9 C-terminus is crucial for transcriptional activity of the complexes that IRF9 forms. Accordingly, mice lacking *IRF9* have partially impaired IFN Type-I as well as Type-II signalling pathways (Kraus et al. 2003). IRF9 activity, unlike other IRFs, is not regulated by phosphorylation events (Paul, Tang, and Ng 2018). However, some studies suggested the role of constitutive DBD phosphorylation in IRF9 activity, as forced dephosphorylation abolished the ability of IRF9 to bind to the ISRE (Veals, Santa Maria, and Levy 1993). Moreover, acetylation of Lys81 is crucial for DNA binding and ISGF3 complex assembly upon IFN-mediated signalling (Tang et al. 2007).

IRF9 (not only as part of ISGF3) is also involved in homeostasis including: regulation of cell proliferation but also pathological conditions e.g., inflammation in the intestines, autoimmune diseases, carcinogenesis and cardiovascular disease (Paul, Tang, and Ng 2018)(Rauch et al. 2015). It was also observed that IRF9 functions as a mediator during hepatic

ischemia/reperfusion injury by diminishing expression of the *SIRT1* gene encoded SIRT1 deacetylase. The decreasing *SIRT1* expression leads to p53 acetylation enhancement. Thus, IRF9 indirectly mediates p-53-dependent hepatocytes apoptosis (P. X. Wang et al. 2015). The functionality of IRF9 as a negative regulator of deacetylase SIRT1 was also shown in studies of neointima formation as a consequence of vascular injury (S. M. Zhang et al. 2014), neuronal death (being a result of cerebral ischemic stroke) and cardiomyocyte death (following ischemia-reperfusion-directed myocardial injuries) (Yan Zhang et al. 2014). In contrary, the IRF9 protective effect has been proven in case of male mice, where low IRF9 levels in the liver correlated with obesity. In those mice, an impaired glucose metabolism, hepatic steatosis and inflammation were observed. Overexpression of IRF9, on the other hand, in obese mice reduced hepatic steatosis, inflammation and insulin resistance (X.-A. Wang et al. 2013). Similarly, Jiang and colleagues, provided evidence for the protective effect of IRF9 in the development of cardiac hypertrophy, both *in vitro* and *in vivo*. Furthermore, researchers indicated myocardin as a IRF9 target as myocardin TAD-IRF9 interactions drastically diminished transcriptional activity of this coactivator (Jiang et al. 2014).

1.3.3.2. IRF1

The *IRF1* gene is located on chromosome 5. Even though, IFN α and β gene activation was not reduced in mice with *IRF1* homozygous deletion, IRF1 plays an important role in IFN Type-II (Paun and Pitha 2007) and IFN Type-I signalling (Antonczyk et al. 2019). Moreover, experiments on *IRF1* K.O. mice showed involvement of the IRF1 protein in a broad range of processes e.g. NK cells development, production of IL-12 in macrophages, maturation of CD8+ T- and Th1-dependent responses, as well as MHC-I expression or apoptosis and in cell-cycle arrest in response to DNA damage (Paun and Pitha 2007)(Taniguchi et al. 2001). On the other hand, IRF1 in complex with IRF8, in general, represses the ISRE-dependent response (Paun and Pitha 2007). However, IRF1 has also been proven to directly regulate ISG expression by recognizing ISREs in ISG promoters alone or in cooperation with other IRFs (Lou et al. 2009).

IRF1 is a GAS-containing gene and its transcription is regulated by binding of the GAF complex in response to IFN Type-II, however, IRF1 expression is induced upon IFN Type-I treatment as well (Stewart et al. 2002)(Michalska et al. 2018). Accordingly, *IRF1* expression is severely impaired in U3C cells that are STAT1 K.O. overexpressing STAT2 (Michalska et al.

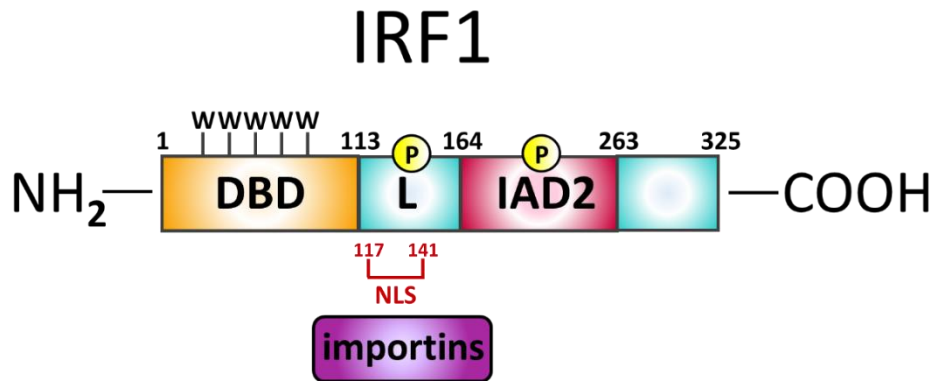


Figure 1.6 The IRF1 protein structure

IRF1, like other IRFs, consists of 2 domains, the DBD and the IAD, separated by the linker. At the N-terminus, the evolutionarily conserved DNA binding domain is located. The DBD contains five tryptophan-rich repeats (W) crucial for interactions with DNA. The Nuclear localization signal (NLS) recognized by importins, is located within the linker, at position 117-141. The IAD of IRF1 (and IRF2) is structurally distinct from those found in IRF3-9 and is therefore named IAD2. Its structure, as in case of the other IADs, dictates specificity of dimerization (Antonczyk et al. 2019)(Yanai, Negishi, and Taniguchi 2012)(Feng et al. 2021).

2018). It was observed, that IRF1 expression correlates with the STAT1 phosphorylation profile. The IRF1 levels are highly increased in the early stages of IFN Type-I and -II responses, and are sustained over time. IRF1 functions as a transcription factor that recognizes IRF-E as well as ISRE elements. Among IRF1 target genes, are *STAT1*, *STAT2*, *IRF9*, as well other ISGs. IRF1 expression is dependent on JAK-STAT signalling but independent of IFN production. Taken together, IRF1 provides functional overlap with ISGF3 (Schoggins et al. 2011) (Michalska et al. 2018).

IRF1 was described to interact with other proteins and transcription factors: IRFs (e.g. IRF2 and IRF8 together with PU.1), STATs (e.g. GAF complex) and NFκB (Antonczyk et al. 2019). Furthermore, in untreated 2fTGH and U3A overexpressing unphosphorylatable STAT1 mutant, the partially overlapping interferon consensus sequence 2 (ICS-2)/GAS elements in the *Low Molecular Mass Polypeptide 2 (LMP2)* gene are occupied by U-STAT1 and IRF1 in a cooperative manner (Chatterjee-Kishore et al. 2000).

1.3.4. The role of the ISGF3 complex in the canonical IFN α -dependent signalling pathway

The IFN α signalling pathway is the ancestral defence system against pathogens. In 2017, Shaw and colleagues (Shaw et al. 2017), performed multispecies comparison that have revealed a group of 62 ‘core’ ISGs, that are common for vertebrates, even for those species that are less phylogenetically related.

As mentioned above, the IFN-dependent signalling cascade starts after binding of IFN to a specific receptor. In case of the Type-I response, IFN α binding to IFNAR triggers activation of JAK1 and TYK2 by their cross-phosphorylation. Once activated, these kinases phosphorylate STAT1 and STAT2 that form a heterodimer (Y. Wang et al. 2021). Coil-coiled domains of STAT1/STAT2 interact with the 160 amino acid region at the N-terminus of the IRF9 protein thereby forming ISGF3. This complex is then translocated to the nucleus, where it recognizes the ISRE in ISG promoters (Wesoly, Szweykowska-Kulinska, and Bluysen 2007)(Veals, Santa Maria, and Levy 1993). It was proven that IRF9 alone is able to bind to DNA but its ISRE-binding affinity is much lower than that of ISGF3 (Ramana et al. 2007)(Kessler et al. 1990). In the canonical IFN Type-I-dependent response, IRF9 is responsible for ISRE binding, while STAT1 stabilizes the ISGF3 complex on DNA and STAT2 provides the transactivation domain (Bluysen and Levy 1997). To ensure a potent antiviral response, assembly of ISGF3 is extremely fast after IFN-receptor activation. ISGF3, that is attached to the DNA, was found in cells just after minutes upon IFN α treatment and the amount of this complex increases robustly and reaches maximum in just 15 minutes (Levy et al. 1989). The rapid formation of ISGF3 is possible due to the presence of pre-existing complexes in the cytoplasm of untreated cells. Unphosphorylated STAT1 (U-STAT1) was found to bind to U-STAT2 in the anti-parallel conformation, but nuclear translocation of this complex is impossible as NLS remains hidden and unrecognizable for importin- α 5. To be translocated to the nucleus, U-STAT1-U-STAT2 needs to be phosphorylated. Phosphorylation provides conformational changes, that allow to uncover NLS, thus plays a key role in IFN signalling (Kevin M. McBride et al. 2002). U-STAT2/IRF9 was detectable in the nucleus and the cytoplasm regardless the IFN α treatment (Martinez-Moczygemba et al. 1997) due to NES/NLS-dependent shuttling (Banninger and Reich 2004). The results of coimmunoprecipitation, obtained by Martinez-Moczygemba and colleagues (Martinez-Moczygemba et al. 1997) showed, that two types of complexes are formed: STAT1/STAT2 and STAT2/IRF9. Taken together, this suggests that ISGF3 formation may occur not, as it was thought previously, in cytoplasm, but on the ISRE sequence in the nucleus.

One possible mechanism, is that STAT2/IRF9, because of its ability to shuttle between the cytoplasm and the nucleus, is binding the DNA already in resting cells. Simultaneously, the STAT1/STAT2 complex stays in the cytoplasm as the NLS remains inactive. Then, after interferon Type-I stimulation, STAT1/STAT2 becomes phosphorylated and its conformation is being changed, what activates NLS. This allows translocation of this complex to the nucleus, where, due to interaction with STAT2/IRF9, formation of ISGF3 takes place. Hereby, U-STAT2/IRF9 functions as a flag of DNA sequence for STAT1/STAT2 complex. On the other hand, recent findings of Platanitis and colleagues (Platanitis et al. 2019), suggested that, in the mouse system, the most probable scenario is replacement of STAT2/IRF9 pre-connected with DNA with ISGF3. In resting cells STAT2/IRF9 binds to DNA, while upon IFN β -treatment a molecular switch between the STAT2/IRF9 and ISGF3 complexes occurs. However, in human cells this kind of switch has not been observed.

Additionally to the canonical ISGF3 complex, researchers have published evidence that unphosphorylated ISGF3 can exist and be functional in the context of gene expression regulation. This topic is discussed in more detail in the chapter 1.4.2.1.

1.3.5. Negative regulation of the IFN Type-I signalling pathway

Canonical IFN Type-I signalling pathway is activated very fast and robust engaging many cellular components as well as it triggers production of huge amounts of cyto- and chemokines. Prolonged state of induced immune response is detrimental to the host cells and the condition of pathological failure to inhibit IFN-dependent pathways activation leads to immunological disorders (such as Sjögren's syndrome, systemic lupus erythematosus, thyrotoxicosis, thyroiditis or pernicious anaemia) what could be observed in the patients after IFN-dependent cancer treatment (Malterer, Glass, and Newman 2014)(Ronnlblom, Alm, and Oberg 1991). That is why mechanisms to suppress an IFN-mediated response are essential.

Suppression mechanisms may be various: cellular or dependent on ISG activity. The first group involves endocytosis and liposomal degradation of IFN-receptors, while the second comprises activity of phosphatases that inactivate JAK-STAT family members and effect of PIAS family (protein inhibitors of activated STATs), However, these events do not operate independently and separately from each other (Malterer, Glass, and Newman 2014).

PIAS proteins, such as the SUMO (small ubiquitin-like modifier) E3-ligases (Ungureanu et al. 2005), are involved in SUMOylation that is based on covalent binding of

target protein to the SUMO and results in the ubiquitination-like process. Furthermore, PIASs may act in the SUMOylation-independent way by blocking connection of transcription factors to gene targets (Malterer, Glass, and Newman 2014). The existence of these two mechanisms have been already proven in case of the inhibition of STAT1 protein (Ungureanu et al. 2005)(Rogers, Horvath, and Matunis 2003).

To the group of ISG-connected suppressors belong the SOCS (suppressor of cytokine signalling) family and the USP18 (ubiquitin-specific peptidase 18) protein. SOCS blocks STAT1 activation by direct interactions with the phosphorylated tyrosine residue of both IFNAR receptor and receptor-related JAK proteins. Then, SOCSs drive receptor ubiquitin-dependent degradation (Malterer, Glass, and Newman 2014)(Ivashkiv and Donlin 2014).

USP18 is protein able to detach ISG15 molecule from its targets in process called deISGylation. USP18 is also binding to the IFNAR2 receptor subunit thus blocking JAK1 attachment. Moreover, USP18 promotes conformational changes in extracellular part of the IFNAR2 subunit, thus makes it unrecognizable for IFN α but not for β . Interestingly, the USP18 role is limited to IFN Type-I response (Malterer, Glass, and Newman 2014)(Ivashkiv and Donlin 2014)(Honke et al. 2016). Additionally, as mentioned before, ISG15 protein has been described as a negative regulator of IFN-dependent immune response since the MH1 ISG15 K.O. cell line displayed elevated and prolonged ISGs expression (Broering et al. 2010).

1.3.6. Prolonged ISGs expression

At the beginning, the IFN α signalling pathway was described as a very simple one. Now, after years of intensive studies, we know it is much more complex and integrates with other signalling pathways.

It was believed for years, that IFN-signalling pathways are triggered quickly and immune response depending on these molecules is transient in time. More and more evidence for that the IFN-mediated response is not extinguished after several hours, but stays prolonged, has been accumulated. For example, Cheon and colleagues, had shown that some ISGs such as *IFI27*, *OAS2*, or *MX1* display high expression up to three days after a single IFN β treatment (H. J. Cheon and Stark 2009)(H. Cheon et al. 2013). Similar data was provided by the team of Sung (Sung et al. 2015). Moreover, both teams observed the same ISGF3 components phosphorylation patterns, where pSTAT1 and pSTAT2 levels are decreasing while their

unphosphorylated forms are accumulating during the time of prolonged IFN treatment. The possible mechanism involved in prolonged ISGs expression will be discussed in the following chapters.

1.4. Non-canonical IFN-signalling pathways

1.4.1. Antiviral response in the absence of the STAT1 protein: the role of the STAT2/IRF9 complex.

The evolution of host-virus interactions is an arms race - who is the first to create the mechanisms to defeat the opponent. Viruses are mutating all the time to develop ways to bypass the host's immune response, so the host immune system has a variety of ISGF3-independent signalling pathways that provide protection for viruses that are trying to slip through antiviral barriers. The mechanisms that provide the antiviral abilities of the host cells are various. To mention only those associated with the interferon signalling pathway, we can distinguish:

- inhibition of JAK/STAT signalling by e.g. blockage of STAT phosphorylation, that is crucial for its activation,
- interfering with STAT dimerization,
- interactions of pathogen proteins with STATs and JAKs, that lead to their deactivation,
- blockage of ISGs expression or translation in general,
- prevention of viral RNA degradation (Beachboard and Horner 2020)(Alcami and Koszinowski 2000).

It was already shown in 1997 that STAT2 is able to form a stable homodimer in response to IFN α -mediated phosphorylation (Bluyssen and Levy 1997). This homodimer, in complex with IRF9, has active NLS/NES (Banninger and Reich 2004) and shuttles in and out the nucleus where it can bind to the ISRE elements triggering ISGs transcription. However, the affinity of the STAT2/IRF9-DNA connection is much lower in comparison to that of ISGF3, as STAT1 is the component that provides additional, stabilizing contacts with DNA (Bluyssen and Levy 1997). The STAT1 knock-out mice have been described to be unable to combat influenza virus infection due to the lack of Type-I and -II IFN signalling pathways (Durbin et al. 2000). However, genome-wide studies of Blaszczyk and colleagues (Blaszczyk et al. 2015) on STAT1 K.O. cells overexpressing STAT2 protein confirmed again that STAT2, when abundant, along

INTRODUCTION

with IRF9, drives expression of the subset of genes similar to ISGF3. Interestingly, the gene expression profiles driven by ISGF3 and STAT2/IRF9 differ from each other. While ISGF3-mediated an average gene expression profile is early and transient, STAT2/IRF9 triggers lower and prolonged response. Two possible mechanisms explaining this phenomenon have been proposed. One is connected to the up-regulation of the *SOCS1* gene whose expression is tightly correlated with the transient nature of IFN α -mediated response (described in chapter 1.3.5.). It was observed that expression of *SOCS1* was diminished in cells lacking STAT1 (Abdul-Sater et al. 2015)(Blaszczyk et al. 2015), thus the changed ISGs expression pattern, in that case, may be a result of prolonged phosphorylation kinetics of STAT2 protein. The second could be a result of the lower affinity of STAT2/IRF9 in comparison to ISGF3 (Bluyssen and Levy 1997).

Nevertheless, even though STAT2/IRF9 drives the distinct ISGs expression profile it is sufficient to combat vesicular stomatitis Indiana virus (VSV) and encephalomyocarditis virus (EMCV) infections in the absence of STAT1 (Blaszczyk et al. 2015). This phenomenon may be explained by the presence of a backup system (see the paragraph below) that provides protection of host cells from lysis by viruses capable of blocking STAT1. Other researchers also highlighted the role of STAT2 in protection from HCV, as the Huh7.5 STAT2 K.O. cells which exhibit abolished IFN α -related response, while in STAT1 K.O. it was only partially attenuated (Yamauchi et al. 2016). Is it also worth noting that the hybrid molecule of IRF9 and STAT2-TAD domain has been proved to be sufficient for triggering ISRE-dependent response and providing the viral protection (Kraus et al. 2003). STAT2/IRF9 was also observed to drive delayed ISG expression in STAT1 K.O. mice (Majoros et al. 2016).

Viruses that interact with the STAT1 protein may use several mechanisms. Few examples of specific STAT1-virus interactions are mentioned further. Extracellular HCV core protein has been established to deregulate IRF7 and STAT1 proteins expression, which leads to accumulation of unphosphorylated STAT1, thus blocking IFN Type-I signalling (Stone et al. 2014). Another example is protein eVP24 from Ebola virus that can impair translocation of P-STAT1 to the nucleus by efficient competition with this protein for binding to KPNA5 (Karyopherin Subunit Alpha 5) that is a member of the karyopherin alpha nuclear transporter family (Wei Xu et al. 2014). Moreover, Sendai viruses have been observed to directly interact with STAT1. From all four proteins of this virus, only SevC is responsible for interactions with STAT1, thereby suppressing antiviral state in the infected, as well as in the neighbouring cells.

Moreover, SevC bound with STAT1 also inhibits directing cells towards programmed cell death (Garcin et al. 2002). Similarly, rotaviral NSP1 protein has been proven to inhibit phosphorylation of STAT1, thus blocking the IFN-dependent response (Sen et al. 2014).

The mechanism protecting the host organism from viruses relying on STAT2-mediated STAT1-independent IFN Type-I signalling was also described in Dengue virus (Perry et al. 2011) and *Legionella pneumophila* infection (Abdul-Sater et al. 2015).

Possible mechanisms underlying the antiviral response in the absence of STAT1 are shown in the Figure 1.8.

1.4.2. The role of the unphosphorylated STAT-based complexes in the IFN α -driven response

1.4.2.1. U-ISGF3

Since the prolonged IFN Type-I-dependent ISG expression has been observed, researchers studied also the mechanisms of this process. One of the considered possibilities is

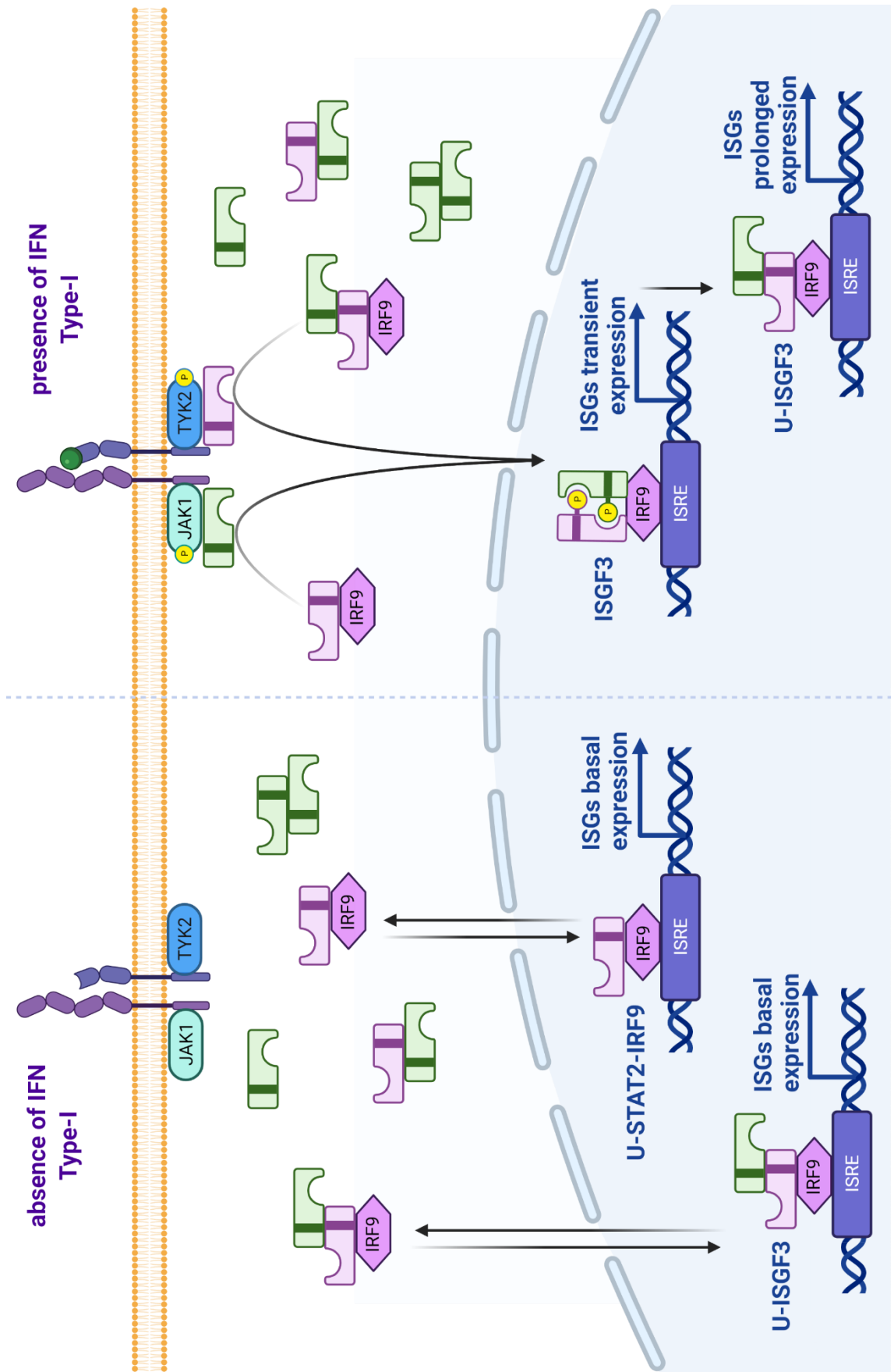
Figure 1.7 The role of ISGF3 components in constitutive and the IFN-dependent ISG expression

In the absence of IFN Type-I treatment (left panel) unphosphorylated STAT2 (pink) can complex with IRF9 (U-STAT2/IRF9) or U-STAT1 (green). U-STAT1 can exist in the cytoplasm as monomers or dimers, so theoretically does U-STAT2. Potentially, U-STAT1, U-STAT2 and IRF9 can form U-ISGF3. U-STAT2/IRF9 is able to shuttle between the cytoplasm and the nucleus. It can bind the ISRE to drive low, basal ISG expression. It can also mark the ISRE for ISGF3 that is formed upon IFN treatment (right panel). Hypothetically, U-ISGF3, alike U-STAT2/IRF9, is also shuttling between the cytoplasm and the nucleus where it can drive constitutive ISG expression. In contrast, both, U-STAT1 monomers and U-STAT1/U-STAT2 dimers, cannot be translocated to the nucleus.

Upon IFN treatment (right panel) different scenarios of ISGF3 formation can be proposed. The U-STAT2/IRF9 and phosphorylated STAT1/STAT2 complexes can be independently translocated to the nucleus, where they form ISGF3 directly on the DNA. On the contrary, ISGF3 could be assembled in the cytoplasm where, on the IFNAR receptor, U-STAT2/IRF9 undergoes phosphorylation and recruits P-STAT1.

The first, rapid IFN Type-I-dependent response is mediated by ISGF3. Increased levels of STAT1, STAT2 and IRF9 and limited phosphorylation could then result in formation of U-ISGF3, that might regulate prolonged ISG expression (Błaszczuk et al. 2016). Possibly, the ISGF3 and U-ISGF3 can cooperate in triggering antiviral response.

(Figure on the next page)



the role of an ISGF3-like complex consisting of the unphosphorylated STAT1 and STAT2 together with IRF9.

The role of this U-ISGF3 complex has been firstly described by Cheon and colleagues in 2013 (H. Cheon et al. 2013) but as early as in 2009 this team suggested U-STAT1 is responsible for prolonging expression of the majority of ISGs regulated also by IFNs (H. J. Cheon and Stark 2009) (Figure 1.7, right panel). Moreover, besides its antiviral role, U-ISGF3 has been proven to participate in maintaining protection from a DNA damage (H. Cheon et al. 2013). More recent data of Sung (Sung et al. 2015), showed that hepatitis C virus infection engages IFN β and λ , but not α , signalling pathways and first phase of response is classic, ISGF3-dependent. However, accumulation of native forms of STAT1 and STAT2, as well as IRF9, leads to formation of U-ISGF3 that regulates prolonged ISGs expression (Figure 1.7, right panel). Interestingly, these two complexes recognize the distinct ISRE sequences and trigger expression of different gene subsets (Sung et al. 2015).

1.4.2.2. U-STAT2/IRF9

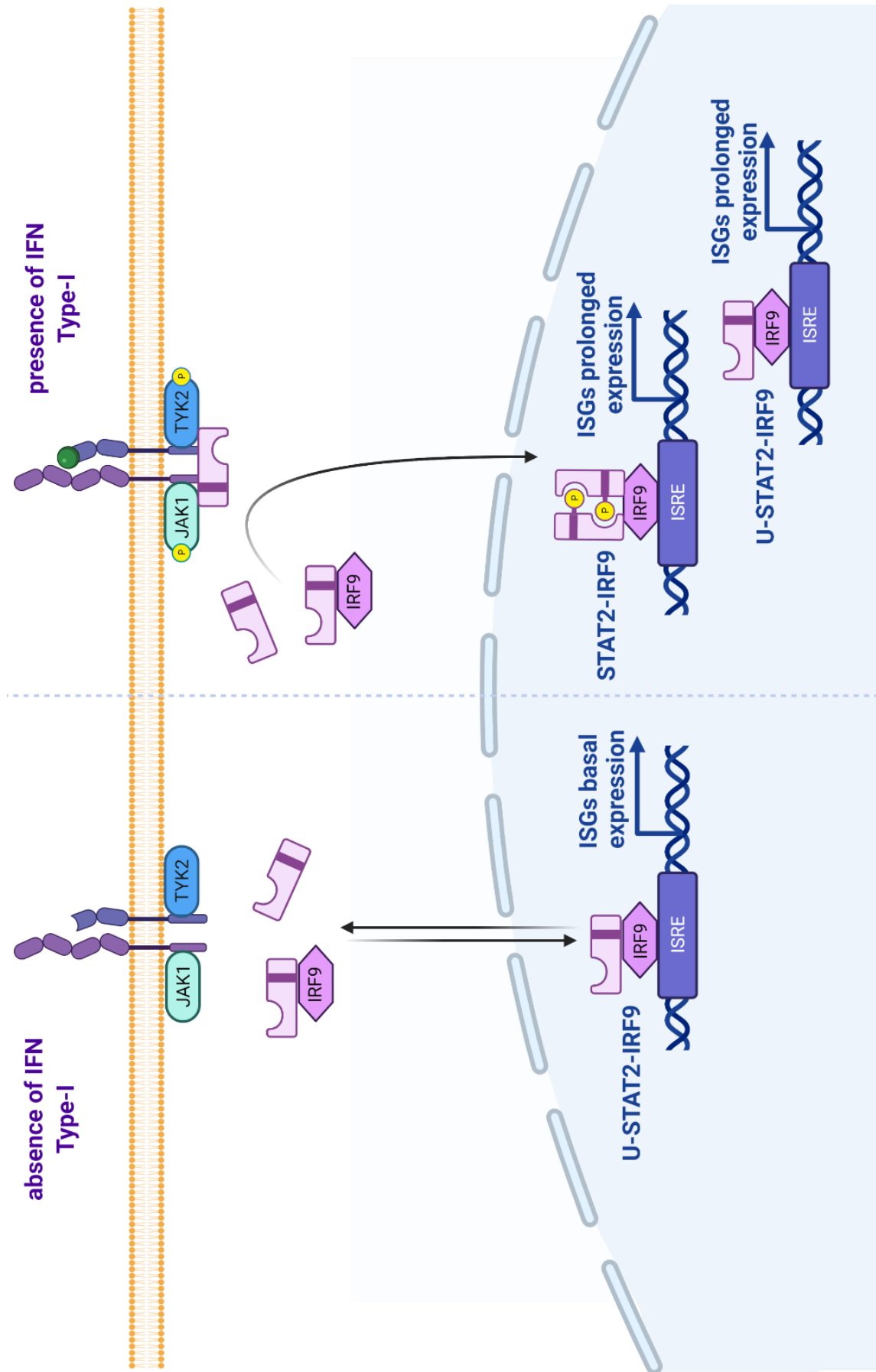
STAT2 was reported to form the complex with IRF9 constitutively in the absence of IFN-signalling (Lau, Parisien, and Horvath 2000) (Figure 1.8, right panel) and these proteins interact with each other with high affinity via region 133-315 aa of C-C domain (STAT2) and region 182-385 aa of IAD (IRF9). Regarding the structure of domains, the members of the STAT and IRF families are evolutionarily conserved, however, regions that are involved in

Figure 1.8 The role of ISGF3 components in constitutive and the IFN-dependent ISG expression in the absence of STAT1

In untreated STAT1-deficient cells (left panel) unphosphorylated STAT2 (U-STAT2; pink) exists as a monomer, dimer or can complex with IRF9 (U-STAT2/IRF9). This complex is able to shuttle between the cytoplasm and the nucleus, where it binds to the ISRE and ensures low, but sustained, ISG expression.

Upon IFN-treatment (right panel) U-STAT2 in complex with IRF9 undergoes phosphorylation and recruits another STAT2. Alternatively, the active, phosphorylated STAT2/IRF9 complex is then translocated to the nucleus, where it recognizes the ISRE in ISG promoters. Both, U-STAT2/IRF9 and its phosphorylated form, mediate prolonged ISG expression. The affinity of STAT2/IRF9 to DNA, compared to ISGF3, is lower, thus triggering of ISG expression requires STAT2 and IRF9 abundance (Blaszczyk et al. 2016).

(Figure on the next page)



cross-interactions of STAT2 and IRF9, enable only this specific contact. Furthermore, studies proved that these regions are essential for ISGF3 functionality (Rengachari et al. 2018) (Figure 1.4 and 1.5).

One role for U-STAT2/IRF9 was already proposed by Martinez-Moczygemba in 1997 (Martinez-Moczygemba et al. 1997). U-STAT2/IRF9 was described in her studies as being an indicator of ISRE elements for phosphorylated STAT1/STAT2 complexes translocated to the nucleus after interferon Type-I stimulation.

Moreover, evidence is accumulating that U-STAT2/IRF9 may be involved in antiviral gene expression regulation in the absence or presence of IFN α treatment, however the details of this complex formation still needs to be studied. U-STAT2/IRF9 has been proposed to have a role in triggering transcription of retinoic acid-induced G (*RIG-G*) gene (Lou et al. 2009). Researchers showed, that the unphosphorylatable STAT2 Y690F mutant, together with IRF9, was able to induce prolonged *RIG-G* expression. However, also IRF1 is involved in *RIG-G* expression regulation in both, U-STAT2/IRF9-dependent and -independent manner.

1.4.3. The role of the unphosphorylated STAT-based complexes in the basal ISGs expression regulation

The IFN signalling pathways are triggered extremely fast. To ensure this rapid response the different STAT and IRF-based complexes are present in the cell before IFN appearance (Figure 1.7 and 1.8, left panels). It has been already known, that unphosphorylated STAT1 and STAT2 are present in the cytoplasm of untreated cells in the anti-parallel conformation. Then, after phosphorylation, their NLSs become active and pSTAT1 and pSTAT2 can be recognized by importin- α . Both, U-STAT2 together with IRF9, are detectable in the nucleus and the cytoplasm as this complex has active NES/NLS signals (Kevin M. McBride et al. 2002)(Banninger and Reich 2004)(Martinez-Moczygemba et al. 1997). U-STAT1 alone has inactive NLS and is not recognized by importin- α , however, the unphosphorylatable Y701F STAT1 mutant was observed to be present in the nucleus. This transport was suggested to involve the interaction with IRF1 (Chatterjee-Kishore et al. 2000) which was mentioned in previous chapter, as well as by direct binding of U-STAT1 to nuclear pore complexes (Reich 2013). In 2011, U-STAT2 was also observed to bind to ISG promoters in ChIP-chip experiments performed by Testoni and colleagues (Testoni et al. 2011).

The role of U-ISGF3 complex in basal ISG expression regulation was highlighted by Wang *et al.* in 2017 (W. Wang et al. 2017). Researchers provide evidence for independency of constitutive ISG expression from upstream JAK-STAT signalling elements by using JAK1 or IFNAR1 deficient cell lines, as well as JAK Inhibitor I. In 2017, Wang and colleagues, provide evidence that together, STAT1, STAT2 and IRF9, are necessary for basal expression of ISGs, therefore for inhibition of HCV and HEV replication. shRNA-mediated knock-out of one of the components of ISGF3 diminishes ISG expression and increases viral replication in each case, while overexpression of STAT1, STAT2 or IRF9 does not change neither ISG expression, nor antiviral abilities. Based on this, researchers hypothesise that these proteins function as U-ISGF3. They also observed, that U-ISGF3 drives ISG expression without IFN stimulation or even when upstream IFN-signalling elements were excluded (W. Wang et al. 2017) (Figure 1.7, left panel).

Together, these findings demonstrated the complexity of mechanisms involved in the basal response of the host cells to fight with viral invasion (Figure 1.7 and 1.8, left panels).

1.5. Genome-wide studies of the IFN Type-I signalling pathway

Studies on IFN α response were conducted since the beginning of the '80 (Samuel and Knutson 1982). The first element described was the ISRE and the studies of IFN α -mediated stimulation were restricted to single genes containing this element due to technical limitations. The XXI century brought capability to extend studies of ISGs expression to a larger scale. Firstly, microarray experiments were performed in order to understand the global transcription effects of IFN α (Geiss et al. 2003). However, microarrays were restricted only to known genomic regions. Next Generation Sequencing (NGS), which was ameliorated for last 15 years, gives opportunity for discovering the exact sequence of whole genome. Besides RNA-Seq, also studies on interaction of transcription factors with DNA became easier and faster since the chromatin-immunoprecipitation methods were combined with sequencing. ChIP-Seq allows to explore the binding of TFs across whole chromosomes and, later, also genome-wide. However, the integrative studies, connecting the global transcription profiles of IFN α -mediated signalling and genome-wide binding of STAT1, STAT2 and IRF9 still need to be conducted.

1.5.1. IFN Type-I dependent

The global transcription effect of IFN α has been characterized firstly with the use of microarray experiments (Geiss et al. 2003), then via NGS, and the results of this types of studies are still accumulating rapidly. In addition to the expression studies, genome-wide approaches based on chromatin immunoprecipitation (such as ChIP-chip and ChIP-Seq) have been conducted. For instance, Hartman et. all (Hartman et al. 2005), using ChIP samples and DNA microarrays containing loci from the 22nd chromosome, identified the binding profiles of STAT1 and STAT2 after IFN α and γ treatment to this genomic region, that is known to comprise many ISGs. Indeed, binding of a transcription factors to ISGs was confirmed, however, new IFN α -mediated non-conserved STAT1 binding sites were also identified. Moreover, the STAT1 binding strongly correlated with that of STAT2. Interestingly, some sites were bound by STAT2, but not STAT1, which points to the greater complexity of STAT proteins binding to their targets in response to IFN.

The data received from studies involving whole-genome approaches are now deposited online in open-access databases and accessible for scientists around the world. For instance, within the Encyclopaedia of DNA Elements project (ENCODE Project Consortium, 2012) the data from ChIP-Seq of K562 cell line treated with both, IFN α and γ , is deposited. For preparing these experiments, antibodies against STAT1, STAT2, as well as IRF1, were used. Based on analysis of this data, Michalska and colleagues (Michalska et al. 2018), showed known, as well as new, binding sites for these TFs. Interestingly, the researchers described pools of genes that contain GAS, ISRE or both. The first group, represented by *ISGF15*, *MX1* or *IFIT3*, contains solely the ISRE and the ISGF3 components is binding to their promoters in response to IFN Type-I and IRF1 in response to IFN Type-I and -II. Expression of the second group, represented by GAS-only genes like: *IRF1*, *ICAM1* and *SOCS3*, is occupied by GAF and GAF-like pSTAT1-pSTAT2 heterodimer. Finally, there are also genes (e.g. *SOCS1*, *AIM2*, *BST2*, *IFI35*, as well as *STAT1*, *STAT2* and *IRF9* themselves), containing both, ISRE and GAS. The expression of these genes is triggered by cooperation of ISGF3, GAF and IRF1 binding in response to both, IFN Type-I and -II. Another available online data base is the ArrayExpress database, where ChIP-Seq data from experiments of Wienerroither and colleagues (Wienerroither et al. 2015) is deposited. They focused on searching of genes co-regulated by ISGF3 and NF- κ B in bone marrow-derived macrophages (BMDM) treated with IFN β , heat-killed *Listeria monocytogenes* or both. This studies showed the cooperation of the NF- κ B

and ISGF3-mediated signalling pathways in regulating of the response to *L. monocytogenes*. First step is promoter priming by NF- κ B and then the core mediator for Pol II binds what is promoted by ISGF3.

The integrative studies that are connecting IFN-dependent gene expression profiles with whole-genome binding of ISGF3 components are, however, still few. One, published by Platanitis et al. (Platanitis et al. 2019), showed binding of STAT1, STAT2 and IRF9 to the majority of known ISGs in mouse BMDMs, mouse embryonic fibroblasts (MEFs) and human monocytes THP-1. This study showed also that in the mouse system basal ISG expression is regulated by the STAT2/IRF9 complex, which is replaced by ISGF3 upon IFN β -treatment.

As mentioned in chapter 1.3.4, Martinez-Moczygemba and colleagues (Martinez-Moczygemba et al. 1997) provided evidence of the STAT2/IRF9 complex presence on the DNA already in the resting cells due to the active NLS-NES presence (Banninger and Reich 2004). This U-STAT2/IRF9/DNA interactions may take part in basal ISG expression regulation (Blaszczyk et al. 2016).

1.5.2. IFN Type-I independent

The binding of ISGF3 components to ISGs promoters after IFN stimulation is a phenomenon quite well described in the literature. The role of these proteins, however, is now extensively studied under IFN α -independent conditions. In 2011, Testoni et al, (Testoni et al. 2011) published very interesting results of ChIP-chip experiments using antibodies against STAT2 and pSTAT2 where they showed that in human hepatocytes U-STAT2 was binding to 62% of target genes in the absence of IFN treatment, with the known ISGs such as IFI6 or MX1 among them. This observation is in agreement with one of the hypotheses concerning ISGF3 formation, where the STAT2/IRF9 heterodimer is present on the DNA already in unstimulated cells, and marking gene promoters for STAT1/STAT2 recruitment to form ISGF3. Another experiment, that showed binding of U-STAT2 to DNA in the absence of IFN-stimulation, was provided by Platanitis et al. (Platanitis et al. 2019). In mice BMDM and MEFs, U-STAT2 was observed to maintain the low basal expression of ISGs in complex with IRF9, but not with STAT1. After IFN β stimulation STAT2/IRF9 is replaced by ISGF3 in the process called by researchers as “molecular switch”. Moreover, investigators obtained different gene subsets

regulated by U-STAT2/IRF9 or ISGF3 in resting cells. This phenomenon is, however, restricted to the mouse system as the STAT2/IRF9 / ISGF3 molecular switch was not observed in human THP-1 monocytes (Platanitis et al. 2019).

1.6. The regulation of *STAT1*, *STAT2*, *IRF9* and *IRF1* gene expression – the positive feedback loop model

Due to the constant exposure to pathogens host cells are prepared for a quick response to this invasion, which means basal ISG expression must be assured (Randall and Goodbourn 2008). The exact mechanisms, that are responsible for this quick antipathogen response, as well as the maintenance of the IFN α response over time and its phosphorylation dependence, has been intensively investigated recently (Figure 1.7 and 1.8). One of the proposed mechanism, that ensure basal *STAT* and *IRF* expression involves unphosphorylated STAT1 and STAT2, that have been observed to shuttle between the cytoplasm and the nucleus in complex with IRF9 in various cell types (Banninger and Reich 2004)(Meyer and Vinkemeier 2004). The U-ISGF3 role in antiviral response was suggested by Wang and colleagues, as in the absence of IFNs,

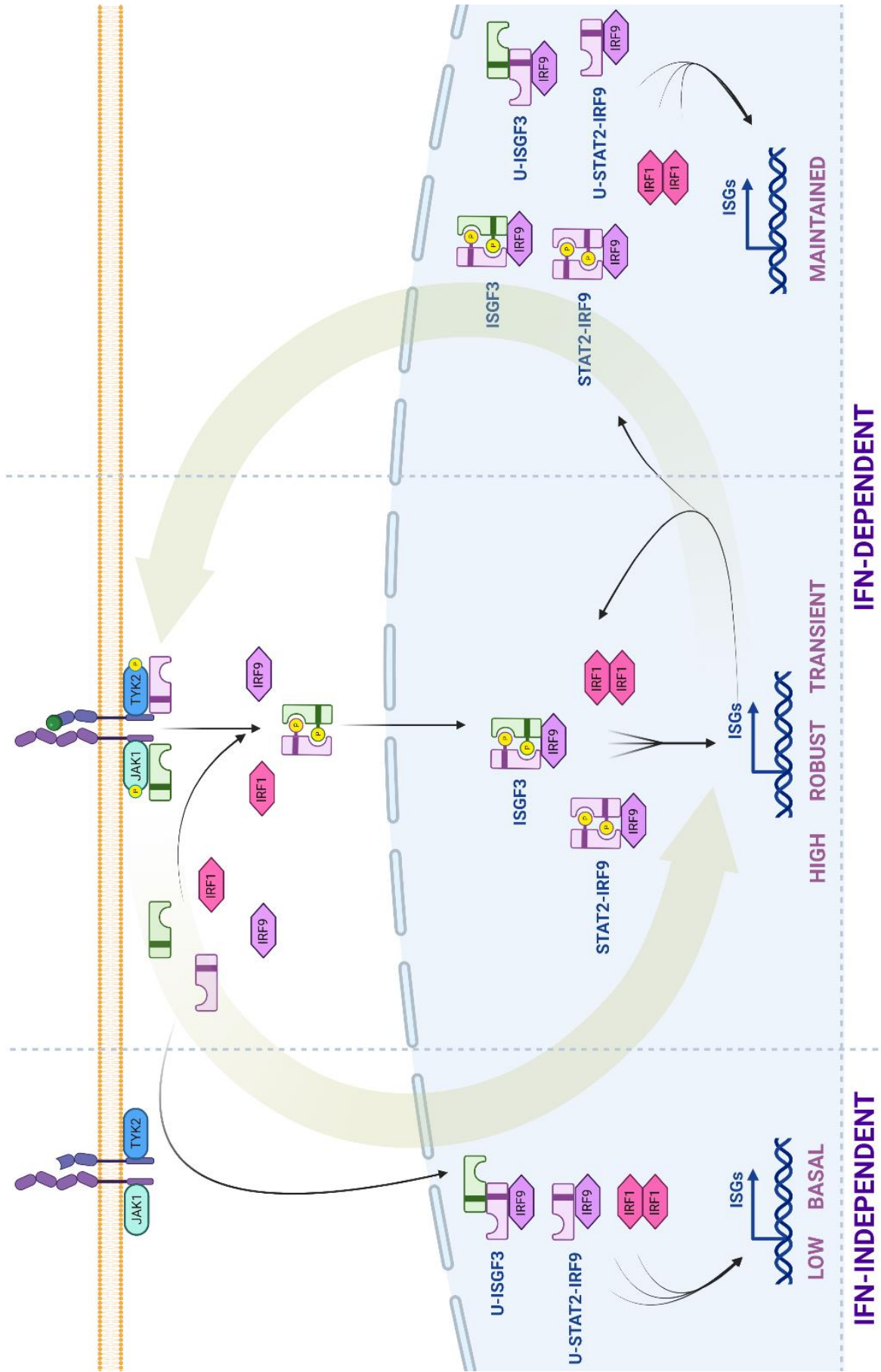
Figure 1.9 The positive feedback loop model

In untreated cells the basal ISG expression is sustained at the low level. Some of these genes encode transcription factors (like STATs and IRFs), that in their unphosphorylated forms can build complexes (U-ISGF3, U-STAT2/IRF9 and the IRF1 homodimer), thus regulate the constitutive ISG expression.

Upon IFN treatment, the IFNAR-connected JAK1 and TYK2 kinases phosphorylated each other, that causes the STAT proteins recruitment to the receptor, where they undergo phosphorylation. The phosphorylated complexes (ISGF3, STAT2/IRF9) are then able to translocate to the nucleus, where recognize the ISRE in promoters of antiviral genes and trigger their robust but transient expression. This leads to accumulation of newly synthesized STAT1, STAT2, IRF1 and IRF9 in the cytoplasm, which can form the mentioned above unphosphorylated complexes. When the level of phosphorylated forms is decreasing, U-ISGF3 and U-STAT2/IRF9, can support or take over the role of ISGF3 and STAT2/IRF9 in prolonging IGS expression at the certain level.

Also IRF1 plays an important role in the positive feedback loop, that regulate ISG expression. IRF1 can bind to ISRE in the promoters of ISGs, both in untreated and IFN Type-I-stimulated conditions, and together with other factors can modulate the antiviral response (Michalska et al. 2018).

(Figure on the next page)



INTRODUCTION

STAT1, STAT2, as well as IRF9, were observed in the nucleus and cells were resistant to HIV or HCV infection (W. Wang et al. 2017). Similarly, U-STAT2/IRF9 drives constitutive ISG expression that decreases susceptibility of cells overexpressing *STAT2* to VSV infection (Blaszczyk et al. 2015). U-ISGF3 was also proposed to be responsible for prolonging the ISG expression initially triggered by IFN β , to maintain long lasting antiviral protection (H. Cheon et al. 2013). In mouse model, by performing ChIP-Seq experiments and transcriptome analysis, researchers selected group of ISGs which basal expression is controlled by STAT2/IRF9 complex. This mechanism is independent of IFN Type-I presence. On the other hand, IFN appearance leads to the formation of ISGF3 complex that switches with STAT2/IRF9 to regulate ISG expression. However, in human model this phenomenon was not observed (Platanitis et al. 2019).

Interestingly, also the IRF1 protein seems to have a significant role in effective antiviral response. This unique antiviral protection is independent of IFN-stimulation but dependent on JAK-STAT signalling and it overlaps with these pathways triggered by IFNs (Schoggins et al. 2011). Surprisingly, *IRF1* gene promoter is bound by STAT1 and STAT2 upon IFN α treatment (Michalska et al. 2018) even though IRF1 is known to be GAS-containing gene, therefore the target for GAF complex, formed in response to IFN γ . Moreover, *STAT1*, *STAT2* and *IRF9* belong to the ISGs that are targets of IRF1 (Schoggins et al. 2011).

Together, all of these data together allowed to propose a positive feedback loop model that regulates antiviral response (Figure 1.9). The basal ISG expression is provided by the unphosphorylated STAT-based complexes and ensures immediate antiviral response. After pathogen detection, phosphorylated STAT-based complexes are getting involved and ISG expression is significantly enhanced. Newly synthesized STATs and IRFs are accumulated that boost the following response. Then, the balance shifts again toward unphosphorylated forms of STATs that allows to maintain long-term antiviral protection (Michalska et al. 2018; Figure “positive feedback loop”). This long-lasting response, dependent on lower, but sustained ISGs expression, provides protection that unlike the strong and fast canonical one, does not debilitate the host organism.

All in all, these findings point to complexity of the IFN-dependent responses and the exact role of phosphorylation status in antiviral protection need still to be discovered. In these studies we used genome-wide approaches such as ChIP-Seq and RNA-Seq to address the question of

the necessity of phosphorylation event in regulation of basal, as well as prolonged ISG expression.

Similar to IFNs themselves, which expression is amplified in the response to the IFN-mediated IRF7 production, positive feedback loop occurs also in case of STAT1, STAT2 and IRF9 proteins. ISGF3-components are ISRE and GAS containing ISGs and their expression is reinforced by the ISGF3 and GAF activity (Michalska et al. 2018). Their expression is regulated by all IFN types but IRF9, in contrast to STAT1 and STAT2, targets ISRE, but not GAS.

However, many issues still remain unclear. What are the exact mechanisms underlying the basal and IFN Type-I-dependent ISG expression? What is the role of phosphorylation in these processes? Does U-ISGF3 have a role in mediating basal and/or prolonged ISG expression under wild type conditions? Does pSTAT2/IRF9 function also under wild type conditions or is it restricted to STAT1-deficient cells? If it is – how its function overlaps with this of ISGF3? Finally, how different ISGF3 components-based complexes integrate in IFN Type-I signalling to provide effective antiviral responses?

1.7. Interferon stimulated genes

Generally, ISGs are the genes which expression depends on the IFN signalling pathways. However, among this large group, containing more than 300 genes, some of them has no antiviral activity. For instance, there are genes belonging to ISGs, that are involved in apoptosis, pathogen recognition processes or cell signalling (Shaw et al. 2017). Comparatively only few ISG products have direct antiviral role. Among them, ISG15 (IFN-stimulated protein of 15 kDa), GTPase MX1 (myxovirus resistance 1), RNaseL (ribonuclease L), PKR (protein kinase R) (Sadler and Williams 2008), ISG20 (IFN-stimulated exonuclease gene 20 protein) and IFIT (interferon-induced protein with tetratricopeptide repeats) family members (Schoggins 2014) are the examples.

ISG15 is inducible not only by IFN Type-I molecules, but also by pathogen-origin stimuli, such as LPS, as well as genotoxic stress or retinoic acid (Perng and Lenschow 2018). By interactions with more than 150 proteins in the process known as a ISGylation, ISG15 takes part in inhibition of viral replication. For example, ISGylation ensures ability to combat viral infection by modification of non-structural protein 1 (NS1) of Influenza A virus (IAV), protease

INTRODUCTION

2 A (2APro) from Coxsackievirus B3, nucleoprotein (NP) of Infectious bronchitis virus (IBV) or capsid protein L1 from Human papilloma virus (HPV) (Perng and Lenschow 2018). Among the targets of ISG15, there are also JAK1, STAT1 and some PRRs such as RIG-I, RNaseL, MX1 and PKR. ISG15 is also known to increase IFN β expression by protection of IRF3 from virus-mediated degradation (Lu et al. 2006). Moreover, ISG15 functions as enzyme modulator. For example, ISGylation rises affinity of eukaryotic translation initiation factor 4E family member 2 (EIF4E2) protein to 5' cap of mRNAs and increases NF- κ B signalling pathway by association with protein phosphatase 1B (PPM1B) which results in its inactivation (Sadler and Williams 2008). ISG15 was found to induce NK cells proliferation, dendritic cells maturation and to stimulate pro-inflammatory cytokines secretion by macrophages and INF γ production by NK or T-cells (Perng and Lenschow 2018). Interestingly, ISG15 works also as a negative regulator of the IFN-signalling pathway, since knocking down of this protein results in significant increase and prolongation of ISGs expression (Broering et al. 2010).

MX1, similarly to the other members of MX family, has GTPase activity due to possessing the large GTPase domain located on its N-terminus. Besides, it contains the central interacting domain (CID) and the C-terminal leucine zipper (LZ) involved in recognition of the viral elements, mostly the viral nucleocapsid-like structures. MX proteins are located near to the smooth ER, where they can screen contents of exocytic vesicles in search of viral fragments, thus rapidly blocking the multiplication of viruses (Sadler and Williams 2008)(Kochs and Haller 1999). Furthermore, MX1 binds to the PB2 polymerase of influenza virus causing impediment in viral transcription (Sadler and Williams 2008).

Another example of ISGs with direct antiviral function is RNaseL and one of OAS (2'-5' oligoadenylate synthetases) proteins duo. Transcription of these proteins is, in contrast to MXs and ISG15, low but constant (Sadler and Williams 2008). OAS proteins, by production of 2'-5' oligomers of adenosine activate latent form of RNaseL. In turn, this enzyme mediates degradation of the various RNA forms (Rebouillat and Hovanessian 1999). However, besides ability to arrest transcription globally, RNaseL also induces apoptosis in infected cells (Silverman 2007). As 2'-5' oligomers of adenosine are unstable, the choice of viral-origin RNA over host RNAs is favoured and depends on OAS synthetase activity in the neighbourhood (Goodbourn, Didcock, and Randall 2000). Then, degraded viral RNA leads to induction of the IFN Type-I response by stimulating cytoplasmic PRRs such as RIG-I and MDA5 (Sadler and Williams 2008).

INTRODUCTION

The ISG20 antiviral activity is also based on viral nucleic acids decay, since it causes degradation of both, ssRNA and DNA. In the contrary to RNaseL, ISG20 activity is more specific, restricted to the viral, not host genetic material. Interestingly, ISG20 does not have any regulatory domains and its selectivity probably is dependent on interactions with co-factors e.g. the post-transcriptional N6-methyladenosine modification pathway may play a role in recruiting ISG20, therefore promote HBV RNA-degradation. Apart from this, ISG20 acts also indirectly by regulating expression of other ISGs, like IFIT1, but this function seems to be cell-specific (Emily Yang and Li 2020).

PKR, as ubiquitously expressed kinase, is able to phosphorylate eukaryotic initiation factor-2 α (eIF2 α), that disrupts formation of eIF2-GTP-Met-tRNA(i) ternary complex and, as a consequence, can block translation. PKR, similarly to OAS and RNaseL, functions as PRR and is activated by presence of viral RNA. Its activation is related to interactions of double RNA-binding motifs located at the N-terminus with viral RNAs (Sadler and Williams 2008).

Another antiviral gene family is IFI. Among this family members, production of only IFI6 and IFI27 is induced by IFNs. Both proteins are conserved paralogues, however IFI6, but not IFI27, has been proven to effectively diminish replication of flaviviruses e.g. Yellow Fever virus, Zika virus, Denga virus and West Nile virus. Interestingly, IFI6 has no role in antiviral signalling mediation, but is acting as a direct effector. The mechanism of this protein function is connected to its location in ER, where *Flaviviridae* are replicated. IFI6 blocks forming of viral organelles, therefore protects neighbouring cells from invasion (Richardson et al. 2018).

Last but not least, IFIT family need to be mentioned. Over the years the antiviral role of these proteins was extensively studied. IFITs consist of IFIT1, IFIT2 and IFIT3 in humans and mice with additional human-specific IFIT5 protein. Their antiviral role comprise the recognition of RNAs containing 5'-triphosphates and lacking 2'-O methylation, as well as the inhibition of protein synthesis by interactions with eiF3C or eiF3E subunits of eIF-3 complex (Schoggins 2019).

2. HYPOTHESIS AND OBJECTIVES

Hypothesis

ISGF3, U-ISGF3, pSTAT2/IRF9 and U-STAT2/IRF9 cooperate in constitutive and IFN-dependent ISG transcriptional regulation and antiviral responses in a time, phosphorylation- and concentration-dependent manner.

Objectives

- To clarify the role of ISGF3 in time-dependent IFN α -activated transcriptional responses,
- To characterize in more details the role of STAT2/IRF9 in time-dependent IFN α -activated transcriptional responses in the absence of STAT1,
- To characterize the role of phosphorylation of ISGF3 and STAT2/IRF9 in time-dependent IFN α -activated transcriptional responses,
- To further characterize the basal ISG expression regulation under conditions with the abundance of ISGF3 components,
- To characterize the role of abundance of ISGF3 components (U-ISGF3) in the regulation of IFN-activated ISG expression.

3. MATERIAL AND METHODS

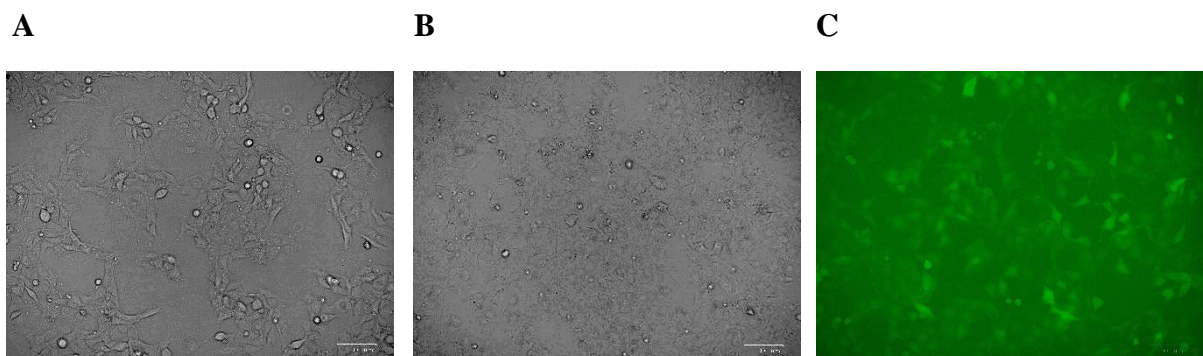
3.1. Cell lines

The human fibrosarcoma 2fTGH cell line, derived from the HPRT negative subline of HT-1080 (McKendry et al. 1991), and the STAT1-deficient U3C cell line, derived from high-frequency mutagenesis screening (Bonjardim 1998), were kind gifts from Dr Sandra Pellegrini (Institute Pasteur, Paris, France). The U3C cell lines, stably overexpressing combinations of ISGF3-components (ST2-U3C, ST2-IRF9-U3C, ST1-ST2-IRF9-U3C), were generated in our laboratory, as described below in subsection 3.2.

The human hepatocellular carcinoma cell line Huh7.5 and Huh7.5 ST1 K.O., that was generated using the CRISPR/Cas9 system (Yamauchi et al. 2016), were kind gifts from Prof. Kiyonao Sada (Department of Genome Science and Microbiology, University of Fukui, Fukui, Japan).

3.1.1. Cell culture

2fTGH, ST2-U3C, ST2-IRF9-U3C and ST1-ST2-IRF9-U3C were cultured in Dulbecco's modified Eagle's medium (DMEM) (Pracownia Chemii Ogólnej, Instytut Immunologii i Terapii Doświadczalnej PAN, Wrocław) supplemented with 10% fetal bovine serum (FBS) (ThermoFisher Scientific), 1% L-glutamine (BioWest) and 1% penicillin/streptomycin/amphotericin B (Sigma-Aldrich). Huh7.5 and Huh7.5 ST1 K.O. were maintained in DMEM supplemented with 10% FBS, 1% L-glutamine, 1% antibiotics solution, and 1% MEM NEAA (ThermoFisher Scientific). Both media are referred later in the manuscript as full culture media. Cell culture was carried out at 37°C and 5% CO₂ level on 10cm dishes and passaged when cell confluency reached ~90%.



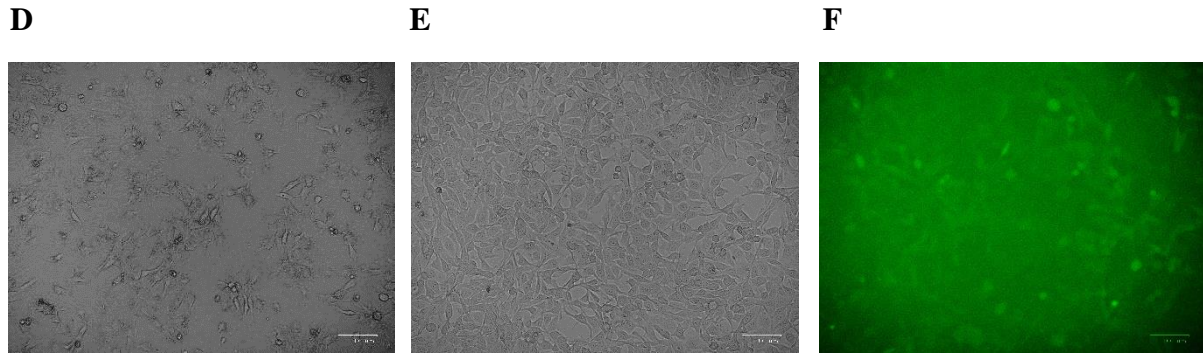


Figure 3.1 Cell lines in culture

2fTGH (A), Huh7.5 (B), ST2-U3C (C), Huh ST1 K.O (D), U3C (E) and ST1-IRF9-U3C (F) cell lines in culture. Pictures have been taken using Zoe Fluorescent Cell Imager under visible or fluorescent light

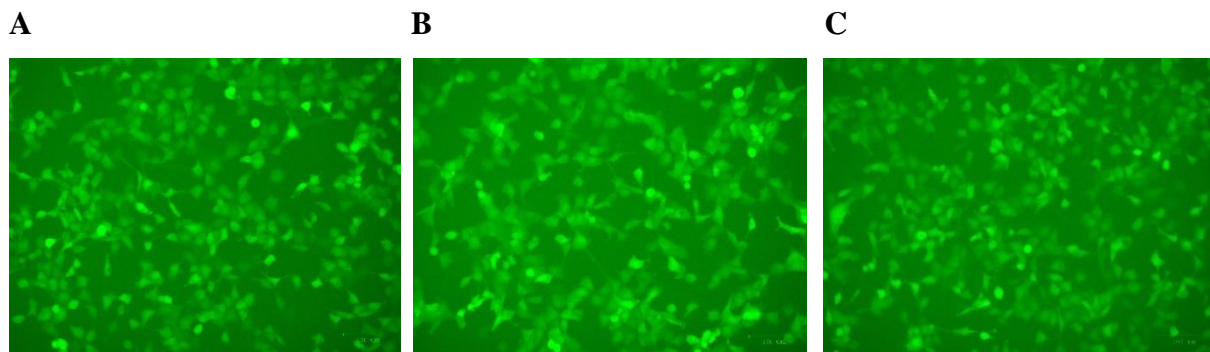


Figure 3.2 The fluorescence of three clones of the cell line stably overexpressing STAT1, STAT2 and IRF9

Clone 1, 2 and 3 shown in A, B and C, respectively. Pictures have been taken using Zoe Fluorescent Cell Imager

3.1.2. Interferon treatment

Depending on the type of experiment, cells were seeded in 6-well plate, 6cm, 10cm, or 15cm dishes in an appropriate volume of the proper type of full culture medium. The next day the full medium was replaced by the starving medium, containing FBS reduced to 1%. The human recombinant interferon alpha 2a (Merck) (referred later as interferon α or IFN α) was added for the indicated time point in the final concentration of 1000U/ml.

3.2. Generation of the cell lines with stable overexpression of ISGF3 components

The cells stably overexpressing different combinations of ISGF3 components were prepared using the X-tremeGENE™ HP DNA Transfection Reagent (Merck), according to the manufacturer’s protocol. Plasmid Migr1 (Figure 3.3.), carries the gene of interest sequence (prepared in our laboratory or provided by colleagues from the National Taiwan University in Taipei) as well as the gene for the Green Fluorescent Protein (GFP) and the pcDNA6/TR

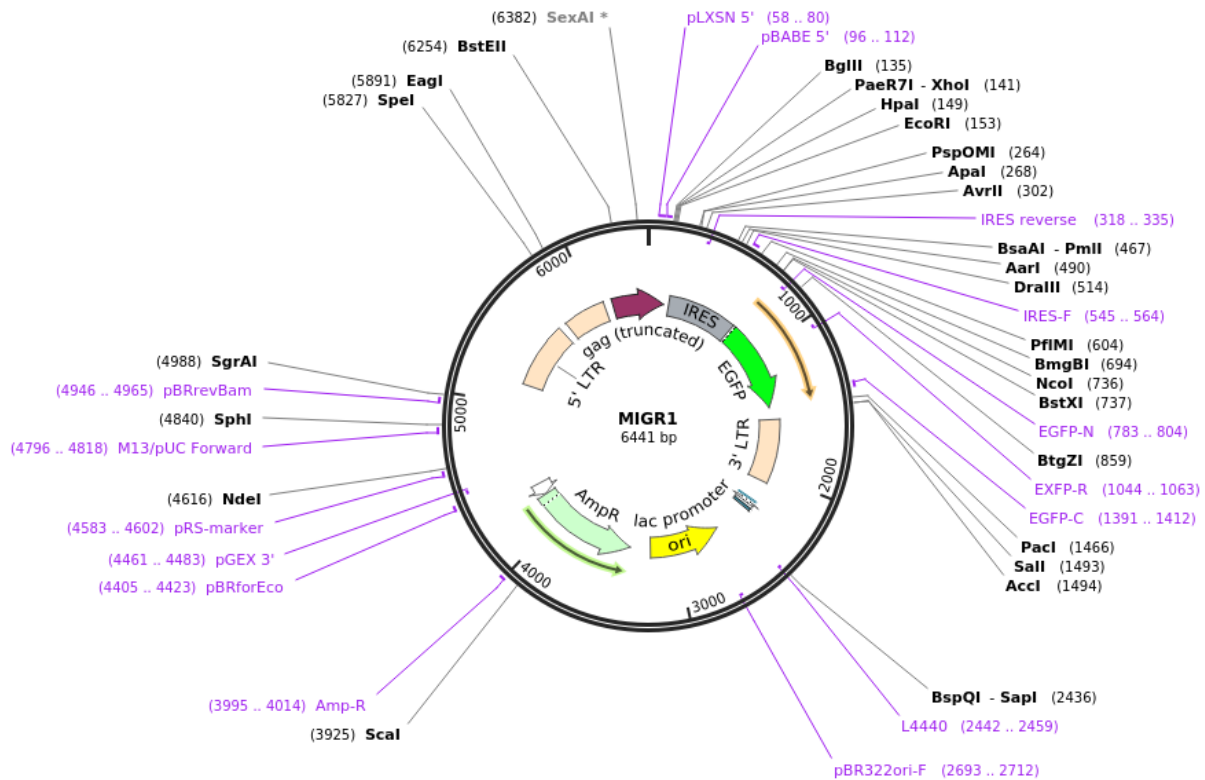


Figure 3.3 The construction of MIGR1 plasmid

The MIGR1 plasmid that was used to prepare the cell lines stably overexpressing different ISGF3 components. Inserts, as well as constructs, were prepared either by our colleagues from Taipei or in our lab.

Source: Addgen.org

(blasticidin-resistance; ThermoFisher Scientific) was mixed with X-tremeGENE reagent and then added to the appropriate confluent U3C in a dropwise manner. After ~24h incubation cells were selected using a selection medium containing blasticidin (5µg/ml; Merck) The individual cell line was then derived from one particular cell that was emitting green fluorescence from GFP.

3.3. RNA isolation and reverse transcription

Total RNA was extracted from the trypsin-treated (Pracownia Chemii Ogólnej, Instytut Immunologii i Terapii Doświadczalnej PAN, Wrocław) cell pellets washed with the pre-warmed PBS (ThermoFisher Scientific) using the GeneMATRIX Universal RNA Purification Kit (EurX), according to the protocol provided by the manufacturer with minor changes (incubation of liquid containing the alcohol precipitated RNA on the column for 15 minutes, elution with the pre-heated to 37°C H₂O and incubation 15 minutes at 37°C). The RNA concentration was estimated spectrophotometrically, using NanoDrop (ThermoFisher Scientific), or fluorescently, using Qubit™ 4 Fluorometer (ThermoFisher Scientific, Qubit RNA BR or HS Assay). The 500 ng of purified total RNA was then reverse-transcribed using ThermoFisher Scientific reagents and the C1000 Touch Thermal Cycler (Bio-Rad), according to the protocol shown step by step in the Table 3/1 on the next page.

Table 3/1. Conditions for reverse transcription reaction.

Step	Reagent	Volume (volume in total)	Incubation conditions	Purpose
1.	RNA (500 ng) + nuclease-free H ₂ O	8µl (8µl)	N/A	N/A
2.	DNase I (1 U) + DNase I reaction buffer (10x)	1µl + 1µl (10µl)	37°C, 30 min	Residual DNA digestion
3.	EDTA (50 mM)	1µl (11µl)	65°C, 10 min	DNase I reaction stopping
4.	Random hexamers (100 µM)	1µl (12µl)	65°C, 5 min	Complementary DNA (cDNA) synthesis
5.	Mix (NF H ₂ O, RT buffer, dNTP, RevertAid Reverse Transcriptase, RiboLock RNase Inhibitor)	9,75µl + 6µl + 0,75µl + 1µl + 0,5µl (30µl)	25°C, 10 min 42°C, 60 min 70°C, 10 min	

Obtained cDNA was then used to assess the gene expression level by qPCR.

3.4. qPCR method (Real-time PCR)

The quantitative PCR (qPCR, Real-time PCR) was performed to assess the gene expression. To conduct the experiments the Maxima SYBR Green/ROX qPCR Master Mix (ThermoFisher Scientific), specific primers for the gene of interest, and nuclease-free water was used in the volumes given in the Table 3/2 on the next page.

Table 3/2. qPCR sample preparation description.

Reagent	Volume
Maxima SYBR Green MM	5 μ l
NF H ₂ O	0,8 μ l
Forward + Reverse primer mix	1,2 μ l
cDNA (12,5x diluted)	3 μ l

The qPCR reactions were performed on the CFX Thermal Cycler System (Bio-Rad) or the Eco Real-Time PCR System (Illumina) using PCR program settings shown in the Table 3/3.

Table 3/3. qPCR reaction conditions.

Step		Conditions	
1.	Initial denaturation	10 min, 95°C	
2.	Denaturation	10 sec, 95°C	35-40 cycles (depending on the procedure)
3.	Primer annealing	1 min, temperature specific for designed primers	
4.	Melting curve	Settings built in the thermocycler Incrementation with 1°C	

MATERIAL AND METHODS

The transcript amount was normalized to reference gene actin beta (*ACTB*) or glyceraldehyde-3-phosphate dehydrogenase (*GAPDH*) levels and was determined with the formulas:

$$\Delta CT_{gene} = CT_{gene} - CT_{ref} *$$

$$\Delta CT_{control} = CT_{gene} - CT_{ref} *$$

$$av. \Delta CT_{control} = \text{arithmetic average of } \Delta CT_{control} \text{ values}$$

$$\Delta \Delta CT = \Delta CT_{gene} - av. \Delta CT_{control}$$

$$Q = 2^{(-\Delta \Delta CT)}$$

* CT_{ref} stays for the reference – the CT value of the housekeeping gene

Results are presented as mean +/- SEM (standard error of the mean) for (if not indicated differently) two independent biological repeats. Graphs were prepared in GraphPad Prism Software. The sequences of used primers are shown in the Table 3/4.

Table 3/4. Primers used for the gene expression experiments are described in subsection 3.4.

Gene name	Primer sequence	
	Forward	Reverse
<i>GAPDH</i>	CAATATGATTCCACCCATGGCAA	GATCTCGCTCCTGGAAGATGG
<i>ACTB</i>	ACAGAGCCTCGCCTTTGCCGAT	ATCATCCATGGTGAGCTGGCGG
<i>IFI27</i>	GTCACTGGGAGCAACTGGAC	GGGCAGGGAGCTAGTAGAAC
<i>IFI6</i>	ATCCTGAATGGGGGCGG	AGATACTTGTGGGTGGCGTAG
<i>OAS2</i>	CAATCAGCGAGGCCAGTAAT	TCCAGGTTGGGAGAAGTCAA
<i>IFIT1</i>	CTTGACAGAAACACCCACTT	CCTCTAGGCTGCCCTTTTGT

3.5. RNA-Seq library preparation and sequencing

RNA sequencing experiments on 2fTGH and ST2-U3C were performed in collaboration with dr Katarzyna Błaszczuk, Human Molecular Genetics Research Unit, Institute of Molecular Biology and Biotechnology, Adam Mickiewicz University in Poznan. RNA sequencing data on

MATERIAL AND METHODS

Huh7.5 and Huh ST1 K.O. was performed by dr Agata Sekrecka, Human Molecular Genetics Research Unit, Institute of Molecular Biology and Biotechnology, Adam Mickiewicz University in Poznan.

RNA quantity was estimated using the Qubit RNA BR assay kit (ThermoFisher Scientific) and quality was assessed by the Agilent 2100 Bioanalyzer using the RNA 6000 Nano kit (Agilent Technologies), according to the protocols provided by manufacturers. RNA degradation was assessed by RIN (RNA integrity number) and samples with RIN higher than 9 were then used for further analysis. RNA libraries were prepared in three biological repeats from 1 µg of total RNA using NEBNext® Ultra™ or Ultra™ II RNA Library Prep Kit for Illumina® (New England Biolabs, NEB) together with NEBNext Poly(A) mRNA Magnetic Isolation Module (NEB) and NEBNext® Multiplex Oligos for Illumina® (NEB), according to the manufacturer's protocol. To select mRNA containing polyA-tails the Oligo dT Beads were added to the total RNA. After elution from the beads, RNA was fragmented into ~200bp sequences which then was used as a matrix to synthesize the First cDNA Strand. Next, Second Strand cDNA was synthesized, DNA ends were repaired and 5'ends were phosphorylated. After the cleaning step, 3'ends were adenylated and the adaptor was ligated. Subsequently, adaptor-ligated DNA was then size-selected using the magnetic AMPure XP beads (Beckman Coulter). The final step was PCR Enrichment in which index primer, specific for each sample, was used. Quality and fragment distribution of prepared libraries were estimated using the Agilent High Sensitivity DNA kit (Agilent Technologies) and quantity was assessed by the Qubit dsDNA HS assay kit (ThermoFisher Scientific). Sequencing (HighOutput SR75, v2 chemistry) was performed on the NextSeq500 (Illumina) in Lexogen, BioCenter in Vienna, Austria.

3.5.1. RNA-Seq data analysis

The bioinformatic analysis of data obtained from RNA-Seq experiments was performed with help provided by dr Katarzyna Kluzek, Human Molecular Genetics Research Unit, Institute of Molecular Biology and Biotechnology, Adam Mickiewicz University in Poznan. Dr Kluzek analyzed raw data, provided all scripts, suggested best tools to use and helped with her expertise during data analysis.

Fastq files were aligned using STAR v2.7.3a (Dobin et al., 2013) against the Homo_sapiens.GRCh38.dna.primary_assembly genome build (release-100). Quality control

MATERIAL AND METHODS

assessments were made using FastQC (Andrews, 2010) and reports combined with MultiQC (Ewels et al., 2016). Gene counts (reads aligned to each gene of each sample) were generated using FeatureCounts v1.6.2 with default parameters (Liao et al., 2014). Genes with low counts (below 10 in all time points) were considered as “non-expressed” and filtered out for the downstream testing.

Differential gene expression analysis (DEG)

Counts were then normalized and DEG analysis were performed using the DESeq2 v1.30.1 package (Love et al., 2014) in R v4.0.3 software (R Core Team, 2021). The Wald Test (for ST1-ST2-IRF9 and U3C) or likelihood ratio test (LRT; for the rest of the cell lines) was used for to identify genes that respond to IFN α treatment over time. These tests compares how well count data of individual gene fit to a “full model” (with independent variables, such as time) compared to a “reduced model” (without these variables). DEG was tested with “replicate” fit as a blocking factor (\sim replicate + time). Relationships between replicates and time of treatment were assessed through a principal component analysis (PCA) plot generated using DESeq2. False discovery rate (FDR)–adjusted q-values (5% threshold) were calculated by Benjamini-Hochberg procedure. The log₂FC (fold change) was also calculated for each gene. Genes with adjusted p-values (padj) less than 0.05 and log₂FC > 0,5 (for ST2-U3C) or log₂FC > 1 (for the rest of the cell lines) were considered as DEGs.

Heatmap generation

Heatmaps visualizing transcriptional response to IFN α stimulation were prepared using pheatmap v1.0.12 (Kolde 2019) and ComplexHeatmap v2.10.0 (Gu, Eils, and Schlesner 2016) packages for R software environment. For selected genes, normalized counts obtained from DESeq2 were extracted and subjected to hierarchical clustering (only by row) with default clustering method: complete, euclidean distance. For plotting, row scaling with Z-scores was performed. Colour scale (from green to burgundy, that represents low and high normalized intensity, respectively) indicates the expression change over time for each sample compared to the expression of the non-stimulated control.

Gene ontology term enrichment analysis

The GO term enrichment analysis was performed using ShinyGO 0.76 software (Ge, Jung, and Yao 2020). False Discovery Rate (FDR), that indicate how likely the enrichment is by chance, was calculated based on nominal P-value from the hypergeometric test. Then Fold Enrichment was defined as a percentage of indicated genes belonging to a pathway, divided by the corresponding percentage in the background. The records were selected by the FDR (the smallest indicate the highest statistical power) and next, sorted by the Fold Enrichment. The network was performed to show summarized correlation among significant pathways in which uploaded genes are involved. The nodes were connected when they share at least 20% of genes.

Selection of commonly upregulated genes

To select commonly upregulated genes Venn diagrams were prepared using jvenn software (Bardou et al. 2014).

3.6. Chromatin immunoprecipitation (ChIP)

To estimate the broad spectrum of transcription factors-DNA interactions we selected four time-points of the IFN α treatments: 0, 2, 24 and 72h. The First 3 time-points represent the early, robust wave of the interferon-dependent response, while 72h stays for prolonged ISGs expression. Samples were prepared according to the following procedure (the buffers made in house are described at the end of this section): the trypsin-treated cells were suspended in PBS in 20 mln cells aliquots and then the protein-DNA connection was fixed, firstly by the use of disuccinimidyl glutarate (DSG, ThermoFisher Scientific) and then by 1% formaldehyde (ThermoFisher Scientific). Formaldehyde activity was blocked by using 1M glycine (Chempur). Then the protein-DNA complexes were washed in PBS and stored at -80°C. Isolation was performed using Lysis Buffer + PIC (cComplete™ Mini Protease Inhibitor Cocktail, Merck; 1 tablet per 10 ml of the buffer) and lysates were sonicated in Sonication Buffer + PIC (1 tablet per 10ml of the buffer) using BioRuptor 300 (Diagenode). Conditions for experiments were previously established experimentally in our lab to obtain the approximately 200-1000bp fragments. The cell wall remnants were then removed by centrifugation and supernatant was diluted in Dilution Buffer + PIC (1 tablet per 50ml of the

MATERIAL AND METHODS

buffer). Antibodies of interest (anti-STAT1, anti-STAT2, anti-IRF9, anti-pSTAT1 and anti-pSTAT2, described in the Table 3/7), as well as normal mouse IgG (negative control, Merck), were added and samples were incubated overnight at 4°C on the Stuart Rotator (Cole-Parmer). To precipitate chromatin-antibody complexes, a mixture of Dynabeads™ Protein A and Protein G (Invitrogen) was added to the samples and the whole liquid was incubated for 6h at 4°C. After incubation, beads were washed six times with Lysis Buffer + PIC (1 tablet per 50ml), two times with 1x TE Buffer, DNA fragments were eluted for 30 minutes with Elution Buffer and de-cross-linked by incubation with 5M NaCl and 0,5M EDTA at 65°C, overnight. In the morning, samples were cooled down and RNA was removed by incubation for 30 min with 1µl RNase A (ThermoFisher Scientific) at 37°C. Proteins were then digested by incubation with 2µl of Proteinase K (A&A Biotechnology) at 45°C. DNA was then purified on columns using the MiniElute PCR Purification kit (Qiagen) according to the protocol provided by the manufacturer. Obtained chromatin was eluted in 25µl of Elution Buffer supplied in the kit.

Buffers of ChIP experiments made *in house*:

- Lysis Buffer: 150mM NaCl (Sigma-Aldrich), 50mM EDTA pH 8.5 (ThermoFisher Scientific), 0,2M Tris-HCl pH 7.5 (ThermoFischer Scientific), 0,5% NP40 (BioShop).
- Sonication Buffer: 20% SDS (BioShop), 0,5M EDTA pH 8.0 (ThermoFisher Scientific), 1M Tris pH 8.0 (ThermoFisher Scientific).
- Dilution Buffer: 20% SDS (BioShop), 1,1 % Triton X-100 (BioShop), 0,5M EDTA pH 8.0 (ThermoFisher Scientific), 5M NaCl (Sigma-Aldrich), 1M Tris-HCl pH 8.0 (ThermoFisher Scientific).

ChIP DNA was then quantified by qPCR and normalized to values obtained for unprecipitated DNA (input). Primers used for assessment of the material quality (positive control *OAS2* and negative control *NANOG*), as well as primers used in ChIP-PCR experiments are listed in the Table 3/5.

The phosphorylated forms of STAT1 and STAT2 exhibit higher affinity to the DNA and the binding profile is more prolonged in case of 2fTGH (Figure 4.1). This may be a result of methodology that was used according to the library preparation protocol, where starting material is 10ng of chromatin or less - estimated to the least concentrated sample from the

particular experiment. This results in reduced differences of the DNA-binding affinity of particular antibodies that are shown in IGV as a peak heights.

Table 3/5. A list of primers used for ChIP-PCR experiments that are described in subsection 3.5.

Gene name	Primer sequence	
	Forward	Reverse
<i>NANOG</i>	TGGTAGACGGGATTAAGTCTGAG	GAAGGCTCTATCACCTTAGA
<i>OAS2</i>	CGCTGCAGTGGGTGGAGAGA	GCCGGCAAGACAGTGAATGG
<i>IFI27</i>	CTTCTGGACTGCGCATGAGG	CCACCCCGACTGAAGCACTG
<i>STAT1 inside peak</i>	CGCTCAGCCAATTAGACGC	GTAAACAGAACGCCAGTTCCC
<i>STAT1 right peak</i>	CTCTCAATCCCAGTCCTTCTC	GAACCGCTTCGGAAACAGC
<i>STAT2 inside peak</i>	TGTCACCAAGCAGGCTGTC	TCTGTTCTGTTAGGCTCAGGC
<i>STAT2 right peak</i>	CTGCCATTCAGTCAAGCC	ACTCCTCCCCTCGTAGAAA
<i>IRF9</i>	AGATGCTGCTGCCCTCTAGT	CCCCTTTCTACAGTCCCCA

3.7. ChIP-Seq

Chromatin obtained in ChIP experiments was quantified using a Qubit dsDNA HS assay kit (ThermoFisher Scientific). Up to 10ng of the DNA per sample was used to prepare ChIP-DNA libraries by using NEBNext® ChIP-Seq Library Prep Reagent Set for Illumina® (New England BioLabs) according to the manufacturer's protocol which is identical to RNA-Seq library preparation described in chapter 3.5. except it starts from the end-repair step. Prepared libraries quality and fragment distribution were estimated using the Agilent High Sensitivity DNA kit (Agilent Technologies) and quantity was assessed by the Qubit dsDNA HS assay kit (ThermoFisher Scientific). Sequencing was done in two biological replicates (HighOutput SR75, v2 chemistry) was done in Lexogen BioCenter in Vienna (Austria) on the NextSeq500 (Illumina).

Binding affinity of pSTAT1 and pSTAT2, expressed by the height of the peaks, is higher when compared to the total STAT1 and STAT2 (Figure 4.8). This may be explained by the quality of particular antibodies.

The ChIP samples for Huh7.5 and Huh ST1 K.O. were prepared and sequenced by dr Agata Sekrecka. The ChIP samples for 2fTGH and ST2-U3C were prepared and sequenced in collaboration with dr Katarzyna Błaszczuk, Human Molecular Genetics Research Unit, Institute of Molecular Biology and Biotechnology, Adam Mickiewicz University in Poznan. The Huh7.5 and Huh ST1 K.O. samples were prepared and sequenced by dr Sekrecka.

3.7.1. ChIP-Seq data analysis

The bioinformatic analysis of data obtained from ChIP-Seq experiments was performed with help provided by dr Katarzyna Kluzek, Human Molecular Genetics Research Unit, Institute of Molecular Biology and Biotechnology, Adam Mickiewicz University in Poznan. Dr Kluzek analyzed raw data, provided all scripts, suggested best tools to use and helped with her expertise during data analysis.

ChIP-Seq data analysis was conducted in two ways. Because of the lack of repeats IDR was performed only for Huh7.5 and Huh ST1 K.O. as explained in A. The analysis for the rest of the cell lines are described in B.

A.

The primary analysis of the raw fastq sequence reads obtained from ChIP-Seq experiments has been carried out as follows: the alignment to the GRCh38.106 human genome assembly was done with Bowtie2 v2.4.1 (Langmead and Salzberg 2012) and BAM files were created and sorted by SAMTools v1.6 (Danecek et al. 2021). PCR duplicates were removed using BamUtil v1.0.15 (Jun et al. 2015). The read enrichments (peaks) of transcription factors were predicted by MACS v2.2.6 (Yong Zhang et al. 2008). During the secondary analysis artefacts were determined and removed based on the blacklisted genes list from the ENCODE project (ENCODE Project Consortium 2012) using BEDTools v2.30.0 (Quinlan and Hall 2010). To annotate the location of a given peak in terms of important genomic features [that includes if a peak is in the TSS (transcription start site), TTS (transcription termination site), Exon (Coding), 5' UTR Exon, 3' UTR Exon, Intronic or Intergenic region] and to associate peaks with nearby genes the annotatePeaks.pl was performed by HOMER v4.11. (Heinz et al. 2010). HOMER was also used to generate motifs. BAM files were converted using bamCoverage using (deepTools2 v3.5.0) (Ramírez et al. 2016) to bigwig format and IGVtools was used for visualization with IGV (Robinson et al. 2011).

B.

All ChIP-Seq experiments were performed in duplicate and were scored against input DNA. After quality assessment of raw reads with FastQC (Andrews, 2010), data obtained from ChIP-Seq experiments was analyzed according to ENCODE Transcription Factor processing pipeline (Figure 3.4) (<https://github.com/ENCODE-DCC/chip-seq-pipeline2>) with default parameters (ENCODE Project Consortium, 2012). Briefly, sequencing reads were aligned to hg38 v29 genome (<https://www.encodeproject.org/files/ENCFF110VAV/>) using Bowtie2 v2.4.1 (Langmead and Salzberg 2012) with mapping quality threshold 30. Subsequently, duplicates were marked using Picard Tools (<http://broadinstitute.github.io/picard/>). Peaks were called with SPP, FDR threshold set to 0.01. Afterward, a statistical procedure called Irreproducible Discovery Rate (IDR), was used to determine an optimal number of reproducible peaks between biological replicates.

It compares a pair of ranked lists of regions and assigns scores that reflect expected probability that the peak belongs to the noise component. An IDR score threshold of 0.02 was used to obtain optimal set of peaks. All peak sets were then screened against a specially curated blacklist of regions in the human genome provided within ENCODE pipeline and peaks overlapping the blacklisted regions were discarded. P-value signal tracks for each replicate and replicates pooled were generated with MACS2.

Quality control reports were generated at each step of data analysis e.g.:

- The complexity of the library was evaluated by calculation of NRF (non-redundant fraction), PBC1 and PBC2 (PCR bottleneck coefficient). Preferred values are: NRF>0.9, PBC1>0.9, and PBC2>10.
- ChIP Quality was estimated by Normalized and Relative Strand Cross-Correlation (NSC and RSC) and Cross-Correlation Plot. ENCODE guidelines recommend that the RSC be > 0.8 and NSC > 1.05.
- For Replicate Concordance inspection IDR Rescue Ratio, IDR Self-Consistency Ratio and IDR Reproducibility Test were used. All samples passed quality check based on thresholds set by ENCODE, detailed description of all parameters can be found at: <https://www.encodeproject.org/datastandards/terms/#concordance>.

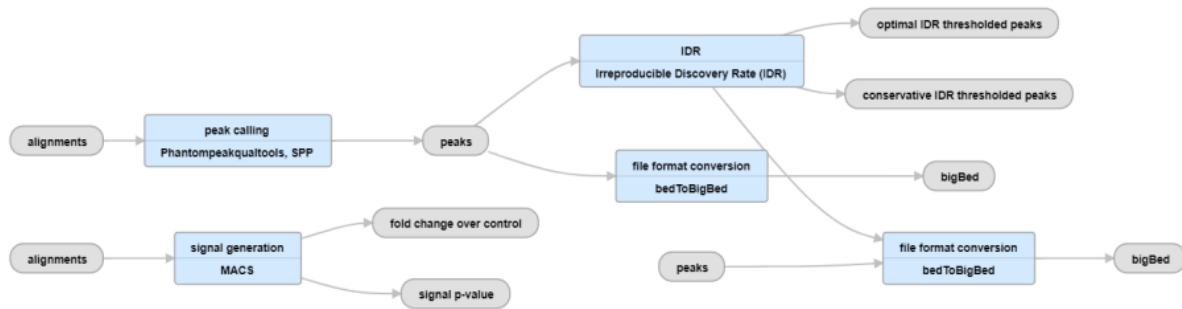


Figure 3.4 Pipeline for ChIP-Seq data processing of a transcription factor

Source of the graph: ENCODE: Encyclopedia of DNA Elements; J. Michael Cherry (<https://www.encodeproject.org/pipelines/ENCPL138KID/>),

Visualization in the Integrative Genomics Viewer

To visualize the ChIP-Seq in the Integrative Genomics Viewer (IGV) (Thorvaldsdóttir et al., 2013) BAM files were prepared using Bowtie2 aligner v2.4.1 (Langmead and Salzberg, 2012) and converted using bamCoverage (deepTools2 v3.5.0) (Ramírez et al., 2016) to bigwig format. Snapshots were taken in order to present them in figures.

Binding profiles

In order to generate STAT1, STAT2, IRF9, STAT1 and pSTAT2 binding profiles upon IFN α treatment at every time-points, the matrices that represent bigWig signal over selected genomic intervals have been quantified. For each treatment, p-value signal tracks from pooled replicates for all time-points and bed file with peaks annotated to promoters of selected 208 (commonly upregulated genes in 2fTGH vs Huh7.5) and 63 (commonly upregulated genes in wild-type vs STAT1 knock-out cell lines) genes were used. Read numbers were computed across 4 kb region centered on ChIP-Seq peak summits with computeMatrix function from deepTools v3.5.0 (reference-point TSS, upstream region 3000 bp, downstream region 1000 bp) (Ramírez et al., 2016). Further steps were performed with profileplyr_1.10.0 package (Carroll and Barrows, 2021). First, k-means clustering of the signal across the genomic intervals of gene promoters was performed with pheatmap package (Kolde, 2019). Mean range signal for each cluster was subsequently visualized as boxplots with ggplot2 (Wickham, 2011).

Binding site motifs identification

Peaks from all samples were prepared with custom R script and used to identify enriched transcription-factor-binding motifs by Hypergeometric Optimization of Motif EnRichment (HOMER) v. 4.9.1 (Heinz et al., 2010). Selected matrices for binding elements annotation (4 for GAS and 3 for ISRE) are shown in Figure 3.5 were applied for binding site annotation using annotatePeaks.pl, program (HOMER). Motif logos were generated using universalmotif package v1.12.1(Tremblay, 2021).

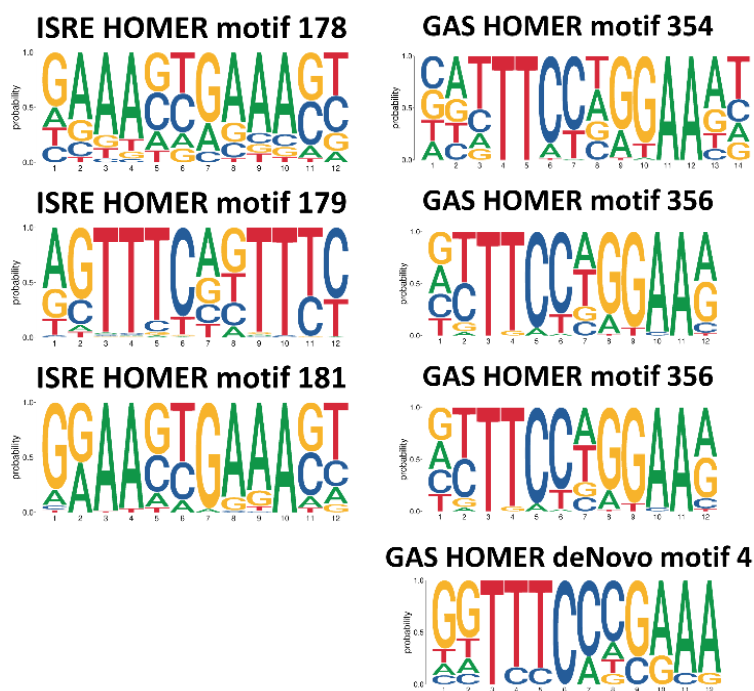


Figure 3.5 HOMER motifs

GAS and ISRE motif sequences selected for binding sites annotation in the peak region from ChIP-Seq experiments.

3.8. Proteins isolation

Protein extract was isolated from trypsin-treated (Pracownia Chemii Ogólnej, Instytut Immunologii i Terapii Doświadczalnej PAN, Wrocław) cell pellets washed with pre-warmed PBS (ThermoFisher Scientific) using made in house RIPA Buffer (150mM NaCl [Sigma-Aldrich], 0,5% Sodium deoxycholate [BioShop], 0,1% SDS [BioShop], 0,01% NP-40 [BioShop], 0,05M Tris-HCl pH=8.0 [ThermoFisher Scientific], 1mM DTT [Sigma-Aldrich], 1% PIC [Sigma-Aldrich], 1% EDTA [Sigma-Aldrich], 0,1 % PMSF [Sigma-Aldrich]). Cell pellets were incubated with RIPA on ice for at least 30 min, vortexed meanwhile several times, and then incubated overnight at -80°C. Ready protein extracts were stored in a -80°C freezer.

Protein concentration was measured using the Pierce™ BCA Protein Assay Kit (ThermoFisher Scientific) according to the manufacturer's protocol. Equal amounts of proteins were incubated for 10 minutes at 70°C with the Bolt™ Sample Reducing Agent and the Bolt™

MATERIAL AND METHODS

LDS Buffer (ThermoFisher Scientific) and separated electrophoretically on pre-casted polyacrylamide gel Blot 4-12% Bis-Tris Plus Gels (Invitrogen) for ~45 minutes under constant voltage of 65V. Proteins were then transferred to a methanol-activated PVDF membrane (pore size 0,45µm, Santa Cruz) using the Pierce™ 1-Step Transfer Buffer (ThermoFisher Scientific) and kurGEL Semi-dry transfer system (VWR) for 10-12 minutes under constant voltage of 25V.

Western blot experiments were carried out on the SNAP i.d.® 2.0 Protein Detection System (Merck Millipore) using the protocol described step-by-step in the Table 3/6, buffers made in-house, listed later in the text and antibodies listed in the Table 3/7. Proteins on the membrane were visualized using ECL protocol on the G:Box System (Syngen).

Table 3/6. Western blotting protocol

Step	Reagent	Condition
Blockage	0,125% non-fat dry milk or 1% BSA in TBS-T	20 min
Primary antibody incubation	Ab listed in Table 3/6	1 – 1,5h
Washing	3x with TBS-T or TBS-T + 0,5M NaCl	N/A
Secondary antibody incubation	Goat anti-rabbit (Sigma-Aldrich)	1:20 000, 13 min
Washing	3x with TBS or TBC + 0,5M NaCl	N/A
Visualizing	Luminata Forte HRP Substrate or Immobilon Forte Western HRP substrate (Merck)	5 min
Stripping	Stripping buffer	1h
Washing	3x TBS-T	10 min

Buffers for WB experiments made *in house*:

- TBS 10x: 0,5 M Tris, 1,4 M NaCl; pH 7.6
- TBS-T: 1x TBS, 0,1% Tween-20 (BioShop)
- TBS + NaCl: 1x TBS, 0,5M NaCl
- TBS-T + NaCl: 1x TBS, 0,5M NaCl, 0,1% Tween-20
- Stripping buffer: 25 mM Glycine (BioShop), 1% SDS (Bio-Shop); pH 2.0

Table 3/7. List of antibodies used in Western blot and chromatin immunoprecipitation experiments

Primary antibodies							
				2FTGH and ST2-U3C		Huh 7.5 and ST1 K.O.	
Company	Host species	Protein target	Blocking solution	Dilution	Condition	Dilution	Condition
CST	Rabbit monoclonal	STAT1	0,125% non-fat dry milk in TBS-T	1:500	1h	1:500	30min
CST	Rabbit monoclonal	pSTAT1 (Tyr701)	1% BSA in TBS-T	1:200	1h 30min	1:200	1h 20min
CST	Rabbit monoclonal	STAT2	0,125% non-fat dry milk in TBS-T	1:500	1h	1:500	30min
CST	Rabbit monoclonal	pSTAT2 (Tyr690)	1% BSA in TBS-T	1:500	1h 30min	1:500	1h 20min
CST	Rabbit monoclonal	IRF9	0,125% non-fat dry milk in TBS-T	1:400	1h 30min	1:300	1h
CST	Rabbit monoclonal	IRF1	0,125% non-fat dry milk in TBS-T	1:200	1h 30min	1:300	1h
Abcam	Rabbit monoclonal	α -Tubulin	0,125% non-fat dry milk in TBS-T	1:2 000	15min	1:2000	15min
Sigma-Aldrich	Goat IgG fraction	Anti-Rabbit Ab	Matching the primary Ab	1:20 000	13min	1:20 000	13min

RESULTS

3.9. Experiments with JAK Inhibitor I

Two sets of particular cells were prepared in appropriate confluence. Cells were stimulated with 1000U/mL of IFN α for the time course showed in the Table 3/8. Next, one set of the cells was treated with 5 μ M JAK Inhibitor I for 6h.

Table 3/8. JAK Inhibitor I treatment schedule

	Time:	0h	1h	2h	4h	8h	24h	48h	72h
Set 1	IFN α	-	+	+	+	+	+	+	+
	JII	-	-	-	-	-	-	-	-
Set 2	IFN α	-	+	+	+	+	+	+	+
	JII	-	-	-	-	+	+	+	+

3.10. Antiviral assay

Antiviral assays were performed in collaboration with the team of Prof. Chien-Kuo Lee, in his lab in The Graduate Institute of Immunology, National Taiwan University College of Medicine, Taipei, Taiwan.

Two different schemes were used for the antiviral assay. One, classical, was done to check the ability of IFN α treated cells to fight viral infection. The second was done on untreated cells.

- The INFa-treated cells:

2fTGH and U3C were seeded into 96-well plates at an appropriate amount per well. The next day, cells were pre-treated with or without 2-fold serial dilutions of IFN α , starting from 50 U/ml for 24, 48 and 72h. Subsequently, vesicular stomatitis Indiana virus (VSV) at a multiplicity of infection (MOI) of 1.0 was added to the cells using serum-free DMEM. Twenty hours post-infection, the medium was removed and cells were fixed with the 10% formaldehyde solution for 20 minutes at room temperature. After fixation, cells were visualized by the crystal violet staining. Excess dye was removed by immersing the plate in water.

RESULTS

- The untreated cells:

ST1-ST2-IRF9-U3C were seeded into 96-well plates at an appropriate amount per well. The next day, cells were pre-treated with 50 U/ml of IFN α for 24h. Subsequently, VSV at the 10-fold serial dilution of VSV starting from MOI of 10.0 was added to the cells using serum-free DMEM. Twenty hours post-infection, the medium was removed and cells were fixed with the 10% formaldehyde solution for 20 minutes at room temperature. After fixation, cells were visualized by the crystal violet staining. Excess dye was removed by immersing the plate in water.

4. RESULTS

To obtain further insight into the IFN α -mediated gene expression regulation and its phosphorylation dependence we performed a number of experiments on different cell lines. The results section is divided into four parts where we address the role of different ISGF3 component-based complexes and their phosphorylation status in canonical IFN α signalling pathway, in the absence of STAT1 protein and in the basal conditions.

PART I

The role of ISGF3 in time-dependent IFN α -activated transcriptional responses

4.1. Characterisation of 2fTGH and Huh7.5 cell lines

Western blotting

The human fibrosarcoma cell line 2fTGH and the human hepatocellular carcinoma cell line Huh7.5 have been widely used to study IFN Type-I signalling and the role of ISGF3 and its components. To obtain further insight into the IFN-I activated transcriptional responses in 2fTGH and Huh7.5 WT cells, we first characterized the IFN α -induced expression and phosphorylation of ISGF3 components i.e. STAT1, STAT2 and IRF9 at the protein level (Figure 4.1). Cells were treated with 1000U/mL of IFN α in time course of 1, 2, 4, 8, 24, 36, 48 and 72h and compared to untreated cells. In 2fTGH phosphorylation of STAT1 and STAT2 was absent in untreated cell, but highly induced upon IFN α treatment with an early, transient increase between 1 and 4 h, after which it rapidly diminished to undetectable levels at 72h (Figure 4.1 A). A similar early and transient IFN α -dependent STAT1 and STAT2 phosphorylation pattern was observed in Huh7.5 (Figure 4.1 B), with a clear drop between 4 and 8h after treatment. However, in these cells the phosphorylation of STAT1 and STAT2 remained slightly higher at later time points, and was still clearly visible after 72h.

In contrast, expression of STAT1 and STAT2 was already detectable in untreated 2fTGH and Huh7.5 cells, and further induced between 4 and 72h after IFN α addition. The same pattern was seen for IRF9, although it was nearly undetectable in resting 2fTGH and absent in untreated

RESULTS

Huh7.5 cells. The IFN α -induced expression of STAT1, STAT2 and IRF9 in both cell types followed the phosphorylation pattern of STAT1 and STAT2 at later time-points (2fTGH: transient; Huh7.5: prolonged) and was correlated with the action of classical ISGF3. On the other hand, the accumulation of STAT1, STAT2 and IRF9 in time, may predict an additional role of U-ISGF3 as well in mediating the prolonged IFN Type-I signalling.

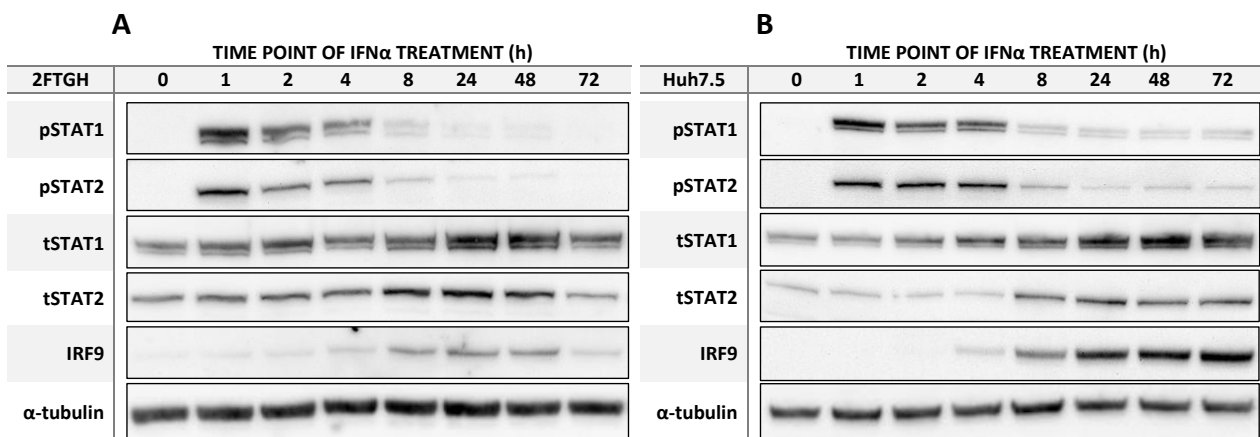


Figure 4.1 The protein levels and phosphorylation profiles in the 2fTGH and Huh7.5 cell lines

Western blot analysis of STAT1, STAT2, IRF9 and IRF1, as well as α -tubulin, were done on 2fTGH (A) and Huh7.5 (B) to estimate the protein levels and their phosphorylation profiles. Cells were treated with 1000U/mL of IFN α for the indicated time course or left untreated.

(p – phosphorylated, t - total)

4.2. The genome-wide characterization of gene expression in 2fTGH and Huh7.5 cell lines

RNA-Seq

To study the whole-genome gene expression mediated by IFN α in wild-type cells RNA-Seq experiments were performed and obtained data was analysed. RNA from 2fTGH and Huh7.5 treated with 1000U/mL IFN α for 0, 1, 2, 4, 8, 24, 36, 48 and 72h was isolated, libraries were prepared and sequencing was performed according to Material and Methods. Differential gene expression analysis (DEG) was performed and genes upregulated in at least one of the time points were selected based on the cut-off of $\log_2FC > 1$ and $p_{adj} < 0,05$. As such, IFN α -induced expression of 1280 genes in 2fTGH and 899 in Huh7.5 cells, of which 208 genes were in common (Figure 4.2).

RESULTS



Figure 4.2 Commonly upregulated genes for 2fTGH and Huh7.5 cell lines

Venn diagram show the upregulated genes for 2fTGH (green) and Huh7.5 (violet) that were obtained in RNA-Seq experiments. Among 208 overlapped genes, the well-known ISGs, like IFIT or OAS family, are present.

The average gene expression profile of the top 100 of these 208 commonly induced genes in the different cell-types, are presented graphically in Figure 4.3. In general, the potency of transcriptional responses in Huh7.5 was higher in comparison to 2fTGH. Nevertheless, a transient expression pattern was observed in both cell lines upon IFN α treatment, with a maximum at 8h followed by a significant drop to still detectable levels over time.

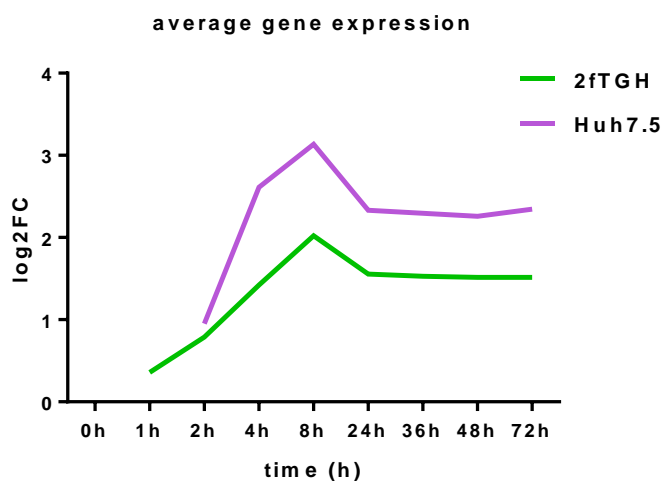


Figure 4.3

Characterization of selected commonly upregulated ISGs in the 2fTGH and Huh7.5 cell lines

The graphs represent gene expression profiles in selected commonly upregulated genes in 2fTGH (A) and Huh7.5 (B). Gene expression is presented in logarithmic form.

Next we examined the expression profiles of a pre-selection of highly induced known ISRE-containing antiviral ISGs (Figure 4.4), including *IFIT1*, *IFIT2*, *IFIT3*, *ISG15*, *IFI6*, *IFI27*, *OAS1* and *OAS2*, as well as the components of ISGF3 (*STAT1*, *STAT2* and *IRF9*).

RESULTS

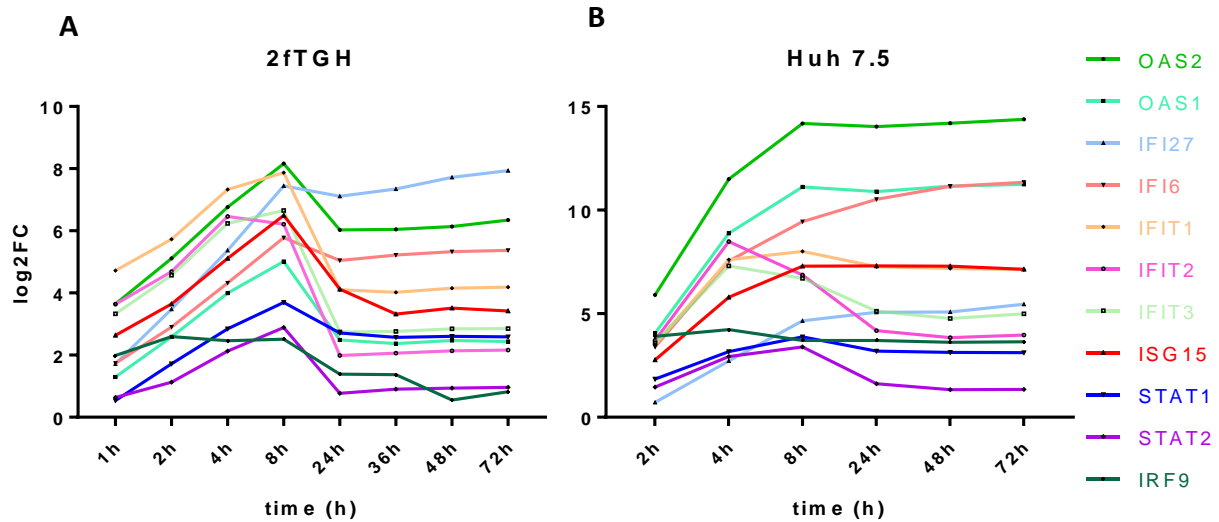


Figure 4.4 Characterization of selected commonly upregulated ISGs in the 2fTGH and Huh7.5 cell lines

The graphs represent gene expression profiles in selected commonly upregulated genes in 2fTGH (A) and Huh7.5 (B). Gene expression is presented in logarithmic form.

In 2fTGH, the majority of these genes exhibited a similar IFN-induced expression profile, with a maximum expression level after 8h of treatment, followed by a significant drop to still detectable levels at 72h (Figure 4.4 left panel). In contrast, in Huh7.5 the expression profiles of these genes were in general more prolonged, reaching maximum expression between 8 and 72h (Figure 4.4 right panel). *IFIT2* and *IFIT3* exhibited a more transient expression profile, as opposed to 2fTGH, showing maximum expression after 4h of IFN treatment. Together, this clearly correlates with the STAT1 and STAT2 phosphorylation profiles induced by IFN α in both cell-types and is consistent with the action of classical ISGF3.

To validate the quality of our RNA-seq dataset in general and the expression profiles observed for the pre-selected ISRE-containing antiviral ISGs, the expression of a number of these genes, including *OAS2*, *IFIT1*, *IFI27* and *IFI6*, was additionally confirmed by qPCR (Figure 4.5).

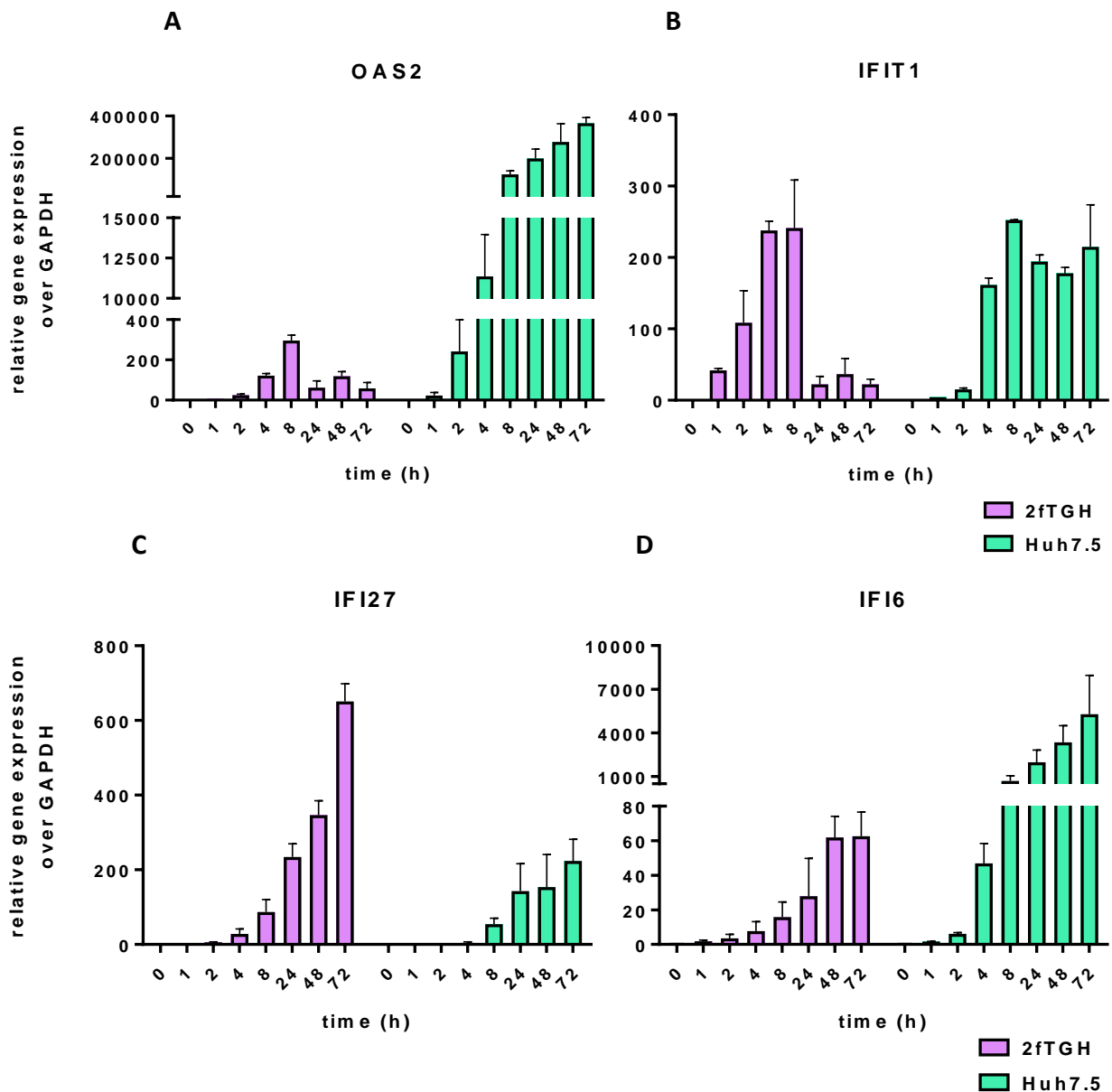


Figure 4.5 The gene expression profile in the 2fTGH and Huh7.5 cell lines

Cells were treated with 1000 U/mL IFN α in indicated time course. The profiles of gene expression for showed ISGs (OAS2, IFIT2, IFI27 and IFI6 on graph A, B, C and D, respectively) were estimated using qPCR method. Relative expression over GAPDH as a reference was estimated; n=2; mean +/- SEM. The expression profiles for 2fTGH are indicated in violet colour, while for Huh7.5 in turquoise.

The commonly IFN α -induced genes in 2fTGH and Huh7.5 were also subjected to GO term enrichment analysis. The most significant pathways, in which these common 208 genes are involved, are shown as a GO Network (Figure 4.6). Biological processes indicated in this GO Network are connected to Type-I signalling as well as broadly defined antiviral response, and recognize these genes among the core subset of antiviral ISGs.

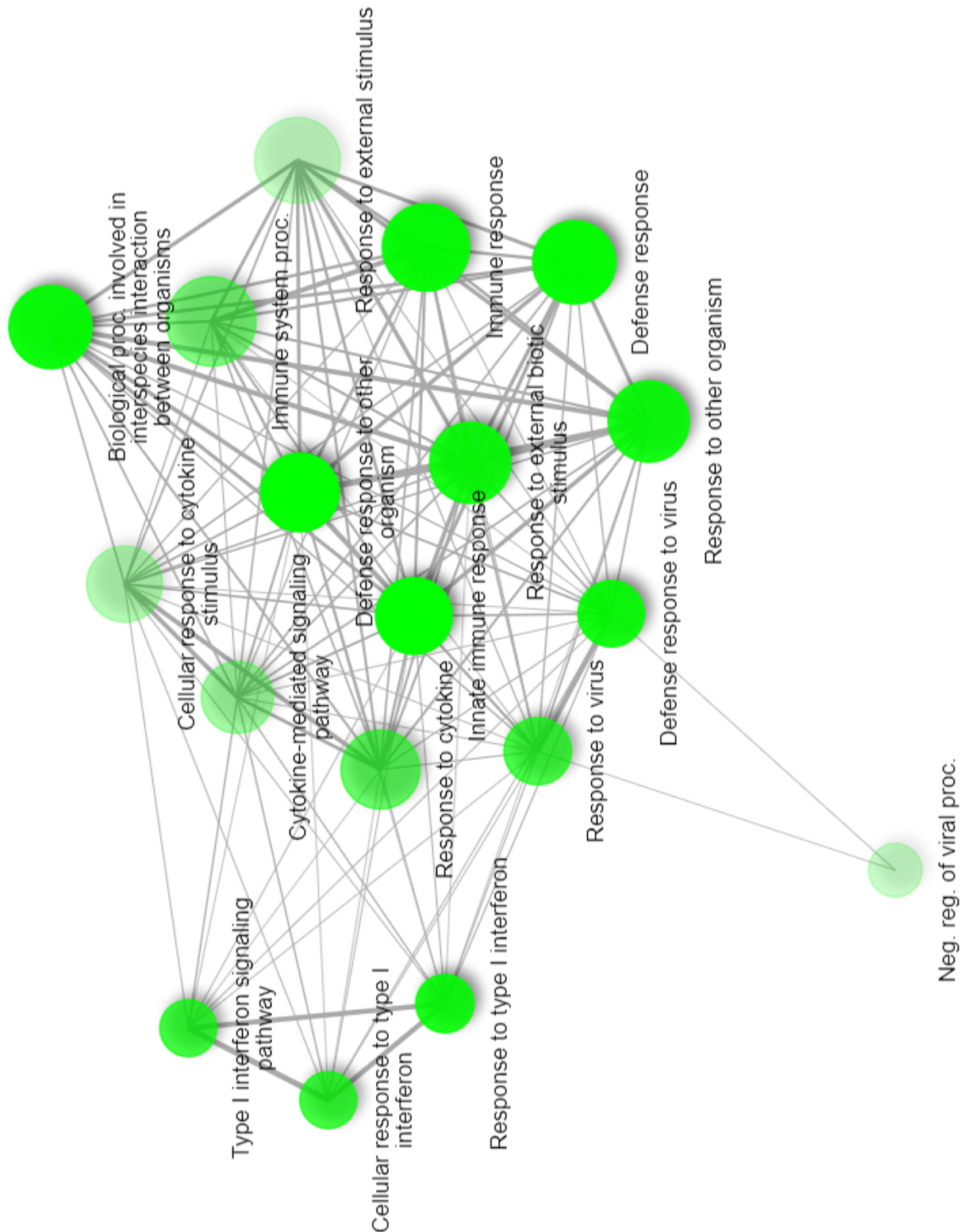


Figure 4.6 Gene Ontology

GO term enrichment analysis was performed on the lists of commonly up-regulated genes in 2fTGH and Huh7.5. The enriched term was considered statistically significant with the $FDR < 0.05$. In A the most significant biological processes are indicated. In B the relationship between enriched pathways. The more intensive colour of the node, the more significant enriched gene set. The bigger node, the larger gene set. The thickness of edges correlates with number of overlapped genes.

RESULTS

Together, these results provide evidence to suggest, that in 2fTGH and Huh7.5 cells a common IFN α -inducible transcriptional mechanism exists, that depends on the ISGF3 components STAT1, STAT2 and IRF9 in a phosphorylation- and time-dependent, as well as cell-type-dependent, manner. It also points to an important role of classical ISGF3 in the regulation of prolonged ISG expressions in both cell types. However, the contribution of U-ISGF3 under these conditions cannot be ruled out.

4.3. The genome-wide chromatin interactions in response to IFN α

ChIP-Seq

Next, we characterized the genome-wide binding of the ISGF3 components to the regulatory regions of the 208 commonly IFN α -induced genes. As such, chromatin immunoprecipitation (ChIP) experiments were performed on chromatin isolated from 2fTGH and Huh7.5 cells treated with 1000U/mL of IFN α for 2, 24 and 72h, using antibodies against STAT1, STAT2, pSTAT1, pSTAT2 and IRF9. The obtained DNA was then sequenced and data was analysed as described in Material and Methods section.

As expected, exposure to IFN α increased the genome-wide number of STAT1, STAT2, pSTAT1, pSTAT2, IRF9 binding peaks in a time-dependent manner (Figure 4.7 A). After statistical analysis, under these conditions, the peak number distribution in 2fTGH followed a transient pattern for all antibodies, with maximum at 2h of IFN α stimulation, and clear dependence on treatment (no basal binding) (Figure 4.7 A, upper graph). Moreover, STAT1, STAT2, pSTAT1, pSTAT2 and IRF9 binding peaks could still be detected after 72 hours. The peak number distribution in Huh7.5 exhibited a more prolonged pattern for all antibodies, being absent in untreated cells and showing high binding scores at 2, 24 and 72h of IFN α stimulation (Figure 4.7 A, lower graph). Collectively, the IFN α - and time-dependent distribution of STAT1, STAT2, pSTAT1, pSTAT2, IRF9 binding in 2fTGH and Huh7.5 correlated with the expression profile observed for the 208 commonly IFN α -induced genes in the individual cell lines (see Figure 4.3).

Subsequently, using HOMER software, ISRE and GAS consensus motifs (see Material and Methods, subsection 3.7.1, Figure 3.5) were mapped to IFN α -induced STAT1, STAT2, pSTAT1, pSTAT2 and IRF9 binding regions of the 208 commonly IFN α -induced genes. The predicted distribution of ISRE and GAS binding sites is depicted in Figure 4.7 B. Accordingly,

RESULTS

60% of these genes contained an ISRE binding site, 15% were mapped with a GAS site and 25% without ISRE or GAS. Motifs are shown in the Material and Methods, Figure 3.5.

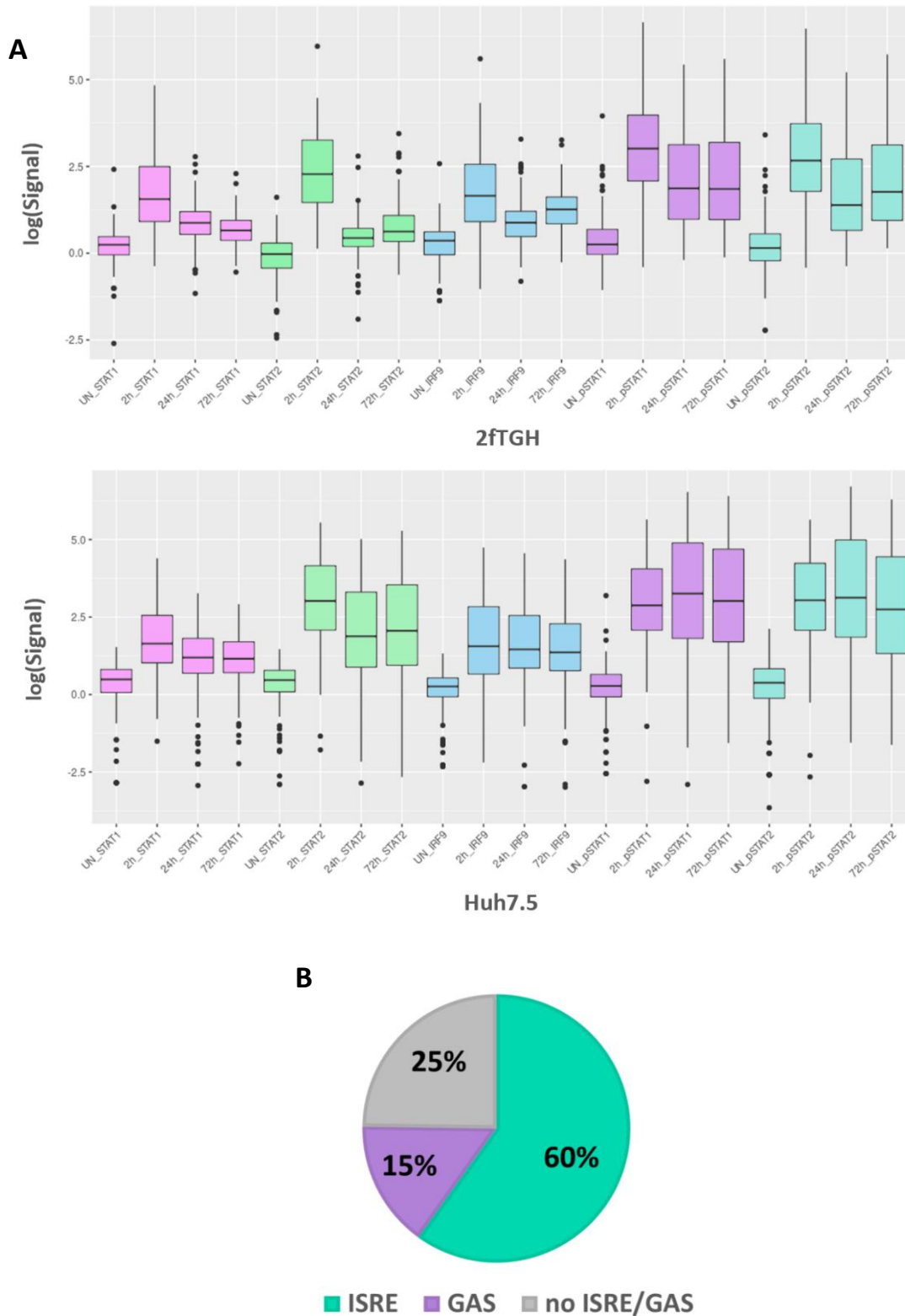


Figure explanation on the next page

Figure 4.7**A. Peak distribution of particular antibodies**

Boxplot represents the normalized scores of STAT1 (pink bars), STAT2 (green bars), IRF9 (blue bars), pSTAT1 (violet bars) and pSTAT1 (turquoise bars) binding peaks to the promoters of 208 commonly upregulated genes in 2fTGH vs Huh7.5.

B. Motif distribution

Graph represents the percentage of ISRE and GAS motifs distributed in 208 commonly upregulated genes in 2fTGH vs Huh7.5. Turquoise part represents the % of genes that possess ISRE (or ISRE and GAS), violet – that possess only GAS while grey shows the % of genes that have no ISRE.

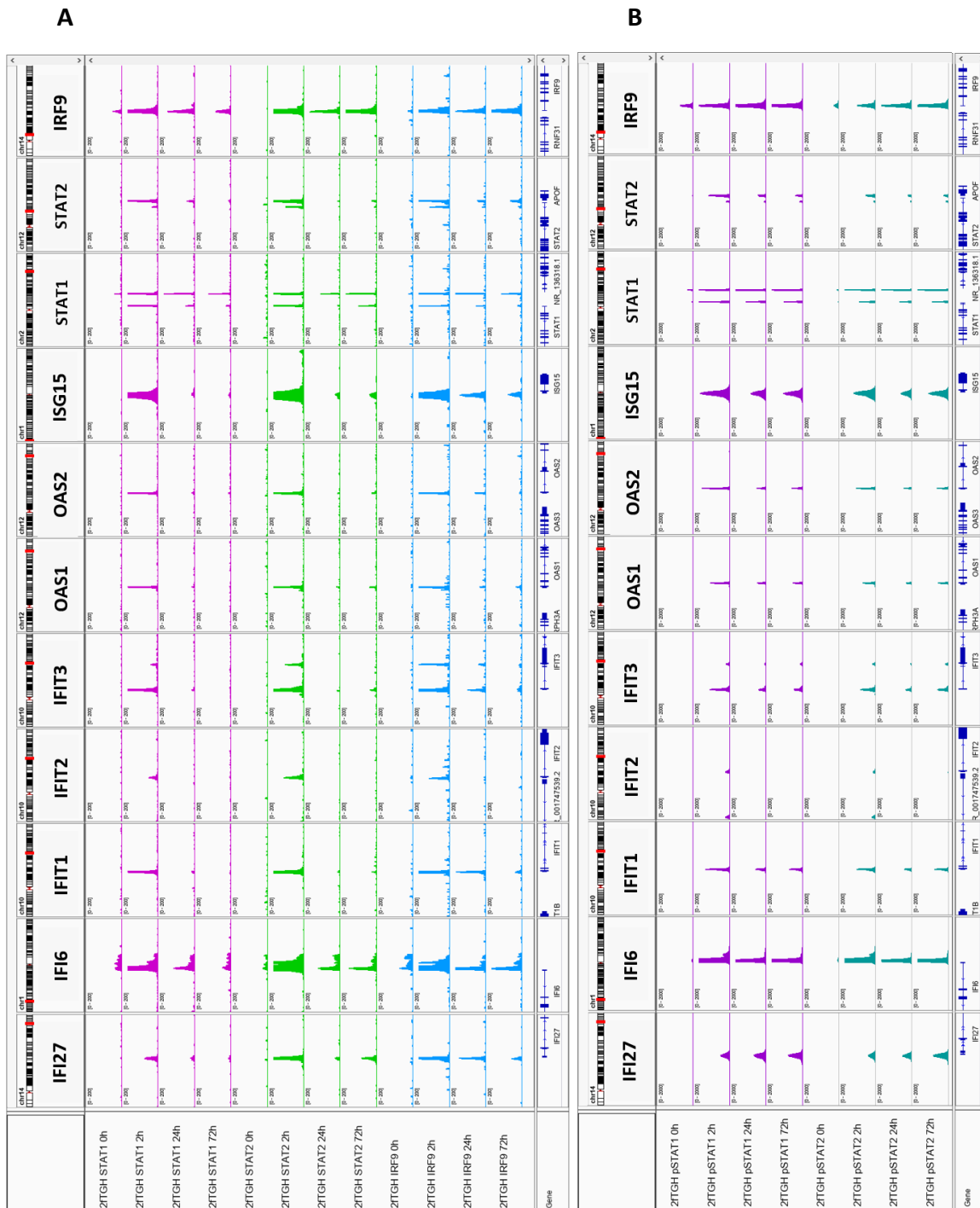
Closer inspection of a pre-selection of the previously characterized ISRE-containing antiviral ISGs (Figure 4.4), confirmed a correlation between gene expression and recruitment of STAT1, STAT2, pSTAT1, pSTAT2 and IRF9 in response to IFN α in 2fTGH and Huh7.5.

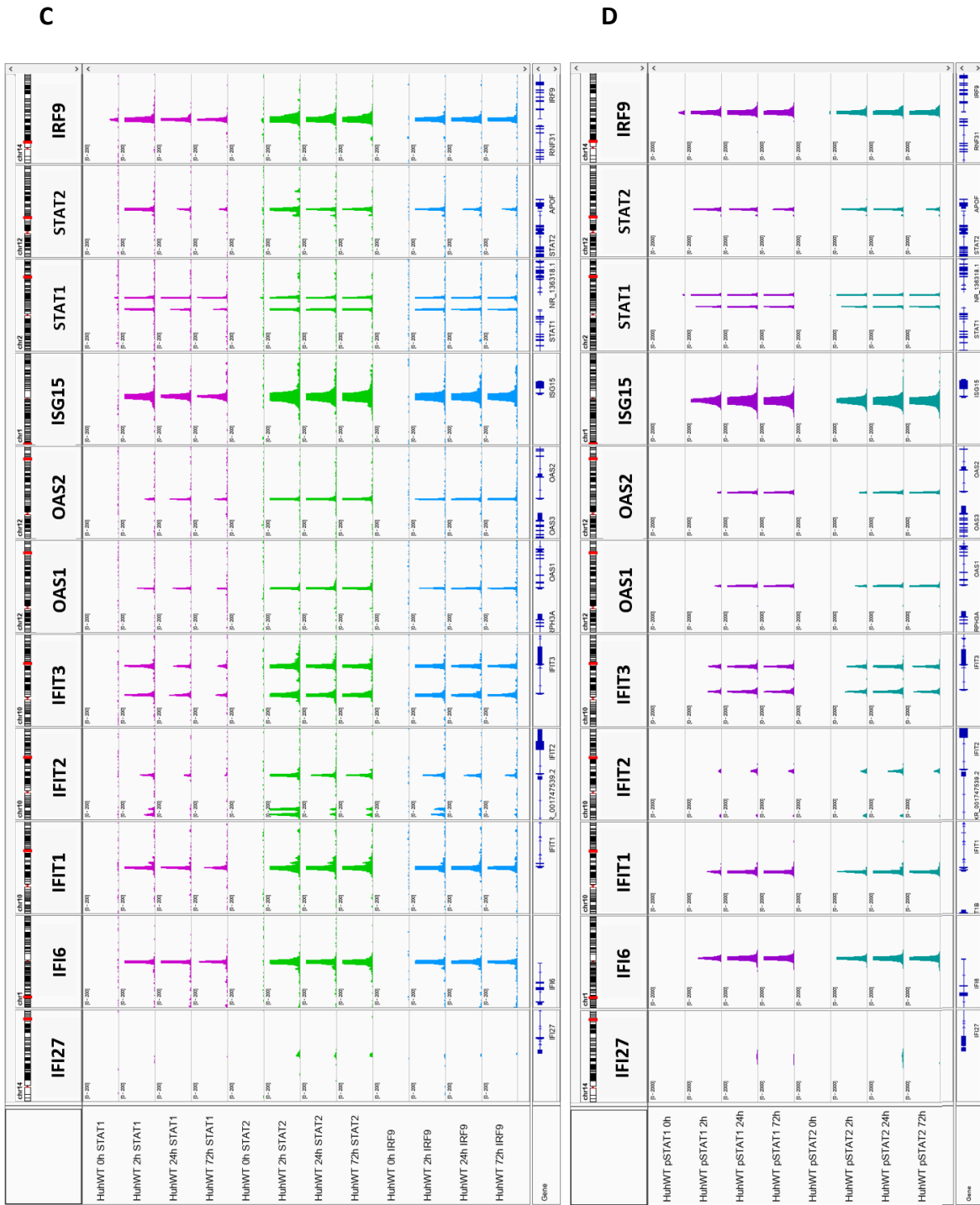
Accordingly, for the majority of the pre-selected genes in 2fTGH the binding profiles of total STAT1, STAT2 and IRF9 resemble the peak distribution as shown in Figure 4.8 A. A transient pattern was detected for all three components, with maximum at 2h of IFN α stimulation, and clear dependence on treatment (no basal binding). Moreover, significant binding could still be detected after 72 hours (Figure 4.8 A). On the contrary, in Huh7.5 the binding of STAT1, STAT2 and IRF9 is, in general higher and much more prolonged (Figure 4.8 C), being absent in untreated cells and showing strong binding at 2, 24 and 72h of IFN α stimulation. A similar cell-type dependent binding pattern was observed for pSTAT1 and pSTAT2, with binding in Huh7.5 being stronger and more prolonged as compared to 2fTGH, and closely resembling the binding patterns of STAT and STAT2 (compare figures 4.8 B and D). These observations are in agreement with the gene expression profiles from both, RNA-Seq, and qPCR results, shown in Figure 4.3, 4.4 and 4.5. It clearly indicates that classical ISGF3 (pSTAT1 + pSTAT2 + IRF9) is important in long-term ISG expression even after 72h.

Figure 4.8 Characterization of different ISGF3 components recruitment/binding to the regulatory regions of ISGs under IFN α treatment

Representative views of the ChIP-Seq peaks detected in the promoter regions of selected ISGs, in the 2fTGH (A and B) and Huh7.5 (C and D) cell lines untreated or treated with IFN α for indicated time course. All peaks were mapped onto the human reference genome hg38 and visualized using the Integrative Genomic Viewer (IGV). In A and C binding of the total STAT1, STAT2 and IRF9 is, while in B and D – binding of pSTAT1 and pSTAT2. Scale for A and C: 0-200, and for B and D: 0-2000.

Figures C and D on the next page





RESULTS

Accordingly, for the majority of the pre-selected genes in 2fTGH the binding profiles of total STAT1, STAT2 and IRF9 resemble the peak distribution as shown in Figure 4.8. A transient pattern was detected for all three components, with maximum at 2h of IFN α stimulation, and clear dependence on treatment (no basal binding). Moreover, significant binding could still be detected after 72 hours (Figure 4.8 A). On the contrary, in Huh7.5 the binding of STAT1, STAT2 and IRF9 is, in general higher and much more prolonged (Figure 4.8 C), being absent in untreated cells and showing strong binding at 2, 24 and 72h of IFN α stimulation. A similar cell-type dependent binding pattern was observed for pSTAT1 and pSTAT2, with binding in Huh7.5 being stronger and more prolonged as compared to 2fTGH, and closely resembling the binding patterns of STAT and STAT2 (compare figures 4.8 B and D). These observations are in agreement with the gene expression profiles from both, RNA-Seq, and qPCR results, shown in Figure 4.3, 4.4 and 4.5. It clearly indicates that classical ISGF3 (pSTAT1 + pSTAT2 + IRF9) is important in long-term ISG expression even after 72h. It also points to a cell-type-dependent role of ISGF3, which correlates with the different phosphorylation and expression profiles and chromatin binding patterns of STAT1, STAT2 and IRF9 observed in 2fTGH and Huh7.5. However, increased protein expression and binding of STAT1, STAT2 and IRF9 at later time points cannot rule out an additional role of U-ISGF3 (U-STAT1 + U-STAT2 + IRF9) in prolonged ISG expression in both cell-types as well.

4.4. The viral protection of 2fTGH upon long-term IFN α stimulation

Antiviral assay

The results presented in previous subsections showed that in 2fTGH ISG expression was sustained at a certain level up to 3 days after IFN α stimulation. To address the question if this low ISG expression was sufficient to ensure the cells to combat viral infection, antiviral assays were performed (Figure 4.9). Cells treated with a 2-fold serial dilution of IFN α [starting from 50U/mL (Figure 4.9 A) or 200U/ml (Figure 4.9 B)] were left for 24, 48 or 72h and then infected with Vesicular stomatitis Indiana virus (VSV) at a MOI of 1.0. As a control the STAT1-deficient U3C cell line, that is unable to combat viral infection, was used and treated similarly. The results show that once treated with IFN α , 2fTGH cells were able to effectively combat VSV infection up to 72h and the viral protection was IFN-dose dependent.

RESULTS

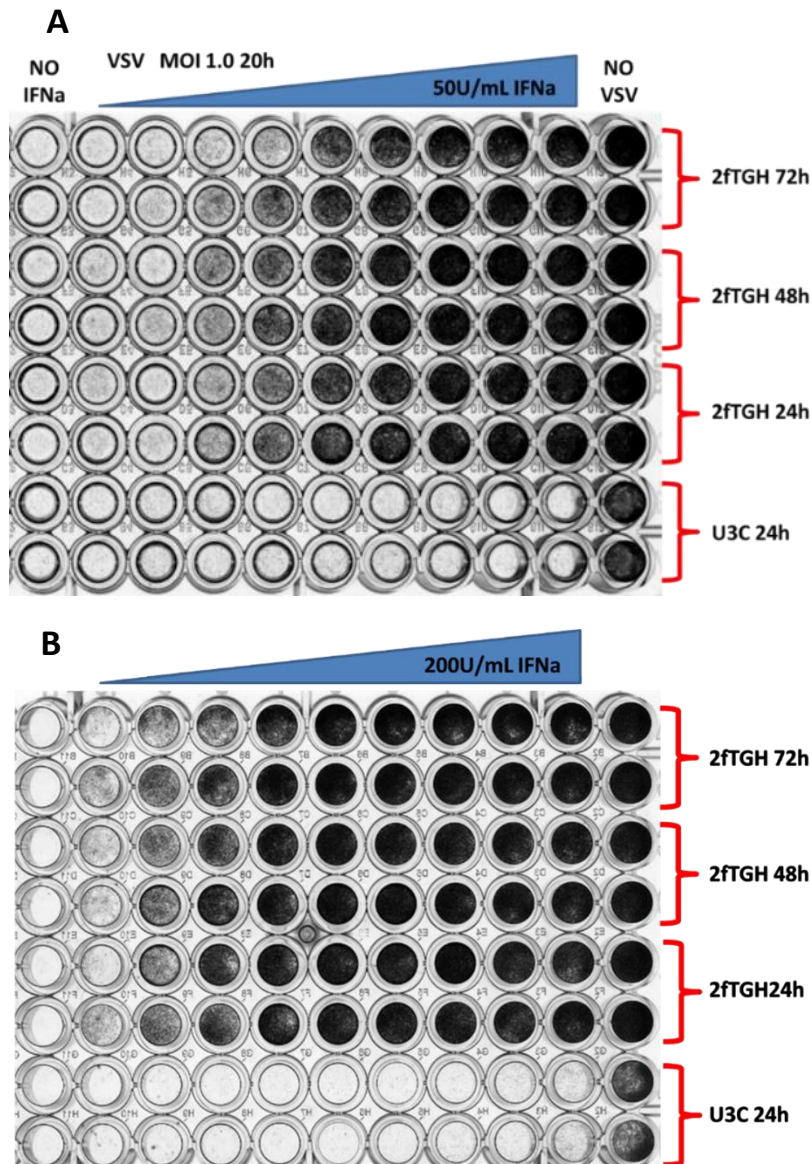


Figure 4.9 The long-lasting antiviral protection upon IFN α stimulation

The 2fTGH cells were pre-treated with 2-fold serial dilution of IFN α starting from 50U/mL (A) or 200U/mL (B) and left for 24, 48 and 72h. After this time cells were infected with VSV at MOI of 1.0 for 20h. One row (leftmost) on the plate contains cells untreated and one (rightmost) – cells uninfected. Next, results were visualized by crystal violet staining - the black wells indicate the living cells.

In combination with observations mentioned in above subsections, we concluded that despite the expression of the majority of ISGs was decreased in the 2fTGH cell line after longer time points, the long lasting viral protection was maintained. Low ISG expression was sufficient for cells to combat viral infection. Together with the shown above results, these findings raise the question of the importance of phosphorylation of the ISGF3 components in mediating the long-term antiviral response, which will be addressed in PART III.

PART II

The role of STAT2/IRF9 in time-dependent IFN α -activated transcriptional responses in the absence of STAT1

4.5. Characterisation of ST2-U3C and Huh7.7 STAT1 K.O. cell lines

Western blotting

To study IFN Type-I signalling in the absence of STAT1 and the role of STAT2/IRF9, the STAT1-deficient human fibrosarcoma cell line U3C overexpressing STAT2 (ST2-U3C) and Huh ST1 knock-out cells (Huh-STAT1 K.O.) have been generated by us and others previously (Blaszczyk et al. 2015)(Yamauchi et al. 2016). To understand in more detail the role of STAT2/IRF9 vs ISGF3 in long-term IFN responses, we first compared IFN α -induced expression and phosphorylation of STAT2/IRF9 and ISGF3 components at the protein level in these cell-lines and in their WT counterparts 2fTGH and Huh7.5 respectively (Figure 4.10).

In case of ST2-U3C a subtle change in the STAT2 phosphorylation profile could be observed as compared to 2fTGH (Figure 4.10 A vs C). The profile remains transient, with an early increase between 1 and 2h, but, in contrast to wild-type cells, the level of pSTAT2 only decreased slowly and stayed still high until 72h. This also corresponds to a higher IFN-induced expression of IRF9 in ST2-U3C at later time-points, and points to a delayed formation of STAT2/IRF9 as compared to ISGF3 in 2fTGH. As STAT2 is overexpressed in these cells, STAT2 expression was not affected by IFN treatment.

Different from ST2-U3C, Huh7.5 STAT1 K.O. displayed a rather shifted STAT2 phosphorylation pattern, being delayed and prolonged as compared to Huh7.5 (Figure 4.10 B and D). Accordingly, in Huh7.5 STAT1 K.O. pSTAT2 levels reached a maximum after 48h of IFN α treatment, while under wild type conditions the maximum phosphorylation was observed just after 2h of treatment and dropped between 4 and 8h. Like in ST2-U3C, in Huh ST1 K.O.

RESULTS

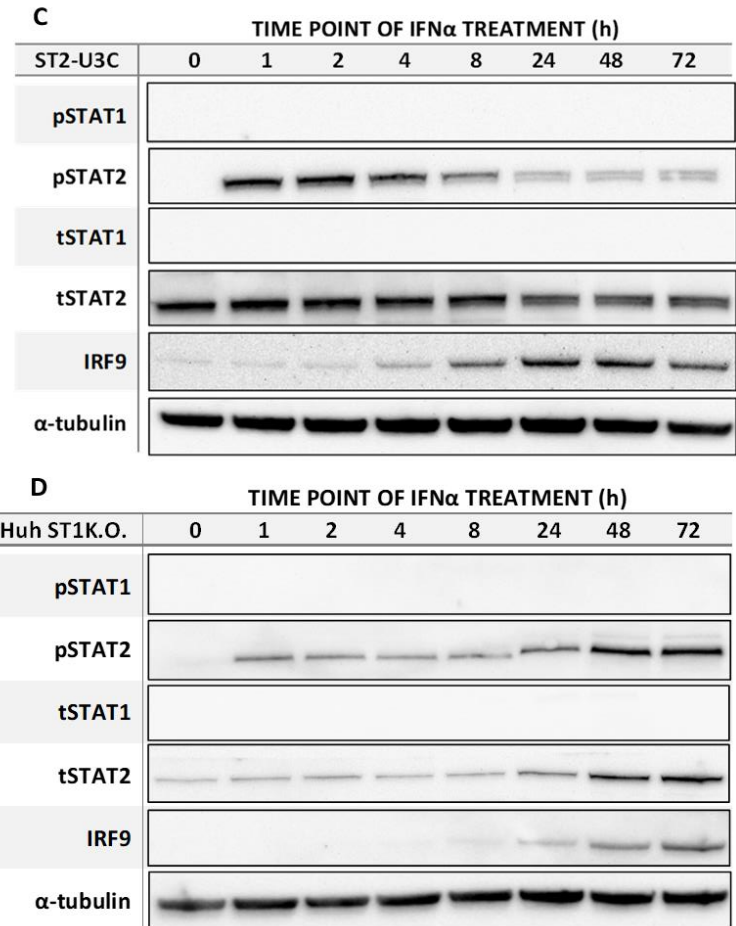
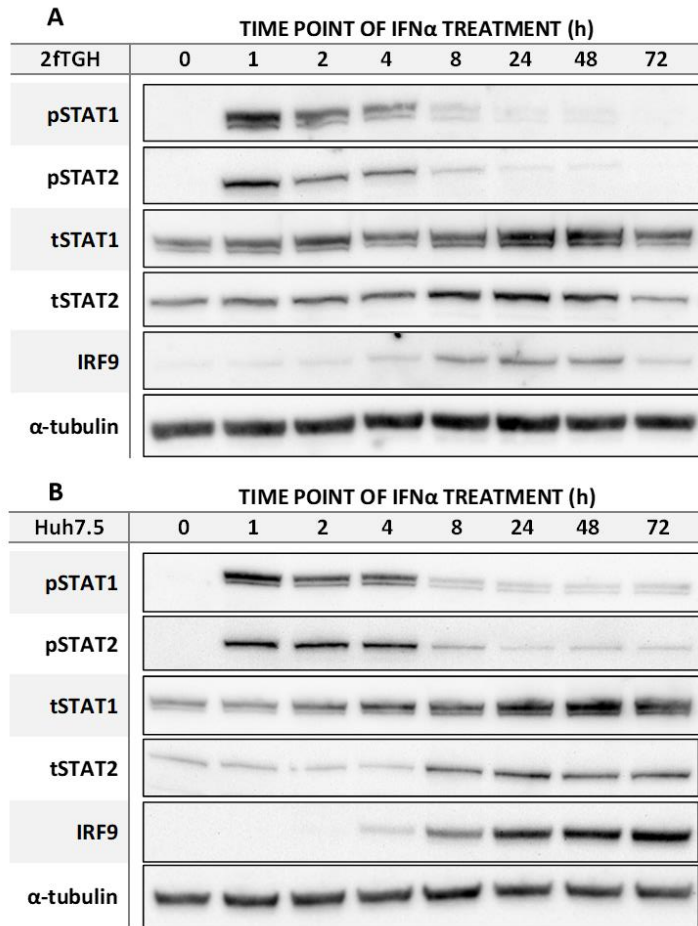


Figure 4.10

The protein levels and phosphorylation profiles in the absence of STAT1

To estimate the protein levels and their phosphorylation profiles Western blot analysis of STAT1, STAT2, IRF9 and IRF1, as well as α -tubulin, were done on the wild type (2fTGH and Huh7.5, A and B, respectively) as well as STAT1 knock-out cells (ST2-U3C and Huh ST1 K.O., C and D, respectively). Cells were treated with 1000U/mL of IFN α for the indicated time course or left untreated.

(p – phosphorylated, t – total)

RESULTS

IFN-dependent accumulation of IRF9, and also STAT2, was observed, however it predominantly occurred at later time points. As a consequence, this points to a possible late formation of STAT2/IRF9 as compared to ISGF3 in Huh7.5, a similar difference as seen in ST2-U3C vs 2fTGH. It also predicts an important role of STAT2/IRF9 in the regulation of prolonged ISG expression in the absence of STAT1 in both cell types. How this depends on phosphorylation of STAT2 and if a contribution of U-STAT2/IRF9 under these conditions exists has not been studied.

4.6. The genome-wide characterization of gene expression in the ST2-U3C and Huh ST1 K.O. cell lines

RNA-Seq

To examine the whole-genome gene expression mediated by IFN α in STAT1 K.O. cells RNA-Seq experiments were performed and obtained data was analysed. RNA from ST2-U3C and Huh ST1 K.O. treated with 1000U/mL IFN α for 0, 1, 2, 4, 8, 24, 48 and 72h was isolated, libraries were prepared and sequencing was performed according to Material and Methods. Differential gene expression analysis (DEG) was performed and genes upregulated in at least one of the time points were selected based on the cut-off of $\log_2FC > 1$ (or $> 0,5$ in case of ST2-U3C) and $padj < 0,05$. As such, IFN α induced expression of 110 genes in STAT2-U3C and 788 in Huh ST1 K.O. cells, of which 84 genes were in common (Figure 4.11 A).

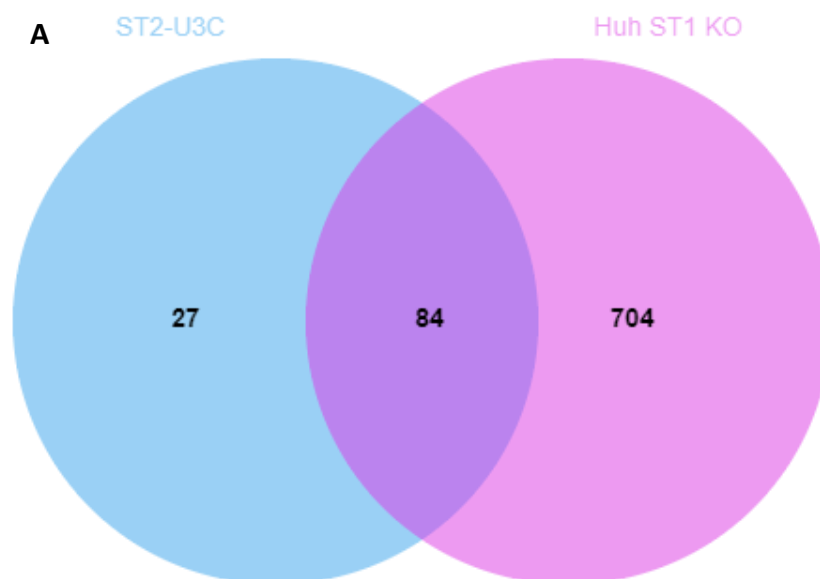


Figure B and explanation on the next page

RESULTS

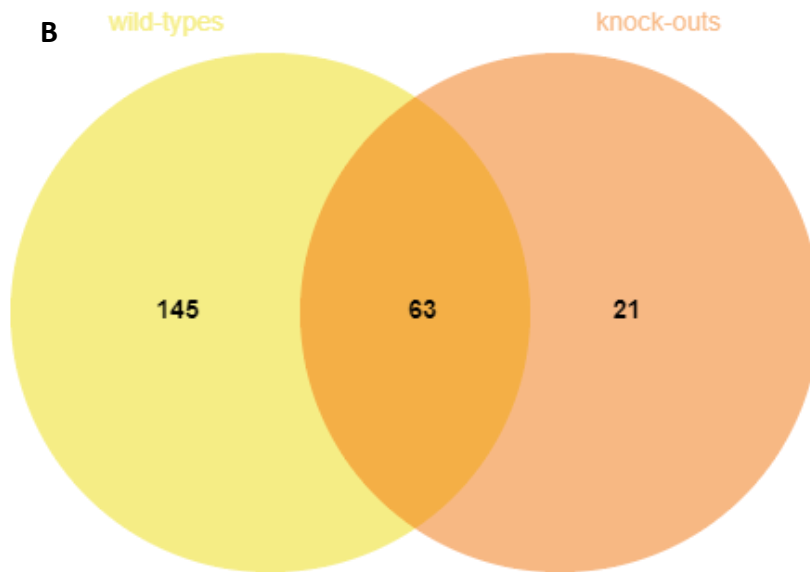


Figure 4.11 Commonly upregulated genes in the 2fTGH, Huh7.5, ST2-U3C and Huh ST1 K.O. cell lines

Venn diagrams, prepared using jvenn tool, represent the commonly upregulated genes in (A) ST2-U3C (blue circle) vs Huh ST1 K.O. (pink circle) and (B) wild type (yellow circle) vs STAT1 knock-out cells (orange circle).

When compared to the 208 commonly IFN α -induced genes from 2fTGH vs Huh7.5, a group of 63 IFN α -inducible genes was recognized that showed overlap between the four different cell lines (Figure 4.11). In addition, 145 genes were specifically induced in WT cells whereas 21 genes were identified as STAT1 K.O.-specific IFN α -inducible genes. The expression profiles of the 63 common genes in IFN α treated 2fTGH, Huh7.5, ST2-U3C and Huh ST1 K.O. cells are presented in the form of a heatmap in Figure 4.12.

Closer examination of this group of genes recognized the presence of the previously characterized pre-selected ISRE-containing antiviral ISGs (Figure 4.4) and identified many additional known ISRE-containing ISGs, including *OAS3*, *IRF1*, *ISG15*, as well as *RSAD2* or *DDX60*.

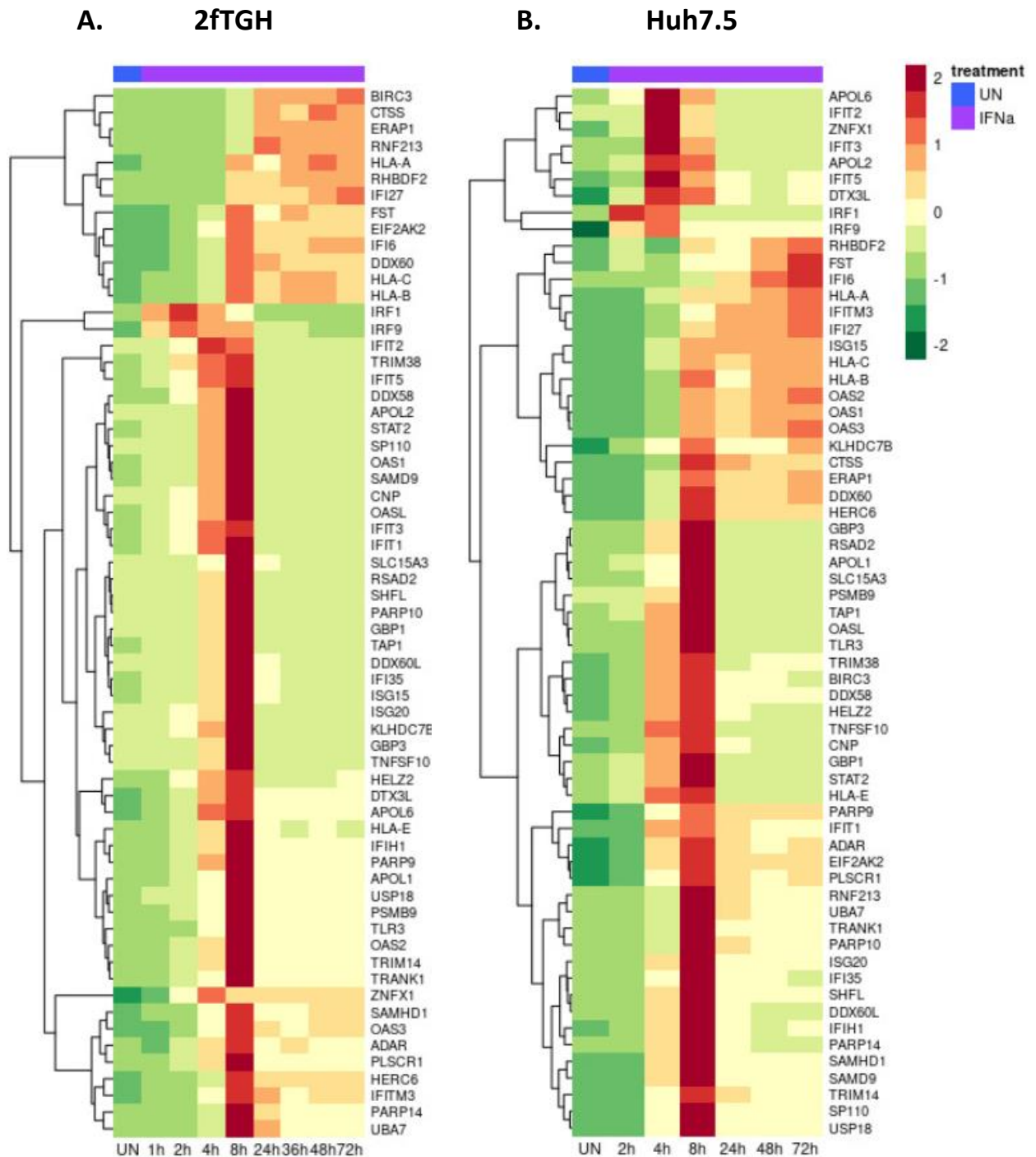
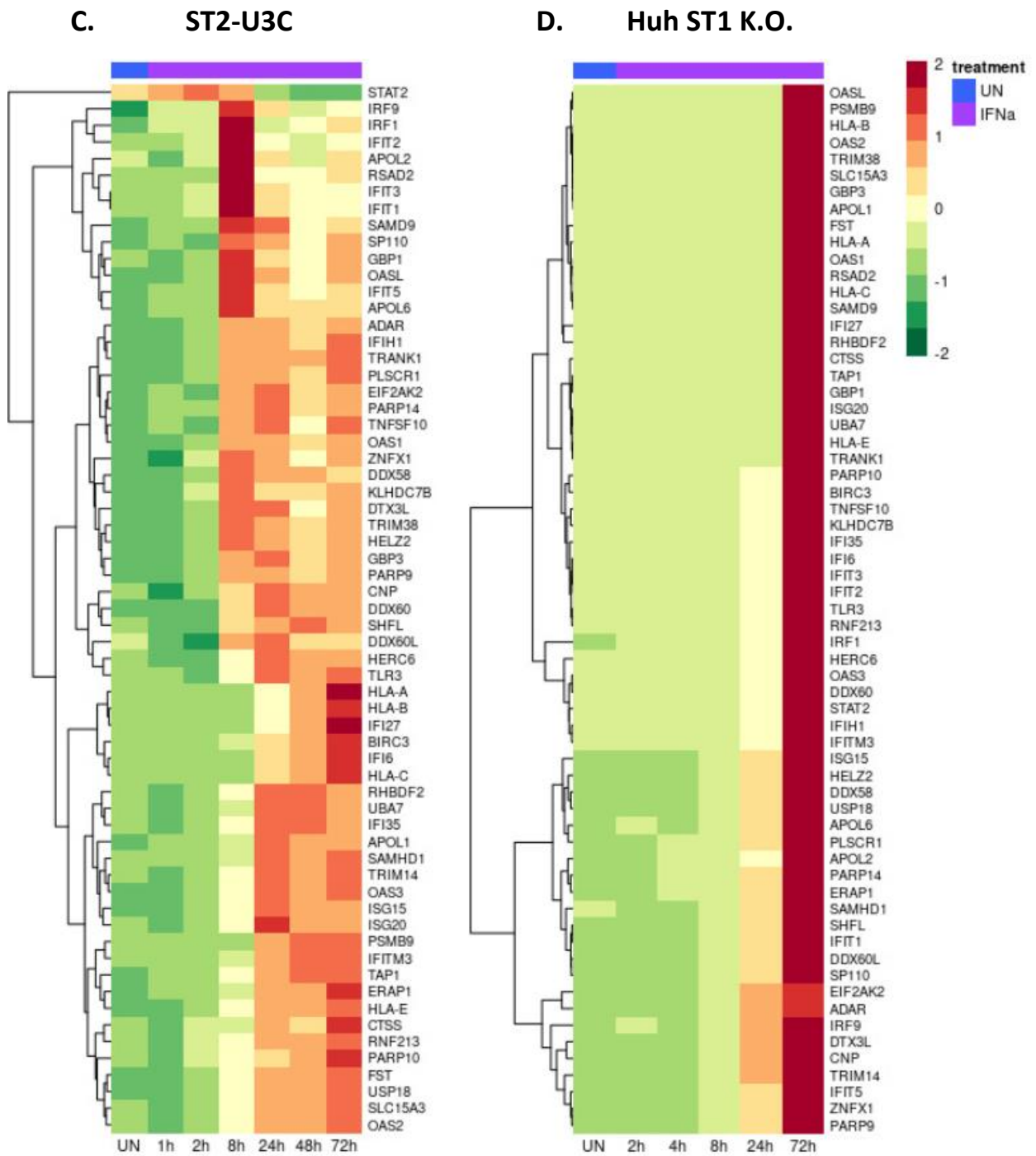


Figure 4.12 Characterization of commonly upregulated ISGs in the wild-type and STAT1 knock-out cell lines

Heatmaps generated from the expression values of 63 commonly upregulated genes in 2fTGH (A), Huh7.5 (B), ST2-U3C (C) and Huh ST1 K.O. (D). Each row represents one gene. Counts were normalized using z-score.

ST2-U3C and Huh ST1 K.O. shown on the next page.

RESULTS



RESULTS

In agreement with the presented above results (Figure 4.12) expression profiles of these 63 commonly IFN α -induced genes exhibited a similar shape in 2fTGH and Huh7.5, with a maximum at 8h. On the other hand, STAT1-deficiency, changed their expression profile completely, resulting in lower and prolonged expression in case of ST2-U3C, and delayed and prolonged expression in case of Huh ST1 K.O. More important, the gene expression patterns of the 63 commonly IFN α -induced genes in these four different cell types reflect the phosphorylation profiles and/or production of ISGF3 and STAT2/IRF9 components, as described above (Figure 4.10).

Next we examined the expression profiles of the previously characterized pre-selected ISRE-containing antiviral ISGs (Figure 4.13). As shown before (Fig 4.4), in 2fTGH, the majority of these genes exhibited a similar IFN-induced expression profile, with a maximum expression level after 8h of treatment, followed by a significant drop to still detectable levels at 72h (Figure 4.13 A). In contrast, in Huh7.5 the expression profiles of these genes were, in general, more prolonged, reaching maximum expression between 8 and 72h. *IFIT2* and *IFIT3* exhibited a more transient expression profile, as opposed to 2fTGH, showing maximum expression after 4h of IFN treatment (Figure 4.13 B).

In ST2-U3C, in general, the expression level of these pre-selected ISGs was much lower and their expression profile more prolonged as compared to 2fTGH. Only the *IFIT* family members had a clear expression peak at 8h (Figure 4.13 C). Likewise, in Huh ST1 K.O. expression of these ISGs was prolonged, but in addition even more delayed, shifting the expression profiles of all selected ISGs towards later time points while reaching comparable levels as in Huh7.5 (Figure 4.13 D). It also further proves, that in Huh ST1 K.O. IFN α -mediated ISG expression clearly depends on both STAT2 and IRF9, as early presence of only STAT2 is not sufficient for triggering gene expression and absence of IRF9 strongly delays the start of transcription, when compared to Huh7.5.

RESULTS

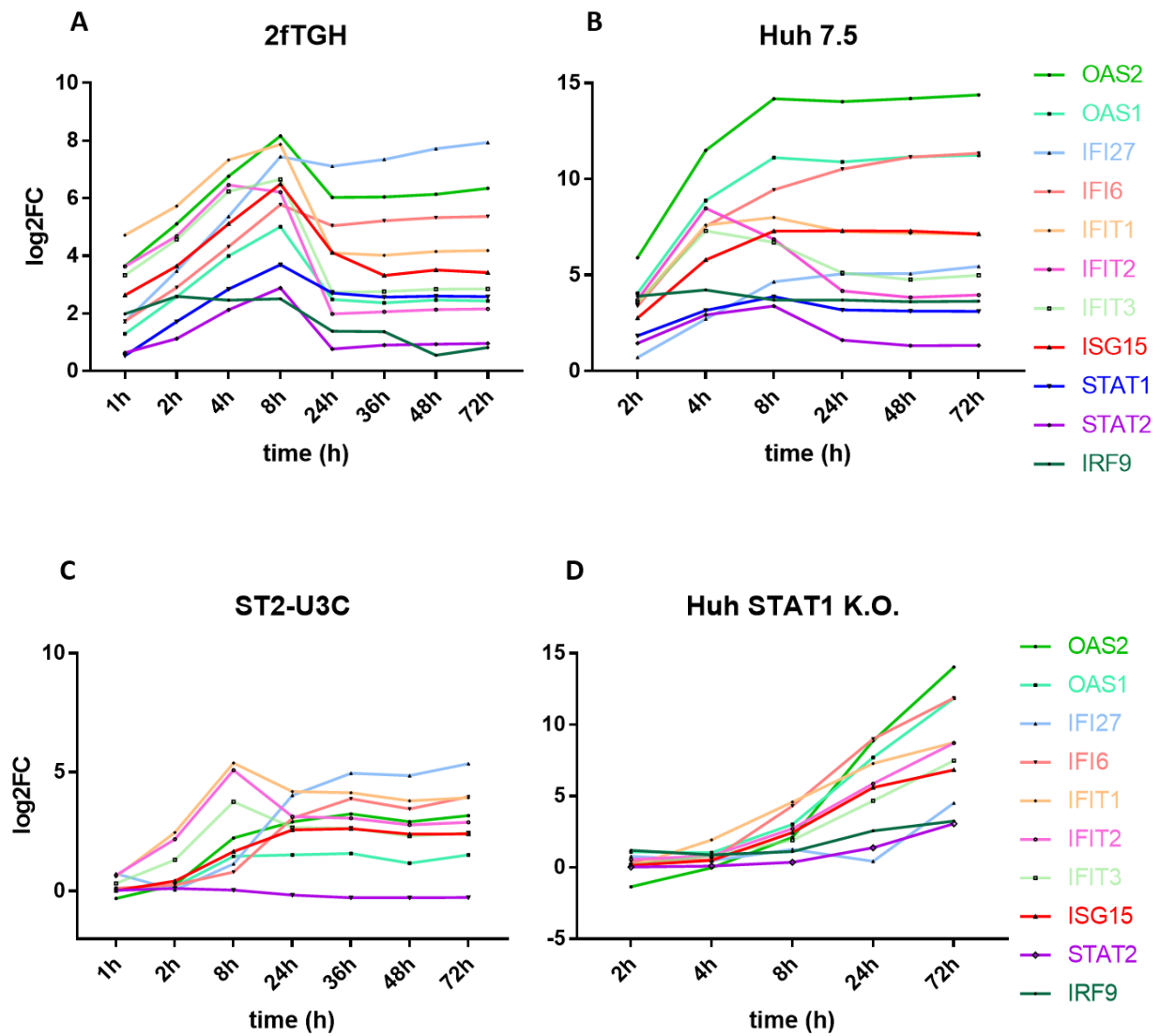
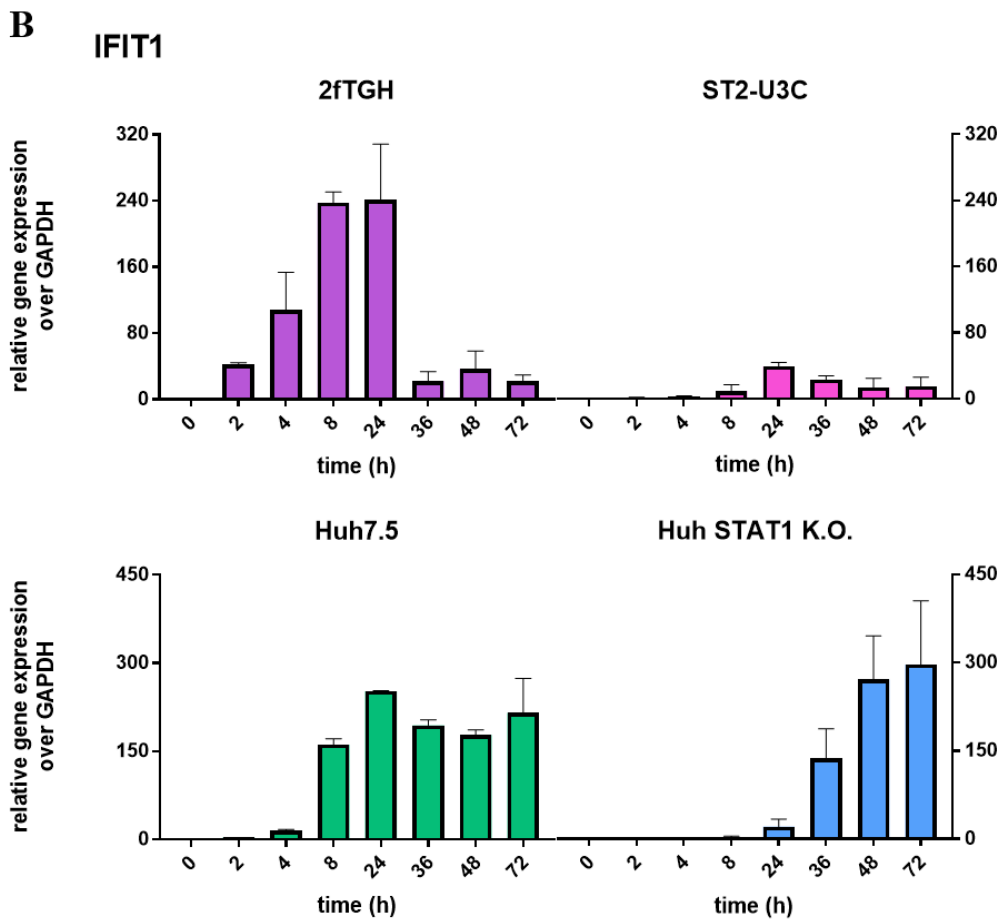
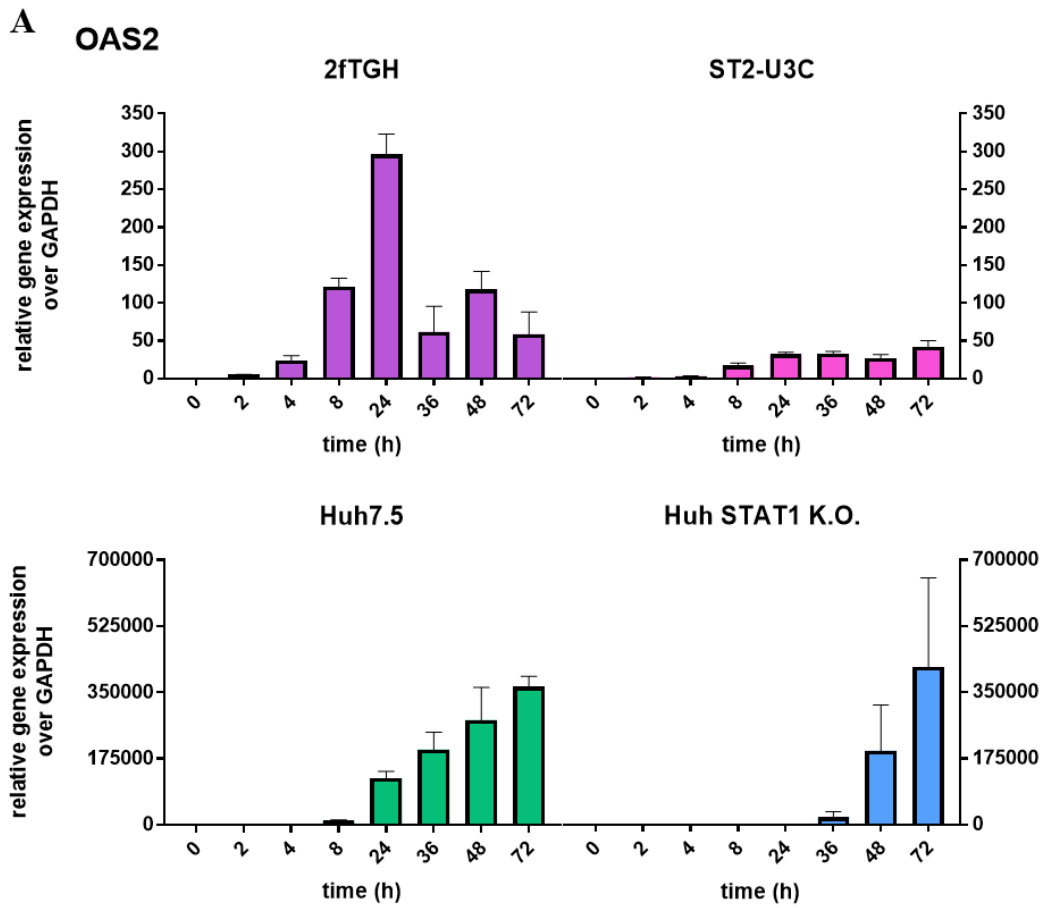


Figure 4.13 Characterization of selected commonly upregulated ISGs in the wild-type and STAT1 knock-out cell lines

The graphs represent gene expression profiles in selected commonly upregulated genes in 2fTGH (A), Huh7.5 (B), ST2-U3C (C) and Huh STAT1 K.O. (D). Gene expression is presented in logarithmic form.

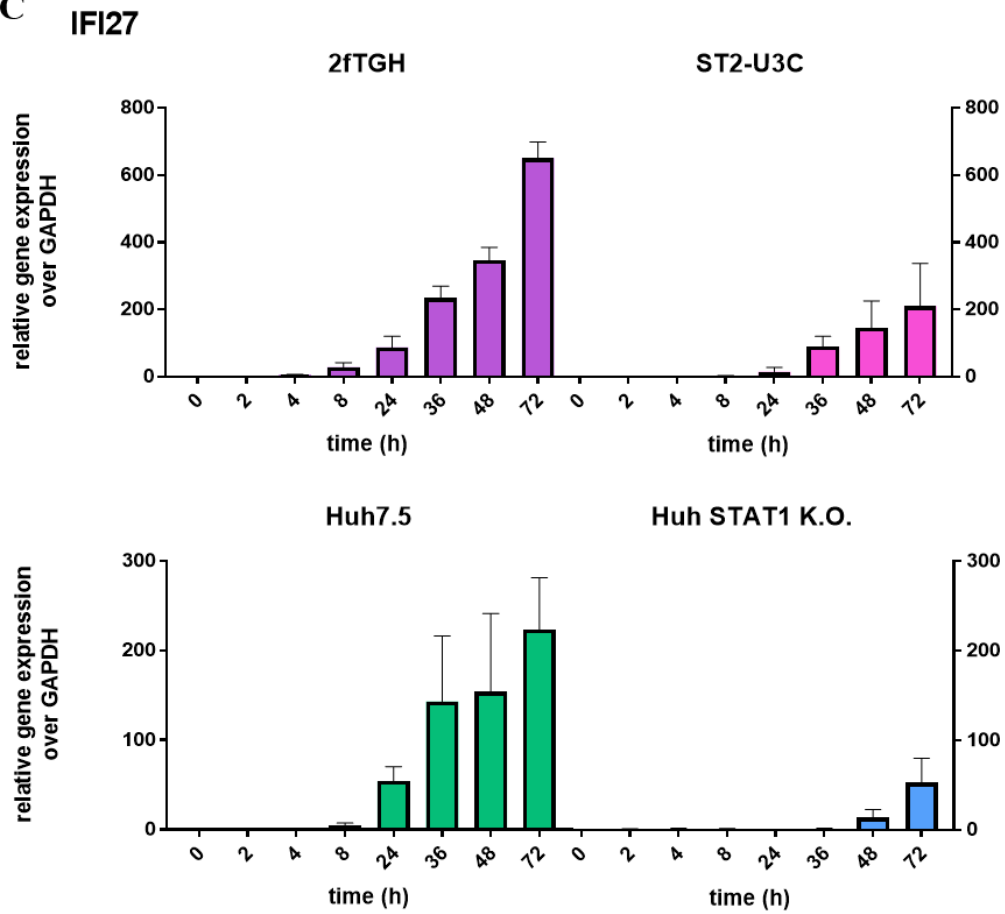
To validate the quality of our RNA-Seq dataset in general and the expression profiles observed for the pre-selected ISRE-containing antiviral ISGs (Fig 4.13), the expression of a number of these genes, including *OAS2*, *IFIT1*, *IFI27* and *IFI6*, was additionally confirmed by qPCR and compared in the four different cell lines (Figure 4.14).

RESULTS

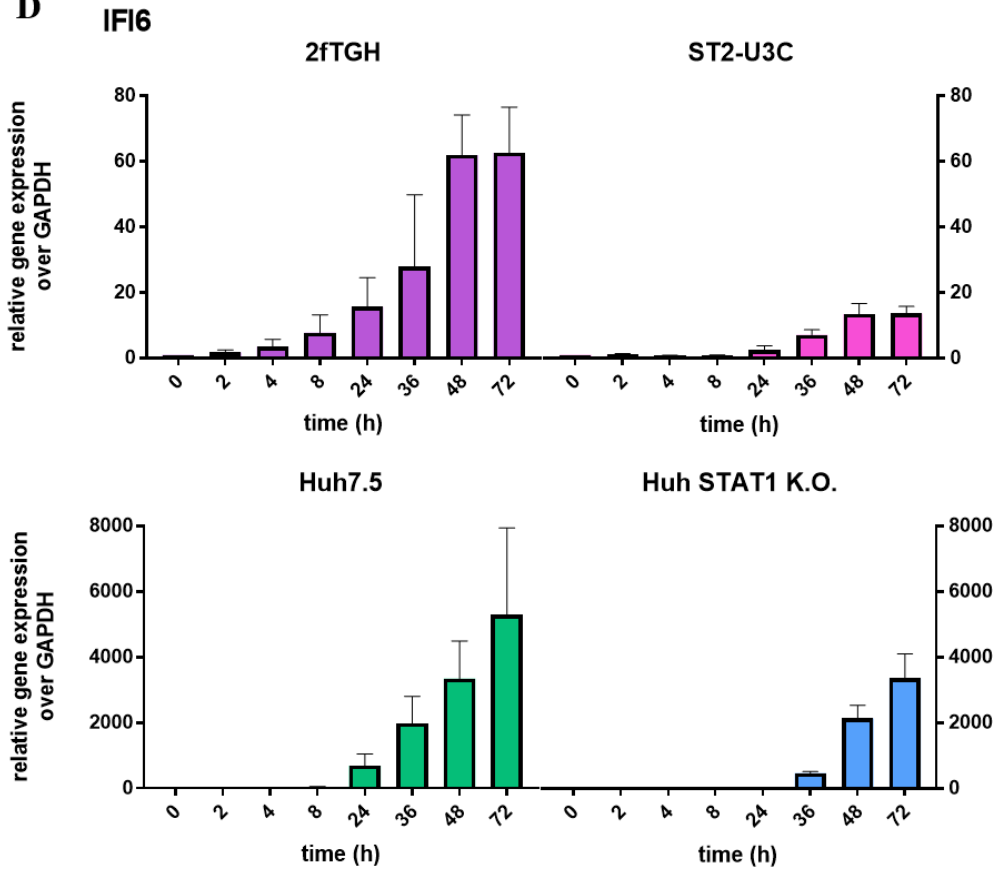


Figures explanation on the page 91

C



D



Figures explanation on the page 91

Figure 4.14. The gene expression profiles in the STAT1-deficient cell lines vs WT

Cells from 2fTGH (violet), ST2-U3C (pink), Huh7.5 (green) and Huh ST1 K.O. (blue) lines were treated with 1000 U/mL IFN α in indicated time course. The profiles of gene expression for selected IGS (OAS2, IFIT1, IFI27 and IFI6, shown in A, B, C and D, respectively) were estimated using qPCR method. Relative expression over GAPDH as a reference was estimated; n=2; mean +/- SEM.

Together these results provide evidence to suggest that in ST2-U3C and Huh ST1 K.O. cells a common IFN α -inducible and STAT1-independent transcriptional mechanism exists, that depends on the STAT2/IRF9 components STAT2 and IRF9 in a phosphorylation- and time-dependent, as well as cell-type-dependent manner. It also provides further prove for the previous observation that STAT2/IRF9 can take over the role of ISGF3 in the absence of STAT1, to regulate expression of a common group of ISRE-containing genes.

4.7. The genome-wide chromatin interactions in response to IFN α **ChIP-Seq**

Next, we characterized the genome-wide binding of the STAT2/IRF9 components to the regulatory regions of the 63 commonly IFN α induced genes. As such, chromatin immunoprecipitation (ChIP) experiments were performed on chromatin isolated from ST2-U3C and Huh ST1 K.O. cells treated with 1000U/mL of IFN α for 2, 24 and 72h, using antibodies against STAT2, pSTAT2 and IRF9. The obtained DNA was then sequenced and data was analysed as described in Material and Methods section.

After statistical analysis, under these conditions, the peak number distribution in ST2-U3C and Huh ST1 K.O. cells followed a prolonged pattern for all antibodies, without binding in untreated cells. The maximal peak number in ST2-U3C was observed at 2h, while in Huh ST1 K.O. it was shifted towards 24h. Moreover, in both cell lines STAT2, pSTAT2 and IRF9 binding peaks could still be detected after 72 hours. Additionally, the peak scores in ST2-U3C were generally much lower than in Huh ST1 K.O., which correlates with the gene expression pattern observed in these two cell lines (Figure 4.15). Collectively, the IFN α - and time-dependent distribution of STAT2, pSTAT2 and IRF9 binding in ST2-U3C and Huh ST1 K.O. correlated with the expression profile observed for the 63 commonly IFN α -induced genes

RESULTS

in the individual STAT1 K.O. cell lines (see Figure 4.10). It also confirms the ability of the STAT2/IRF9 complex to take over the role of ISGF3 in the absence of STAT1.

Subsequently, using HOMER software, ISRE consensus motifs (see Material and Methods, subsection 4.7.1.) were mapped to IFN α -induced STAT2, pSTAT2 and IRF9 binding regions of the 63 commonly IFN α -induced genes. Not surprisingly, all of these genes contained an ISRE binding site (not shown).

Closer inspection of the previously characterized pre-selected ISRE-containing antiviral ISGs (Figure 4.4), in general confirmed a correlation between gene expression and recruitment of STAT2, pSTAT2 and IRF9 in response to IFN α in ST2-U3C and Huh ST1 K.O..

Accordingly, for the majority of these genes in both cell lines, the binding profiles of STAT2, pSTAT2 and IRF9 were prolonged [as compared to their WT counterparts 2fTGH and Huh7.5 (Figure 4.8)] and resemble the peak distribution as shown in Figure 4.15. In ST2-U3C, a prolonged pattern was detected for all three components, with maximum at 2h of IFN α stimulation, and clear dependence on treatment (no basal binding). Moreover, significant binding could still be detected at 24 and 72 hours (Figure 4.16 A). On the contrary, in Huh ST1 K.O. the binding of STAT1, STAT2 and IRF9 was, in general, higher and much more prolonged (Figure 4.16 B), while being absent in untreated cells and showing minimal binding at 2h and strong binding at 24 and 72h of IFN α stimulation. Importantly, a similar cell-type dependent binding pattern was observed for pSTAT2 and STAT2 in the two STAT1 K.O. cell lines, as was also true for pSTAT1 and pSTAT2 vs STAT1 and STAT2 in both WT cell lines (compare Figures 4.8 and 4.16).

RESULTS

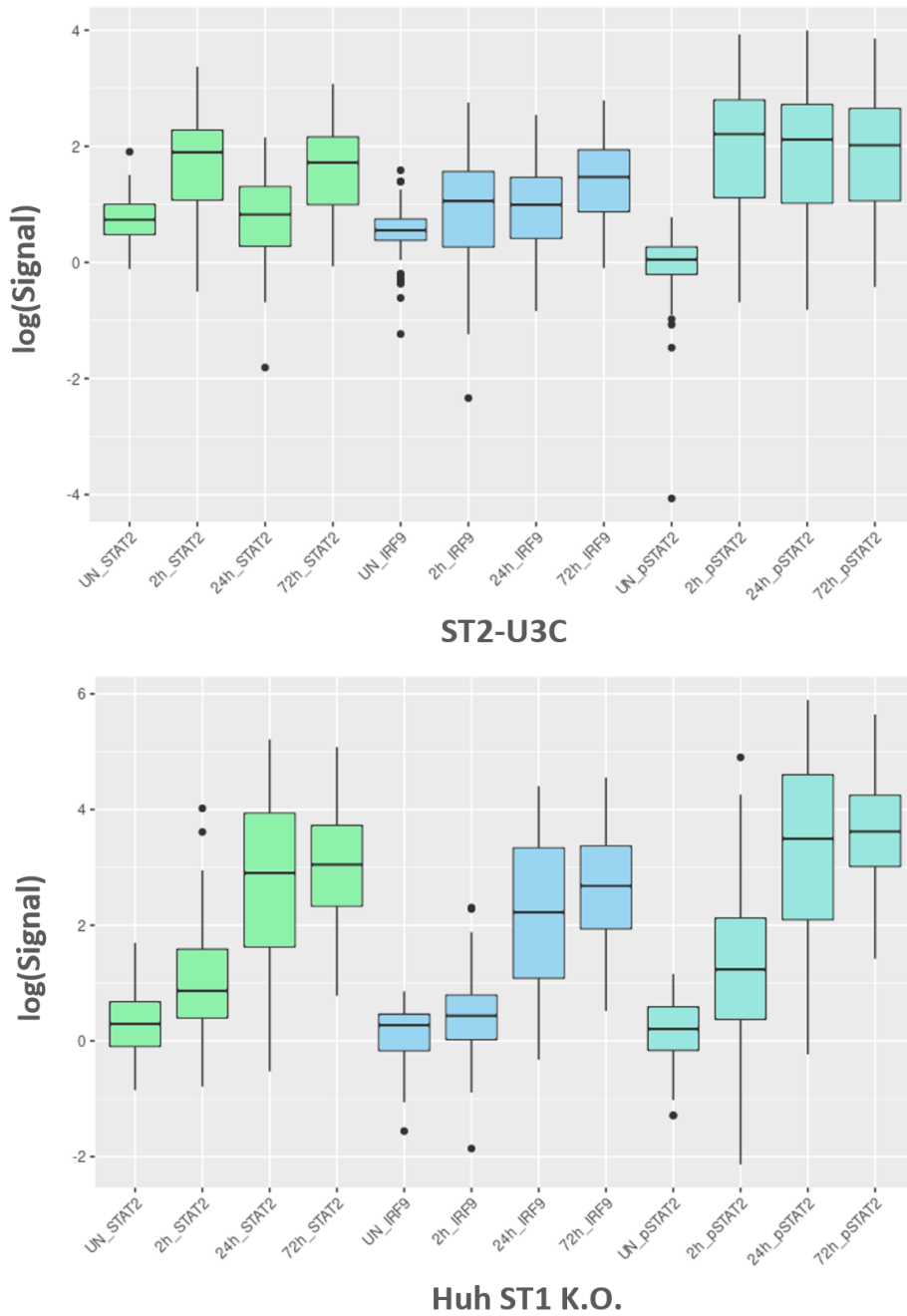


Figure 4.15 Peak distribution of particular antibodies

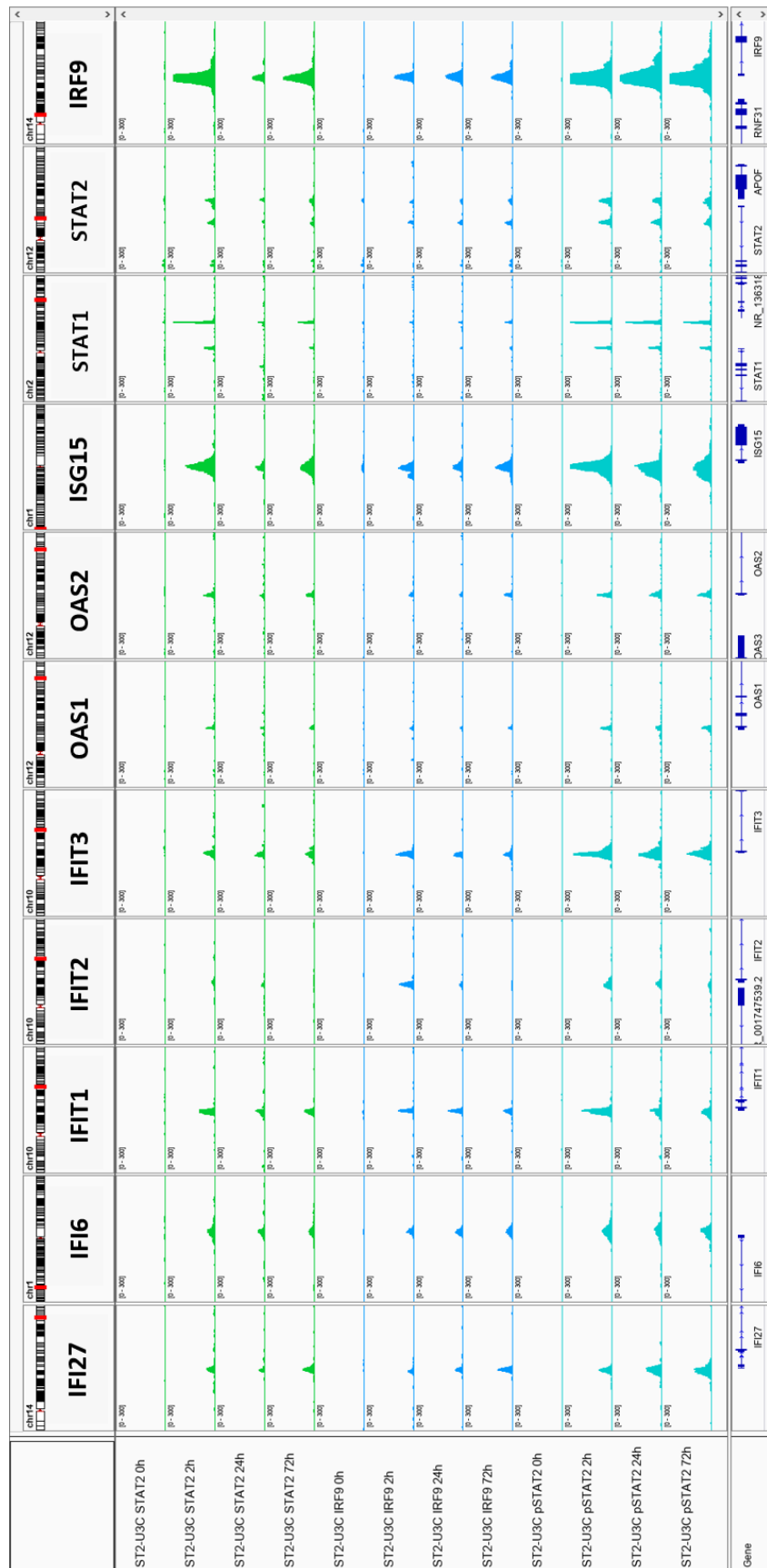
Boxplot represents the normalized scores of STAT2 (green bars), IRF9 (blue bars) and pSTAT1 (turquoise bars) binding peaks to the promoters of 63 commonly upregulated genes in ST2-U3C and Huh ST1 K.O. vs 2fTGH and Huh7.5 (see Figure 4.11 and text on the page 84)

Figure 4.16
Characterization of different ISGF3 components recruitment to the regulatory regions of ISGs under IFN α treatment in the absence of STAT1 protein

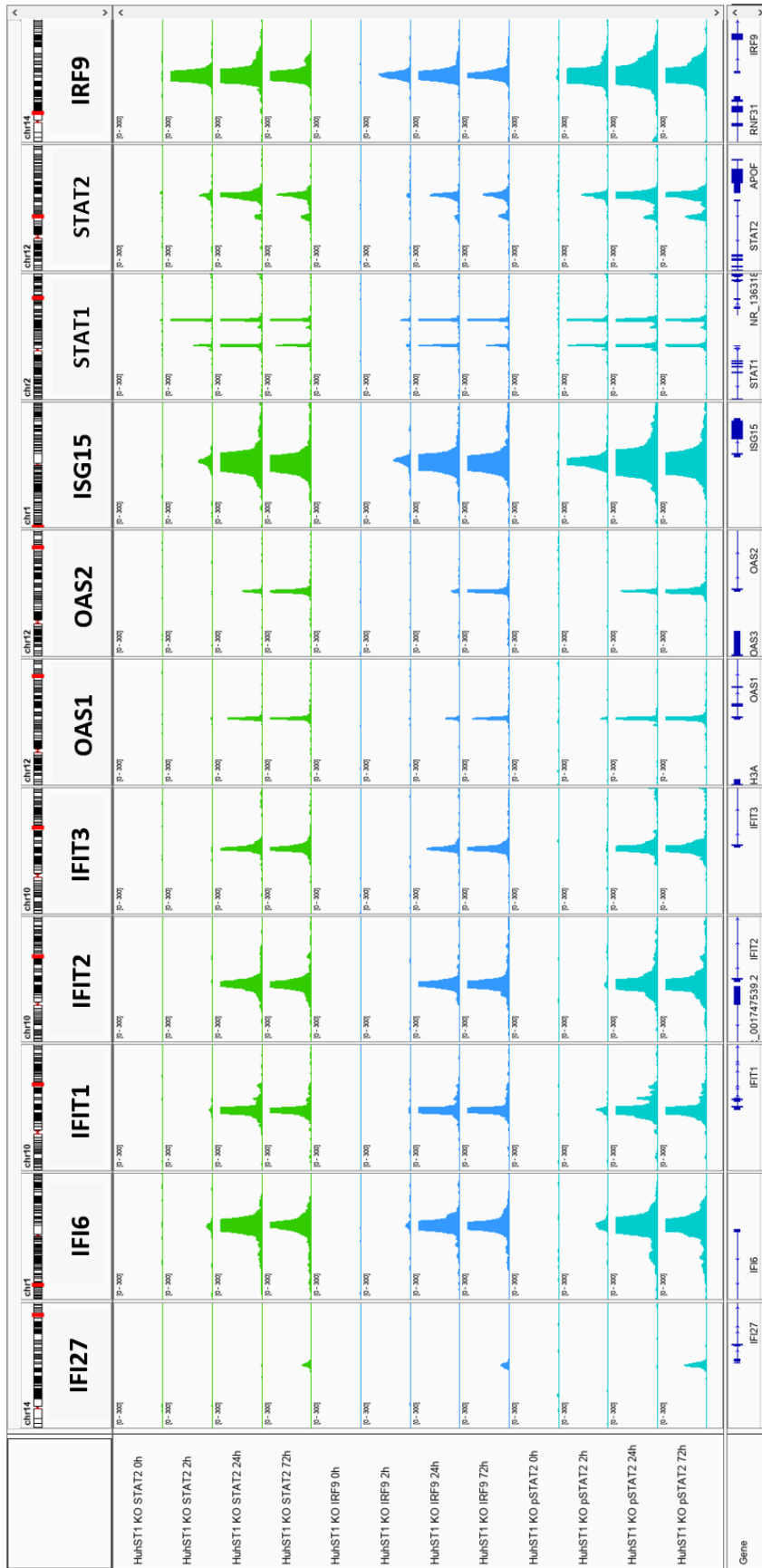
Representative views of the ChIP-Seq peaks detected in the promoter regions of selected ISGs, in the ST2-U3C (A) and Huh ST1 K.O. (B) cell lines untreated or treated with IFN α for indicated time course. All peaks were mapped onto the human reference genome hg38 and visualized using the Integrative Genomic Viewer (IGV). Scale is 0-300.

Figure B showed on the next page

A



B



RESULTS

These observations are in agreement with the gene expression profiles from both, RNA-Seq, and qPCR results shown in Figure 4.3, 4.5 and 4.6. It clearly indicates, that in the absence of STAT1, STAT2/IRF9 (pSTAT2 + IRF9) is important in long-term ISG expression even after 72h. It also points to a cell-type-dependent role of STAT2/IRF9, which correlates with the different phosphorylation and expression profiles and chromatin binding patterns of STAT2 and IRF9 observed in ST2-U3C and Huh ST1 K.O.. However, increased protein expression and binding of STAT2 and IRF9 at later time points cannot rule out an additional role of U-STAT2/IRF9 (U-STAT2 + IRF9) in prolonged ISG expression in both cell-types as well.

Summarizing the results described in PART I and II, we can conclude that gene expression profile correlates with phosphorylation pattern of STAT1 and/or STAT2 together with IRF9 under wild-type, as well as STAT1 K.O. conditions. Additionally, these observations correspond to interactions of tested transcription factors with the ISG promoters in all tested cell types. This confirm the function of STAT2/IRF9 as a potent equivalent of ISGF3. However, the accumulation of unphosphorylated forms of STAT1 and STAT2, as well the IRF9 protein rises a question of the role of phosphorylation in the regulation of the long lasting antiviral response. To prove or exclude the role of the phosphorylation event we performed a series of experiments with the use of JAK inhibitor I, which results are presented below, in the PART III. Additionally, we observed the increased basal ISGs expression in ST2-U3C when compare to wild-type cells. This made us to consider the potential role of unphosphorylated ISGF3-based complexes in mediating constitutive ISG expression. This hypothesis will be tested in the PART IV A.

PART III

The role of phosphorylation of ISGF3 and STAT2/IRF9 in time-dependent IFN α -activated transcriptional responses

4.8. The role of phosphorylation of ISGF3 in the regulation of prolonged ISG expression under wild type conditions

Western blotting and qPCR

As shown in Figure 4.1 A, in 2fTGH phosphorylation of STAT1 and STAT2 was highly induced upon IFN α treatment with an early, transient increase between 1 and 4 h, after which it rapidly diminished to undetectable levels at 72h. A similar early and transient IFN α -dependent STAT1 and STAT2 phosphorylation pattern was observed in Huh WT (Figure 4.1 B), with a clear drop between 4 and 8h after treatment. However, in these cells the phosphorylation of STAT1 and STAT2 remained slightly higher at later time points, and was still clearly visible after 72h.

To address the role of phosphorylation of STAT1 and STAT2, especially in long-term IFN-I activated transcriptional responses, experiments with JAK Inhibitor I (JII) were performed. JII is a potent compound that inhibits activity of all 4 Janus kinases, and because of this, it blocks IFN α -dependent phosphorylation of STAT1 and STAT2.

Accordingly, 2fTGH and Huh7.5 cells treated with 1000U/mL of IFN α alone for 0, 1, 2, 4, 8, 24, 36, 48 and 72h were compared to cells treated with IFN α alone for 0, 1, 2, 4h, and for 8, 24, 36, 48 and 72h together with JII (added after 6h of IFN treatment, at each time-point) (Figure 4.17). As becomes clear, addition of JII resulted in a complete block of STAT1 and STAT2 phosphorylation in 2fTGH at 8, 24, 36, 48 and 72h. Likewise, in Huh7.5 phosphorylation was inhibited at each of these time-points, except at 8h, where weak phosphorylation of STAT1 and STAT2 was still visible. In both cell types, increased production of total STAT1, STAT2 and IRF9, observed after long-term IFN α -treatment, was also impacted by the addition of JAK Inhibitor I. However, expression was still detectable. This predicts a role of STAT1 and STAT2 phosphorylation in the long-term expression of ISGF3 components and in the action of the ISGF3, and potentially U-ISGF3, complexes at later time-points in 2fTGH and Huh7.5 cells.

RESULTS

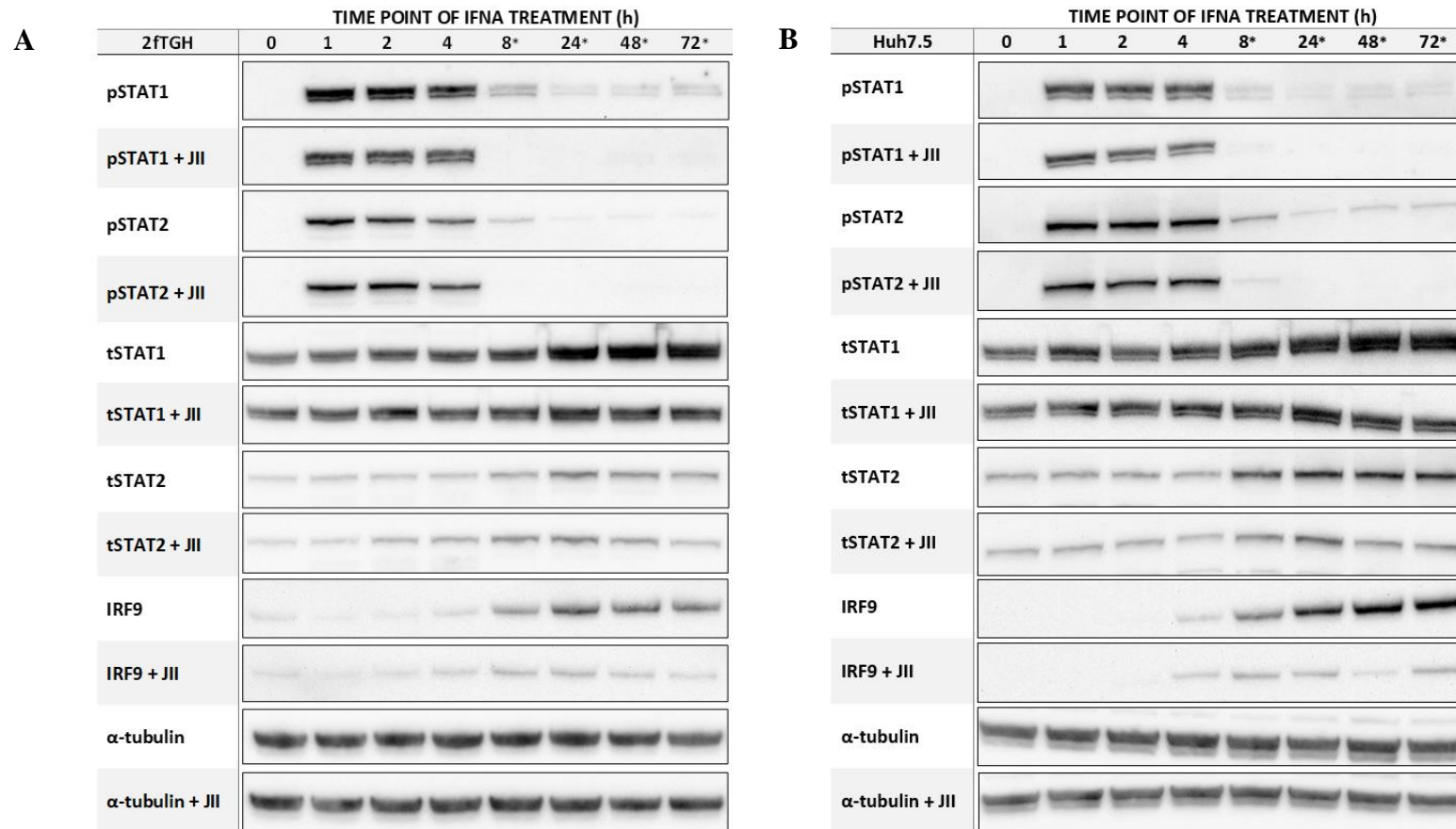


Figure 4.17 The protein levels and phosphorylation profiles in the 2fTGH and Huh7.5 cell lines upon treatment with JAK Inhibitor I

Western blot analysis of STAT1, STAT2, IRF9 and IRF1, as well as α-tubulin, were done on 2fTGH (A) and Huh7.5 (B) to estimate the protein levels and their phosphorylation profiles. Two sets of cells were stimulated with 1000U/mL of IFNα for the indicated time course or left untreated. Next, cells in time points of 8, 24, 48 and 72h in one set (marked with *) were treated with JAK Inhibitor I (JII) for 6h after each IFNα addition and left till the end of treatment.

(p – phosphorylated, t - total)

RESULTS

Under the same conditions, we studied the effect of JII treatment on the long-term IFN α -induced expression of a selection of ISGs, including *OAS2*, *IFIT1*, *IFI27* and *IFI6*, by qPCR (Figure 4.18 and 4.19, respectively). In both cell lines, addition of JII dramatically decreased expression of these genes after 8h of IFN α treatment, which correlated with a block in STAT1 and STAT2 phosphorylation. Interestingly, gene expression was not completely inhibited under these conditions, and was still present above basal levels.

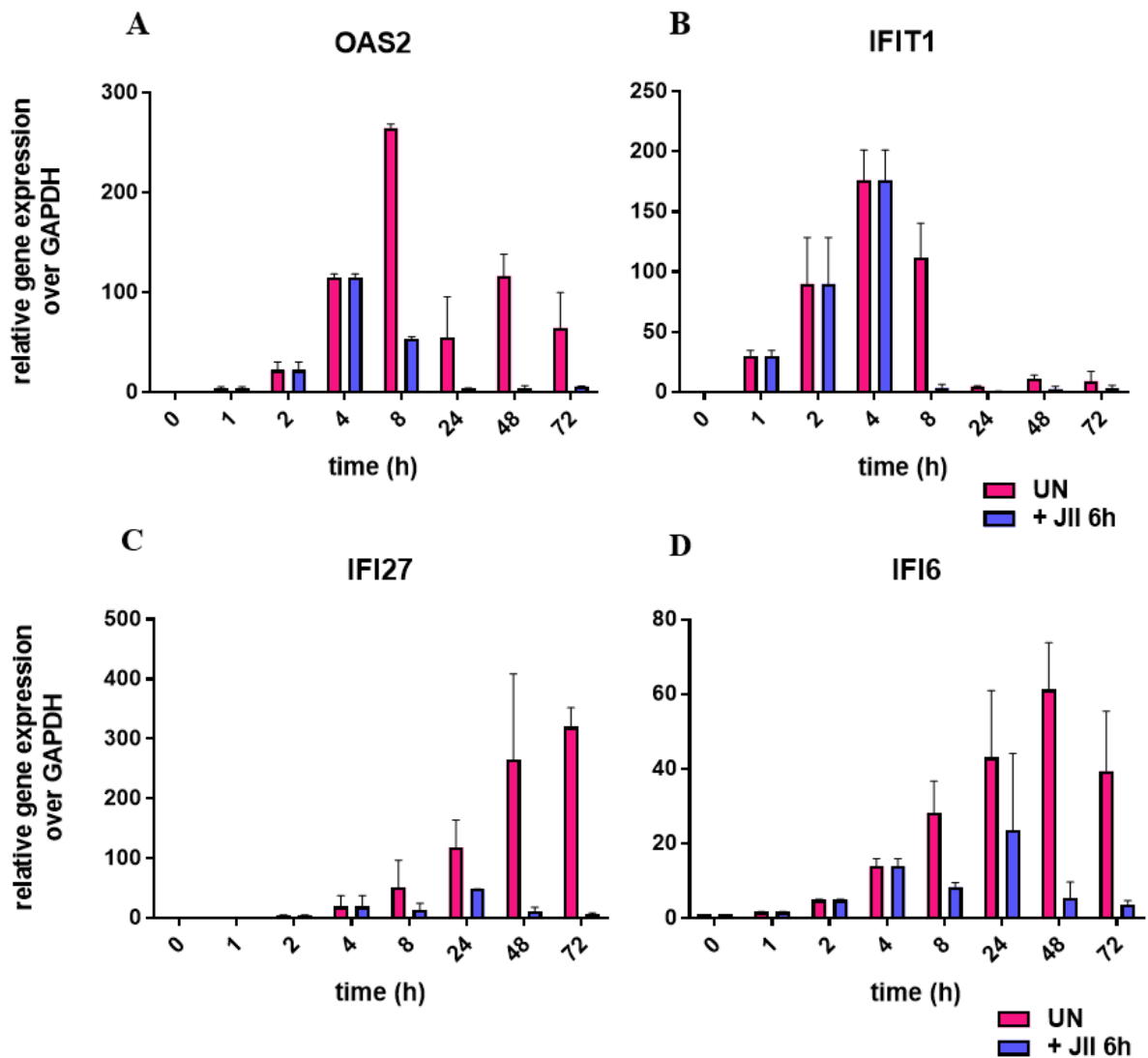


Figure 4.18 The gene expression profile in the 2fTGH cell lines untreated and treated with JAK Inhibitor I

Two sets of cells were stimulated with 1000 U/mL IFN α in indicated time course. Next, cells in time points of 8, 24, 48 and 72h in one set were also treated with JAK Inhibitor I (JII) for 6h. The profiles of gene expression for showed ISGs (*OAS2*, *IFIT2*, *IFI27* and *IFI6* on graph A, B, C and D, respectively) were estimated using qPCR method. Relative expression over GAPDH as a reference was estimated; n=2; mean \pm SEM. The expression profiles for 2fTGH treated with JII are indicated in orange colour, while untreated in green.

RESULTS

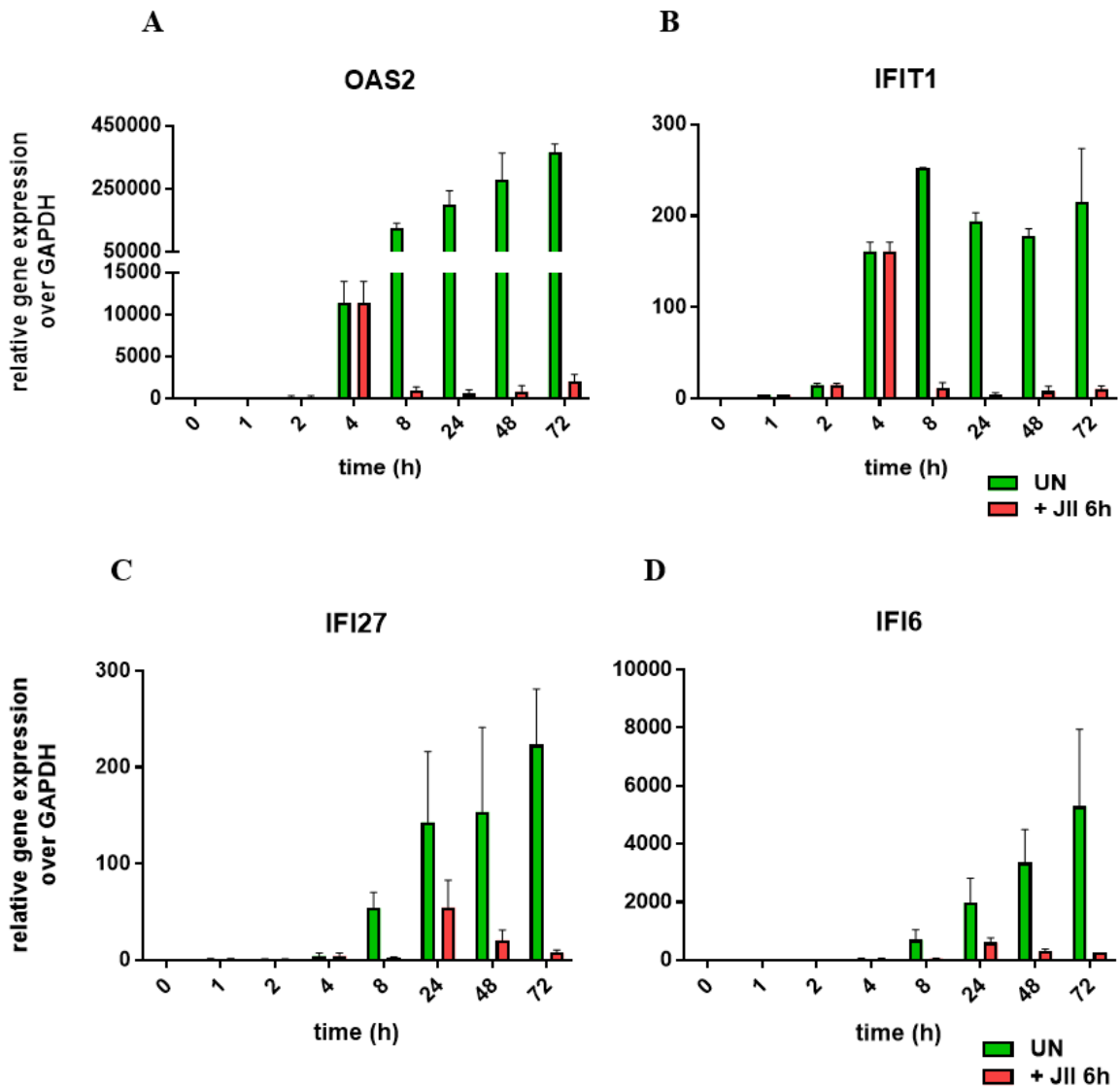


Figure 4.19 The gene expression profile in the Huh7.5 cell lines untreated and treated with JAK Inhibitor I

Two sets of cells were stimulated with 1000 U/mL IFN α in indicated time course. Next, cells in time points of 8, 24, 48 and 72h in one set were also treated with JAK Inhibitor I (JII) for 6h after each IFN α addition and left till the end of treatment. The profiles of gene expression for showed ISGs (OAS2, IFIT2, IFI27 and IFI6 on graph A, B, C and D, respectively) were estimated using qPCR method. Relative expression over GAPDH as a reference was estimated; n=2; mean +/- SEM. The expression profiles for Huh7.5 treated with JII are indicated in orange colour, while untreated in green.

RESULTS

Together, these findings show that phosphorylation is a key factor in the regulation of prolonged ISG expression in 2fTGH and Huh7.5. It also strongly suggests that classical ISGF3 is the predominant complex that mediates both early and prolonged ISG expression. However, low but sustained levels of IFN-activated ISG expression, still detected in the presence of JII, correlates with the low, but significant, levels of unphosphorylated STAT1, STAT2 and IRF9, which may form U-ISGF3 and regulate transcription.

4.9. The role of phosphorylation of STAT2/IRF9 in prolonged IFN α signalling in the absence of STAT1

Western blotting and qPCR

To study the role of phosphorylation in prolonged IFN α signalling in the absence of STAT1, experiments with the use of JAK Inhibitor I in ST2-U3C and Huh ST1 K.O. cells were performed, similar to those performed on wild-type cells (see above, Figure 4.17). As expected, phosphorylation of STAT2 was significantly diminished after treatment with JII and no longer detectable in both ST2-U3C and Huh ST1 K.O after 48 and 72h of IFN α treatment (Figure 4.20, A and B, respectively). Interestingly, when compared to wild-type cells, in STAT1-deficient cells phosphorylation of STAT2 upon JII addition was observed much longer – it was still detectable at 24h (Compare with figures 4.18 and 19). This may suggest, that in the absence of STAT1, STAT2 phosphorylation is stronger than in wild-type cell lines. Like in WT cells, JII addition also significantly hampered the IFN-dependent increased production of STAT2 and IRF9, although more dramatically in Huh ST1 K.O cells than in ST2-U3C. In Huh ST1 K.O. expression of IRF9 was even no longer detectable upon JII treatment.

These observations suggest, that in the STAT1-deficient cell lines, long-term expression of STAT2 and IRF9 is highly dependent on phosphorylation of STAT2 itself. It also points to the crucial role of STAT2/IRF9, and potentially U- STAT2/IRF9, in prolonged IFN α signalling in the absence of STAT1 in ST2-U3C and Huh ST1 K.O cells.

RESULTS

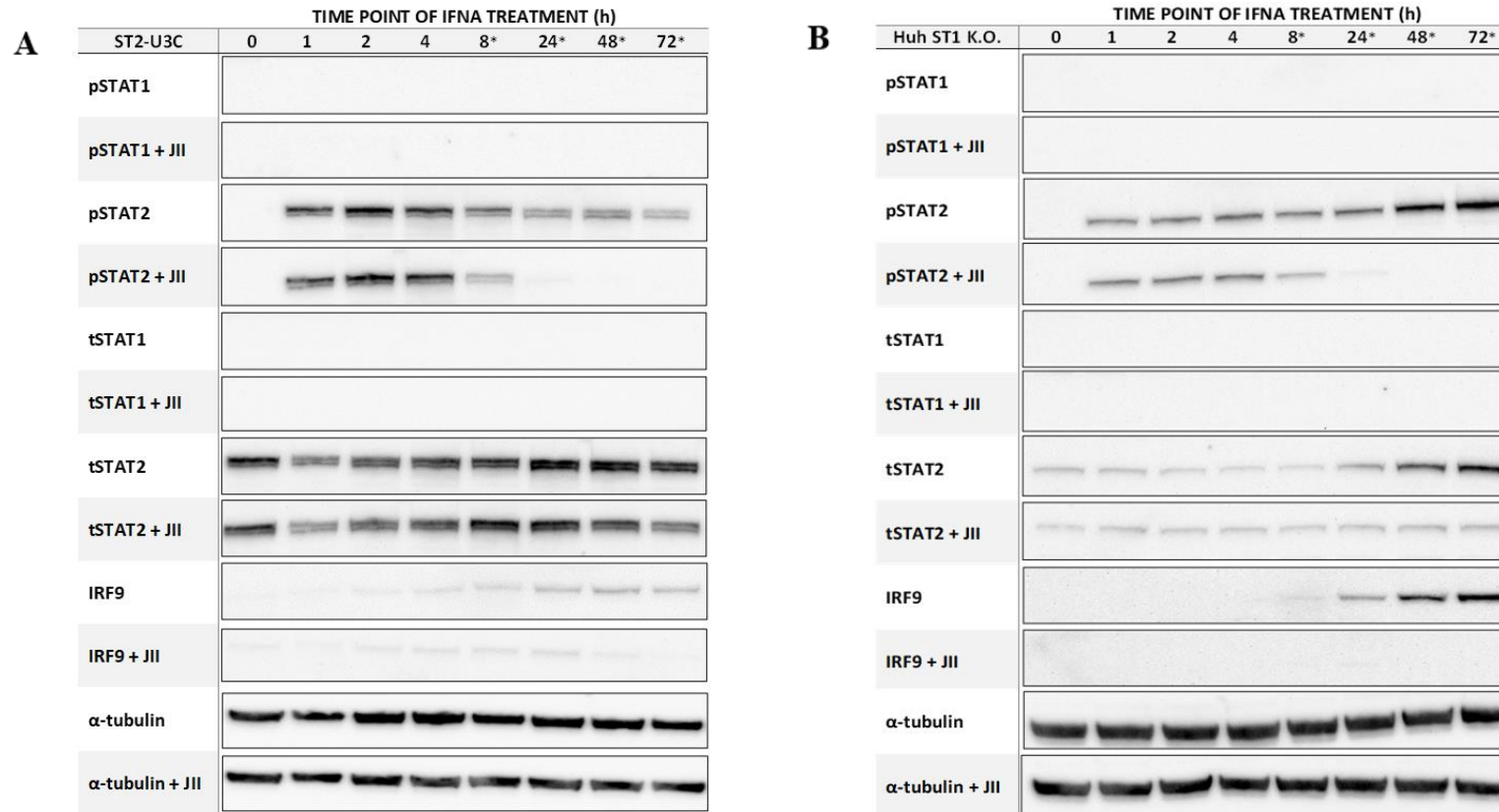


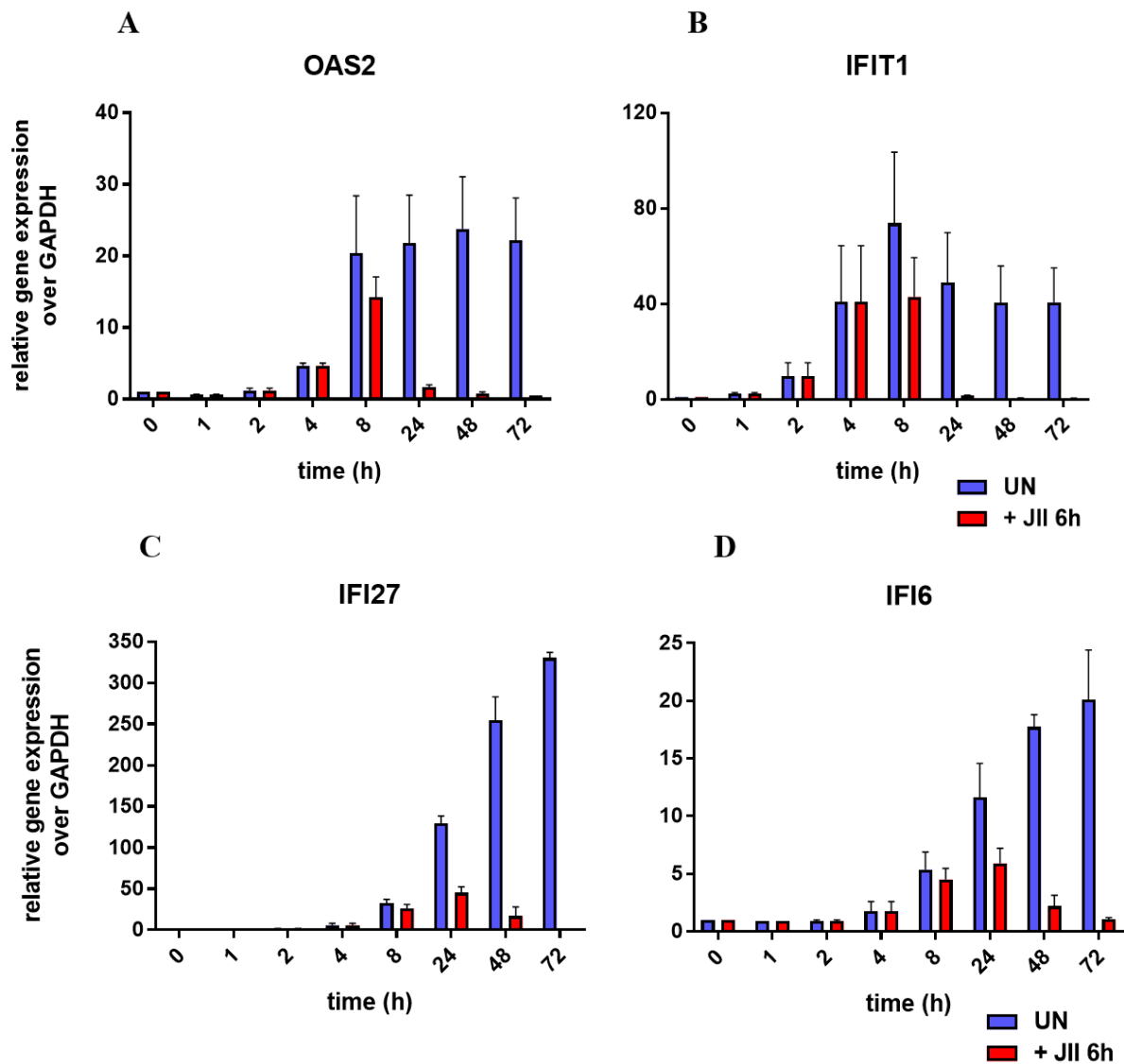
Figure 4.20 The protein levels and phosphorylation profiles in the ST2-U3C and Huh ST1 K.O. cell lines upon treatment with JAK Inhibitor I

Western blot analysis of STAT1, STAT2, IRF9 and IRF1, as well as α-tubulin, were done on ST2-U3C (A) and Huh ST1 K.O. (B) to estimate the protein levels and their phosphorylation profiles. Two sets of cells were stimulated with 1000U/mL of IFNα for the indicated time course or left untreated. Next, cells in time points of 8, 24, 48 and 72h in one set (marked with *) were treated with JAK Inhibitor I (JII) for 6h after each IFNα addition and left till the end of treatment.

(p – phosphorylated, t - total)

RESULTS

Under the same conditions, we studied the effect of JII treatment on the long-term IFN α -induced expression of *OAS2*, *IFIT1*, *IFI27* and *IFI6*, in the absence of STAT1, in ST2-U3C and Huh ST1 K.O. by qPCR (Figure 4.21 and 4.22, respectively). In both cell lines, addition of JII dramatically decreased expression of *OAS2*, *IFIT1*, *IFI27* to undetectable levels at 48 and/or 72h of IFN α treatment. This correlated with a block in STAT2 phosphorylation. Interestingly, expression of *IFI6* was not completely inhibited under these conditions, suggesting involvement of a phosphorylation-independent mechanism for this gene.



Figures explanation on the next pages

Figure 4.21 The gene expression profile in the ST2-U3C cell lines untreated and treated with JAK Inhibitor I

Two sets of cells were stimulated with 1000 U/mL IFN α in indicated time course. Next, cells in time points of 8, 24, 48 and 72h in one set were also treated with JAK Inhibitor I (JII) for 6h after each IFN α addition and left till the end of treatment. The profiles of gene expression for showed ISGs (OAS2, IFIT2, IFI27 and IFI6 on graph A, B, C and D, respectively) were estimated using qPCR method. Relative expression over GAPDH as a reference was estimated; n=2; mean +/- SEM. The expression profiles for ST2-U3C treated with JII are indicated in blue colour, while untreated in red.

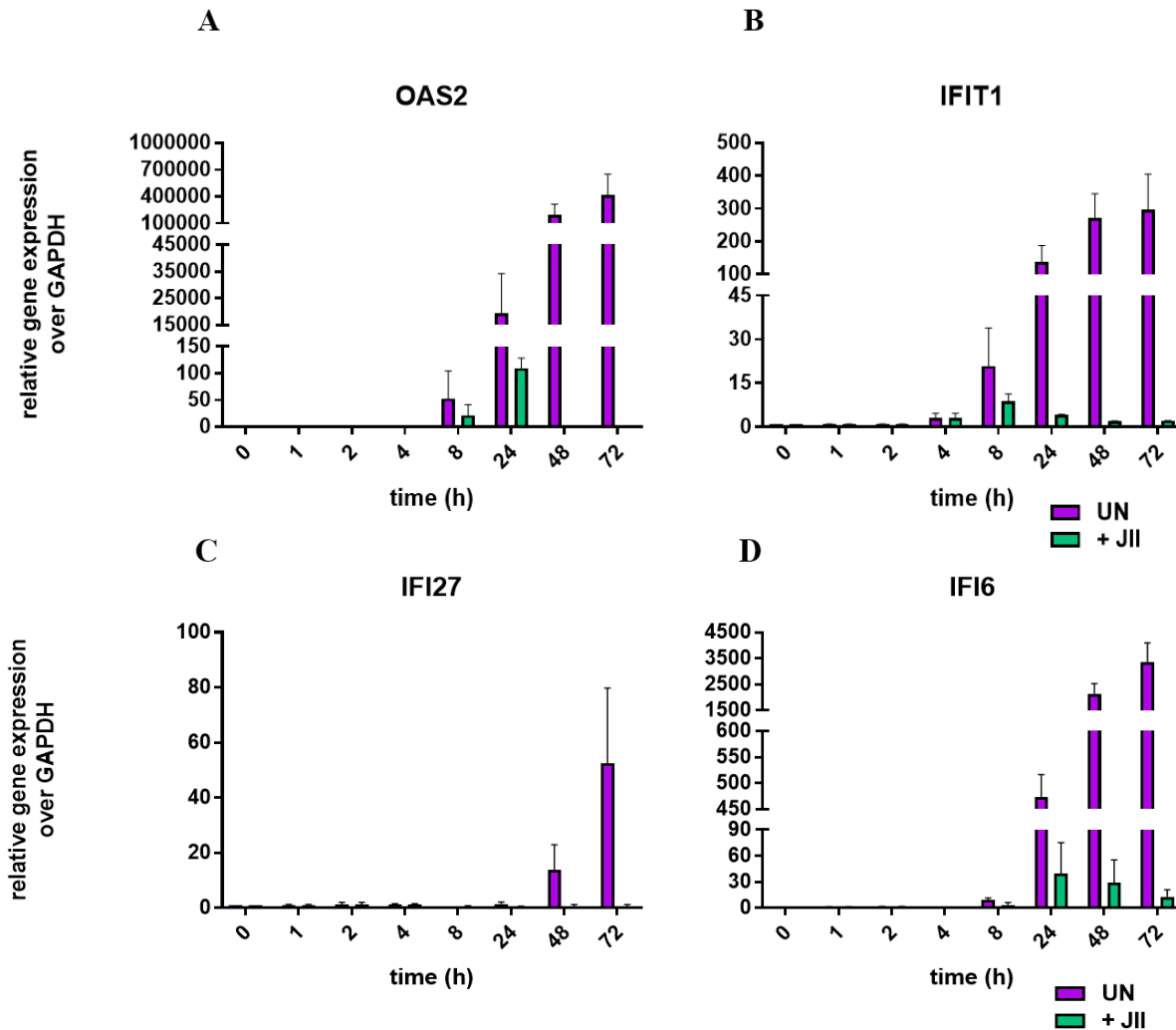


Figure 4.22 The gene expression profile in the Huh ST1 K.O. cell lines untreated and treated with JAK Inhibitor I

Two sets of cells were stimulated with 1000 U/mL IFN α in indicated time course. Next, cells in time points of 8, 24, 48 and 72h in one set were also treated with JAK Inhibitor I (JII) for 6h after each IFN α addition and left till the end of treatment. The profiles of gene expression for showed ISGs (OAS2, IFIT2, IFI27 and IFI6 on graph A, B, C and D, respectively) were estimated using qPCR method. Relative expression over GAPDH as a reference was estimated; n=2; mean +/- SEM. The expression profiles for Huh ST1 K.O. treated with JII are indicated in violet colour, while untreated in turquoise.

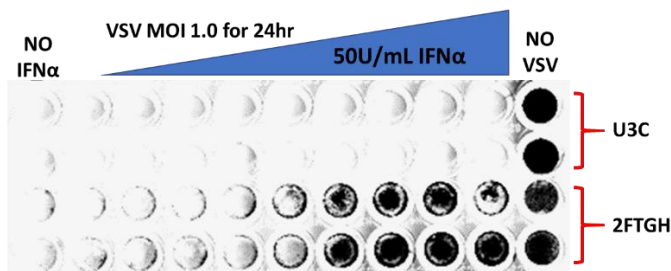
RESULTS

Together, these findings show, that phosphorylation is a key factor in the regulation of prolonged ISG expression in the absence of STAT1. It also strongly suggests, that STAT2/IRF9 is the predominant complex that mediates both early and prolonged ISG expression in ST2-U3C and Huh ST1 K.O. cells. In STAT1 deficient cells, especially in Huh ST1 K.O., the IRF9 level was no longer detectable in 72h, that excludes the possibility of forming U-STAT2/IRF9, that could drive the long-lasting ISG expression. Moreover, only *IFI6* expression was clearly sustained in these cells.

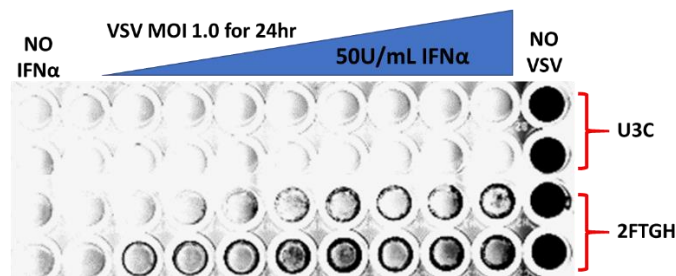
4.10. The role of phosphorylation in viral protection of the 2fTGH cells

To address the role of phosphorylation in protection of 2fTGH cells from viral infection, we performed the antiviral assay and examined the effect of JII treatment (Figure 4.23).

A. no JII



B. + JII 4h



C. + JII 25h

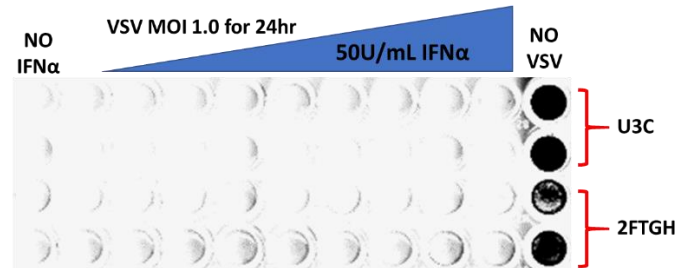


Figure 4.23 The role of phosphorylation in antiviral protection of the 2fTGH cells

The 2fTGH cells were treated with 2-fold serial dilution of IFNα starting from 50U/mL left for 24h. After this time cells were infected with VSV at MOI of 1.0 for 24h. During this infection time, cells on the middle plate (B) were treated with JII for 4h, cells on lower plate (C) – for 25h, and cells on the upper plate (A) left untreated. Finally, results were visualized by crystal violet staining - the black wells indicate the living cells.

RESULTS

Like in Figure 4.9 cells were treated with a 2-fold serial dilution of IFN α [starting from 50U/mL (Figure 4.23)] and left for 24h and then infected with Vesicular stomatitis Indiana virus (VSV) at a MOI of 1.0. During this infection time, cells were treated with JII for 4h or 25h. The STAT1-deficient U3C cell line was used as a control. The results clearly showed that in 2fTGH, viral protection is strongly dependent on phosphorylation. Consequently, addition of JAK Inhibitor I rendered these cells more sensitive to VSV infection. Pre-treatment of cells with IFN α could not effectively protect from virus-dependent lysis. Importantly, 4h of stimulation with JII only partially impaired IFN α -mediated 2fTGH viral protection. However, addition of JII for 25h completely blocked viral protection. As shown above (Figure 4.17), this correlates not only with the inhibition of IFN-induced phosphorylation of STAT1 and STAT2, but also of the long-term expression of STAT1, STAT2 and IRF9. This provides additional proof for the importance of phosphorylation and increased expression of the ISGF3 components in mediating long-term IFN-dependent antiviral responses.

Taking into account the results presented in PART I, II and III, we can conclude, that there is high dependence of prolonged ISG expression on the phosphorylation event in both, wild-type and STAT1-deficiency conditions. As so, ISGF3 is the key mediator of IFN α - and time-dependent response in 2fTGH and Huh7.5, and STAT2/IRF9 – in ST2-U3C and Huh ST1 K.O. However, showed data, especially the accumulation of total STAT1, STAT2 and IRF9 over time, together with the sustained low ISG expression upon JII treatment may imply the potential role of U-ISGF3. Nevertheless, in the STAT1 K.O. cells, the prolonged ISG expression is diminished faster to basal level (with an exclusion of *IFI6*) and IRF9 is undetectable upon JII stimulation, thus the role of U-STAT2/IRF9 is excluded.

PART IV A

**The basal ISG expression regulation under conditions
with the abundance of ISGF3 components**

4.11. The role of abundance of ISGF3 components in the regulation of the basal ISG expression

A role of unphosphorylated STATs has been shown in the transcriptional regulation of ISGs in an IFN- α -independent manner (W. Wang et al. 2017)(H. Cheon et al. 2013). In this respect, increased basal expression of a selection of ISGs was observed in ST2-U3C cells, as compared to U3C in the absence of IFN α treatment (Błaszczyk et al. 2015). Recently, we generated the ST2-IRF9-U3C variant, overexpressing both STAT2 and IRF9, and studied the IFN α -dependent and -independent ISG expression in comparison to ST2-U3C and U3C (Figure 4.24). As expected, IFN-induced expression of *OAS2*, *IFI27* and *IFI6* was the highest in

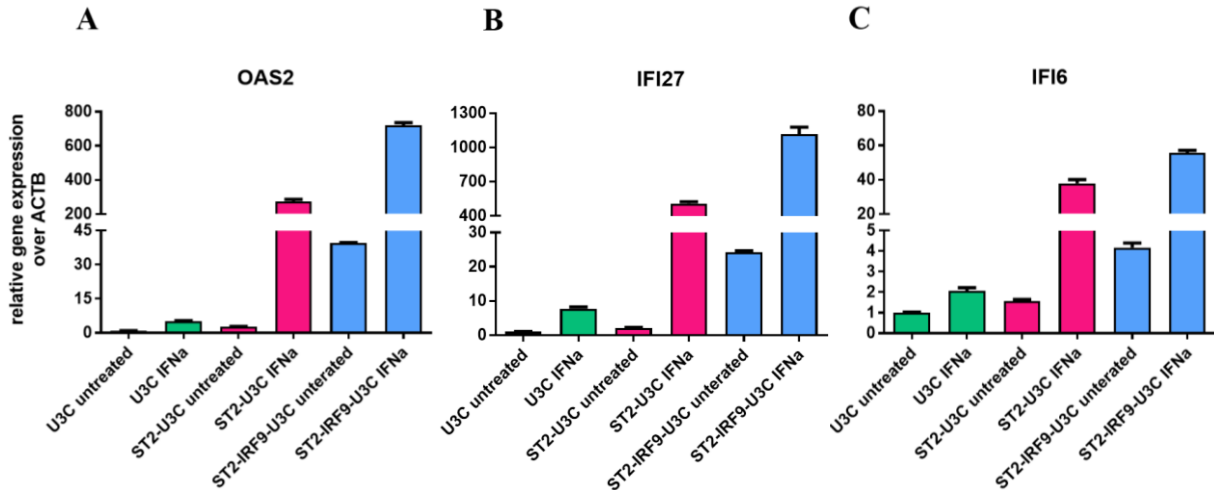


Figure 4.24 The gene expression level in the U3C, ST2-U3C and ST2-IRF9-U3C cell lines upon IFN α stimulation

The U3C (green) ST2-U3C (pink) and ST2-IRF9-U (blue) cell lines were stimulated with 1000 U/mL IFN α for 24h. The profiles of gene expression for showed ISGs (*OAS2*, *IFI27* and *IFI6* on graph A, B and C, respectively) were estimated using qPCR method. Relative expression over ACTB as a reference was estimated; n=2; mean +/- SEM.

The ST2-U3C and ST2-IRF9-U3C cell lines were generated by Katarzyna Błaszczyk and Aleksandra Antończyk, respectively.

RESULTS

ST2-IRF9-U3C, correlating with the increased levels of phosphorylated ISGF3 components (not shown). Likewise, IFN-independent expression of these genes was also significantly higher in ST2-IRF9-U3C, which could point to a regulatory role of U-ISGF3 or U-STAT2/IRF9 in basal ISG expression (Figure 4.24).

4.12. The characterization of STAT1 K.O. U3C cell lines overexpressing the STAT1, STAT2 and IRF9 proteins

To examine in more detail the possible role of U-ISGF3 in mediating basal ISG expression, we first generated the U3C-based cell lines, overexpressing the ISGF3 components STAT1, STAT2 and IRF9 (comparison of different clones in Figure 4.25 and 4.26). Based on the expression profile of these three proteins, as compared to U3C, from twelve clones three (10, 1 and 4, named in the following text as clone 1, 2 and 3, respectively) have been chosen for further analysis (Figure 4.26).

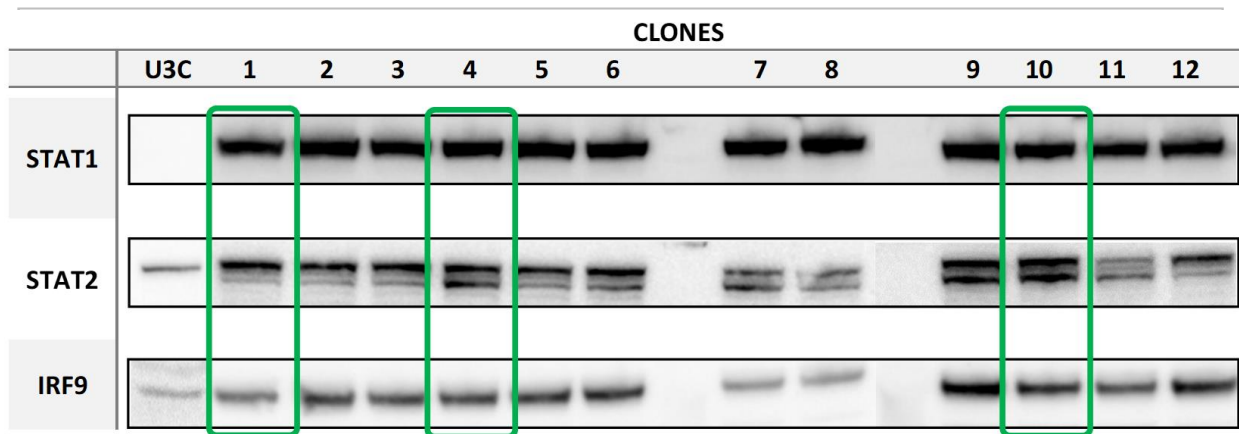


Figure 4.25 *The protein levels in different clones of cells overexpressing STAT1, STAT2 and IRF9*

Western blot analysis of STAT1, STAT2 and IRF9 were done on different clones of ST1-ST2-IRF9-U3C, as well as U3C as a control, to estimate the protein levels. Three clones (1, 4 and 10, marked in green) have been chosen for the further analysis.

To assess the basal antiviral gene expression in these cells we performed qPCR experiments for *OAS2* and *IFI27* in these three clones in the absence of IFN α treatment (Figure 4.25).

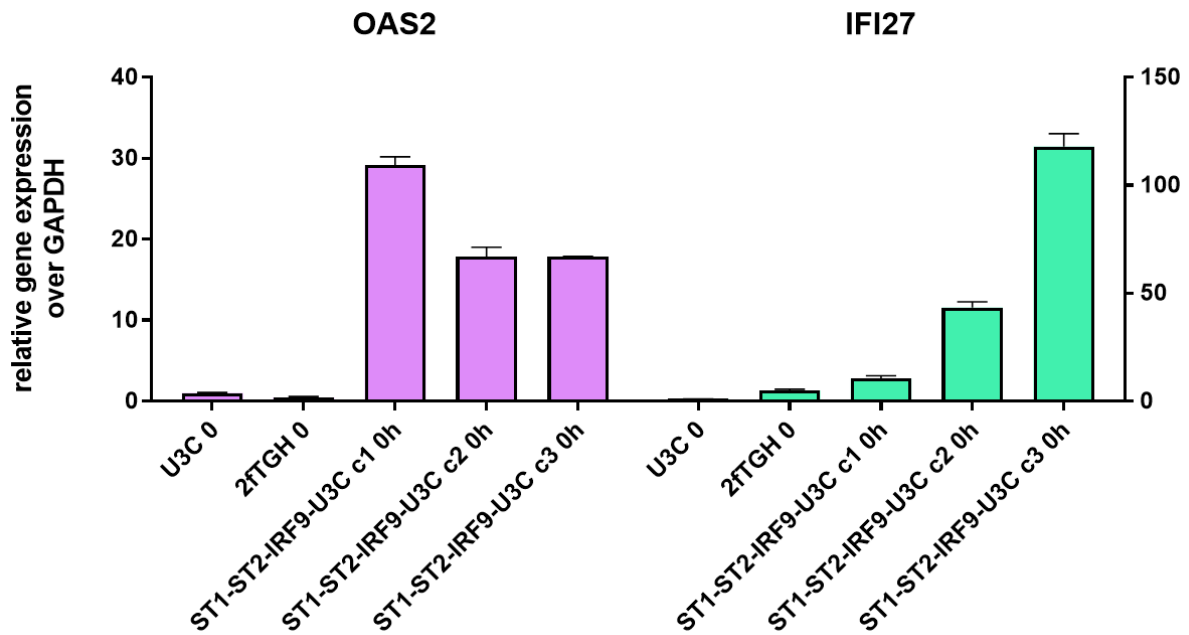


Figure 4.26 The gene expression level in the U3C, 2fTGH and ST1-ST2-IRF9-U3C cell lines without IFN α stimulation

The expression of OAS2 (violet) and IFI27 (turquoise) in untreated cell lines: U3C, 2fTGH and three clones of ST1-ST2-IRF9-U3C was estimated using qPCR method. Relative expression over GAPDH as a reference was calculated; n=2; mean +/- SEM.

Similar to the U3C cells overexpressing STAT2 alone (ST2-U3C) or together with IRF9 [(ST2-IRF9-U3C), Figure 4.24], also cells with abundance of all ISGF3 components exhibited higher basal expression of OAS2 and IFI27. Based on the comparative relative gene expression over GAPDH, for the rest of the experiments, we decided to continue with clone 3, ST1-ST2-IRF9-U3C-c3 (Fig 4.26).

4.13. The genome-wide characterization of basal gene expression in cells overexpressing STAT1, STAT2 and IRF9

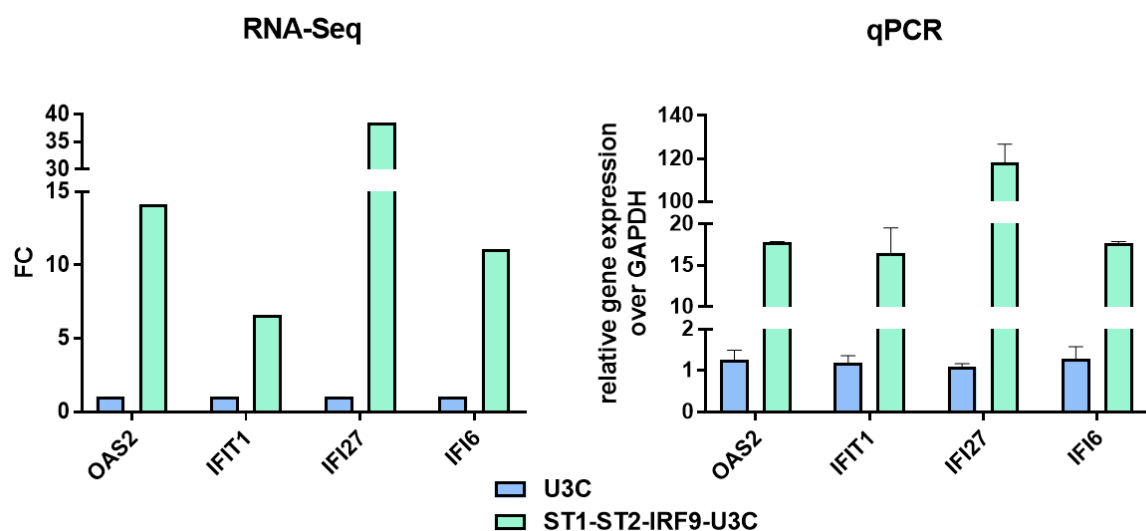
To examine the genome-wide basal gene expression in ST1-ST2-IRF9-U3C-c3 as compared to U3C, we performed RNA-Seq on RNA from three independent repeats. Differential gene expression analysis (DEG) was performed and upregulated genes were selected based on the cut-off of $\log_2FC > 1$ and $padj < 0,05$. As such, 251 genes were identified in ST1-ST2-IRF9-U3C-c3 cells with increased basal expression (Fig 4.27). After comparing these genes with the 208 commonly IFN α -induced genes in WT cells (Figure 4.2), 41 genes

RESULTS

were in common (Figure 4.27) and included the previously characterized pre-selected ISRE-containing antiviral ISGs (Figure 4.4), as well as many additional known ISRE-containing ISGs, including *DDX60*, *ISG20*, *IFITM1* and 3 as well as *BST2*.



To validate the quality of our RNA-seq dataset in general, the expression of a number of previously characterized ISRE-containing antiviral genes, including *OAS2*, *IFIT1*, *IFI27* and *IFI6*, was additionally confirmed by qPCR and compared to their RNAseq FC values (Figure 4.28). Indeed, for all of these genes the basal expression in ST1-ST2-IRF9-U3C-c3 was dramatically increased as compared to U3C cells.



Figures explanation on the next page

Figure 4.28 RNA-Seq results and their confirmation by qPCR

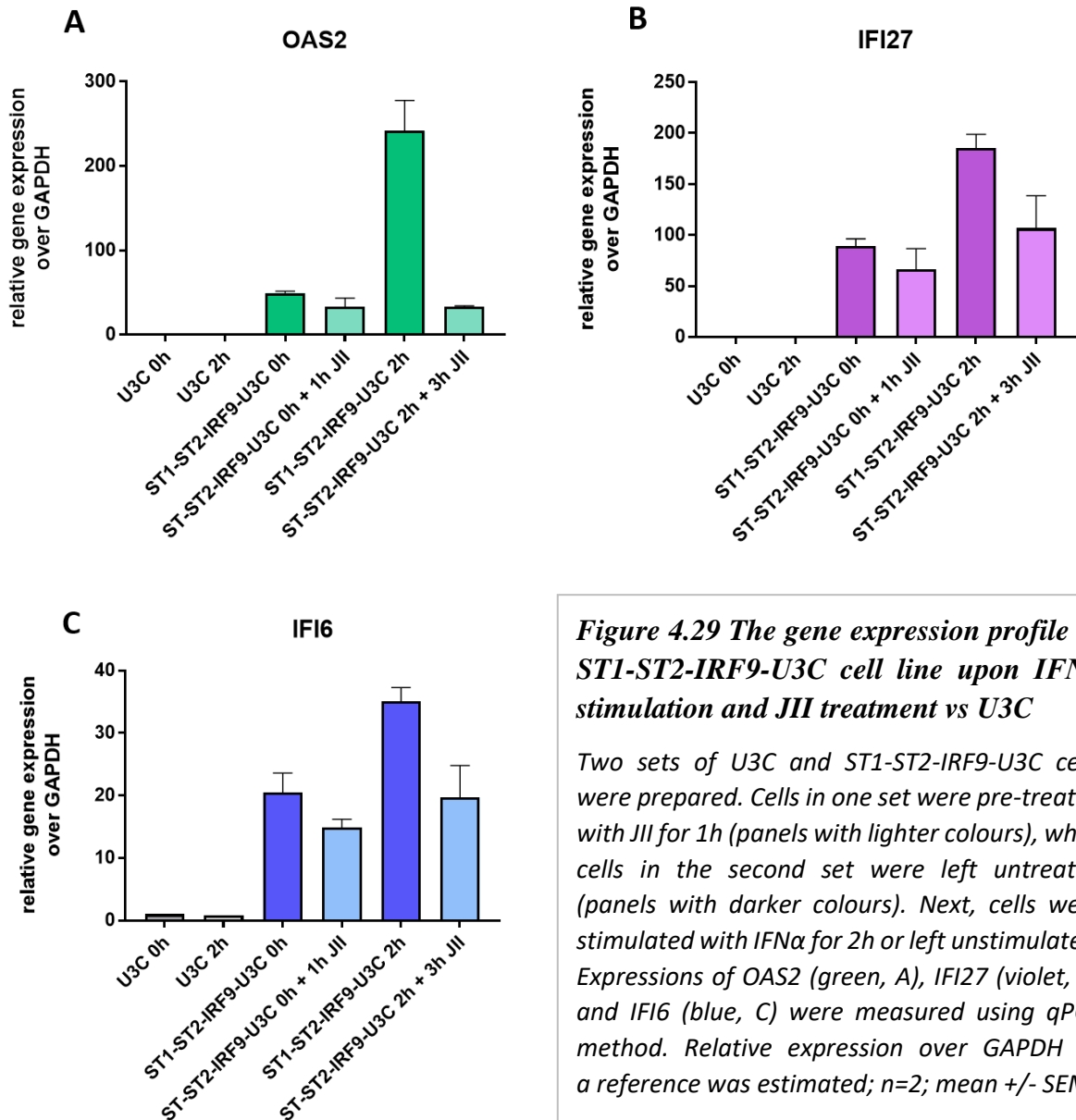
RNA from untreated U3C (blue) and ST1-ST2-IRF9-U3C (turquoise) were isolated and RNA-Seq or qPCR experiments were performed. For selected ISGs (*OAS2*, *IFIT1*, *IFI27* and *IFI6*) RNA-Seq results (presented as fold-change differences; left panel) and qPCR (as relative expression over *GAPDH* as a reference; right panel) are presented; for qPCR $n=2$; mean \pm SEM.

Together, this could point to a role of unphosphorylated ISGF3 components in the formation of U-ISGF3 and/or U-STAT2/IRF9 to regulate basal ISG expression and increase protection against viral infection.

4.14. The role of unphosphorylated ISGF3 components in basal ISG expression

To study the role of phosphorylation in basal ISG expression in ST1-ST2-IRF9-U3C-c3 as compared to U3C cells, experiments with the use of JAK Inhibitor I were performed (Figure 4.29). Pre-treatment with JII for 1h did not significantly lower the basal expression of *OAS2*, *IFI27* and *IFI6* in untreated ST1-ST2-IRF9-U3C-c3. Treatment with IFN α for 2h increased the expression levels of these genes, returning to basal levels upon JII pre-treatment.

This is in agreement with the role of phosphorylation in IFN- α activated transcriptional responses and provides further evidence for a phosphorylation-independent mechanism involved in the regulation of basal ISG expression in ST1-ST2-IRF9-U3C-c3.



4.15. The basal chromatin binding of ISGF3 components in cells overexpressing these components

Next, we characterized the chromatin interactions of the ISGF3 components to the regulatory regions of *OAS2*, *IFI27*, *STAT1*, *STAT2* and *IRF9*, by ChIP-PCR. As such, chromatin was isolated from untreated ST1-ST2-IRF9-U3C-c3 cells, using antibodies against STAT1, STAT2, and IRF9 (Figure 4.30). Preliminary results, showed clear binding for all three components to the majority of the genes. Surprisingly, STAT2 binding to the regulatory regions of *OAS2* and *STAT1*, seemed significantly weaker.

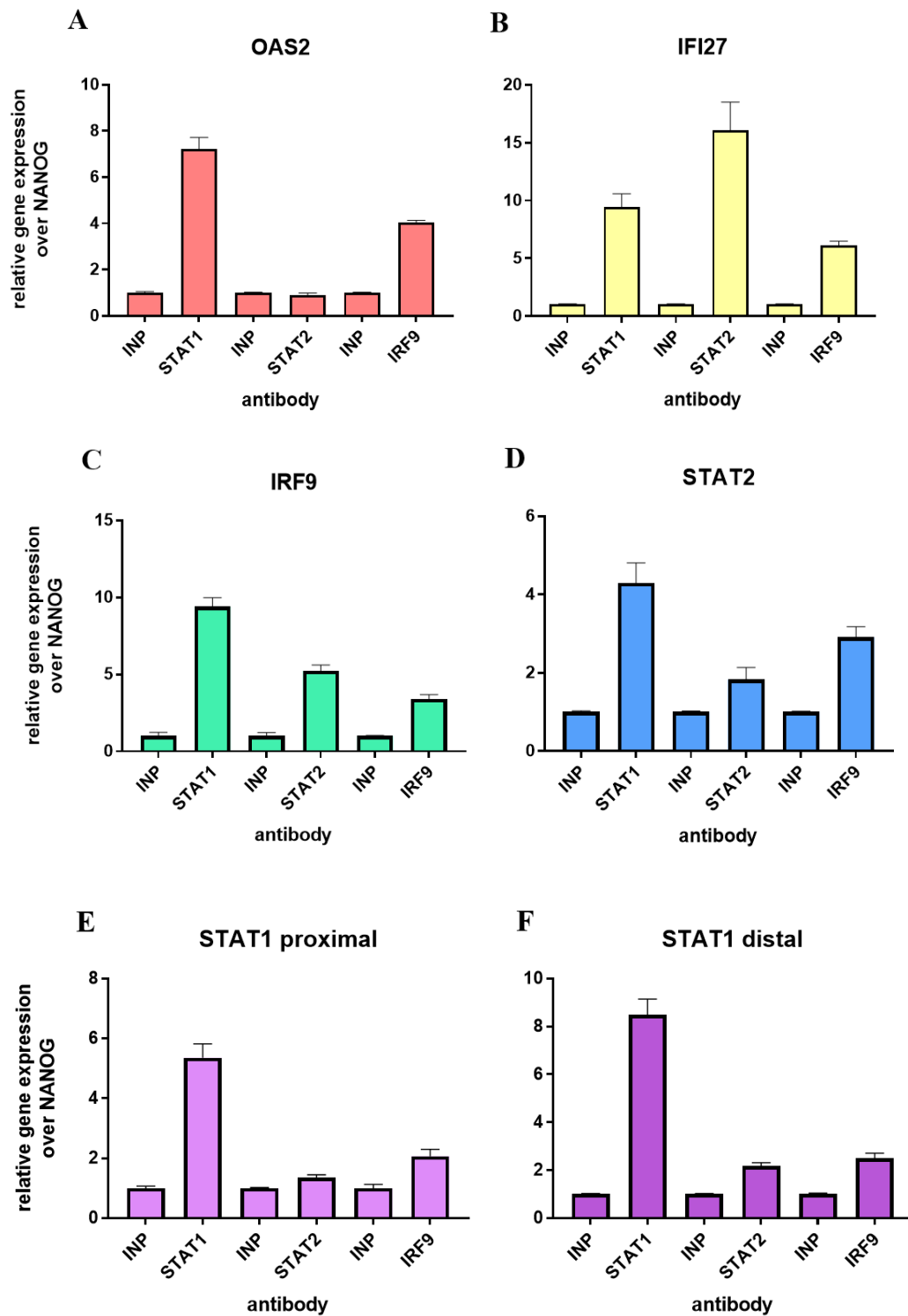


Figure 4.30 Characterization of STAT1, STAT2 and IRF9 recruitment to ISG promoters without IFN α stimulation in ST1-ST2-IRF9-U3C

ChIP experiments were done on the untreated ST1-ST2-IRF9-U3C cells using STAT1, STAT2 and IRF9 antibodies. ChIP-PCR were performed to estimate the binding of these antibodies to the promoter regions in OAS2 (A), IFI27 (B), IRF9 (C), STAT2 (D) and STAT1 (E and F) genes. Relative gene expression was estimated using 2^{ddCT} method over NANOG and with U3C ChIP-PCR CT values as a reference; n=2; mean +/- SEM

4.16. The role of unphosphorylated ISGF3 components in the viral protection in the absence of IFN α stimulation

To study the ability of abundance of unphosphorylated ISGF3 components to combat viral infection in the absence of IFN treatment, antiviral assays were performed. Various cell lines were infected with serial 10-fold dilutions of Vesicular stomatitis Indiana virus starting from MOI=10 (Figure 4.31). U3C, as well as 2fTGH, were not able to fight with the virus at MOI more than 0.001. Oppositely, the clone overexpressing STAT1, STAT2 and IRF9, even without the pre-stimulation with IFN α , was protected 10x more (up to MOI=0.1).

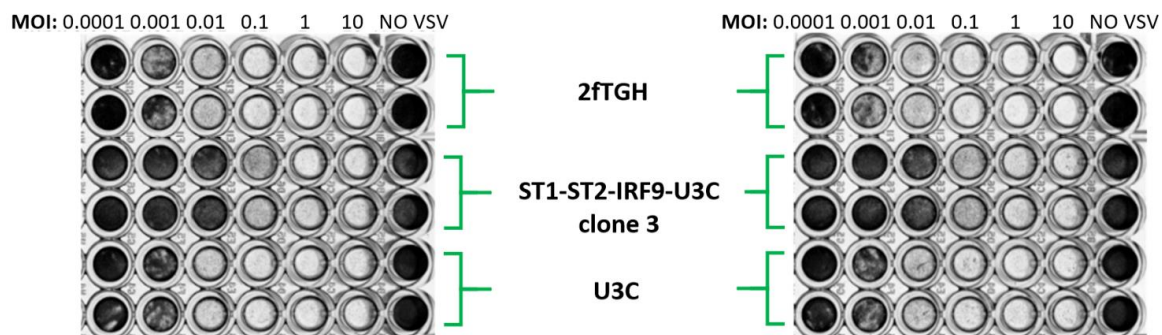


Figure 4.31 *The long-lasting antiviral protection without IFN α stimulation*

Two experiments of antiviral assay (left and right panel) were done. U3C, 2fTGH and clone 3 of ST1-ST2-IRF9-U3C were infected with serial 10-fold dilution of VSV starting from MOI=10 or left uninfected. Next, after 20h of incubation, the results were visualized by crystal violet staining - the black wells indicate the living cells.

To study the effect of JAK Inhibitor I, cells were subsequently pre-treated with JAK Inhibitor I for 2 or 24h, and next infected with VSV (Figure 4.32). Results of these experiments clearly showed, that phosphorylation has no role in viral protection of ST1-ST2-IRF9-U3C-c3 cells, as its blockage did not diminish the ability of these cells to combat viral infection (Compare 4.32; A: no JII vs B: JII 2h and C: JII 24h).

RESULTS

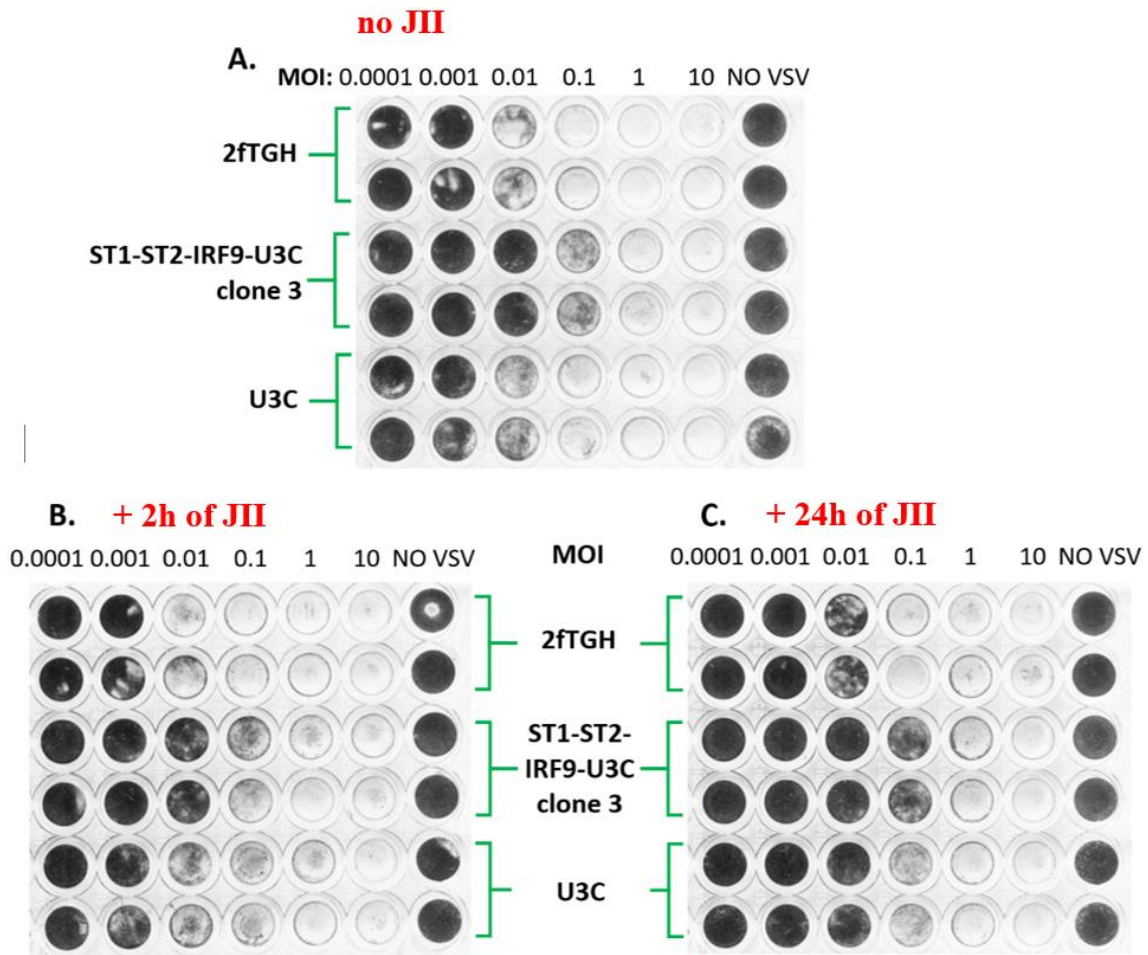


Figure 4.32 *The role of phosphorylation in ensuring antiviral protection without IFN α stimulation*

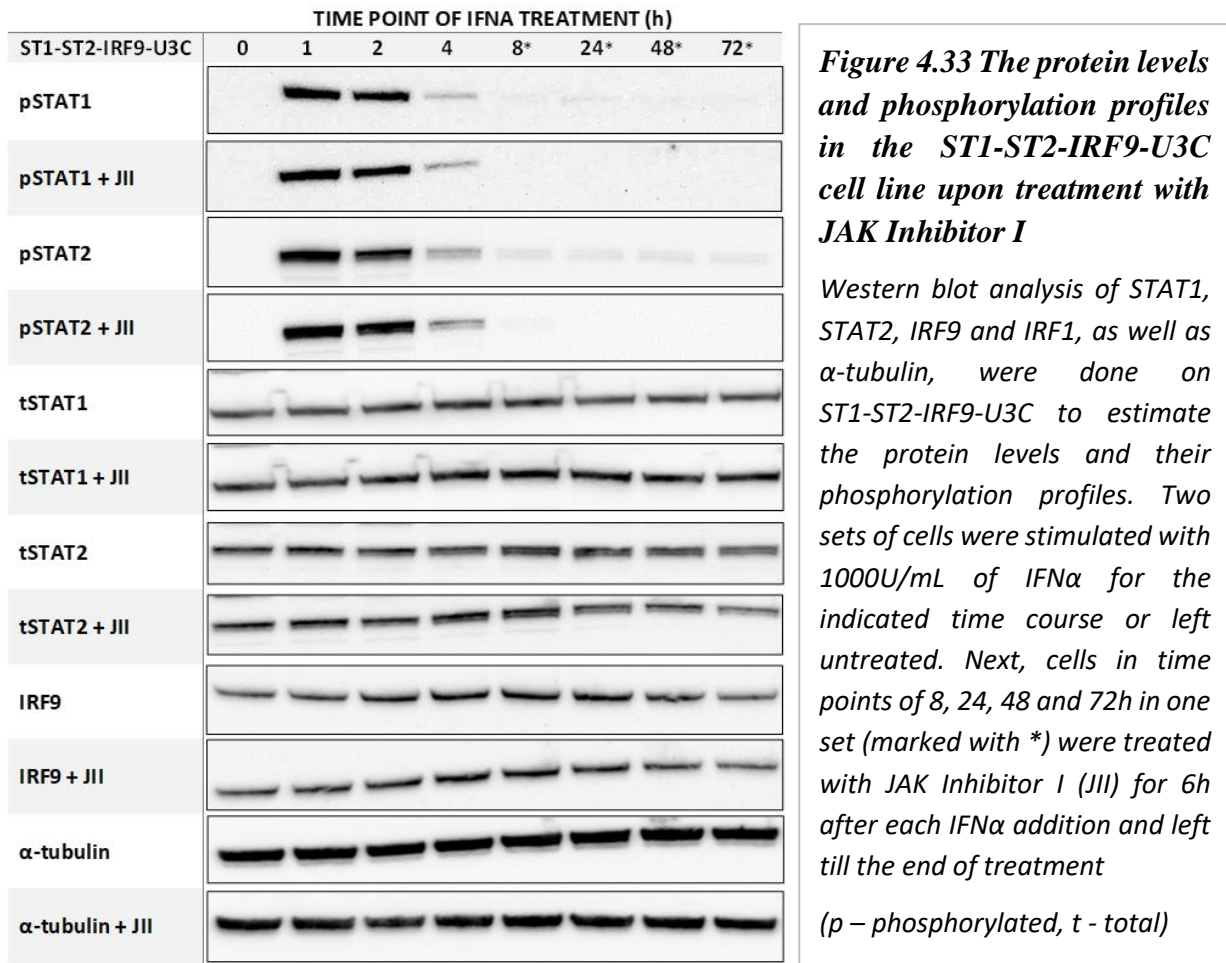
Three experiments of antiviral assay were done. U3C, 2fTGH and ST1-ST2-IRF9-U3C were infected with serial 10-fold dilution of VSV starting from MOI=10 or left uninfected. Next, after 2h (B) or 24h (C) of incubation cells were treated with JAK Inhibitor I or left untreated (A). The results were visualized by crystal violet staining after 24h - the black wells indicate the living cells.

Together, these results provide further evidence for a role of U-ISFG3 in the regulation of constitutive ISG expression in ST1-ST2-IRF9-U3C-c3 cells. Moreover, they also suggest that a certain threshold of STAT1, STAT2 and IRF9 expression and levels of U-ISGF3 has to be reached to be able to trigger basal gene expression and mediate IFN-independent viral protection.

PART IV B**The role of abundance of ISGF3 components (U-ISGF3) in the regulation of IFN-activated ISG expression****4.17. The role of phosphorylation in prolonged IFN α signalling under conditions with abundance of ISGF3 components****Western blotting and qPCR**

To examine in more detail the possible role of U-ISGF3 in mediating IFN α -induced long-term ISG expression, several experiments with the use of JAK Inhibitor I were performed on ST1-ST2-IRF9-U3C-c3 cells. Western blot was used to examine the protein production and their phosphorylation status in the absence after JII treatment (added after 6h of IFN treatment, at each time-point) (Figure 4.33). As became clear, in ST1-ST2-IRF9-U3C-c3, cells phosphorylation of STAT1 and STAT2 was absent in untreated cells, but highly induced upon IFN α treatment with an early, transient increase between 1 and 4 h, after which it diminished to still detectable levels at 72h (Figure 4.33). Addition of JII resulted in a dramatic drop in STAT1 and STAT2 phosphorylation at 8, 24, 48 and 72h. On the other hand, no effect was seen on the native levels of STAT1, STAT2 as well as IRF9.

RESULTS



4.18. The role of phosphorylation in prolonged IFN α signalling in the cells overexpressing STAT1, STAT2 and IRF9

To study the role of phosphorylation on ISG expression, ST1-ST2-IRF9-U3C-c3 cells were treated with IFN α for up to 24h and pre-treated with JAK Inhibitor I, 1h in advance of each time-point (Figure 4.34). Results obtained from the qPCR experiments on selected ISGs show that phosphorylation is crucial for triggering the IFN-induced gene expression in these cells. Indeed, phosphorylation blockage significantly inhibited *OAS2*, *IFIT1*, *IFI27* and *IFI6* expression. However, expression of all of these ISGs never dropped below the basal level observed in untreated ST1-ST2-IRF9-U3C-c3 cells.

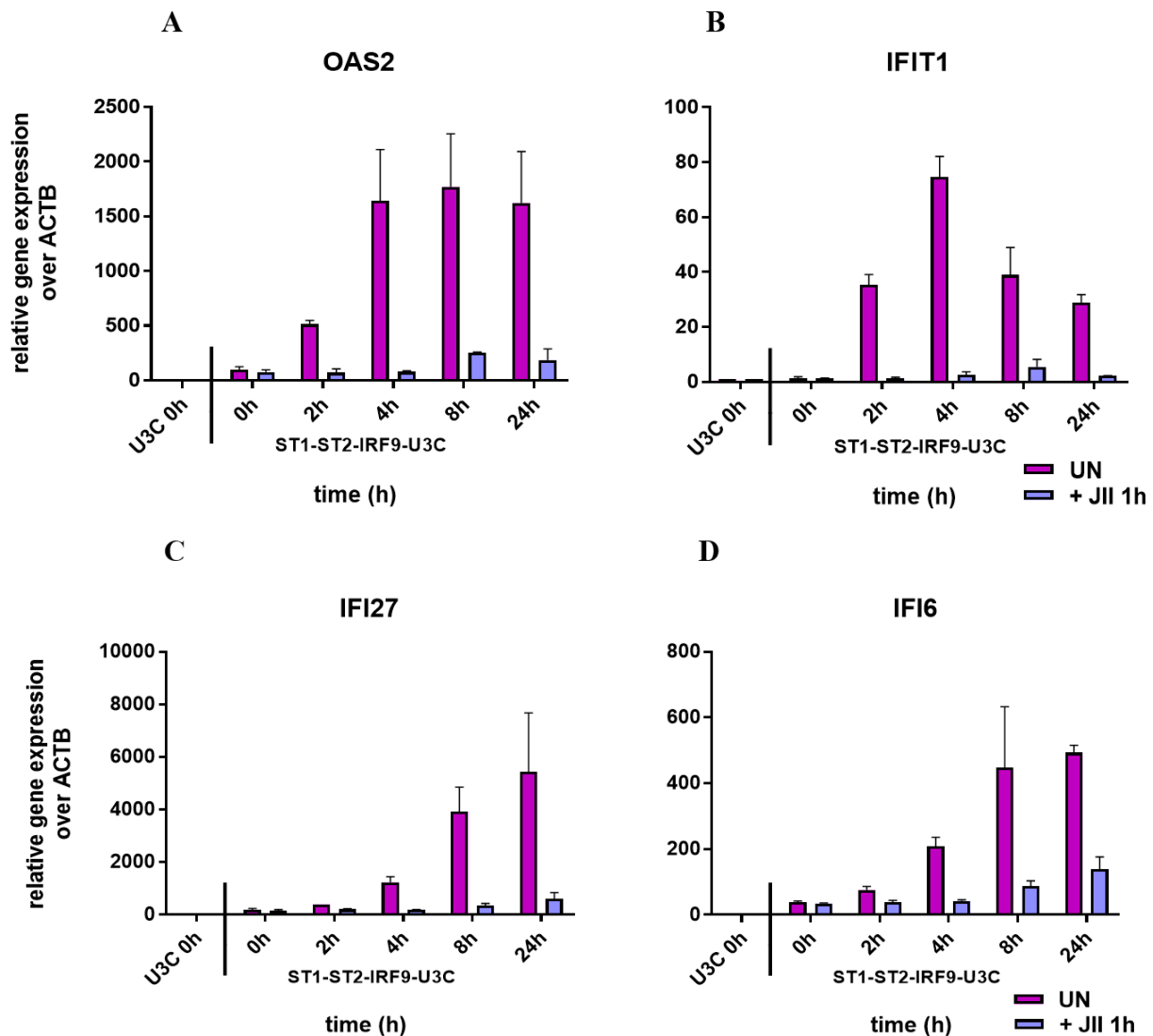


Figure 4.34 The effect of phosphorylation inhibition on gene expression

Two sets of the ST1-ST2-IRF9-U3C and U3C cells were treated with IFN α (violet) for shown time course. Previously, cells in one set were pre-treated with JAK Inhibitor I for 1h (blue). The expression of OAS2 (A), IFIT1 (B), IFI27 (C) and IFI6 (D) was estimated using qPCR method with the untreated U3C as a reference. Relative expression over ACTB was estimated; $n=2$; mean \pm SEM.

4.19. The role of phosphorylation in antiviral protection upon the abundance of STAT1, STAT2 and IRF9

To address the role of phosphorylation in protection of IFN-treated ST1-ST2-IRF9-U3C-c3 cells from viral infection, we performed the antiviral assay and examined the effect of JII treatment. In comparison to 2fTGH and U3C, ST1-ST2-IRF9-U3C-c3 cells were treated with 50U/mL of IFN α for 24h in three independent sets of experiments. Then, one set was stimulated with JII (5 μ M) for 4h, second – for 25h

RESULTS

(so JII was added 1h before IFN) and third – left unstimulated. Finally, all sets were infected by VSV at MOI=1.0 for 24h (Figure 4.35). We prepared this experiment also using higher concentration of JII (20 μ M) and obtained the same results (data not shown).

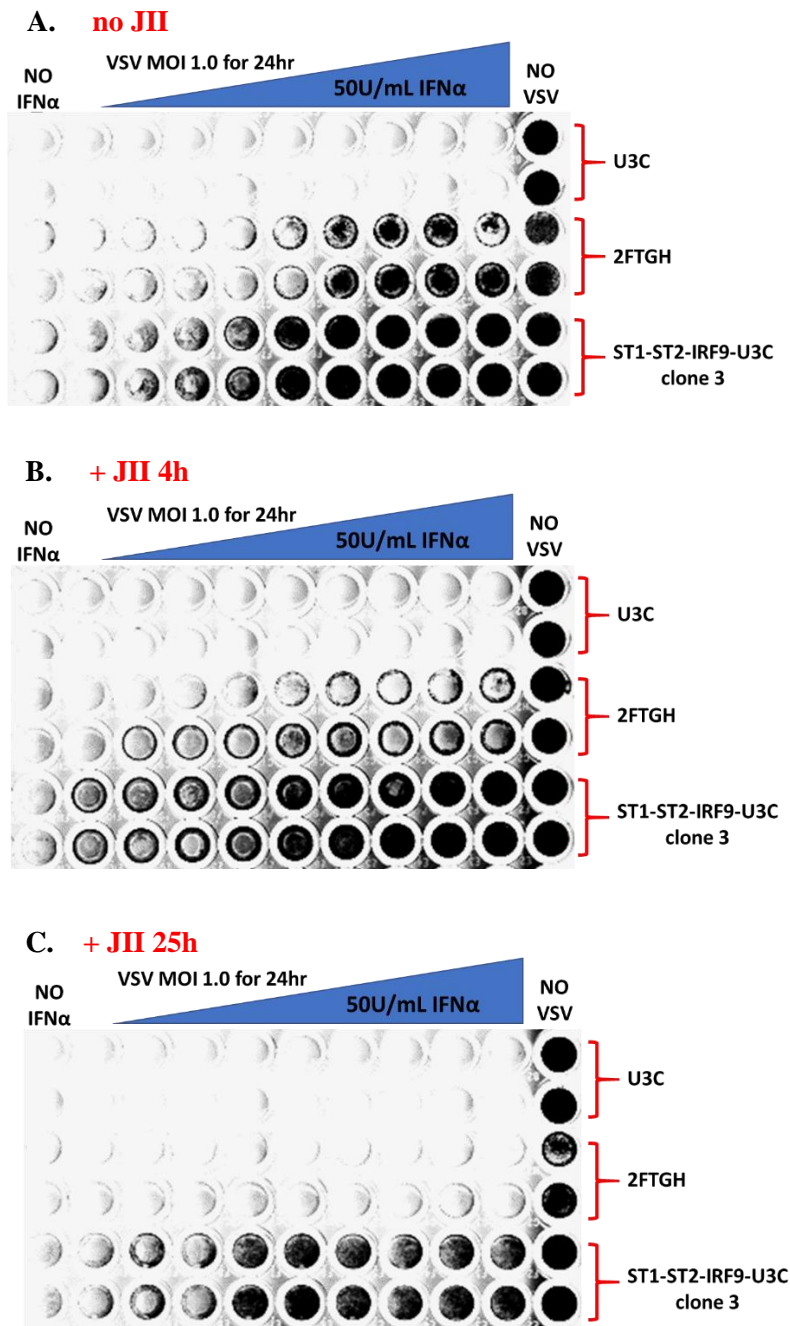


Figure 4.35 The role of phosphorylation in antiviral protection

The cell lines: ST1-ST2-IRF9-U3C, 2FTGH and U3C as a control, were treated with 2-fold serial dilution of IFN α starting from 50U/mL left for 24h. After this time cells were infected with VSV at MOI of 1.0 for 24h. During this infection time, cells on the middle plate (B) were treated with JII for 4h (5 μ M), cells on lower plate (C) – for 25h, and cells on the upper plate (A) left untreated. Finally, results were visualized by crystal violet staining - the black wells indicate the living cells.

RESULTS

Results of these experiments clearly show that blocking of phosphorylation has no major effect on IFN-induced viral protection of ST1-ST2-IRF9-U3C-c3 cells. qPCR results (Figure 4.36) under these conditions indeed confirmed that expression of *OAS2*, *IFI27* and *IFI6* never dropped below the basal level observed in untreated ST1-ST2-IRF9-U3C-c3 cells and is sufficient to protect cells from lysis by VSV.

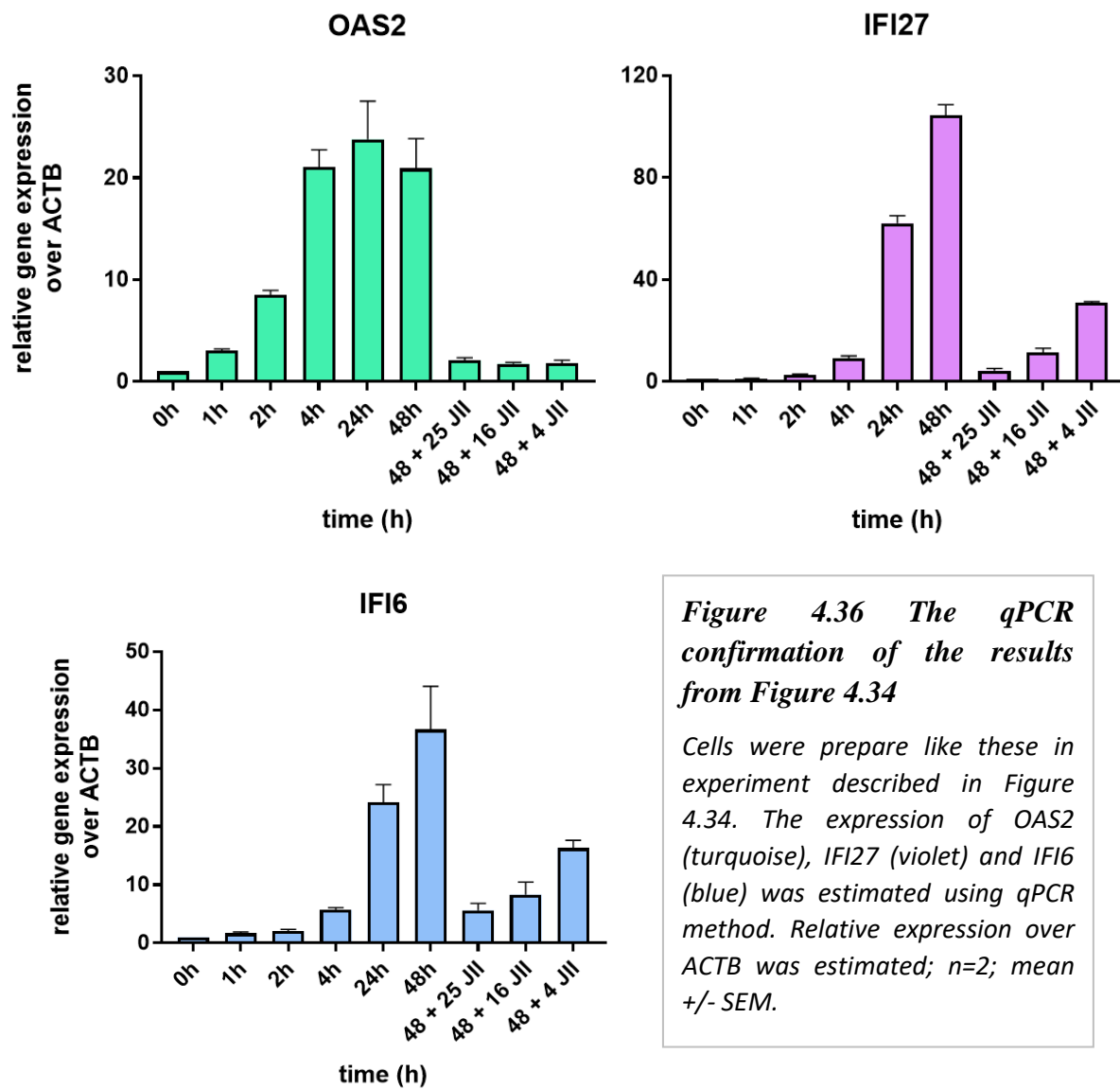


Figure 4.36 The qPCR confirmation of the results from Figure 4.34

Cells were prepared like these in the experiment described in Figure 4.34. The expression of *OAS2* (turquoise), *IFI27* (violet) and *IFI6* (blue) was estimated using the qPCR method. Relative expression over ACTB was estimated; n=2; mean \pm SEM.

RESULTS

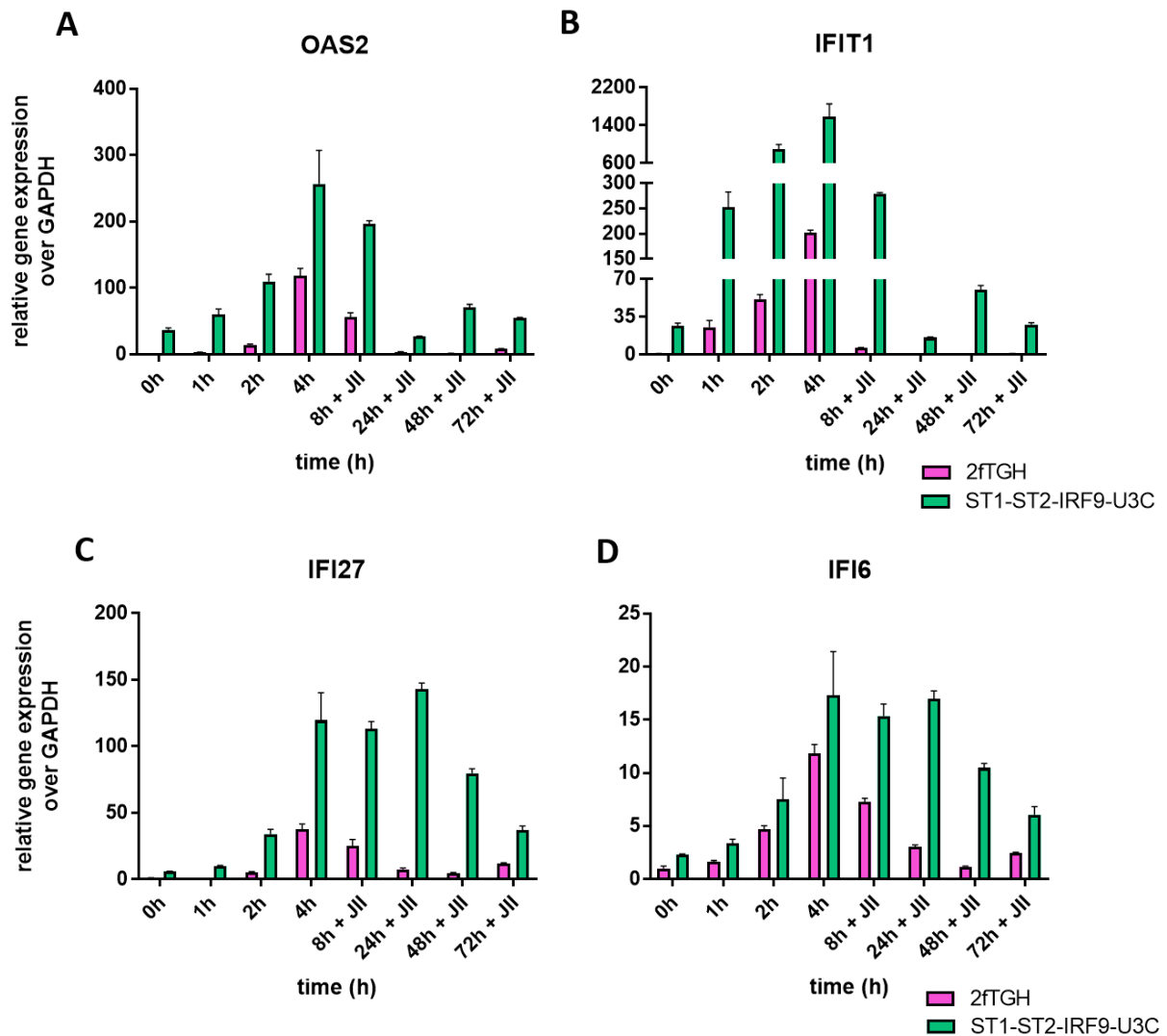


Figure 4.37 The comparison of the gene expression profiles in ST1-ST2-IRF9-U3C and 2fTGH upon IFN α stimulation and JII treatment

2fTGH (pink) and ST1-ST2-IRF9-U3C (green) cells were pre-stimulated with IFN α for indicated time course. 6h later cells in time points 8, 24, 48 and 72h were treated with JII. Expressions of OAS2 (A), IFIT1 (B), IFI27 (C) and IFI6 (D) were measured using qPCR method. Relative expression over GAPDH as a reference was estimated; n=2; mean +/- SEM.

Finally, comparison of IFN-stimulated 2fTGH and ST1-ST2-IRF9-U3C-c3 cells, treated with JII, revealed a dramatic difference in gene expression levels of *IFIT1*, *OAS2*, *IFI27* and *IFI6* after long-term IFN α and JII treatment (Figure 4.37). This is in agreement with previous observations and confirms a potential role of U-ISFG3 in the regulation of constitutive and possibly long-term IFN α -treated ISG expression in ST1-ST2-IRF9-U3C-c3 cells. As a consequence, together with classical ISGF3, U-ISGF3 could be instrumental in IFN-dependent and independent ISG transcription and in combatting viral infection.

5. DISCUSSION

The classical IFN Type-I response is based on ISGF3 complex that is composed of phosphorylated forms of STAT1 and STAT2 together with IRF9. In ISGF3, IRF9 is responsible for recognizing of DNA, STAT1 stabilizes this connection, and STAT2 provides the transactivation domain. ISGF3 is formed in the response to the IFN Type-I production, and while present in the nucleus, is able to trigger expression of many genes with antiviral function by recognizing ISRE in their promoters. Over the years, intensive studies of IFN Type-I signalling revealed that other than ISGF3 complexes, may be functional. The examples are U-ISGF3 (that is composed of unphosphorylated forms of STAT1 and STAT2 together with IRF9) and complexes of STAT2 and IRF9, both, in phosphorylated or unphosphorylated form. The role of all mentioned complexes was tested in this thesis.

5.1. The role of ISGF3 phosphorylation in time-dependent IFN α -activated regulation of ISGs

The main role of ISGF3 is triggering fast and robust expression of more than 300 genes in response to the IFN Type-I function (Blaszczyk et al. 2016)(Schoggins 2019). This is possible due to the pre-existence of STAT1, STAT2 and IRF9 in the resting cells. Due to this, it was always thought that ISGF3 is transcription factor that work transiently and is active only during the early IFN-dependent response (Darnell, Kerr, and Stark 1994). This was the reason why the whole-genome approaches, as microarrays, were done on samples after IFN-treatment restricted up to 24h (Geiss et al. 2003). However, ISG expression is prolonged in time, what prompted researchers to wonder, how this process is regulated. In our studies we tried to address the question about the importance of the phosphorylation event in regulation of IFN α - and time-dependent ISG expression and viral protection. We, as one of the first, considered the role of ISGF3 in sustaining low ISG expression up to 72h.

In 2fTGH, as well as in Huh7.5, drop in phosphorylation of STAT1 and STAT2 is observed and both, gene expression profiles, as well as TFs-DNA interactions, correlate with this decreased phosphorylation. Similar IFN-dependent phosphorylation decline is a general phenomenon and was documented e.g. in case of bronchial respiratory epithelial cells (RECs)(Novatt et al. 2016). The possible mechanism underlying observed drop in phosphorylation is the function of negative regulators, such as the SOCS or PIAS family

DISCUSSION

members (Malterer, Glass, and Newman 2014)(Ivashkiv and Donlin 2014)(Ungureanu et al. 2005)(Rogers, Horvath, and Matunis 2003). The slight differences in gene expression profiles between 2fTGH and Huh7.5 are the results of the IFN-induced phosphorylation patterns of STAT1 and STAT2 in these cells. According to the RNA-Seq performed by us, the ISG expression is higher and more prolonged in Huh7.5 what mirrors the longer detectable phosphorylation, when compared to 2fTGH (Figure 4.1, 4.3 and 4.4). This all is in agreement with the documented dynamics of ISGF3 formation and function. It is important to notice that ISGF3-mediated response is potent and once treated with IFN α 2fTGH cells are able to combat viral infection up to three days (Figure 4.10). This, strong protection of IFN α -stimulated 2fTGH against Vesicular stomatitis Indiana virus, complies with the observations of other researchers (Weidner et al. 2010)(W. Wang et al. 2017)(Blaszczyk et al. 2016).

The genome-wide binding approaches based on chromatin immunoprecipitation allow us to examine the interaction patterns of ISGF3 components with the regulatory regions in ISG promoters. According to our results, we can conclude that upon IFN α -stimulation all the ISGF3 component are recruited to the promoters of all well-known ISGs. Profound examination of results and comparison with those obtained from RNA-Seq and Western blot experiments revealed that binding pattern of these TFs are consistent with their production and phosphorylation profiles. Hartman et al. (Hartman et al. 2005) was studying the STAT1 and STAT2 binding to the chromosome 22 upon IFN α or γ treatment and showed the correlation between the binding of STAT1 and STAT2 in the response to IFN α . Additionally, in ENCODE database (ENCODE Project Consortium, 2012) we can find ChIP-Seq experiment results performed using anti-STAT1 and -STAT2 antibodies on the cell line K562. Michalska et al., analysed these data, showing similar pattern of STAT1 and STAT2 binding when compared to 2fTGH (Michalska et al. 2018). Also Platanitis (Platanitis et al. 2019) and colleagues performed ChIP-Seq experiments on the mouse BMDM and MEF, as well as human THP-1. However, all of these studies concerned only the early IFN-stimulation (up to 6h). In the opposite, as the first, we extended the studies for longer (up to 72h) IFN α treatment time-points. The binding of pSTAT1 and pSTAT2 antibodies are clearly stronger than those of total STAT1 and STAT2, although they exhibit similar binding patterns, which may be a result of the quality of the antibodies themselves. Anti-total STAT1 and -total STAT2 were purchased from the Santa Cruz Biotechnologies, while anti-pSTAT1 and -pSTAT2 – by the Cell Signalling Technologies (CST). Using Santa-Cruz antibodies to perform Western blot experiments, we were not able to detect pSTAT1 and pSTAT2 after 24h of IFN α treatment (data not shown). In contrast, when

DISCUSSION

CST antibodies were used on the same treatment schedule and on the same cell line phosphorylation of STATs is clearly seen up to 72h (Figure 4.1). This stands for the much better quality of CST vs Santa-Cruz antibodies.

To study the role of phosphorylation in time-dependent IFN α -mediated transcriptional response we performed experiments with the use of JAK Inhibitor I that potently blocks the STAT phosphorylation events by interacting with JAK family members (Pedranzini et al. 2006). Thus, JII prevents forming of ISGF3 that is main complex involved in the regulation of the antiviral gene expression upon IFN α stimulation (Levy et al. 1988). Under the treatment with JII, the phosphorylation of STAT1, as well as STAT2, is no longer detectable in both, 2fTGH and Huh7.5 (Figure 4.17), and ISG expression, is dramatically decreased (Figure 4.18 and 4.19). Moreover, it is clear that protection against the viral infection in these cells is strongly dependent on phosphorylation, as IFN α -stimulated 2fTGH treated then with JII for 4h after VSV infection become much more sensitive to the virus-caused lysis (Figure 4.23 B). This, together with observed correlation of ISG expression and STATs phosphorylation, stands for the pivotal role of phosphorylation of the ISGF3 components in context of prolonged transcriptional response in tested wild-type cell lines.

Our results give further insight into complicated pathways that regulate IFN α -dependent ISG expression. By conducting whole-genome approaches, and, as the first, long time IFN α treatment we could study the many aspects, such protein-DNA interactions and large-scale gene expression, at the same time.

5.2. The role of STAT2/IRF9 in time-dependent IFN α -activated regulation of ISGs in the absence of STAT1

Nowadays, more and more evidence is accumulating for the functionality of the STAT2/IRF9 complex that has been proved to be formed in cells untreated (Lau, Parisien, and Horvath 2000) or stimulated with IFN α in the absence of STAT1. The STAT2/IRF9 may serve as a backup system that can provide protection for example against the viruses with the ability to block STAT1 function. Of them, Sendai viruses should be mentioned. The SevC protein can directly interacts with STAT1, thus not only inhibits STAT1 activity, but also precludes apoptosis of infected cells (Garcin et al. 2002). This is interesting field for understanding the mechanism and development of mechanisms of suppressing the replication of viruses that in

DISCUSSION

the course of evolution have acquired the ability to block of ISGF3 formation through various interactions with STAT1.

As was already proven by Bluysen and Levy, in the response to IFN α stimulation, STAT2 homodimer, together with IRF9 recognizes and binds ISRE in the promoters of many genes (Bluysen and Levy 1997). Studies on U3C overexpressing STAT2 that were conducted in our laboratory by Blaszczyk and colleagues (Blaszczyk et al. 2015), proved ability of STAT2/IRF9 to take over ISGF3 function and providing potent anti-VSV and -EMCV response. Similar results were obtained by the Yamauchi and colleagues (Yamauchi et al. 2016) from experiments performed on the Huh7.5 STAT1 mutant cells. Researchers showed that HCV replication is inhibited by IFN α in the STAT1-independent but STAT2-dependent manner. STAT2-mediated STAT1-independent IFN Type-I signalling pathway was described by Perry and colleagues in Dengue virus (Perry et al. 2011) and by Abdul-Sater in *Legionella pneumophila* (Abdul-Sater et al. 2015). This non-canonical pathway may act as a backup system to fighting with STAT1-blocking viruses such as Sendai viruses (Garcin et al. 2002), Rotaviruses (Sen et al. 2014) or Ebola (Wei Xu et al. 2014).

Data obtained from our RNA-Seq experiments performed on the cell lines, showed 84 upregulated genes that are common for ST2-U3C and Huh ST1 K.O. (Figure 4.11 A). 63 of them are commonly expressed in wild-type and STAT1-knock-out cell lines upon IFN α stimulation (Figure 4.11 B). Deeper examination revealed that ISG expression levels in ST2-U3C are significantly lower, but with distinctly prolonged profiles, generally, without the strong marked maximum (figure 4.12 and 4.13 C vs A) as compared to wild-type cells. This correlates with STAT2 and IRF9 production, as well as with the STAT2 phosphorylation pattern. In this cells, as STAT1 production is abolished, ISGF3 can no longer be formed. The STAT2/IRF9-DNA interactions are, however, weaker, than those of ISGF3 (Bluysen and Levy 1997) that is why the ISG expression is lower than in 2fTGH. Nevertheless, recruitment of phosphorylated STAT2 to the regulatory regions of ISGs has similar pattern to this observed in case of total STAT2. This also agrees with suggestion that phosphorylation plays a key role in ensuring ISG expression.

Similarly to ST2-U3C, in liver cells Huh ST1 K.O., the gene expression profiles are changed as compared to wild type Huh7.5. Moreover, we identified 84 genes that are commonly upregulated in both, ST2-U3C and Huh STAT1 K.O. 63 of these genes are common in WT's vs K.O.'s, among them well-known ISGs, such as: *IFIT* family, *OAS* family, *IFI* family or *ISG15* and *ISG20*. All of these genes have similar expression profile (Figure 4.12 and 4.13 D

DISCUSSION

vs B). The ISG expression pattern in these cells is now significantly shifted towards the much later time points of IFN α treatment. In this case, we can also observe the delay in the IRF9 production and STAT2 phosphorylation (Figure 4.10 D vs B). This clear connection between the delayed pSTAT2 and IRF9 production, as well as with the pSTAT2 and IRF9 binding in ChIPseq, and shifted gene expression also confirms the STAT2/IRF9 functionality. In U3C the STAT2 level is too low to form STAT2/IRF9 that is why, this STAT1 K.O. cells are not responsive to the IFN α stimulation, and are completely incapable of combating viral infection [Figure 4.9 and 4.23; (Błaszczuk et al. 2016)]. Unlike U3C, in Huh ST1 K.O., the basal STAT2 level is already enough to provide the antiviral gene expression upon IFN treatment. However, the production of STAT2 and IRF9 is hindered by the lack of STAT1, what causes the delay in start of ISG expression.

In both tested STAT1-deficient cell lines, similar to the wild-type cells, JII administration severely decreased the ISG expression (Figure 4.21 and 4.22). This, together with the binding of pSTAT2 to the ISG regulatory regions observed in 72h (Figure 4.15), prove the crucial role of phosphorylation in regulation of prolonged ISG expression, also under the STAT1-deficient conditions

As the first, we used the genome-wide approaches, such as RNA-Seq and ChIP-Seq on the two different STAT1-deficient cell types treated with IFN α up to 72h, which results shed light on the role of phosphorylation status of STAT2/IRF9 in the prolonged ISG expression. However, many questions still need to be answered, e.g. is prolonged ISG expression regulated only by STAT2/IRF9 or is there any role of U-STAT2/IRF9. To address this question ChIP-Seq experiments need to be done on STAT1-deficient cells upon JII treatment.

5.3. ISGF3 vs STAT2/IRF9

Main function of ISGF3 is to trigger rapid and robust IFN Type-I-related responses by regulating ISG expression (Malterer, Glass, and Newman 2014). This early potent and time-restricted response, on the one hand, provides the ability to suppress viral infection, and on the other hand, prevents damage caused by cachexia after prolonged antiviral activation of the cells. Already in 1989, Levy and colleagues, proved that ISGF3 is present in the cell just in minutes after IFN α stimulation (Levy et al. 1989). This coincides with transient phosphorylation profiles observed in case of STAT1 and STAT2 (Figure 4.11), as well as with the binding pattern of all ISGF3 components to the DNA, and, overall, confirm the transient nature of ISGF3-dependent response.

DISCUSSION

In contrast to the transient ISGF3-related ISG expression, STAT2/IRF9-dependent one is lower and prolonged [Figure 4.13 C; (Blaszczyk et al. 2015)]. This is, most probably, the result of lower DNA affinity of STAT2/IRF9, when compared to ISGF3 (Bluyssen and Levy 1997). This correlates with the prolonged pSTAT2 phosphorylation and weaker DNA-promoter interactions that were presented in this thesis (Figure 4.10 and 4.15, respectively). Our RNA-Seq experiment performed on wild-type, as well as STAT1-deficient cell lines showed that 63 genes (among them well-known ISGs such as *IFIT*, *IFI* and *OAS* family members) are commonly upregulated by ISGF3 and STAT2/IRF9. However, 145 and 21 gene expressions were specifically regulated by this complexes, respectively. Currently, we do not know what is the role of those genes and it would be very exciting to supplement our data with the analysis covering also this issue. This is definitely part of our future plans.

The cooperative function of ISGF3 and STAT2/IRF9 in BDMD, was described by Platanitis and colleagues. Using a mouse models and ChIP-Seq technique, researchers identified the gene group of which the expression in resting cells is regulated by STAT2/IRF9 that, upon IFN β stimulation, is replaced by classical ISGF3, in the process named by researchers as the ‘molecular switch’. This, however, was not observed in human THP-1 cells (Platanitis et al. 2019). Our RNA- and ChIP-Seq data also do not confirm the presence of the ‘molecular switch’ between STAT2/IRF9 and ISGF3. Neither in Huh7.5, nor in 2fTGH we did observe exclusive STAT2 and IRF9 recruitment to the ISG promoters. We also insightfully examined our ChIP-Seq results in terms of genes selected by Platanitis team. We did not found STAT2 and IRF9 binding in case of any from 29 genes that are, according to the researchers, the STAT2/IRF9 targets in mouse macrophages and embryonic fibroblasts. Our results are supporting the hypothesis that ‘molecular switch’ phenomenon is restricted only to mouse system.

5.4. The role of U-ISGF3 and U-STAT2/IRF9 in basal and IFN-mediated expression of IFN α -induced genes

During our JII experiments analysis we noticed that in wild-type and STAT1 knock-out cells IFN-induced ISG expression is not completely abolished (Figure 4.18, 19, 21 and 22), what together with the observed significant drop of STATs phosphorylation and U-STATs accumulation might point to possible function of unphosphorylated STATs-based complexes: U-ISGF3 and U-STAT2/IRF9. U-ISGF3 function was already proposed by Cheon et al. (H. Cheon et al. 2013) and Wang et al. (W. Wang et al. 2017) and was suggested to have

DISCUSSION

a protective role in chronic HCV infection (Sung et al. 2015). According to our results, overexpression of STAT2 increases the basal ISG expression and, similarly, overexpression of both, STAT2 and IRF9, enlarges the gene expression even more (Figure 4.24). This prompted us to explore the potential role of U-ISGF3 in IFN α -induced and -independent transcriptional response by generating cell lines with stable overexpression of STAT1, STAT2 and IRF9 (ST1-ST2-IRF9-U3C). Indeed, in these cells, constitutive ISG expression is higher, when compared to U3C or 2fTGH (Figure 4.26 or 4.28). To extend studies to the whole genome, we conducted NGS and examined genome-wide gene expression in ST1-ST2-IRF9-U3C. Our results for the first time presented the genome-wide IFN α -independent ISG expression that is sufficient to provide antiviral protection (Figure 4.27 and 31). It appeared that 41 genes (Figure 4.27) that are already expressed in the untreated cells, with the abundance of STAT1, STAT2 and IRF9, are engaged in the IFN α -connected signalling, as well as in the defence against pathogens (data not shown). Additionally, to exclude the role of the phosphorylation event in sustained basal ISG expression, we used JII (Figure 4.29). These experiments proved that phosphorylation is completely redundant and increased constitutive ISG expression depends, most probably, on the U-ISGF3 complex. This is in line with the observations made by Wang (W. Wang et al. 2017). In these studies, they proved the role of all: STAT1, STAT2 and IRF9, in protecting the Huh7.5 cell line that overexpress these proteins, against the HCV and HEV infection, by triggering ISG expression in the absence of IFN α treatment. Moreover, conducted experiments suggested that all of these proteins are crucial, but their phosphorylation is not required. Researchers concluded that constitutive antiviral gene expression is mediated by the function of the U-STAT1, U-STAT2 and IRF9 as an U-ISGF3 complex. According to the co-IP results, shown by Cheon and colleagues (H. Cheon et al. 2013), U-STAT1, U-STAT2 and IRF9 interacts which each other in the nucleus of hTERT-HME1 overexpressing STAT1, STAT2 and IRF9 without IFN-stimulation, what again pointed to potential role of U-ISGF3. Researchers, by performing qPCR experiments and antiviral assays on fibroblasts (BJ) and the epithelial cells (hTERT-HME1) transfected with unphosphorylatable mutant of STAT1, suggested that prolonged ISG expression and antiviral protection is mediated by U-ISGF3. They identified 29 genes that were induced by U-ISGF3, but not ISGF3 in tested cell lines and showed that these complexes recognizes slightly different ISREs, however, the core sequence for U-ISGF3 and ISGF3-only targets remain the same (H. Cheon et al. 2013). Among U-ISGF3 targets, genes with known antiviral function, such as *IFI27*, *OAS* family, *IFIT 1 and 3* as well as *MX* family members, can be found. However, the role of STAT2 in these processes has not been studied. Researchers used only unphosphorylatable STAT1 mutant, while the STAT2

DISCUSSION

protein remained unchanged. Thus, they could not exclude the U-STAT2/IRF9 in the protection against VSV and EMCV. In this publication, authors claimed that after 16-days of daily administration with low IFN β concentration the phosphorylation of STATs is absent with simultaneous accumulation of native forms. As ISG expression after this time is maintained they suggested the role of U-ISGF3 under the IFN-treated conditions. Wang and colleagues, ruled out the phosphorylation possibility, by creating Huh7.5 cells overexpressing unphosphorylatable Y701F STAT1 mutant, STAT2 and IRF9. All this is in agreement with the results obtained by us on the ST-STAT2-IRF9-U3C treated with JII. However, no one ever proved U-ISGF3 genome-wide binding to the regulatory regions of ISGs. Wang et al. (W. Wang et al. 2017) presented the CHIP-Seq data from ENCODE database, where shown binding of STAT1 to the promoters of large group of genes (186), among them *ISG15*, *IRF9*, *IRF1* and *STAT1* itself. We also see this in case of 2fTGH CHIP-Seq (compare Figure 4.8), however, STAT1 binding is restricted to only a limited number of genes (Figure 4.8 A). Strikingly, pSTAT1 (and also pSTAT2) exhibits the 0h binding to the *STAT1* and *IRF9* regulatory region that is even higher than this of total STAT1 (Figure 4.8 B; notice the scale: 200 in case of anti-total proteins antibodies and 2000 in case of anti-phospho-proteins, so we considered is rather as a false positive, as in untreated cells pSTAT1 and pSTAT2 could not be detectable by Western blot method using the same antibodies. So far we cannot explain this phenomenon. After overexpressing of the ISGF3 components in the U3C cells we proved the binding of STAT1, STAT2 and IRF9 to the promoters of *IFI27*, *STAT2*, *IRF9*, *STAT1* and *OAS2* (this last two with lower binding of the STAT2; Figure 4.30). It is tempting to speculate about whole-genome binding of unphosphorylated forms of STAT1, STAT2 as well as IRF9 in these cells, expectably in form of U-ISGF3. To examine this, we plan to perform CHIP-Seq experiments.

As described above, abundance of ISGF3 components were shown to drive constitutive ISG expression, potentially in the form of U-ISGF3. Interesting issue to consider is also the potential role of this complex under wild-type conditions.

In 2fTGH, as the total STAT1 and STAT2, as well as IRF9, levels are increasing over time, and pSTATs drops significantly, is tempting to speculated that the long-term viral protection depends on the levels of ISGF3 components, and hence, of antiviral protein production. Without IFN-induced intensified STAT1, STAT2 and IRF9 production, cells may have not enough of these TFs to exceed the threshold required for intensified ISG expression, but once treated, the phosphorylation can decrease severely to the almost undetectable levels, but without the significant effect on the cells survivability (Figure 4.9). This also may point to the role of

DISCUSSION

U-ISGF3 in term of long-lasting IFN α -mediated response. The JII administration in 2fTGH, however, made the cells sensitive to the VSV lysis, and long-term ISG expression in these cells was significantly, but not totally, diminished. On the data held, it cannot be distinguished, if low level of long-lasting ISG expression in the presence of JII is only the remnant of the earlier wave of ISGF3-dependent response or is maintained by the U-ISGF3. Even considering the mRNA stability, which half-life ranges from several minutes to even days (X. L. Li et al. 2000) depending on the type of the coding protein (transcripts for housekeeping genes are, in general, more stable (Edward Yang et al. 2003), it is impossible, beyond any doubt, to prove or exclude the role of U-ISGF3 in prolonged ISG expression regulation, at the moment. To reveal this, more experiments with JII, especially ChIP-Seq experiments, need to be done.

The U-ISGF3 role was now studied extensively, however, also U-STAT2/IRF9 may be functional independently of IFN stimulation.

U-STAT2/IRF9 forming and function was already proposed to serve as an indicator for the STAT1/STAT2 recruitment to the ISRE (Martinez-Moczygemba et al. 1997) and was observed to drive *RIG-G* expression (Lou et al. 2009). Under STAT1-deficiency, in U3C, the increased gene expression is not observed [Figure 4.24; (Blaszczyk et al. 2016)], thus U3C are totally unable to fight viral infection [Figure 4.23; (Blaszczyk et al. 2016)] even after IFN α stimulation. This is possibly due to the low STAT2 level. This is consistent with observation that STAT2 overexpression in these cells allows the ISGs to be constitutively expressed (Blaszczyk et al. 2016). This suggest the quantity-dependence of the ISG signalling also under the STAT1-deficiency conditions. This is in agreement with the Western blot results, where the ISG expression start is shifted to the later time-points that corresponds with the delay in IRF9 and STAT2 production and STAT2 phosphorylation in response to IFN α (Figure 4.10). Upon JII treatment, IRF9 production in this cells is partially (in case of ST2-U3C) or totally abolished (in case of Huh ST1 K.O.) (Figure 4.20 A and B, respectively), thus U-STAT2/IRF9 formation is impossible.

Like with ISGF3, also in case of STAT2/IRF9 function, the reaching the minimal levels of proteins, seems to be crucial. Platanitis and colleagues (Platanitis et al. 2019), observed that knock-out of all ISGF3 components abolished STAT2/IRF9 targeted gene expression, but, simultaneously, as showed by Majoros *et al.* (Majoros et al. 2016) lack of IRNAR or STAT1, as well as the presence of Y701F STAT1 mutant permanently disrupt the basal expression of STAT2/IRF9 targets. According to the results of Platanitis team, constitutive expression of STAT1, STAT2 and IRF9 relies on the binding of them to their own promoters (Platanitis et al.

DISCUSSION

2019). Michalska and colleagues, (Michalska et al. 2018) proposed the positive feedback loop mechanism, where IFN-induced accumulation of U-STATs, IRF9 and IRF1 over time leads to formation of U-ISGF3 and U-STAT2/IRF9 that maintain prolonged ISG expression. As in case of knock-out cells, the threshold level cannot be reached, STAT2/IRF9 forming is not maintained.

Taking all this into consideration, it is tempting to speculate that gene expression in ST2-U3C and Huh ST1 K.O. (similar to the wild-type cells) is triggered when the level of particular TFs is reached. For ISGF3 these levels are much lower and this complex can be already formed even though IRF9 could not be detectable by the Western blot. In contrast, for U-STAT2/IRF9 and U-ISGF3 the triggering of ISG expression requires the abundance of STAT1 and/or STAT2 as well as IRF9. This threshold levels are apparently not exceeded in any of the tested wild-type cells in the absence of IFN.

In the cells overexpressing all three ISGF3 components we clearly see the elevated basal ISG expression when compared to wild-type cells. After IFN α treatment, we observed enormous gene expression which maximum is much higher than in WT cells. This elevated expression is also sustained after JII administration (Figure 4.37) and, most likely, STAT phosphorylation blockade returns ISG expression to basal levels. Nevertheless, when compared to 2fTGH, the JII effect on transcriptional response in ST1-ST2-IRF9-U3C is clearly less severe, and ISG expression decreased slower.

5.5. Increased complexity of basal and IFN α -dependent transcriptional responses

Intensive studies of IFN-dependent signalling revealed the complexity of the mechanisms that regulate antiviral response. Each year new discoveries appear that bring another puzzle to complete the gaps, however, many threads still remain unsolved.

In this paragraph, based on the available data from this thesis and the literature, we would like to clarify these complex mechanism that function in different cell types.

Under wild-type conditions (Figure 5.1), basal ISG expression is not sufficient to provide viral protection, as the levels of U-STAT1, U-STAT2 and IRF9 are too low. IFN α -stimulation induces STATs phosphorylation, ISGF3 formation, and robust ISG expression. Only then the threshold is exceeded, and cells are able to combat infection. JII addition, block STATs phosphorylation thus robustly reduces gene expression that is decreasing until it drops below

DISCUSSION

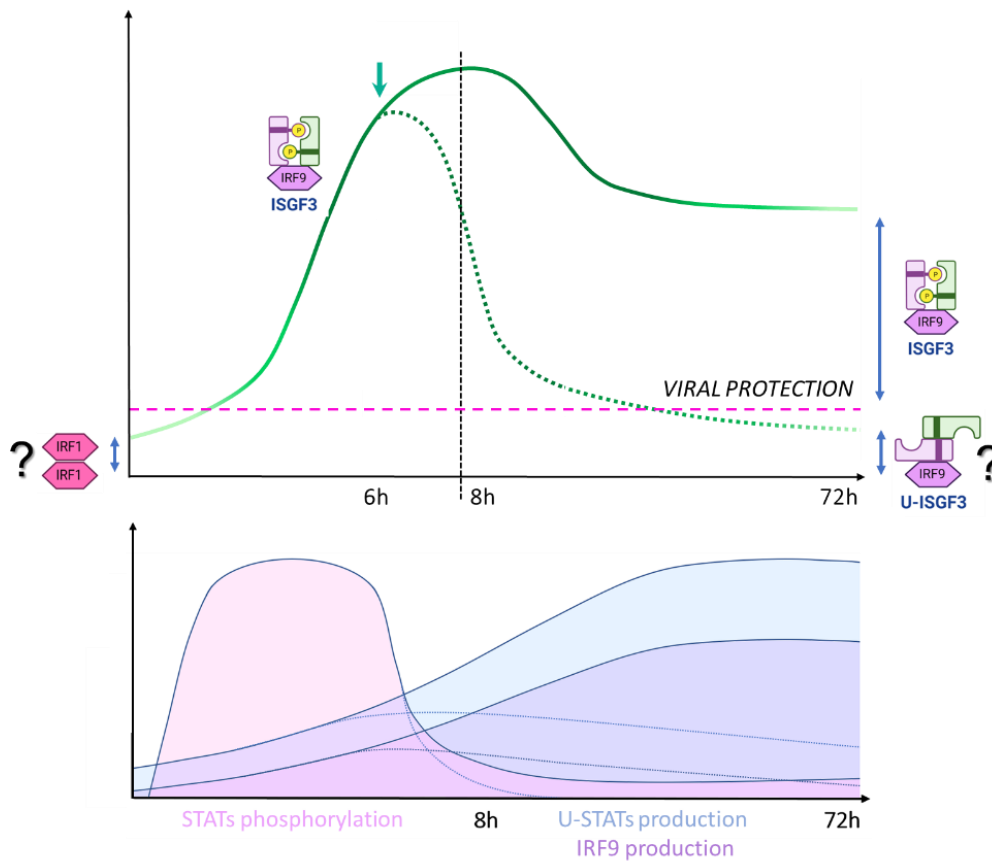


Figure 5.1 *The complex model of the phosphorylation-dependent regulation of IFN α - induced transcriptional response under wild-type conditions*

Upper part of the scheme presents the ISG expression profile in wild-type cells upon long time IFN α treatment (solid green line) and IFN α + JII treatment (dotted green line). Addition of JII in 6h is indicated by the turquoise arrow. Pink dotted line indicates the threshold required to provide the viral protection.

Lower part of the scheme presents the STATs phosphorylation profile (pink), U-STATs production (blue) and IRF9 production (violet) up to 72h of IFN α treatment. Dotted lines present situation after JII stimulation at 6h.

Fast and robust ISG expression and viral protection is ensured by ISGF3, and this complex is also involved in their maintaining up to 72h. After JII treatment, ISG expression, as well as U-STATs and IRF9 production, drastically decrease, what is an effect of the STAT1 and STAT2 phosphorylation blockage. The level of U-STATs is not high enough to provide

the threshold, making the cells sensitive to viral lysis again. JII usage, however, not only blocks STATs phosphorylation, but also inhibits phosphorylation-induced production of native STAT1 and STAT2, as well as IRF9. Therefore, is not possible to distinguish beyond reasonable doubt if the abolished longer ISG expression is caused by lack of phosphorylation

DISCUSSION

or by too low minimal U-STATs and IRF9 levels. Nevertheless, in wild-type cells basal ISG expression is elevated slightly and this could be the result of U-ISGF3 function. On the other hand, some researchers, put forward a hypothesis, for IRF1 to have a role in regulating constitutive ISG expression as its production can be detected in many cell. For example, using CHIP-chip, Hassan and colleagues (Abou El Hassan et al. 2017), have found 28 binding sites occupied by IRF1 in untreated cells, that accounted for 14,3% of all IFN γ -induced sites. Another study, showing the role of IRF1 in untreated cells, is that of Lou *et al.* (Lou et al. 2009). Researchers observed that IRF1 is involved in *RIG-G* expression regulation in both, U-STAT2/IRF9-dependent and -independent manner. IRF1 can also interact with the U-STAT1 to drive *LMP2* basal expression, as was presented by Chatterjee-Kishore and colleagues (Chatterjee-Kishore et al. 2000). *LMP2* promoter region has been found to be occupied by both, STAT1 and IRF1, in the resting 2fTGH cells and U3A that overexpressed unphosphorylatable form of STAT1. This strongly points to the role of IRF1, alone or in the complex with U-, not pSTAT1, in the *LMP2* transcription regulation. Similarly, in HeLa cells, basal *PSMB9* and *TAP2* expression requires the binding of IRF1 to their promoters types (Abou El Hassan et al. 2017). Researchers identified also the STAT1-IRF1 target genes, among them *IFIT* and *IFI* family members that are occupied in the absence of IFN-treatment. However, according to our CHIP-Seq results, we do not see U-STATs binding in case of cells tested by us.

In the absence of STAT1 (Figure 5.2), in Huh ST1 K.O. the production of IRF9 is delayed. After IFN α treatment, STAT2 becomes phosphorylated and together with IRF9 forms the STAT2/IRF9 complex that is able to take over the role of ISGF3. In this case, STAT2/IRF9 forming is delayed because of not sufficient levels of IRF9. However, in the ST2-U3C (Figure 5.3), elevated STAT2 level is sufficient for IRF9 production in the early time-points. The basal ISG expression is also higher in these cells, when compared to 2fTGH. This suggests the role of U-STAT2 in the mediation of basal ISG expression. Nevertheless, this elevated ISG level is not sufficient to provide potent VSV or EMCV protection (Błaszczuk et al. 2015). JII administration in both cell lines, decreased the STAT2 and IRF9 production. Low *IFI6* expression is, however, sustained up to 72h, but the role of U-STAT2/IRF9 in this case is questionable, as IRF9 production is decreased severely, especially in Huh ST1 K.O., where is completely undetectable by the Western blot method.

DISCUSSION

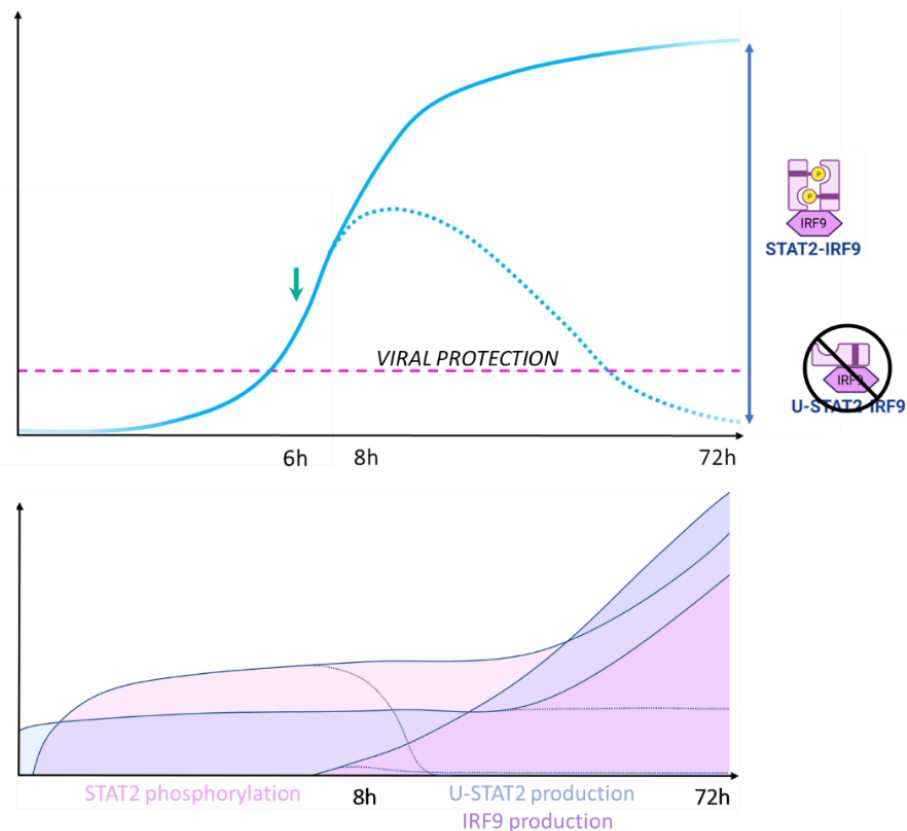


Figure 5.2 The complex model of the phosphorylation-dependent regulation of IFN α - induced transcriptional response in the Huh ST1 K.O. cell line

Upper part of the scheme presents the ISG expression profile in STAT1-deficient Huh cells upon long time IFN α treatment (solid blue line) and IFN α + JII treatment (dotted blue line). Addition of JII in 6h is indicated by the turquoise arrow. Pink dotted line indicates the threshold required to provide the viral protection.

Lower part of the scheme presents the STAT2 phosphorylation profile (pink), U-STAT2 (blue) and IRF9 (violet) production up to 72h of IFN α treatment. Dotted lines present situation after JII stimulation at 6h.

Because of the lack of STAT1, the ISGF3 role is taken over by STAT2/IRF9. IRF9 production and ISG expression start is delayed, and this complex is also involved in their maintaining up to 72h. After JII treatment, ISG expression, as well as U-STATs and IRF9 production drastically decrease, what is an effect of the STAT2 phosphorylation blockage. The level of U-STATs and IRF9 is not high enough to provide viral protection. Completely abolished IRF9 production under basal condition and JII treatment exclude the role of U-STAT2/IRF9 in these cells.

Under conditions of STAT1, STAT2 and IRF9 overexpression (Figure 5.4), abundance of these TFs is enough to provide constitutive ISG expression that ensures potent protection against VSV (Figure 4.28 and 31) and is independent of phosphorylation (Figure 4.35 and 36). JII addition blocks STATs phosphorylation but does not have significant effect on the gene

DISCUSSION

expression and viral protection of these cells. U-ISGF3 is the most probable complex that is involved in this process. Discussed above IRF1 could also participate, but our RNA-Seq results do not show any significant differences in expression of IRF1 between ST1-ST2-IRF9-U3C vs U3C as a control (data not shown). In this instance, the IRF1 role may be restricted to its activity, e.g. interactions with other factors and cofactors, and not connected to its production.

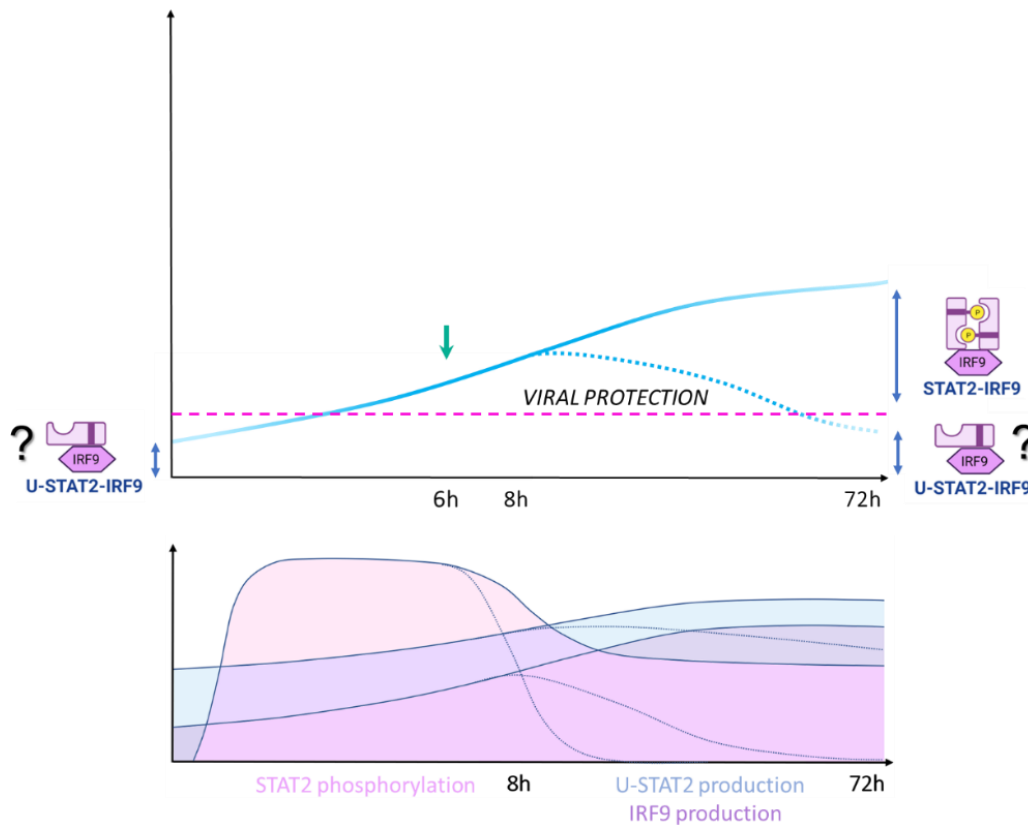


Figure 5.3 The complex model of the phosphorylation-dependent regulation of IFN α - induced transcriptional response in the STAT2-U3C cell line

Upper part of the scheme presents the ISG expression profile in STAT1-deficient cells overexpressing STAT2 upon long time IFN α treatment (solid blue line) and IFN α + JII treatment (dotted blue line). Addition of JII in 6h is indicated by the turquoise arrow. Pink dotted line indicates the threshold required to provide the viral protection.

Lower part of the scheme presents the STAT2 phosphorylation profile (pink), U-STAT2 (blue) and IRF9 (violet) production up to 72h of IFN α treatment. Dotted lines present situation after JII stimulation at 6h.

In the lack of STAT1 the ISGF3 role cannot be formed and its role is taken over STAT2/IRF9. STAT2 overexpression is sufficient to increase IRF9 production, thus most probably STAT2/IRF9 triggers low basal ISG expression. However, potency of STAT2/IRF9 is weaker, when compared to ISGF3, and, in general, this complex mediates much lower ISG expression. After JII treatment, gene expression, as well as U-STAT2 and IRF9 production radically decrease, what is an effect of the STAT2 phosphorylation blockage. The level of U-STAT2 and IRF9 is not high enough to provide protection.

DISCUSSION

In conclusion, our results provide further evidence that in WT cells an IFN α -inducible transcriptional mechanism exists, that relies on the ISGF3 components STAT1, STAT2 and IRF9 in a phosphorylation- and time-dependent manner. It also points to an important role of classical ISGF3 in the regulation of prolonged ISG expressions and viral protection. However, the contribution of U-ISGF3 under these conditions cannot be ruled out.

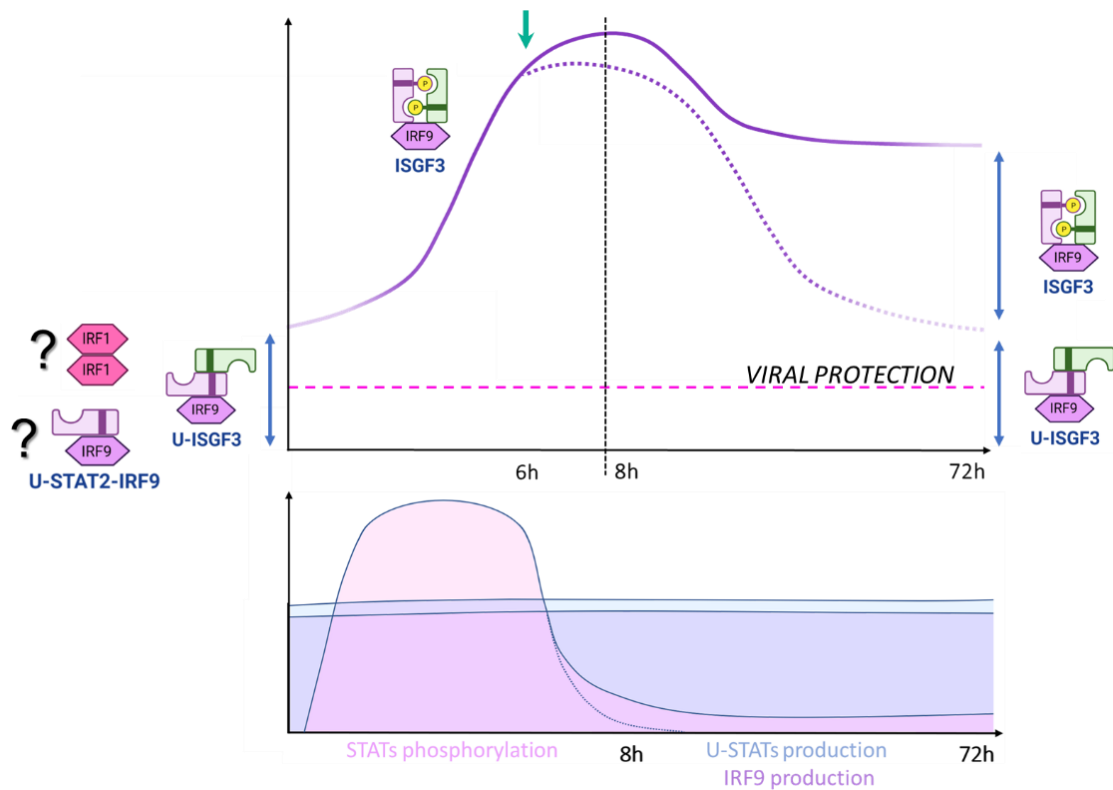


Figure 5.4 *The complex model of the phosphorylation-dependent regulation of IFN α -induced transcriptional response under the overexpression of STAT1, STAT2 and IRF9*

Upper part of the scheme presents the ISG expression profile in cells overexpressing STAT1, STAT2 and IRF9 upon long time IFN α treatment (solid violet line) and IFN α + JII treatment (dotted violet line). Addition of JII in 6h is indicated by the turquoise arrow. Pink dotted line indicates the threshold required to provide the viral protection.

Lower part of the scheme presents the STATs phosphorylation profile (pink), U-STATs (blue) and IRF9 (violet) production up to 72h of IFN α treatment. Dotted lines present situation after JII stimulation at 6h.

Because of the overexpression the level of STAT1, STAT2 and IRF9 is constant, even after IFN α treatment. Simultaneously, abundance of these U-STATs and IRF9 is sufficient to increase constitutive ISG expression and exceed the threshold that provides viral protection. JII administration blocks STATs phosphorylation, thus decreases gene expression, however, it never goes below the basal level. For this reason, U-ISGF3 seems to be key factor that is responsible for this elevated ISG expression.

DISCUSSION

Likewise, in cells lacking STAT1, an IFN α -inducible and STAT1-independent transcriptional mechanism exists, that depends on the STAT2/IRF9 components STAT2 and IRF9 in a phosphorylation- and time-dependent manner. It also provides further prove for the previous observation that STAT2/IRF9 can take over the role of ISGF3 in the absence of STAT1, to regulate expression of a common group of ISRE-containing genes and provide protection against viral infection.

Finally, comparative experiments in STAT1-KO cells overexpressing all ISGF3 components, revealed a potential role of U-ISFG3, and possibly U-STAT2/IRF9, in the regulation of constitutive and long-term IFN α -treated ISG expression and viral protection. This strongly suggests that a certain threshold of STAT1, STAT2 and IRF9 expression and levels of U-ISGF3 (and/or U-STAT2/IRF9) has to be reached to be able to trigger ISG transcription. As a consequence, together with classical ISGF3, U-ISGF3 and U-STAT2/IRF9, could be instrumental in IFN-dependent and independent ISG transcription and in combatting viral infection.

References

- Abdul-Sater, Ali A. et al. 2015. “Different STAT Transcription Complexes Drive Early and Delayed Responses to Type I IFNs.” *The Journal of Immunology* 195(1): 210–16.
- Abou El Hassan, Mohamed et al. 2017. “Properties of STAT1 and IRF1 Enhancers and the Influence of SNPs.” *BMC Molecular Biology* 18(1): 1–19.
- Alcami, Antonio, and Ulrich H. Koszinowski. 2000. “Viral Mechanisms of Immune Evasion.” *Trends in Microbiology* 8(9): 410–18.
- Ali, Shafaqat et al. 2019. “Sources of Type I Interferons in Infectious Immunity: Plasmacytoid Dendritic Cells Not Always in the Driver’s Seat.” *Frontiers in Immunology* 10(APR).
- Antonczyk, Aleksandra et al. 2019. “Direct Inhibition of IRF-Dependent Transcriptional Regulatory Mechanisms Associated with Disease.” *Frontiers in Immunology* 10(MAY): 1–23.
- Arzt, Lisa et al. 2014. “Signal Transducer and Activator of Transcription 1 (STAT1) Acts like an Oncogene in Malignant Pleural Mesothelioma.” *Virchows Archiv* 465(1): 79–88.
- Banninger, Gregg, and Nancy C. Reich. 2004. “STAT2 Nuclear Trafficking.” *Journal of Biological Chemistry* 279(38): 39199–206. <http://dx.doi.org/10.1074/jbc.M400815200>.
- Bardou, Philippe et al. 2014. “Jvenn: An Interactive Venn Diagram Viewer.” *BMC Bioinformatics* 15(1): 293. <https://doi.org/10.1186/1471-2105-15-293>.
- Barnes, Betsy, Barbora Lubyova, and Paula M. Pitha. 2002. “On the Role of IRF in Host Defense.” *Journal of Interferon and Cytokine Research* 22(1): 59–71.
- Beachboard, Dia C, and Stacy M Horner. 2020. “Innate Immune Evasion Strategies of DNA and RNA Viruses.” (January).
- Bhattacharya, S. et al. 1996. “Cooperation of Stat2 and P300/CBP in Signalling Induced by Interferon- α .” *Nature* 383(6598): 344–47.
- Bianchi, Marco E. 2007. “DAMPs, PAMPs and Alarmins: All We Need to Know about Danger.” *Journal of Leukocyte Biology* 81(1): 1–5.
- Blaszczyk, Katarzyna et al. 2015. “STAT2/IRF9 Directs a Prolonged ISGF3-like Transcriptional Response and Antiviral Activity in the Absence of STAT1.” *Biochemical Journal* 466(3): 511–24.
- Blaszczyk, Katarzyna et al. 2016. “The Unique Role of STAT2 in Constitutive and IFN-Induced Transcription and Antiviral Responses.” *Cytokine & growth factor reviews* 29: 71–81.
- Blyussen, Hans A.R., Joan E. Durbin, and David E. Levy. 1996. “ISGF3 γ P48, a Specificity Switch for Interferon Activated Transcription Factors.” *Cytokine and Growth Factor Reviews* 7(1): 11–17.
- Blyussen, Hans A.R., and David E. Levy. 1997. “Stat2 Is a Transcriptional Activator That Requires Sequence-Specific Contacts Provided by Stat1 and P48 for Stable Interaction with DNA.” *Journal of Biological Chemistry* 272(7): 4600–4605.
- Bonjardim, C. A. 1998. “JAK/STAT-Deficient Cell Lines.” *Brazilian Journal of Medical and Biological Research* 31(11): 1389–95.

REFERENCES

- van Boxel-Dezaire, Anette H.H., M. R. Sandhya Rani, and George R. Stark. 2006. “Complex Modulation of Cell Type-Specific Signaling in Response to Type I Interferons.” *Immunity* 25(3): 361–72.
- Broering, Ruth et al. 2010. “The Interferon Stimulated Gene 15 Functions as a Proviral Factor for the Hepatitis C Virus and as a Regulator of the IFN Response.” *Gut* 59(8): 1111–19.
- Chatterjee-Kishore, Moitreyee, Kenneth L. Wright, Jenny P.Y. Ting, and George R. Stark. 2000. “How Stat1 Mediates Constitutive Gene Expression: A Complex of Unphosphorylated Stat1 and IRF1 Supports Transcription of the LMP2 Gene.” *EMBO Journal* 19(15): 4111–22.
- Cheng, Zhangliang et al. 2020. “The Interactions between CGAS-STING Pathway and Pathogens.” *Signal Transduction and Targeted Therapy* 5(1).
<http://dx.doi.org/10.1038/s41392-020-0198-7>.
- Cheon, Hyeon Joo, and George R. Stark. 2009. “Unphosphorylated STAT1 Prolongs the Expression of Interferon-Induced Immune Regulatory Genes.” *Proceedings of the National Academy of Sciences of the United States of America* 106(23): 9373–78.
- Cheon, Hyeonjoo et al. 2013. “IFN β -Dependent Increases in STAT1, STAT2, and IRF9 Mediate Resistance to Viruses and DNA Damage.” *EMBO Journal* 32(20): 2751–63.
<http://dx.doi.org/10.1038/emboj.2013.203>.
- Chodisetti, Sathi Babu et al. 2020. “Serine Phosphorylation of the STAT1 Transactivation Domain Promotes Autoreactive B Cell and Systemic Autoimmunity Development.” *The Journal of Immunology* 204(10): 2641–50.
- Consortium, The ENCODE Project. 2012. “An Integrated Encyclopedia of DNA Elements in the Human Genome.” *Nature* 489(7414): 57–74.
- Danecek, Petr et al. 2021. “Twelve Years of SAMtools and BCFtools.” *GigaScience* 10(2): 1–4.
- Darnell, James E., Ian M. Kerr, and George R. Stark. 1994. “Jak-STAT Pathways and Transcriptional Activation in Response to IFNs and Other Extracellular Signaling Proteins.” *Science* 264(5164): 1415–21.
- Decker, Thomas, Pavel Kovarik, and Andreas Meinke. 1997. “GAS Elements: A Few Nucleotides with a Major Impact on Cytokine-Induced Gene Expression.” *Journal of Interferon and Cytokine Research* 17(3): 121–34.
- Delgoffe, Greg M., and Dario A.A. Vignali. 2013. “STAT Heterodimers in Immunity: A Mixed Message or a Unique Signal?” *Jak-Stat* 2(1): e23060.
<https://www.landesbioscience.com/journals/jak-stat/article/23060/>.
- Durbin, Joan E. et al. 2000. “Type I IFN Modulates Innate and Specific Antiviral Immunity.” *The Journal of Immunology* 164(8): 4220–28.
- Erickson, Andrea K., and Michael Gale. 2008. “Regulation of Interferon Production and Innate Antiviral Immunity through Translational Control of IRF-7.” *Cell Research* 18(4): 433–35.
- Fagerlund, Riku, Krister Mélen, Leena Kinnunen, and Ilkka Julkunen. 2002. “Arginine/Lysine-Rich Nuclear Localization Signals Mediate Interactions between Dimeric STATs and Importin Alpha 5.” *The Journal of biological chemistry* 277(33): 30072–78.
- Feng, Hui et al. 2021. “Interferon Regulatory Factor 1 (IRF1) and Anti-Pathogen Innate

REFERENCES

- Immune Responses.” *PLoS Pathogens* 17(1): 1–22.
<http://dx.doi.org/10.1371/journal.ppat.1009220>.
- Feusterl, Volker, and Ganes C. Sen. 2009. “Interferons and Viral Infections.” *BioFactors* 35(1): 14–20.
- Ferrao, Ryan, and Patrick J. Lupardus. 2017. “The Janus Kinase (JAK) FERM and SH2 Domains: Bringing Specificity to JAK-Receptor Interactions.” *Frontiers in Endocrinology* 8(APR): 1–11.
- Fujii, Yoshifumi et al. 1999. “Crystal Structure of an IRF-DNA Complex Reveals Novel DNA Recognition and Cooperative Binding to a Tandem Repeat of Core Sequences.” *EMBO Journal* 18(18): 5028–41.
- Gallucci, Stefania, Sowmya Meka, and Ana M. Gamero. 2021. “Abnormalities of the Type I Interferon Signaling Pathway in Lupus Autoimmunity.” *Cytokine* 146(April): 155633.
<https://doi.org/10.1016/j.cyto.2021.155633>.
- Garcin, Dominique et al. 2002. “All Four Sendai Virus C Proteins Bind Stat1, but Only the Larger Forms Also Induce Its Mono-Ubiquitination and Degradation.” *Virology* 295(2): 256–65.
- Ge, Steven Xijin, Dongmin Jung, and Runan Yao. 2020. “ShinyGO: A Graphical Gene-Set Enrichment Tool for Animals and Plants.” *Bioinformatics* 36(8): 2628–29.
<https://doi.org/10.1093/bioinformatics/btz931>.
- Geiss, Gary K. et al. 2003. “Gene Expression Profiling of the Cellular Transcriptional Network Regulated by Alpha/Beta Interferon and Its Partial Attenuation by the Hepatitis C Virus Nonstructural 5A Protein.” *Journal of virology* 77(11): 6367–75.
<http://www.ncbi.nlm.nih.gov/pubmed/12743294>.
- Ghoreschi, Kamran, Arian Laurence, and John J. O’Shea. 2009. “Janus Kinases in Immune Cell Signaling.” *Immunological Reviews* 228(1): 273–87.
- Gitlin, Leonid et al. 2006. “Essential Role of Mda-5 in Type I IFN Responses to Polyriboinosinic: Polyribocytidylic Acid and Encephalomyocarditis Picornavirus.” *Proceedings of the National Academy of Sciences of the United States of America* 103(22): 8459–64.
- Goodbourn, S., L. Didcock, and R. E. Randall. 2000. “Interferons: Cell Signalling, Immune Modulation, Antiviral Responses and Virus Countermeasures.” *Journal of General Virology* 81(10): 2341–64.
- Gu, Zuguang, Roland Eils, and Matthias Schlesner. 2016. “Complex Heatmaps Reveal Patterns and Correlations in Multidimensional Genomic Data.” *Bioinformatics* 32(18): 2847–49.
- Harper, Thomas M., and Dylan J. Taatjes. 2018. “The Complex Structure and Function of Mediator.” *Journal of Biological Chemistry* 293(36): 13778–85.
<http://dx.doi.org/10.1074/jbc.R117.794438>.
- Hartman, Stephen E. et al. 2005. “Global Changes in STAT Target Selection and Transcription Regulation upon Interferon Treatments.” *Genes and Development* 19(24): 2953–68.
- Heinz, Sven et al. 2010. “Simple Combinations of Lineage-Determining Transcription Factors Prime Cis-Regulatory Elements Required for Macrophage and B Cell Identities.” *Molecular Cell* 38(4): 576–89. <http://dx.doi.org/10.1016/j.molcel.2010.05.004>.

REFERENCES

- Hemann, Emily A., Michael Gale, and Ram Savan. 2017. "Interferon Lambda Genetics and Biology in Regulation of Viral Control." *Frontiers in Immunology* 8(DEC).
- Honda, Kenya et al. 2005. "IRF-7 Is the Master Regulator of Type-I Interferon-Dependent Immune Responses." *Nature* 434(7034): 772–77. <http://www.ncbi.nlm.nih.gov/pubmed/15800576>.
- Honke, Nadine et al. 2016. "Multiple Functions of USP18." *Cell Death and Disease* 7(11): 1–9.
- Huang, Lily Jun shen, Stefan N. Constantinescu, and Harvey F. Lodish. 2001. "The N-Terminal Domain of Janus Kinase 2 Is Required for Golgi Processing and Cell Surface Expression of Erythropoietin Receptor." *Molecular Cell* 8(6): 1327–38.
- Ivashkiv, Lionel B., and Laura T. Donlin. 2014. "Regulation of Type I Interferon Responses." *Nature Reviews Immunology* 14(1): 36–49. <http://www.nature.com/articles/nri3581>.
- Janjua, S., A. Stephanou, and D. S. Latchman. 2002. "The C-Terminal Activation Domain of the STAT-1 Transcription Factor Is Necessary and Sufficient for Stress-Induced Apoptosis." *Cell Death and Differentiation* 9(10): 1140–46.
- Jefferies, Caroline A. 2019. "Regulating IRFs in IFN Driven Disease." *Frontiers in immunology* 10(MAR): 325. <http://www.ncbi.nlm.nih.gov/pubmed/30984161>.
- Jiang, Ding Sheng et al. 2014. "Interferon Regulatory Factor 9 Protects against Cardiac Hypertrophy by Targeting Myocardin." *Hypertension* 63(1): 119–27.
- Jun, Goo, Mary Kate Wing, Gonçalo R. Abecasis, and Hyun Min Kang. 2015. "An Efficient and Scalable Analysis Framework for Variant Extraction and Refinement from Population-Scale DNA Sequence Data." *Genome Research* 25(6): 918–25.
- Kaplan, Daniel H. et al. 1998. "Demonstration of an Interferon γ -Dependent Tumor Surveillance System in Immunocompetent Mice." *Proceedings of the National Academy of Sciences of the United States of America* 95(13): 7556–61.
- Kato, Hiroki et al. 2005. "Cell Type-Specific Involvement of RIG-I in Antiviral Response." *Immunity* 23(1): 19–28.
- Kato, Hiroki et al. 2006. "Differential Roles of MDA5 and RIG-I Helicases in the Recognition of RNA Viruses." *Nature* 441(1): 101–5.
- Kaur, Ashwinder, Learn Han Lee, Sek Chuen Chow, and Chee Mun Fang. 2018. "IRF5-Mediated Immune Responses and Its Implications in Immunological Disorders." *International Reviews of Immunology* 37(5): 229–48. <https://doi.org/10.1080/08830185.2018.1469629>.
- Kawai, Taro, and Shizuo Akira. 2011. "Toll-like Receptors and Their Crosstalk with Other Innate Receptors in Infection and Immunity." *Immunity* 34(5): 637–50. <http://dx.doi.org/10.1016/j.immuni.2011.05.006>.
- Kessler, D. S., S. A. Veals, X. Y. Fu, and D. E. Levy. 1990. "Interferon- α Regulates Nuclear Translocation and DNA-Binding Affinity of ISGF3, a Multimeric Transcriptional Activator." *Genes and Development* 4(10): 1753–65.
- Kilbourne MD, Edwin D. 1990. "A Real and Potential Problem Without Boundaries." *JAMA* 264: 68–70.
- Kisseleva, T., S. Bhattacharya, J. Braunstein, and C. W. Schindler. 2002. "Signaling through the JAK/STAT Pathway, Recent Advances and Future Challenges." *Gene* 285(1–2): 1–24.

REFERENCES

- Kiu, Hiu, and Sandra E Nicholson. 2012. "Biology and Significance of the JAK/STAT Signalling Pathways." *Growth factors (Chur, Switzerland)* 30(2): 88–106.
<https://www.ncbi.nlm.nih.gov/pmc/articles/PMC3624763/pdf/nihms412728.pdf>.
- Kochs, Georg, and Otto Haller. 1999. "Interferon-Induced Human MxA GTPase Blocks Nuclear Import of Thogoto Virus Nucleocapsids." *Proceedings of the National Academy of Sciences of the United States of America* 96(5): 2082–86.
- Kolde, Raivo. 2019. "Pheatmap: Pretty Heatmaps. R Package Version 1.0. 12." CRAN. *R-project.org/package=pheatmap*.
- Kraus, Thomas A., Joe F. Lau, Jean Patrick Parisien, and Curt M. Horvath. 2003. "A Hybrid IRF9-STAT2 Protein Recapitulates Interferon-Stimulated Gene Expression and Antiviral Response." *Journal of Biological Chemistry* 278(15): 13033–38.
<http://dx.doi.org/10.1074/jbc.M212972200>.
- Kumar, Aseem et al. 1997. "Defective TNF- α -Induced Apoptosis in STAT1-Null Cells Due to Low Constitutive Levels of Caspases." *Science* 278(5343): 1630–32.
- Langmead, Ben, and Steven L. Salzberg. 2012. "Fast Gapped-Read Alignment with Bowtie 2." *Nature Methods* 9(4): 357–59.
- Lau, Joe F. et al. 2003. "Role of Metazoan Mediator Proteins in Interferon-Responsive Transcription." *Molecular and Cellular Biology* 23(2): 620–28.
- Lau, Joe F., Jean Patrick Parisien, and Curt M. Horvath. 2000. "Interferon Regulatory Factor Subcellular Localization Is Determined by a Bipartite Nuclear Localization Signal in the DNA-Binding Domain and Interaction with Cytoplasmic Retention Factors." *Proceedings of the National Academy of Sciences of the United States of America* 97(13): 7278–83.
- Lazear, Helen M. et al. 2013. "IRF-3, IRF-5, and IRF-7 Coordinately Regulate the Type I IFN Response in Myeloid Dendritic Cells Downstream of MAVS Signaling." *PLoS Pathogens* 9(1).
- Lazear, Helen M., John W. Schoggins, and Michael S. Diamond. 2019. "Shared and Distinct Functions of Type I and Type III Interferons." *Immunity* 50(4): 907–23.
<https://doi.org/10.1016/j.immuni.2019.03.025>.
- Lee, Cheol Jung et al. 2020. "FBXW7-Mediated Stability Regulation of Signal Transducer and Activator of Transcription 2 in Melanoma Formation." *Proceedings of the National Academy of Sciences of the United States of America* 117(1): 584–94.
- Lei, Jin et al. 2021. "Interferon Regulatory Factor Transcript Levels Correlate with Clinical Outcomes in Human Glioma." *Aging* 13(8): 12086–98.
- Levy, D. E. et al. 1988. "Interferon-Induced Nuclear Factors That Bind a Shared Promoter Element Correlate with Positive and Negative Transcriptional Control." *Genes & development* 2(4): 383–93.
- Levy, D. E., D. S. Kessler, R. Pine, and J. E. Darnell. 1989. "Cytoplasmic Activation of ISGF3, the Positive Regulator of Interferon-Alpha-Stimulated Transcription, Reconstituted in Vitro." *Genes & development* 3(9): 1362–71.
- Li, X, S Leung, I M Kerr, and G R Stark. 1997. "Functional Subdomains of STAT2 Required for Preassociation with the Alpha Interferon Receptor and for Signaling." *Molecular and Cellular Biology* 17(4): 2048–56.
- Li, Xiao Ling et al. 2000. "Rnase-l-Dependent Destabilization of Interferon-Induced MRNAs.

REFERENCES

- A Role for the 2-5A System in Attenuation of the Interferon Responses.” *Journal of Biological Chemistry* 275(12): 8880–88. <http://dx.doi.org/10.1074/jbc.275.12.8880>.
- Lim, Cheh Peng, and Xinmin Cao. 2006. “Structure, Function, and Regulation of STAT Proteins.” *Molecular BioSystems* 2(11): 536–50.
- Lindenmann, J., D. C. Burke, and Isaacs A. 1957. “Studies on the Production, Mode of Action and Properties of Interferon.” *British journal of experimental pathology* 38(5): 551–62.
- Liu, Yong Jun. 2005. “IPC: Professional Type 1 Interferon-Producing Cells and Plasmacytoid Dendritic Cell Precursors.” *Annual Review of Immunology* 23(3): 275–306.
- Lotfi, Ramin, James J. Lee, and Michael T. Lotze. 2007. “Eosinophilic Granulocytes and Damage-Associated Molecular Pattern Molecules (DAMPs): Role in the Inflammatory Response within Tumors.” *Journal of Immunotherapy* 30(1): 16–28.
- Lotze, Michael T., Albert Deisseroth, and Anna Rubartelli. 2007. “Damage Associated Molecular Pattern Molecules.” *Clinical Immunology* 124(1): 1–4.
- Lou, Ye Jiang et al. 2009. “Ifr-9/Stat2 Functional Interaction Drives Retinoic Acid-Induced Gene g Expression Independently of Stat1.” *Cancer Research* 69(8): 3673–80.
- Lu, G et al. 2006. “ISG15 Enhances the Innate Antiviral Response by Inhibition of IRF-3 Degradation.” *Cellular and molecular biology (Noisy-le-Grand, France)* 52(1): 29–41. <http://europepmc.org/abstract/MED/16914094>.
- Majoros, Andrea et al. 2016. “Response to Interferons and Antibacterial Innate Immunity in the Absence of Tyrosine-Phosphorylated STAT1.” *EMBO reports* 17(3): 367–82. <http://www.ncbi.nlm.nih.gov/pubmed/26882544>.
- Majoros, Andrea et al. 2017. “Canonical and Non-Canonical Aspects of JAK-STAT Signaling: Lessons from Interferons for Cytokine Responses.” *Frontiers in Immunology* 8(JAN).
- Malterer, Melanie B, Samantha J Glass, and Joseph P Newman. 2014. “Interferon-Stimulated Genes: A Complex Web of Host Defenses.” *Annual Review of Immunology* 44(3): 735–45.
- Manoochehrabadi, Saba et al. 2019. “Analysis of STAT1, STAT2 and STAT3 MRNA Expression Levels in the Blood of Patients with Multiple Sclerosis.” *Human Antibodies* 27(2): 91–98.
- Marcus, Philip I. 1999. “Intereferons.” : 854–62.
- Marg, Andreas et al. 2004. “Nucleocytoplasmic Shuttling by Nucleoporins Nup153 and Nup214 and CRM1-Dependent Nuclear Export Control the Subcellular Distribution of Latent Stat1.” *Journal of Cell Biology* 165(6): 823–33.
- Marie, I. 1998. “Differential Viral Induction of Distinct Interferon-Alpha Genes by Positive Feedback through Interferon Regulatory Factor-7.” *The EMBO Journal* 17(22): 6660–69.
- Martinez-Moczygemba, Margarita, Michael J. Gutch, Deborah L. French, and Nancy C. Reich. 1997. “Distinct STAT Structure Promotes Interaction of STAT2 with the P48 Subunit of the Interferon- α -Stimulated Transcription Factor ISGF3.” *Journal of Biological Chemistry* 272(32): 20070–76. <http://dx.doi.org/10.1074/jbc.272.32.20070>.
- McBride, K. M. 2000. “Nuclear Export Signal Located within TheDNA-Binding Domain of the STAT1transcription Factor.” *The EMBO Journal* 19(22): 6196–6206.
- McBride, Kevin M., Gregg Banninger, Christine McDonald, and Nancy C. Reich. 2002.

REFERENCES

- “Regulated Nuclear Import of the STAT1 Transcription Factor by Direct Binding of Importin- α .” *EMBO Journal* 21(7): 1754–63.
- McKendry, R. et al. 1991. “High-Frequency Mutagenesis of Human Cells and Characterization of a Mutant Unresponsive to Both α and γ Interferons.” *Proceedings of the National Academy of Sciences of the United States of America* 88(24): 11455–59.
- Mertens, Claudia et al. 2006. “Dephosphorylation of Phosphotyrosine on STAT1 Dimers Requires Extensive Spatial Reorientation of the Monomers Facilitated by the N-Terminal Domain.” *Genes and Development* 20(24): 3372–81.
- Meyer, Thomas, and Uwe Vinkemeier. 2004. “Nucleocytoplasmic Shuttling of STAT Transcription Factors.” *European Journal of Biochemistry* 271(23–24): 4606–12.
- Michalska, Agata, Katarzyna Blaszczyk, Joanna Wesoly, and Hans A.R. Bluysen. 2018. “A Positive Feedback Amplifier Circuit That Regulates Interferon (IFN)-Stimulated Gene Expression and Controls Type I and Type II IFN Responses.” *Frontiers in Immunology* 9(MAY): 1–17.
- Mowen, Kerri A. et al. 2001. “Arginine Methylation of STAT1 Modulates IFN α/β -Induced Transcription.” *Cell* 104(5): 731–41.
- Neculai, Dante et al. 2005. “Structure of the Unphosphorylated STAT5a Dimer.” *Journal of Biological Chemistry* 280(49): 40782–87. <http://dx.doi.org/10.1074/jbc.M507682200>.
- Nguyen, Vinh Ph  c et al. 2002. “Stat2 Binding to the Interferon- α Receptor 2 Subunit Is Not Required for Interferon- α Signaling.” *Journal of Biological Chemistry* 277(12): 9713–21.
- Novatt, Hilary et al. 2016. “Distinct Patterns of Expression of Transcription Factors in Response to Interferon β and Interferon λ 1.” *Journal of Interferon and Cytokine Research* 36(10): 589–98.
- de Oliveira, Roberta Taiane Germano et al. 2021. “ERVs-TLR3-IRF Axis Is Linked to Myelodysplastic Syndrome Pathogenesis.” *Medical Oncology* 38(3): 1–12. <https://doi.org/10.1007/s12032-021-01466-1>.
- Otto, Shirley E. 2003. “Understanding the Immune System: Overview for Infusion Assessment.” *Journal of Infusion Nursing* 26(2): 79–85.
- Park, Jinah et al. 2018. “Novel Identification of STAT1 as a Crucial Mediator of ETV6-NTRK3-Induced Tumorigenesis.” *Oncogene* 37(17): 2270–84. <http://dx.doi.org/10.1038/s41388-017-0102-2>.
- Parrini, Matthias et al. 2018. “The C-Terminal Transactivation Domain of STAT1 Has a Gene-Specific Role in Transactivation and Cofactor Recruitment.” *Frontiers in Immunology* 9(December): 1–16.
- Paul, Alvin, Thean Hock Tang, and Siew Kit Ng. 2018. “Interferon Regulatory Factor 9 Structure and Regulation.” *Frontiers in Immunology* 9(AUG): 1–9.
- Paulson, Matthew et al. 2002. “IFN-Stimulated Transcription through a TBP-Free Acetyltransferase Complex Escapes Viral Shutoff.” *Nature Cell Biology* 4(2): 140–47.
- Paun, A., and P. M. Pitha. 2007. “The IRF Family, Revisited.” *Biochimie* 89(6–7): 744–53.
- Pedranzini, Laura et al. 2006. “Pyridone 6, a Pan-Janus-Activated Kinase Inhibitor, Induces Growth Inhibition of Multiple Myeloma Cells.” *Cancer Research* 66(19): 9714–21.
- Perng, Yi Chieh, and Deborah J. Lenschow. 2018. “ISG15 in Antiviral Immunity and

REFERENCES

- Beyond.” *Nature Reviews Microbiology* 16(7): 423–39.
<http://dx.doi.org/10.1038/s41579-018-0020-5>.
- Perry, Stuart T. et al. 2011. “STAT2 Mediates Innate Immunity to Dengue Virus in the Absence of STAT1 via the Type I Interferon Receptor.” *PLoS Pathogens* 7(2).
- Pestka, Sidney. 2007. “The Interferons: 50 Years after Their Discovery, There Is Much More to Learn.” *Journal of Biological Chemistry* 282(28): 20047–51.
<http://dx.doi.org/10.1074/jbc.R700004200>.
- Pitha, P.M., and Various. 2007. 117 *International Journal of Food Microbiology Interferon: The 50th Anniversary*.
- Platanitis, Ekaterini et al. 2019. “A Molecular Switch from STAT2-IRF9 to ISGF3 Underlies Interferon-Induced Gene Transcription.” *Nature Communications* 10(1): 1–17.
<http://dx.doi.org/10.1038/s41467-019-10970-y>.
- Prokunina-olsson, Ludmila et al. 2013. “A Variant Upstream of IFNL3 (IL28B) Creating a Novel Interferon Gene IFNL4 Is Associated with Impaired Clearance of Hepatitis C Virus.” 45(2): 164–71.
- Quinlan, Aaron R., and Ira M. Hall. 2010. “BEDTools: A Flexible Suite of Utilities for Comparing Genomic Features.” *Bioinformatics* 26(6): 841–42.
- Ramana, Chilakamarti V. et al. 2007. “The STAT Family of Proteins in Cytokine Signaling.” *Progress in Biophysics and Molecular Biology* 18(5–6): 96–101.
<http://dx.doi.org/10.1074/jbc.R700004200>.
- Ramírez, Fidel et al. 2016. “DeepTools2: A next Generation Web Server for Deep-Sequencing Data Analysis.” *Nucleic Acids Research* 44(W1): W160–65.
- Randall, Richard E., and Stephen Goodbourn. 2008. “Interferons and Viruses: An Interplay between Induction, Signalling, Antiviral Responses and Virus Countermeasures.” *Journal of General Virology* 89(1): 1–47.
- Rauch, Isabella et al. 2015. “Noncanonical Effects of IRF9 in Intestinal Inflammation: More than Type I and Type III Interferons.” *Molecular and Cellular Biology* 35(13): 2332–43.
- Rebouillat, Dominique, and A R A G Hovanessian. 1999. “Interferon-Induced Proteins with Unique Enzymatic Properties AC TIVITIES DEPENDENT ON DsRNA.” 308: 2–5.
- Reich, Nancy C. 2013. “STATs Get Their Move On.” *Jak-Stat* 2(4): e27080.
- Rengachari, Srinivasan et al. 2018. “Structural Basis of STAT2 Recognition by IRF9 Reveals Molecular Insights into ISGF3 Function.” *Proceedings of the National Academy of Sciences of the United States of America* 115(4): E601–9.
- Richardson, R. Blake et al. 2018. “A CRISPR Screen Identifies IFI6 as an ER-Resident Interferon Effector That Blocks Flavivirus Replication.” *Nature Microbiology* 3(11): 1214–23.
- Robinson, James T et al. 2011. “Integrative Genome Viewer.” *Nature Biotechnology* 29(1): 24–26.
- Rogers, Richard S., Curt M. Horvath, and Michael J. Matunis. 2003. “SUMO Modification of STAT1 and Its Role in PIAS-Mediated Inhibition of Gene Activation.” *Journal of Biological Chemistry* 278(32): 30091–97. <http://dx.doi.org/10.1074/jbc.M301344200>.
- Roh, Jong Seong, and Dong Hyun Sohn. 2018. “Damage-Associated Molecular Patterns in Inflammatory Diseases.” *Immune Network* 18(4): 1–14.

REFERENCES

- Ronnlblom, L. E., G. V. Alm, and K. E. Oberg. 1991. "Autoimmunity after Alpha-Interferon Therapy for Malignant Carcinoid Tumors." *Annals of Internal Medicine* 115(3): 178–83.
- Sadler, Anthony J., and Bryan R.G. Williams. 2008. "Interferon-Inducible Antiviral Effectors." *Nature Reviews Immunology* 8(7): 559–68.
- Samuel, C. E. 2001. "Antiviral Actions of Interferons." *Clinical Microbiology Reviews* 14(4): 778–809.
- Samuel, C E, and G S Knutson. 1982. "Mechanism of Interferon Action. Kinetics of Induction of the Antiviral State and Protein Phosphorylation in Mouse Fibroblasts Treated with Natural and Cloned Interferons." *Journal of Biological Chemistry* 257(19): 11791–95. <https://linkinghub.elsevier.com/retrieve/pii/S002192581833833X>.
- Schindler, Christian, David E. Levy, and Thomas Decker. 2007. "JAK-STAT Signaling: From Interferons to Cytokines." *Journal of Biological Chemistry* 282(28): 20059–63. <http://dx.doi.org/10.1074/jbc.R700016200>.
- Schoggins, John W. et al. 2011. "A Diverse Range of Gene Products Are Effectors of the Type I Interferon Antiviral Response." *Nature* 472(7344): 481–85.
- Schoggins, John W. et al. 2019. "Interferon-Stimulated Genes: What Do They All Do?" *Annual Review of Virology* 6(1): 567–84. <https://www.annualreviews.org/doi/10.1146/annurev-virology-092818-015756>.
- Schoggins, John W. 2014. "Interferon-Stimulated Genes: Roles in Viral Pathogenesis." *Current Opinion in Virology* 6(January): 40–46. <https://linkinghub.elsevier.com/retrieve/pii/S1879625714000662>.
- Sen, A. et al. 2014. "Rotavirus NSP1 Protein Inhibits Interferon-Mediated STAT1 Activation." *Journal of Virology* 88(1): 41–53.
- Seong, Seung Yong, and Polly Matzinger. 2004. "Hydrophobicity: An Ancient Damage-Associated Molecular Pattern That Initiates Innate Immune Responses." *Nature Reviews Immunology* 4(6): 469–78.
- Shaw, Andrew E. et al. 2017. "Fundamental Properties of the Mammalian Innate Immune System Revealed by Multispecies Comparison of Type I Interferon Responses." *PLoS Biology* 15(12): 1–23.
- Shuai, Ke. 1999. "The STAT Family of Proteins in Cytokine Signaling." *Progress in Biophysics and Molecular Biology* 71(3–4): 405–22.
- Silverman, Robert H. 2007. "Viral Encounters with 2',5'-Oligoadenylate Synthetase and RNase L during the Interferon Antiviral Response." *Journal of Virology* 81(23): 12720–29.
- Sironi, Juan J., and Toru Ouchi. 2004. "STAT1-Induced Apoptosis Is Mediated by Caspases 2, 3, and 7." *Journal of Biological Chemistry* 279(6): 4066–74. <http://dx.doi.org/10.1074/jbc.M307774200>.
- Sommereyns, Caroline, Sophie Paul, Peter Staeheli, and Thomas Michiels. 2008. "IFN-Lambda (IFN-λ) Is Expressed in a Tissue-Dependent Fashion and Primarily Acts on Epithelial Cells in Vivo." *PLoS Pathogens* 4(3): 1–12.
- Stark, George R. 2007. "How Cells Respond to Interferons Revisited: From Early History to Current Complexity." *Cytokine and Growth Factor Reviews* 18(5–6): 419–23.
- Steen, Håkan C. et al. 2013. "Identification of STAT2 Serine 287 as a Novel Regulatory Phosphorylation Site in Type I Interferon-Induced Cellular Responses." *Journal of*

REFERENCES

- Biological Chemistry* 288(1): 747–58.
- Stewart, M. David et al. 2002. “Roles of Stat1, Stat2, and Interferon Regulatory Factor-9 (IRF-9) in Interferon Tau Regulation of IRF-1.” *Biology of Reproduction* 66(2): 393–400.
- Stone, Amy E.L. et al. 2014. “Hepatitis C Virus Core Protein Inhibits Interferon Production by a Human Plasmacytoid Dendritic Cell Line and Dysregulates Interferon Regulatory Factor-7 and Signal Transducer and Activator of Transcription (STAT) 1 Protein Expression.” *PLoS ONE* 9(5): 1–8.
- Sue, Paul K., Michal Meir, and Maite de la Morena. 2018. Principles and Practice of Pediatric Infectious Diseases *Immunologic Development and Susceptibility to Infection*. Fifth Edit. Elsevier Inc. <http://dx.doi.org/10.1016/B978-0-323-40181-4.00009-8>.
- Sung, Pil Soo et al. 2015. “Roles of Unphosphorylated ISGF3 in HCV Infection and Interferon Responsiveness.” *Proceedings of the National Academy of Sciences of the United States of America* 112(33): 10443–48.
- Szelag, Malgorzata et al. 2016. “Targeted Inhibition of STATs and IRFs as a Potential Treatment Strategy in Cardiovascular Disease.” *Oncotarget* 7(30): 48788–812.
- Szelag, Malgorzata, Anna Czerwonec, Joanna Wesoly, and Hans A.R. Bluysen. 2015. “Identification of STAT1 and STAT3 Specific Inhibitors Using Comparative Virtual Screening and Docking Validation.” *PLoS ONE* 10(2): 1–22.
- Tang, Xiaoli et al. 2007. “Acetylation-Dependent Signal Transduction for Type I Interferon Receptor.” *Cell* 131(1): 93–105.
- Taniguchi, Tadatsugu, Kouetsu Ogasawara, Akinori Takaoka, and Nobuyuki Tanaka. 2001. “IRF Family of Transcription Factors as Regulators of Host Defense.” *Annual review of immunology* 19: 623–55. <http://www.ncbi.nlm.nih.gov/pubmed/11244049>.
- Tapper, Michael L. 2006. “Emerging Viral Diseases and Infectious Disease Risks.” *Haemophilia* 12(SUPPL. 1): 3–7.
- Testoni, Barbara et al. 2011. “Chromatin Dynamics of Gene Activation and Repression in Response to Interferon Alpha (IFN(Alpha)) Reveal New Roles for Phosphorylated and Unphosphorylated Forms of the Transcription Factor STAT2.” *The Journal of biological chemistry* 286(23): 20217–27. <http://dx.doi.org/10.1074/jbc.M111.231068>.
- Turvey, Stuart E., and David H. Broide. 2010. “Innate Immunity.” *Journal of Allergy and Clinical Immunology* 125(2 SUPPL. 2): S24–32. <http://dx.doi.org/10.1016/j.jaci.2009.07.016>.
- Ungureanu, Daniela et al. 2005. “SUMO-1 Conjugation Selectively Modulates STAT1-Mediated Gene Responses.” *Blood* 106(1): 224–26.
- Ungureanu, Daniela et al. 2011. “The Pseudokinase Domain of JAK2 Is a Dual-Specificity Protein Kinase That Negatively Regulates Cytokine Signaling.” *Nature structural & molecular biology* 18(9): 971–76. <http://www.ncbi.nlm.nih.gov/pubmed/4504201>.
- Veals, S A, T Santa Maria, and D E Levy. 1993. “Two Domains of ISGF3 Gamma That Mediate Protein-DNA and Protein-Protein Interactions during Transcription Factor Assembly Contribute to DNA-Binding Specificity.” *Molecular and Cellular Biology* 13(1): 196–206.
- Wang, Pi Xiao et al. 2015. “Interferon Regulatory Factor 9 Is a Key Mediator of Hepatic Ischemia/Reperfusion Injury.” *Journal of Hepatology* 62(1): 111–20.

REFERENCES

- <http://dx.doi.org/10.1016/j.jhep.2014.08.022>.
- Wang, Wenshi et al. 2017. “Unphosphorylated ISGF3 Drives Constitutive Expression of Interferon-Stimulated Genes to Protect against Viral Infections.” *Science Signaling* 10(476): 1–13.
- Wang, Xin-An et al. 2013. “Interferon Regulatory Factor 9 Protects against Hepatic Insulin Resistance and Steatosis in Male Mice.” *Hepatology (Baltimore, Md.)* 58(2): 603–16. <https://www.ncbi.nlm.nih.gov/pmc/articles/PMC3624763/pdf/nihms412728.pdf>.
- Wang, Yuxin et al. 2021. “A Virus-Induced Conformational Switch of STAT1-STAT2 Dimers Boosts Antiviral Defenses.” *Cell Research* 31(2): 206–18. <http://dx.doi.org/10.1038/s41422-020-0386-6>.
- Weidner, Jessica M. et al. 2010. “Interferon-Induced Cell Membrane Proteins, IFITM3 and Tetherin, Inhibit Vesicular Stomatitis Virus Infection via Distinct Mechanisms.” *Journal of Virology* 84(24): 12646–57.
- Wesoly, Joanna, Zofia Szweykowska-Kulinska, and Hans A.R. Bluysen. 2007. “STAT Activation and Differential Complex Formation Dictate Selectivity of Interferon Responses.” *Acta Biochimica Polonica* 54(1): 27–38.
- Wienerroither, Sebastian et al. 2015. “Cooperative Transcriptional Activation of Antimicrobial Genes by STAT and NF- κ B Pathways by Concerted Recruitment of the Mediator Complex.” *Cell Reports* 12(2): 300–312.
- Wojciak, Jonathan M., Maria A. Martinez-Yamout, H. Jane Dyson, and Peter E. Wright. 2009. “Structural Basis for Recruitment of CBP/P300 Coactivators by STAT1 and STAT2 Transactivation Domains.” *EMBO Journal* 28(7): 948–58. <http://dx.doi.org/10.1038/emboj.2009.30>.
- Xu, Darui et al. 2012. “Sequence and Structural Analyses of Nuclear Export Signals in the NESdb Database.” *Molecular biology of the cell* 23(18): 3677–93. <http://www.ncbi.nlm.nih.gov/pubmed/22833565>.
- Xu, Wei et al. 2014. “Ebola Virus VP24 Targets a Unique NLS Binding Site on Karyopherin Alpha 5 to Selectively Compete with Nuclear Import of Phosphorylated STAT1.” *Cell Host and Microbe* 16(2): 187–200. <http://dx.doi.org/10.1016/j.chom.2014.07.008>.
- Xu, Weijing et al. 2004. “Geldanamycin, a Heat Shock Protein 90-Binding Agent, Disrupts Stat5 Activation in IL-2-Stimulated Cells.” *Journal of Cellular Physiology* 198(2): 188–96.
- Yamauchi, Shota et al. 2016. “STAT1 Is Essential for the Inhibition of Hepatitis C Virus Replication by Interferon- λ but Not by Interferon- α .” *Scientific Reports* 6(November): 1–11.
- Yanai, Hideyuki, Hideo Negishi, and Tadatsugu Taniguchi. 2012. “The IRF Family of Transcription Factors Inception, Impact and Implications in Oncogenesis.” *OncImmunology* 1(8): 1376–86.
- Yang, Edward et al. 1999. “The Linker Domain of Stat1 Is Required for Gamma Interferon-Driven Transcription.” *Molecular and Cellular Biology* 19(7): 5106–12.
- Yang, Edward et al. 2003. “Decay Rates of Human MRNAs: Correlation with Functional Characteristics and Sequence Attributes.” *Genome research* 13(8): 1863–72. <http://www.ncbi.nlm.nih.gov/pubmed/12902380>.
- Yang, Emily, and Melody M H Li. 2020. “All About the RNA: Interferon-Stimulated Genes

REFERENCES

- That Interfere With Viral RNA Processes.” *Frontiers in immunology* 11(December): 605024. <http://www.ncbi.nlm.nih.gov/pubmed/33362792>.
- Yuemaier, Munire et al. 2020. “Identification of the Prognostic Value and Clinical Significance of Interferon Regulatory Factors (IRFs) in Colon Adenocarcinoma.” *Medical Science Monitor* 26.
- Zanin, Natacha, Christine Viaris de Lesegno, Christophe Lamaze, and Cedric M. Blouin. 2021. “Interferon Receptor Trafficking and Signaling: Journey to the Cross Roads.” *Frontiers in Immunology* 11(January): 1–15.
- Zhang, Shu Min et al. 2014. “Interferon Regulatory Factor 9 Is Critical for Neointima Formation Following Vascular Injury.” *Nature Communications* 5.
- Zhang, Yan et al. 2014. “Interferon Regulatory Factor 9 Is an Essential Mediator of Heart Dysfunction and Cell Death Following Myocardial Ischemia/Reperfusion Injury.” *Basic Research in Cardiology* 109(5).
- Zhang, Yong et al. 2008. “Model-Based Analysis of ChIP-Seq (MACS).” *Genome Biology* 9(9): R137. <https://doi.org/10.1186/gb-2008-9-9-r137>.
- Zhao, Guang Nian, Ding Sheng Jiang, and Hongliang Li. 2015. “Interferon Regulatory Factors: At the Crossroads of Immunity, Metabolism, and Disease.” *Biochimica et Biophysica Acta - Molecular Basis of Disease* 1852(2): 365–78. <http://dx.doi.org/10.1016/j.bbadis.2014.04.030>.
- Zhu, X, Z Wen, L Z Xu, and J E Darnell. 1997. “Stat1 Serine Phosphorylation Occurs Independently of Tyrosine Phosphorylation and Requires an Activated Jak2 Kinase.” *Molecular and Cellular Biology* 17(11): 6618–23.
- Zouein, Fouad A. et al. 2015. “Pivotal Importance of STAT3 in Protecting the Heart from Acute and Chronic Stress: New Advancement and Unresolved Issues.” *Frontiers in Cardiovascular Medicine* 2(January 2016).

List of Figures

INTRODUCTION

Figure 1.1 The Interferon signalling pathways.....**page 9**

Figure 1.2 Simplified scheme of the IFN Type-I production**page 12**

Figure 1.3 The STAT1 protein structure.....**page 19**

Figure 1.4 The STAT2 protein structure.....**page 22**

Figure 1.5 The IRF9 protein structure.....**page 26**

Figure 1.6 The IRF1 protein structure.....**page 28**

Figure 1.7 The role of ISGF3 components in constitutive and the IFN-dependent ISG expression**page 35**

Figure 1.8 The role of ISGF3 components in constitutive and the IFN-dependent ISG expression in the absence of STAT1 **page 37**

Figure 1.9 The positive feedback loop model.....**page 43**

MATERIAL AND METHODS

Figure 3.1 Cell lines in culture.....**page 49-50**

Figure 3.2 The fluorescence of three clones of the cell line stably overexpressing STAT1, STAT2 and IRF9.....**page 50**

Figure 3.3 The construction of MIGR1 plasmid.....**page 51**

Figure 3.4 Pipeline for ChIP-Seq data processing of a transcription factor.....**page 61**

RESULTS

Figure 4.1 The protein levels and phosphorylation profiles in the 2fTGH and Huh7.5 cell lines.....**page 69**

Figure 4.2 Commonly upregulated genes for 2fTGH and Huh7.5 cell lines.....**page 70**

Figure 4.3 Characterization of selected commonly upregulated ISGs in the 2fTGH and Huh7.5 cell lines.....**page 70**

Figure 4.4 Characterization of selected commonly upregulated ISGs in the 2fTGH and Huh7.5 cell lines.....**page 71**

Figure 4.5 The gene expression profile in the 2fTGH and Huh7.5 cell lines.....**page 72**

Figure 4.6 Gene Ontology.....**page 73**

Figure 4.7 Peak distribution of particular antibodies and Motif distribution.....**page 75**

LIST OF FIGURES

- Figure 4.8** Characterization of different ISGF3 components recruitment/binding to the regulatory regions of ISGs under IFN α treatment.....**page 77-78**
- Figure 4.9** The long-lasting antiviral protection upon IFN α stimulation.....**page 80**
- Figure 4.10** The protein levels and phosphorylation profiles in the absence of STAT1.....**page 82**
- Figure 4.11** Commonly upregulated genes in the 2fTGH, Huh7.5, ST2-U3C and Huh ST1 K.O. cell lines.....**page 83-84**
- Figure 4.12** Characterization of commonly upregulated ISGs in the wild-type and STAT1 knock-out cell lines.....**page 85-86**
- Figure 4.13** Characterization of selected commonly upregulated ISGs in the wild-type and STAT1 knock-out cell lines.....**page 88**
- Figure 4.14** The gene expression profiles in the STAT1-deficient cell lines vs WT.....**page 89-91**
- Figure 4.15** Peak distribution of particular antibodies.....**page 93**
- Figure 4.16** Characterization of different ISGF3 components recruitment to the regulatory regions of ISGs under IFN α treatment in the absence of STAT1 protein.....**page 94-95**
- Figure 4.17** The protein levels and phosphorylation profiles in the 2fTGH and Huh7.5 cell lines upon treatment with JAK Inhibitor I.....**page 98**
- Figure 4.18** The gene expression profile in the 2fTGH cell lines untreated and treated with JAK Inhibitor I.....**page 99**
- Figure 4.19** The gene expression profile in the Huh7.5 cell lines untreated and treated with JAK Inhibitor I.....**page 100**
- Figure 4.20** The protein levels and phosphorylation profiles in the ST2-U3C and Huh ST1 K.O. cell lines upon treatment with JAK Inhibitor I.....**page 102**
- Figure 4.21** The gene expression profile in the ST2-U3C cell lines untreated and treated with JAK Inhibitor I.....**page 103-104**
- Figure 4.22** The gene expression profile in the Huh ST1 K.O. cell lines untreated and treated with JAK Inhibitor I.....**page 104**
- Figure 4.23** The role of phosphorylation in antiviral protection of the 2fTGH cells.....**page 105**
- Figure 4.24** The gene expression level in the U3C, ST2-U3C and ST2-IRF9-U3C cell lines upon IFN α stimulation.....**page 107**
- Figure 4.25** The protein levels in different clones of cells overexpressing STAT1, STAT2 and IRF9.....**page 108**
- Figure 4.26** The gene expression level in the U3C, 2fTGH and ST1-ST2-IRF9-U3C cell lines without IFN α stimulation.....**page 109**

LIST OF FIGURES

- Figure 4.27** Commonly upregulated genes in 2fTGH and Huh7.5 vs ST1-ST2-IRF9-U3C.....**page 110**
- Figure 4.28** RNA-Seq results and their confirmation by qPCR.....**page 110-111**
- Figure 4.29** The gene expression profile in ST1-ST2-IRF9-U3C cell line upon IFN α stimulation and JII treatment vs U3C.....**page 112**
- Figure 4.30** Characterization of STAT1, STAT2 and IRF9 recruitment to ISG promoters without IFN α stimulation in ST1-ST2-IRF9-U3C.....**page 113**
- Figure 4.31** The long-lasting antiviral protection without IFN α stimulation.....**page 114**
- Figure 4.32** The role of phosphorylation in ensuring antiviral protection without IFN α stimulation.....**page 115**
- Figure 4.33** The protein levels and phosphorylation profiles in the ST1-ST2-IRF9-U3C cell line upon treatment with JAK Inhibitor I.....**page 117**
- Figure 4.34** The effect of phosphorylation inhibition on gene expression.....**page 118**
- Figure 4.35** The role of phosphorylation in antiviral protection.....**page 119**
- Figure 4.36** The qPCR confirmation of the results from Figure 4.34.....**page 120**
- Figure 4.37** The comparison of the gene expression profiles in ST1-ST2-IRF9-U3C and 2fTGH upon IFN α stimulation and JII treatment.....**page 121**

DISCUSSION

- Figure 5.1** The complex model of the phosphorylation-dependent regulation of IFN α - induced transcriptional response under wild-type conditions.....**page 132**
- Figure 5.2** The complex model of the phosphorylation-dependent regulation of IFN α - induced transcriptional response in the Huh ST1 K.O. cell line.....**page 134**
- Figure 5.3** The complex model of the phosphorylation-dependent regulation of IFN α - induced transcriptional response in the STAT2-U3C cell line.....**page 135**
- Figure 5.4** The complex model of the phosphorylation-dependent regulation of IFN α - induced transcriptional response under the overexpression of STAT1, STAT2 and IRF9.....**page 136**

List of Tables

Table 3/1. Conditions for reverse transcription reaction.....*page 52*

Table 3/2. qPCR sample preparation description.....*page 53*

Table 3/3. qPCR reaction conditions.....*page 53*

Table 3/4. Primers used for the gene expression experiments that are described in subsection 3.4.....*page 54*

Table 3/5. A list of primers used for ChIP-PCR experiments that are described in subsection 3.6.....*page 58*

Table 3/6. Western blotting protocol.....*page 64*

Table 3/7. List of antibodies used in Western blot and chromatin immunoprecipitation experiments.....*page 65*

Table 3/8. JAK Inhibitor I treatment schedule.....*page 66*

Abbreviations

C-C	- coiled-coil domain
cDC	- classical dendritic cell(s)
ChIP	- chromatin immunoprecipitation
DAMP	- damage-associated molecular patterns
DBD	- DNA binding domain
DC	- dendritic cell(s)
GAF	- gamma activation factor
GAS	- gamma-activated sequence
IAD	- IRF-associated domain
IFN	- interferon
IFNAR	- interferon- α/β receptor
IGV	- Integrative Genomics Viewer
IL	- interleukin
IRF	- interferon regulatory factors
ISG	- interferon stimulated genes
ISGF3	- Interferon-Stimulated Gene Factor 3
ISRE	- IFN-Stimulated Regulatory Element
JAK	- Janus kinase
JH	- Jak homology region
JII	- JAK Inhibitor I
K.O.	- knock-out
LPS	- lipopolysaccharide
M ϕ	- macrophage
ND	- N-terminal domain
NES	- nuclear export signal
NF- κ B	- nuclear factor kappa-light-chain-enhancer of activated B cells
NGS	- next generation sequencing
NK	- natural killer
NLS	- nuclear localization signal
PAMP	- pathogen-associated molecular patterns

ABBREVIATIONS

pDC	- plasmacytoid dendritic cell(s)
PRR	- pattern recognition receptors
SH2	- Src homology 2 domain
STAT	- signal transducer and activator of transcription
TAD	- transactivation domain
TF	- transcription factor
TLR	- toll-like receptor
U-ISGF3	- unphosphorylated Interferon-Stimulated Gene Factor 3
U-STAT	- unphosphorylated-STAT
VSV	- vesicular stomatitis Indiana virus
WT	- wild-type

List of publications

1. Renata Kontek, **Hanna Nowicka**,
The modulatory effect of melatonin on genotoxicity of irinotecan in healthy human lymphocytes and cancer cells;
Drug and Chemical Toxicology; 2013
doi: 10.3109/01480545.2012.737805.
IF: 1.29; MP: 15
2. Stefan Chmielewski, Adam Olejnik, Krzysztof Sikorski, Jaroslav Pelisek, **Hanna Nowicka**, Alma Zerneck, Uwe Heemann, Joanna Wesoly, Marcus Baumann, Hans A.R. Bluysen,
STAT1-dependent signal integration between IFN γ and TLR4 in vascular cells reflect pro-atherogenic responses in human atherosclerosis;
PloS One; 2014
doi: 10.1371/journal.pone.0113318.
IF: 4.24; MP: 40
3. Katarzyna Blaszczyk, Adam Olejnik, Yi-Ling Chen, Stefan Chmielewski, Kaja Kostyrko, **Hanna Nowicka**, Joanna Wesoly, Chien-Kuo Lee, Hans A.R. Bluysen,
STAT2/IRF9-mediated IFN α signaling directs ISGF3-dependent and -independent transcription and antiviral activity without STAT1;
Biochem J.; 2015
doi: 10.1042/BJ20140644.
IF: 5.02; MP: 35
4. Katarzyna Blaszczyk, **Hanna Nowicka**, Kaja Kostyrko, Aleksandra Antonczyk, Joanna Wesoly, Hans A.R. Bluysen,
The unique role of STAT2 in constitutive and IFN-induced transcription and antiviral responses;
Cytokine Growth Factor Rev.; 2016
doi: 10.1016/j.cytogfr.2016.02.010.
IF: 6.79; MP: 40
5. Mahdi Eskandarian Boroujeni, Agata Sekrecka, Aleksandra Antonczyk, Sanaz Hassani, Michal Sekrecki, **Hanna Nowicka**, Natalia Lopacinska, Arta Olya, Katarzyna Kluzek, Joanna Wesoly, Hans A.R. Bluysen,
Dysregulated Interferon Response and Immune Hyperactivation in Severe COVID-19: Targeting STATs as a Novel Therapeutic Strategy;
Frontiers in Immunology; 2022
doi: 10.3389/fimmu.2022.888897.
IF: 6.429; MP: 140
6. **Hanna Nowicka**, Katarzyna Błaszczyk, Katarzyna Kluzek, Anastasia Aliesa Hermosaningtyas, Chien Kuo Lee, Joanna Wesoly, Hans AR Bluysen,
U-ISGF3 mediates constitutive ISG expression and viral protection in a concentration-dependent and IFN-independent manner;
Publication in preparation

Acknowledgments

I would like to thank my supervisor, prof. Hans Bluysen for the endless discussions and invaluable advice that gave this dissertation its final shape.

I would like to thank prof. dr hab. J. Jaruzelska, dr hab. M. Dawidowska and dr hab. inż P. Pawlak for taking the time to evaluate my work.

Special thanks goes to:

Dr. Katarzyna Kluzek, our "Zen master" without whom bioinformatic analysis would be impossible, and therefore this thesis would not have been written.

Dr Natalia Derebecka - our lab "language error corrector" and my best friend who always supported me, especially when I was losing hope.

And I would like to thank all my colleagues from the Lab, who made me happy to go to work each day.

My thank goes also to Prof. Lee, and his Team in Taipei, for opportunity to learn new, very useful technics, and Ting-Ting for providing friendly atmosphere far away from home.

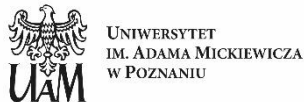
Na końcu chciałaby podziękować moim Rodzicom za to, że dzięki nim jestem taka jaka jestem, że zawsze mogłam na nich liczyć i za olbrzymią motywację. Mojej Teściowej za nieocenioną pomoc, za to, że była zawsze wtedy kiedy potrzebowałam, dzięki czemu mogłam skupić się na pracy. Moim przyjacielom, Wice i Marcinowi, za wsparcie i odskocznię od pracy. Wreszcie mojemu mężowi Markowi za nieprzebrane pokłady cierpliwości i za bycie moją ostoją, każdego dnia. No i mojej Córeczce Lusi, która dzielnie znosiła nieobecność mamy zajętej pisaniem tej pracy.

FUNDING

Funding

Research presented in this doctoral thesis was supported by:

"Passport to the future - Interdisciplinary doctoral studies at the Faculty of Biology UAM"
POWR.03.02.00-00-I006/17



UNIA EUROPEJSKA
EUROPEJSKI
FUNDUSZ SPOŁECZNY



PRELUDIUM research grant UMO-2016/21/N/NZ2/01720:

The cooperation/role of unphosphorylated and phosphorylated ISGF3 components in the regulation of ISG expression and viral protection

Project leader: MSc Hanna Janina Nowicka

OPUS research grant 2012-07-B-NZ1-02710:

STAT1 and IRF8-mediated signal integration between IFN γ and TLRs: a pathophysiological role in vascular disease

Project leader: Prof. Johannes A.R. Bluysen

OPUS research grant 2013/11/B/NZ2/02569:

Genome-wide characterization of type I IFN-induced transcriptomes and identification of novel ISGs and their antiviral functions

Project leader: Prof. Johannes A.R. Bluysen



NATIONAL SCIENCE CENTRE
POLAND

Summary

Interferons belong to the family of cytokines that play crucial role in triggering of antiviral response and are divided into three subfamilies: Type-I, -II and -III. IFN α -dependent response, in the most classical form, is based on Signal Transducer and Activator of Transcription (STAT) family members STAT1 and STAT2 that become phosphorylated and together with interferon regulatory factor 9 (IRF9) form ISGF3. This complex recognizes the specific ISRE sequences in the regulatory regions of ISGs, thus mediating their expression and providing ability to combat viral infections.

Over the years evidence is accumulating that this system is not as simple. It becomes clear that besides canonical ISGF3-dependent signalling, also other pathways function, and may cooperate to provide effective viral protection.

In this thesis, we focused on the role of phosphorylation in both, basal as well as IFN- and -time dependent transcriptional responses under wild-type and STAT1-deficiency conditions, we as well considered the dependence of viral protection on the amount of the native STAT1, STAT2 and IRF9.

Using different molecular techniques, among them whole-genome approaches, such as RNA-Seq and ChIP-Seq, we provide further evidence that in WT cells an IFN α -inducible transcriptional mechanism exists, that relies on the ISGF3 components STAT1, STAT2 and IRF9 in a phosphorylation- and time-dependent manner. It also points to an important role of classical ISGF3 in the regulation of prolonged ISG expressions and viral protection. However, the contribution of U-ISGF3 under these conditions cannot be ruled out.

Likewise, in cells lacking STAT1, an IFN α -inducible and STAT1-independent transcriptional mechanism exists, that depends on the STAT2/IRF9 components STAT2 and IRF9 in a phosphorylation- and time-dependent manner. It also provides further prove for the previous observation that STAT2/IRF9 can take over the role of ISGF3 in the absence of STAT1, to regulate expression of a common group of ISRE-containing genes and provide protection against viral infection.

Finally, comparative experiments in STAT1-KO cells overexpressing all ISGF3 components, revealed a potential role of U-ISFG3, and possibly U-STAT2/IRF9, in the regulation of constitutive and long-term IFN α -treated ISG expression and viral protection. This

SUMMARY

strongly suggests that a certain threshold of STAT1, STAT2 and IRF9 expression and levels of U-ISGF3 (and/or U-STAT2/IRF9) has to be reached to be able to trigger ISG transcription. As a consequence, together with classical ISGF3, U-ISGF3 and U-STAT2/IRF9, could be instrumental in IFN-dependent and independent ISG transcription and in combatting viral infection.

Streszczenie w języku polskim

Interferony, należące do rodziny cytokin, są podzielone na trzy grupy (IFN Typu I, II oraz III) i pełnią kluczową rolę we wzbudzeniu przeciwwirusowej odpowiedzi immunologicznej. W swojej najbardziej klasycznej formie odpowiedź zależna od interferonu alfa (IFN α) jest oparta na kompleksie ISGF3, składającym się z ufosforylowanych białek STAT1 i STAT2 należących do rodziny STAT (od ang. *Signal Transducer and Activator of Transcription*) oraz białka IRF9 (od ang. *interferon regulatory factor 9*). Ten kompleks rozpoznaje specyficzne sekwencje ISRE w promotorach genów o aktywności przeciwwirusowej, w ten sposób regulując ich ekspresję i zapewniając możliwość zwalczania infekcji.

Badania prowadzone w ostatnich latach wykazały, że system ten jest bardziej złożony. Staje się jasne, że oprócz kanonicznej sygnalizacji zależnej od kompleksu ISGF3 w proces ten zaangażowane są również inne szlaki, które mogą uzupełniać się wzajemnie, aby zapewnić skuteczną ochronę wirusową.

W tej pracy skupiliśmy się na roli, jaką w odpowiedzi konstytutywnej, a także zależnej od interferonu i czasu, odgrywa proces fosforylacji. Zbadaliśmy dwa rodzaje linii komórkowych: typu dzikiego, oraz pozbawione białka STAT1 (z ang. *STAT1 knock-out*), i na tej podstawie wyciągnęliśmy wnioski dotyczące zależności ochrony przeciwwirusowej od ilości białek STAT1, STAT2 i IRF9 w komórce.

Stosując różne techniki biologii molekularnej, w tym także metody całogenomowe (takie jak RNA-Seq i ChIP-Seq), dostarczyliśmy kolejnych dowodów na to, że w komórkach typu dzikiego istnieje mechanizm transkrypcyjny indukowany przez IFN α , opierający się, w sposób zależny od procesu fosforylacji i czasu, na białkach STAT1, STAT2 i IRF9, będących składnikami kompleksu ISGF3. W pracy podkreślamy także, jak ważną rolę pełni klasyczny kompleks ISGF3 w regulacji przedłużonej ekspresji ISG i skutecznej odpowiedzi przeciwwirusowej. Nie jesteśmy jednak w stanie wykluczyć także udziału alternatywnego kompleksu U-ISGF3.

Podobnie w liniach komórkowych pozbawionych białka STAT1 istnieje mechanizm transkrypcyjny indukowany przez IFN α , niezależny od białka STAT1, który oparty jest w sposób zależny od fosforylacji i czasu na kompleksie STAT2/IRF9, składającym się z białek STAT2 i IRF9. Ta praca dostarcza kolejnych dowodów potwierdzających zaobserwowane wcześniej zjawisko, w którym pod nieobecność białka STAT1, kompleks STAT2/IRF9 przejmuje rolę

ISGF3 w regulacji ekspresji wspólnej grupy genów zawierających sekwencje ISRE, zaangażowanych w skuteczną ochronę przeciw wirusom.

Co więcej, eksperymenty porównawcze na komórkach pozbawionych STAT1, ze stabilną nadprodukcją wszystkich składników kompleksu ISGF3, wykazały potencjalną rolę U-ISGF3 (i prawdopodobnie także U-STAT2/IRF9) w regulacji konstytutywnej oraz indukowanej IFN α przedłużonej ekspresji ISG i ochronie przeciwwirusowej. To sugeruje, że musi zostać przekroczony pewien minimalny poziom białek STAT1, STAT2 i IRF9 w komórce (a co za tym idzie kompleksów U-ISGF3 i/lub U-STAT2/IRF9), aby doszło do zapoczątkowania ekspresji ISG. W konsekwencji, wraz z klasycznym kompleksem ISGF3, także U-ISGF3 i U-STAT2/IRF9 mogą odgrywać zasadniczą rolę w zależnej i niezależnej od IFN α transkrypcji ISG oraz w zwalczaniu infekcji wirusowych.